# On the Lugiato-Lefever Model for Frequency Combs in a Dual-Pumped Ring Resonator

## with an Appendix on Band Structures for Periodic Fractional Schrödinger Operators

Zur Erlangung des akademischen Grades eines

Doktors der Naturwissenschaften

von der KIT-Fakultät für Mathematik des
Karlsruher Insituts für Technologie (KIT)
genehmigte

Dissertation

von
Elias Gasmi

Referent: Prof. Dr. Wolfgang Reichel

Korreferent: Prof. Dr.-Ing. Christian Koos

Korreferent: Prof. Dr. Michael Plum

Tag der mündlichen Prüfung: 16.11.2022

# Acknowledgement

At this point, I would like to thank a lot of people who contributed to the success of this thesis. The following list may be incomplete since our group has grown exponentially in the last years, that this margin is too narrow to contain.

First of all I thank my supervisor Prof. Dr. Wolfgang Reichel who has been with me as a lecturer since the first semester and who motivated me to start my PhD. Thank you for excellent supervision, many fruitful ideas and never losing optimism. Especially, thank you for never skipping one of our regular meetings, even during the very stressful time as dean of studies.

Moreover, I would like to thank Prof. Dr.-Ing. Christian Koos for co-supervising me. The collaboration with IPQ was very inspiring. Thank you for your willingness to meet at late hours and for all the helpful input.

I would also like to thank Prof. Dr. Michael Plum for reviewing this thesis and for the advice to try a sesquilinear form approach.

Furthermore, I thank the CRC 1173 for giving me the opportunity to do research within this great environment in the very exciting interdisciplinary project B3.

Thanks also to Dr. Huanfa Peng for several explanations concerning the physics of frequency combs and for the invitation to the laboratory. It was a pleasure to watch you capturing the 1-soliton.

In the last years I really enjoyed the great atmosphere in the group Nonlinear Partial Differential Equations. Special thanks goes to Lukas Bengel for many more or less fruitful discussions and for proofreading parts of this thesis. Thanks also to Sebastian Ohrem for proofreading the Appendix and to Dr. Rainer Mandel for mentioning "Leray-Schauder" and "a-priori bounds" at the right time. Many thanks to Marion Ewald for supporting me with organizational stuff and to Dr. Jonathan Wunderlich for many helpful advices. Moreover, I would like to thank Prof. Dr. Tobias Jahnke and Michael Kirn for the successful cooperation and for giving the initial start for analyzing traveling waves.

Last but not least I am very grateful to Anastasia and my family as a whole for their continuous support.

# Contents

# 1. Introduction

Frequency combs are optical signals consisting of a multitude of equally spaced frequency lines. The first generation of frequency combs was realized in 1998 and is due to the group of Theodor Hänsch who introduced them as a new approach to measure the frequency of light with femtosecond laser pulses emitted from a mode-locked laser [66]. Their discovery initiated research on a wide range of applications. In timekeeping, they allow a very precise type of atomic clock and with that improvements in satellite navigation systems [45]. In astronomy, they can be used for detecting exoplanets outside the solar system [14, 71] and possibly even for measuring the expansion of the universe [17]. In optical communications, they allow for high speed data transmission [52]. Due to the huge impact of frequency combs in these and other research fields, Theodor Hänsch and John Hall received both one fourth of the Nobel prize for physics in 2005 "for their contributions to the development of laser-based precision spectroscopy, including the optical frequency comb technique" [28, 27]. Although comb sources implemented by mode-locked lasers are still considered as rather bulky and expensive scientific systems they are still the most common commercially available frequency comb source [24]. For technical applications it is necessary to reduce the cost, size and energy consumption of these devices. Also the physical properties of the emitted frequency combs, such as the covered spectral range of the emitted spectral lines or the comb line spacing (free spectral range, FSR), can be inappropriate for some applications [63]. A comb generator with smaller optical length has a larger FSR as needed in systems like optical telecommunication networks based on wavelength division multiplexing [63]. Therefore, nonlinear Kerr microresonators with a size down to a few cubic centimeter and a total power consumption down to 100 mW have become particularly relevant comb sources [12, 60]. These are photonic structures in which monochromatic light from a separate pump laser can be converted into a frequency comb through the Kerr-nonlinearity by degenerate and non-degenerate four-wave mixing [63]. The experimental setup is depicted in Figure 1 [19].
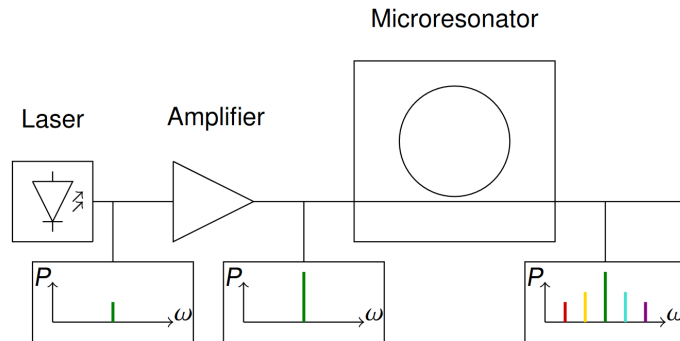


Figure 1. Generation of Kerr frequency combs. A continuous wave laser emits light at frequency $\omega_p$ which is first amplified and then coupled into a microresonator where it is converted into a frequency comb through the Kerr-nonlinearity by degenerate and non-degenerate four-wave mixing.

## 1. Introduction

The frequency $\omega_p$ of the pump laser is set close to a resonance frequency of the microresonator such that light is coupled into one of its resonant modes. Inside the microresonator degenerate four-wave mixing converts two photons of the same frequency $\omega_p$ into two new photons with frequencies $\omega_p + \alpha$ and $\omega_p - \alpha$. In a next step, non-degenerate four-wave mixing converts two photons with different frequencies $\omega_p + \alpha$ and $\omega_p + \beta$ into two different photons with frequencies $\omega_p + \gamma$ and $\omega_p + \alpha + \beta - \gamma$. In this way, a frequency comb is formed [37]. Varying the power and the frequency of the input pump can lead to many different forms of Kerr frequency combs due to the complex nonlinear dynamics. Among these, the stable single-soliton state is most important for applications due to its smooth spectrum, its large optical bandwidth and the high coherence among all comb lines [63].

In 2010, Kerr comb dynamics were described mathematically by Chembo and Yu via a modal expansion approach [8]. They introduced a system of nonlinear coupled ordinary differential equations describing the dynamics of each resonator mode. Indeed, numerical simulations of this model are in agreement with experiments [7]. This formalism enabled the understanding of many essential features such as threshold phenomena and the role of dispersion [8]. However, this modal expansion approach becomes less useful when a large number of modes is excited since it results in high computational effort [8]. By considering the spatiotemporal slowly varying envelope of the total field, Chembo and Menyuk showed in [6] that under suitable simplifications the modal expansion approach is equivalent to a single PDE, the Lugiato-Lefever equation (LLE), which allows a less complex numerical and analytical investigation. The LLE is a nonlinear Schrödinger equation that includes damping, driving and detuning. In dimensionless, normalized quantities the LLE reads

$$\mathrm{i} a_\tau = (\zeta - \mathrm{i})a - d a_{xx} - |a|^2 a + \mathrm{i} f, \qquad a \text{ } 2\pi\text{-periodic in } x. \qquad (1.1)$$

Here, $a(\tau, x)$ represents the optical intracavity field as a function of normalized time $\tau$ and angular position $x \in [0, 2\pi]$ within the ring resonator. The detuning parameter $\zeta$ denotes the normalized frequency mismatch between the frequency of the input pump and the closest resonance frequency of the microresonator. The parameter $d$ quantifies the dispersion in the system (the case $d < 0$ amounts to normal and the case $d > 0$ to anomalous dispersion) and $f$ represents the normalized power of the input pump. Stationary solutions of (1.1) are of particular interest due to their invariance in time. Among these, highly localized states are most important as they feature a broad comb in the frequency domain. Equation (1.1) admits constant solutions $a_0 \in \mathbb{C}$ which correspond to the case where only the primary mode is excited. Hence, these states do not form frequency combs themselves but under modulation instability they serve as starting point for a bifurcation analysis in order to find highly localized, stable states. This has been thoroughly studied, e.g. in [11, 18, 25, 26, 41, 43, 48, 49, 50, 51, 59]. In [18] the authors presented a heuristic algorithm for detecting the optimal choice of the detuning offset $\zeta$ leading to the most localized single-soliton. They use the full-width at half-maximum (FWHM) as quantification of localization, cf. Figure 2. The heuristic given in [18] relies on numerical path continuation methods. Based on this approach, a

8

quantitative characterization of most localized solitons using the comb bandwidth and the pump-to-comb power conversion efficiency as performance metrics was given for many different values of $d$ and $f$.
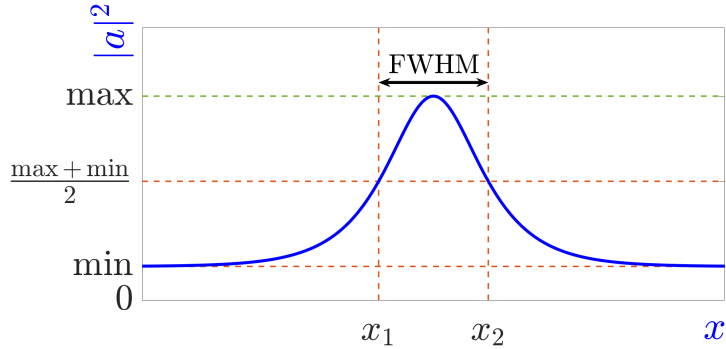


Figure 2. Full-width at half-maximum of a single-peak state, defined as difference between the two values where the average of maximum and minimum is attained.

Future progress in applications based on nonlinear Kerr microresonators highly relies on possibilities to increase the pump-to-comb power conversion efficiency and the comb bandwidth. Usually, Kerr frequency combs are generated by using a monochromatic pump which only excites one single primary mode of the microresonator. However, the simultaneous pumping of two or more different modes permits us to achieve the Kerr frequency comb generation with the appealing benefits of thresholdless comb generation in both normal and anomalous dispersion regimes [29, 38], stabilization of the comb repetition-rate [47], and manipulation of the comb mode spacing [61], which attracted significant attention in recent years. In the present thesis we theoretically analyze the dual pumping scheme (two pumped modes) and demonstrate that in the anomalous dispersion regime $d > 0$ the pumping of two modes leads to Kerr frequency combs with both higher pump-to-comb power conversion efficiency and higher comb bandwidth as compared with single mode pumping.

In Section 2 we derive the Lugiato-Lefever model for a dual-pumped ring resonator starting from an adapted modal expansion approach which models the situation with a second pumped mode [62]. In dimensionless, normalized quantities this modified LLE reads

$$\mathrm{i}a_\tau = (\zeta - \mathrm{i})a - da_{xx} - |a|^2 a + \mathrm{i}f_0 + \mathrm{i}f_1 \mathrm{e}^{\mathrm{i}(k_1 x - \nu_1 \tau)}, \qquad a \ 2\pi\text{-periodic in } x. \qquad (1.2)$$

Compared to (1.1) the forcing term now includes a second expression $\mathrm{i}f_1 \mathrm{e}^{\mathrm{i}(k_1 x - \nu_1 \tau)}$. Here, $k_1 \in \mathbb{N}$ denotes the difference of the mode indices of the two pumped modes and the parameter $f_1$ describes the normalized power of the second input pump. Since there are now two pumped modes there are also two detuning parameters denoted by $\zeta$ and $\zeta_1$ which are taken into account in (1.2) by the parameter $\nu_1 = \zeta - \zeta_1 + dk_1^2$. At some places we will also use the notation $\zeta_0$ for the first detuning $\zeta$.

9

# 1. Introduction

Section 3 is based on the preprint [21] which is joint work with Tobias Jahnke, Michael Kirn and Wolfgang Reichel. Here, we provide several existence results as well as a uniqueness result for time-periodic and spatially $2\pi$-periodic traveling wave solutions of (1.2). We also provide numerical illustrations of our analytical results. The particular form of the forcing term $\mathrm{i}f_0 + \mathrm{i}f_1\mathrm{e}^{\mathrm{i}(k_1 x - \nu_1 \tau)}$ of (1.2) suggests to change into a moving coordinate variable $s = x - \omega\tau$ with $\omega = \frac{\nu_1}{k_1}$ and study solutions of (1.2) of the form $a(\tau, x) = u(x - \omega\tau)$. These traveling wave solutions propagate with speed $\omega$ in the resonator and their profile $u$ solves the stationary ODE

$$-du'' + \mathrm{i}\omega u' + (\zeta - \mathrm{i})u - |u|^2 u + \mathrm{i}f_0 + \mathrm{i}f_1\mathrm{e}^{\mathrm{i}k_1 s} = 0, \qquad u \ 2\pi\text{-periodic.} \tag{1.3}$$

Since the specific form of the forcing term is not essential for many of our results we choose a slightly more general approach in Section 3 and consider

$$-du'' + \mathrm{i}\omega u' + (\zeta - \mathrm{i})u - |u|^2 u + \mathrm{i}f(s) = 0, \qquad u \ 2\pi\text{-periodic,} \tag{1.4}$$

where

$$f(s) = f_0 + f_1 e(s)$$

with a $2\pi$-periodic (not necessarily continuous) function $e : \mathbb{R} \to \mathbb{C}$ and $f_0, f_1 \in \mathbb{R}$. Our main results on the existence of solutions to (1.4) consist of

- Theorem 3.1 which is based on a-priori bounds and ensures the existence of a solution of (1.4) in the general case where $f_1$ does not need to vanish,

- Theorem 3.6 and Corollary 3.8 which describe how a constant solution of (1.4) for $f_1 = 0$ can be continued into the regime $f_1 \neq 0$ and which also describe nonlocal properties of this continuation,

- Theorem 3.9 and Corollary 3.10 which show how a non-constant solution from the case $f_1 = 0$ can be continued to $f_1 \neq 0$ and which again also describe nonlocal properties of this continuation.

In Figure 3 we visualize how a constant solution of (1.3) for $f_1 = 0$ can be continued into the regime $f_1 \neq 0$. The parameter choices are $\omega = 1$, $d = -0.1$, $f_0 = 2$ and $k_1 = 1$. The black curve represents the trivial solution curve of (1.3) for $f_1 = 0$ and $f_0 = 2$, and the colored branches show the continuations of selected points on that curve into the $f_1$-direction. One can observe that some of these continuations seem to be unbounded while others form closed loops. This will be described analytically in Theorem 3.6 using some kind of global implicit function theorem. In Figure 4 we visualize how a non-constant solution of (1.3) for $f_1 = 0$ can be continued into the regime $f_1 \neq 0$. Here the parameter choices are $\omega = 0$, $d = -0.1$, $f_0 = 2$ and $k_1 = 1$. Since $\omega = 0$, this time we find additional primary and secondary bifurcation branches (colored in grey and brown) for $f_1 = 0$ which consist of non-constant solutions. For $\zeta \in \{3, 3.3, 3.6, 3.9\}$ one can observe that continuations into the $f_1$-direction also happens from those non-constant solutions. This will be described analytically in Theorem 3.9 using the Crandall-Rabinowitz Theorem of
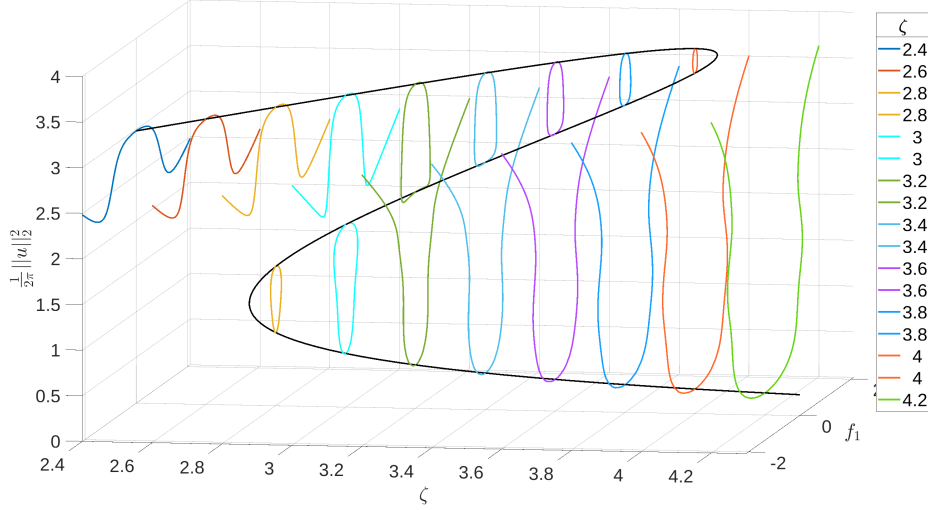
Figure 3. Colored branches show continuations of selected constant solutions into the $f_1$-direction. The parameter choices are $\omega = 1$, $d = -0.1$, $f_0 = 2$ and $k_1 = 1$.

bifurcation from a simple eigenvalue. Appendix B listed in Section 3.8 is not part of the preprint and contains results on a-priori bounds and uniqueness that are tailor-made for the original two mode equation (1.3). In fact, the generalized forcing term used in (1.4) enforced some estimates in Section 3 which can be avoided in case of equation (1.3). The results presented in Appendix B recover for $f_1 = 0$ those stated in [41] for the one mode equation.
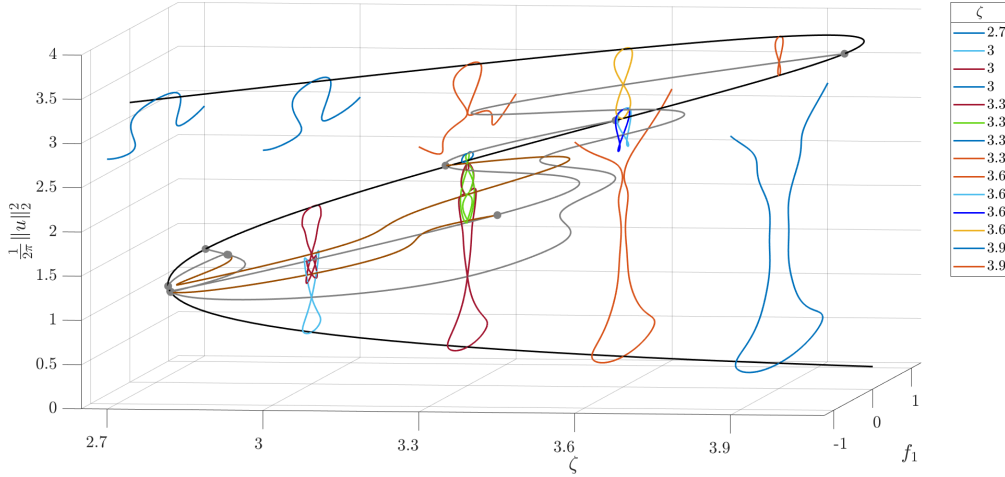


Figure 4. Grey and brown branches for $f_1 = 0$ are bifurcation branches. Other colored branches show continuations of constant and non-constant solutions into the $f_1$-direction. The parameter choices are $\omega = 0$, $d = -0.1$, $f_0 = 2$ and $k_1 = 1$.

Section 4 consists of the preprint [22]. This preprint is joint work with Christian Koos, Huanfa Peng and Wolfgang Reichel. Here, we theoretically demonstrate that the quality of Kerr frequency combs in resonators with anomalous group-velocity dispersion $d > 0$ can be significantly improved by pumping two resonator modes instead of only a single one. The main outcome of our study was found using numerical path continuation methods, and can be summarized as follows:

(1) We show that pumping two modes is advantageous to pumping only one mode.

(2) We present heuristic insights for finding the optimal detuning parameters that provide the most localized 1-soliton states.

(3) We determined the optimal power distribution between the two pumped modes. It is given by a symmetrical distribution where 50% of the power is pumped into each mode, and it simultaneously optimizes all performance metrics (comb bandwidth, full-width at half-maximum, and pump-to-comb power conversion efficiency). Also the two detuning offsets between pump and nearest resonant mode are then equal.

(4) Under optimal power distribution we determined trends of the performance metrics w.r.t. varying dispersion and normalized total input power.

In Figure 5 we illustrate the simultaneous optimization of comb bandwidth, full-width at half-maximum and pump-to-comb power conversion efficiency stated in (3). Here, the power distribution is described as $(f_0, f_1) = (f \cos \varphi, f \sin \varphi)$ with $\varphi \in [0, 2\pi)$ and the normalized total input power $f^2 = f_0^2 + f_1^2$.
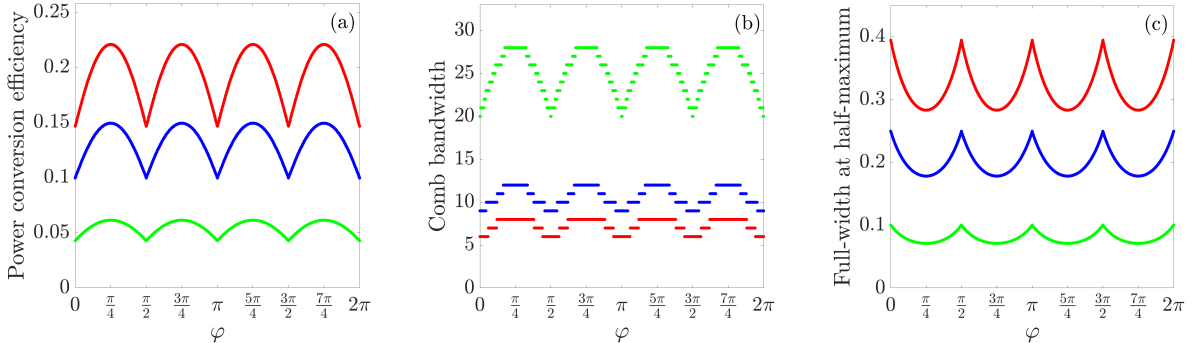


Figure 5. Pump-to-comb power conversion efficiency, comb bandwidth and full-width at half-maximum as a function of $\varphi$ for three different examples. The blue curves correspond to $d = 0.1$ and $f = 2$, the red ones to $d = 0.25$ and $f = 2$ as well as the green ones to $d = 0.1$ and $f = 5$.

## 1. Introduction

In Section 5 we discuss the time-dependent Lugiato-Lefever equation

$$\mathrm{i}a_t = (-\mathrm{i} + \zeta)a - da_{xx} - |a|^2 a + \mathrm{i}f, \qquad a \; 2\pi\text{-periodic in } x, \qquad (1.5)$$

and the time-dependent two mode modification

$$\mathrm{i}a_t = (-\mathrm{i} + \zeta)a - da_{xx} - |a|^2 a + \mathrm{i}f_0 + \mathrm{i}f_1 \mathrm{e}^{\mathrm{i}(k_1 x - \nu_1 t)}, \qquad a \; 2\pi\text{-periodic in } x. \qquad (1.6)$$

Note that in contrast to (1.1) and (1.2) here we write $t$ instead of $\tau$ for the normalized time since it is mathematically more common. In Section 5.1 we present some first results on the question whether all time-periodic solutions of (1.5) are constant in $t$. This includes Theorem 5.2 which is based on Bendixson's negative criterion and which shows that this is true in the case $d = 0$, and Theorem 5.5 which is based on a-priori bounds and shows that for $|f| \ll 1$ all time-periodic solutions of (1.5) are actually constant both in $t$ and in $x$. Likewise, in Section 5.2 we present some first results on the question whether all time-periodic solutions of (1.6) are traveling waves, i.e. of the form $a(t, x) = u(x - \omega t)$, where $u$ is a solution of (1.3) and $\omega = \frac{\nu_1}{k_1}$. In a first step towards this we establish the local uniqueness result Theorem 5.10 which is based on the implicit function theorem and the global uniqueness result Theorem 5.18 which is based on a-priori bounds and holds for $f_0^2 + f_1^2 \ll 1$.

Section 6 is dedicated to approximation results. In [68], Wabnitz used an approximation formula for soliton solutions of the following variant of the stationary LLE

$$-da'' + (-\mathrm{i}\alpha + \zeta)a - |a|^2 a + \mathrm{i}f_* = 0 \text{ on } \mathbb{R}, \qquad a'(0) = 0. \qquad (1.7)$$

It is based on the following explicit solution family for $\alpha = 0$ and $f_* = 0$,

$$a_\theta(x) = \sqrt{2\zeta} \operatorname{sech}\left(\sqrt{\frac{\zeta}{d}} x\right) \mathrm{e}^{\mathrm{i}\theta}, \quad \theta \in [0, 2\pi)$$

and reads as

$$a(x) \approx a_\infty + a_{\theta^*}(x),$$

where $\cos\theta^* = \frac{\alpha\sqrt{8\zeta}}{\pi f_*}$ and where the constant background $a_\infty \in \mathbb{C}$ denotes the solution with smallest magnitude of

$$(-\mathrm{i}\alpha + \zeta)a_\infty - |a_\infty|^2 a_\infty + \mathrm{i}f_* = 0.$$

In Section 6.1 we provide a mathematically rigorous approximation theorem for the equation

$$-dw'' + (-\mathrm{i}\varepsilon + \zeta)w - |w|^2 w + \mathrm{i}\varepsilon f = 0 \text{ on } \mathbb{R}, \quad w'(0) = 0. \qquad (1.8)$$

We use a bifurcation approach based on the Crandall-Rabinowitz Theorem of bifurcation from a simple eigenvalue and consider $\varepsilon$ as bifurcation parameter. We provide mathematical background on the approximation formula used by Wabnitz and a first order correction term. In Section 6.2 we discuss a generalization to the two mode case.

13

In Section 7 we give an outlook on the situation of pumping more than two modes. Starting from an adapted modal expansion approach we derive a modified LLE which models the situation of $n$ distinct pumped modes. We discuss constraints which allow for traveling wave solutions and present initial investigations indicating that it is beneficial to pump as many modes as possible.

Summing up, one of the main objectives of this thesis is to present for the first time a detailed analysis of traveling waves in the dual pumping scheme based on a-priori bounds, fixed point theorems, the implicit function theorem and bifurcation theory both for anomalous and normal dispersion. The second main goal is to use numerical path continuation methods in order to demonstrate that the quality of Kerr frequency combs in resonators with anomalous dispersion can be significantly improved by pumping two modes instead of only a single one.

Appendix A contains an independent topic not related to frequency combs. Here, we study the spectrum of fractional Schrödinger operators with periodic potentials which formally read as $L = (-\Delta)^s + V(x) + \alpha\delta_{\mathrm{per}}(x_n)$. Here, $s \in (^1/_2, 1)$, $\alpha \in \mathbb{R}$, $V \in L^\infty(\mathbb{R}^n, \mathbb{R})$ is $2\pi$-periodic in $x_1, ..., x_n$ and $\delta_{\mathrm{per}}$ denotes a $2\pi$-periodic Dirac comb. In the case $\alpha = 0$ we even allow $s \in (0, 1)$. Our proceeding is motivated by the following considerations, cf. [16, Chapter 3]. The most important tool for the spectral theory of differential operators with periodic coefficients is the so-called Floquet-Bloch theory. Let

$$\mathcal{L} = \sum_{|\alpha| \leq 2} c_\alpha(x)\partial_\alpha$$

denote an uniformly elliptic and formally symmetric second order differential operator on $\mathbb{R}^n$. The (sufficiently smooth) coefficients are complex-valued and assumed to be $2\pi$-periodic in $x_1, ..., x_n$. Viewed as self-adjoint operator

$$A : H^2(\mathbb{R}^n) \subset L^2(\mathbb{R}^n) \to L^2(\mathbb{R}^n), \quad Au := \mathcal{L}u,$$

the spectrum $\sigma(A)$ can be represented in terms of the spectra of associated operators $A_k$ acting on the periodicity cell $\mathcal{P}^n := (0, 2\pi)^n$. For $k \in \mathcal{B}^n := [-^1/_2, ^1/_2]^n$ the operator $A_k$ is defined on the domain

$$D(A_k) = \left\{ u|_{\mathcal{P}^n} : u \in H^2_{\mathrm{loc}}(\mathbb{R}^n), \ u(x + 2\pi e_j) = \mathrm{e}^{2\pi \mathrm{i}k_j} u(x) \text{ for } j = 1, ..., n \right\} \subset H^2(\mathcal{P}^n)$$

by

$$A_k : D(A_k) \subset L^2(\mathcal{P}^n) \to L^2(\mathcal{P}^n), \quad A_k u := \mathcal{L}u.$$

Elements of $D(A_k)$ are said to satisfy quasiperiodic boundary conditions. Floquet-Bloch theory now gives the important connection

$$\sigma(A) = \bigcup_{k \in \mathcal{B}^n} \sigma(A_k).$$

The operators $A_k$ have purely discrete spectrum $\sigma(A_k) = \{\lambda_l(k) : l \in \mathbb{N}\}$ with real eigenvalues

$$\lambda_1(k) \leq \lambda_2(k) \leq ... \leq \lambda_l(k) \xrightarrow{l \to \infty} \infty.$$

The sets $I_l := \{\lambda_l(k) : k \in \mathcal{B}^n\}$ are compact intervals, whence $\sigma(A) = \bigcup_{l \in \mathbb{N}} I_l$ has so-called band structure. In Appendix A we generalize this result to the fractional Schrödinger operator $L = (-\Delta)^s + V(x) + \alpha \delta_{\mathrm{per}}(x_n)$. For $\alpha = 0$ this was already done in [23]. Floquet-Bloch theory does not answer the question whether gaps really occur in the spectrum or whether the bands actually overlap. Using the one-dimensional examples $L = (-\Delta)^s \pm 2\pi \delta_{\mathrm{per}}(x)$, we show the existence of at least one spectral gap in the fractional case $s \in (1/2, 1)$.

# 2. From an adapted modal expansion approach to the Lugiato-Lefever model for a dual-pumped ring resonator

In this section we derive the LLE model (1.2) for a dual-pumped ring resonator starting from an adapted modal expansion approach, cf. [62, 32]. When a resonant cavity is pumped by two continuous wave lasers with frequencies $\omega_{p_0}$ and $\omega_{p_1}$ a system of nonlinear coupled mode equations can be used to describe the evolution of the field inside the cavity. The numbering $k$ of the resonant modes in the cavity is relative to the mode $k_0 = 0$. We use the cold cavity dispersion relation $\omega_k = \omega_0 + d_1 k + d_2 k^2$ for the resonant frequencies $\omega_k$, where $d_1$ corresponds to the FSR of the resonator and $2d_2$ to the difference between two neighboring FSRs at the center frequency $\omega_0$. With $\widetilde{k}_0, \widetilde{k}_1 \in \mathbb{Z}$, $\widetilde{k}_0 < \widetilde{k}_1$, we denote the two pumped modes. If $\hat{A}_k$ is the mode amplitude of the $k$-th resonant mode normalized such that $|\hat{A}_k|^2$ is the number of quanta in the $k$-th mode, then the simplified set of equations reads as follows, cf. [62, 32]:

$$\frac{\partial \hat{A}_k}{\partial t} = -\frac{\kappa}{2}\hat{A}_k + \sum_{j=0}^{1} \delta_{k\widetilde{k}_j}\sqrt{\kappa_{\text{ext}}}\, s_j \mathrm{e}^{-\mathrm{i}(\omega_{p_j}-\omega_{\widetilde{k}_j})t}\mathrm{e}^{\mathrm{i}\phi_j}$$
$$+ \mathrm{i}g \sum_{k'+k''-k'''=k} \hat{A}_{k'}\hat{A}_{k''}\bar{\hat{A}}_{k'''}\mathrm{e}^{-\mathrm{i}(\omega_{k'}+\omega_{k''}-\omega_{k'''}-\omega_k)t}. \tag{2.1}$$

The first term on the right-hand side of equation (2.1) is a damping term, where $\kappa = \kappa_0 + \kappa_{\text{ext}}$ denotes the cavity decay rate as a sum of intrinsic decay rate $\kappa_0$ and coupling rate to the waveguide $\kappa_{\text{ext}}$. The second term describes the inflow of photons by the two input lasers. Here, $\phi_0$ and $\phi_1$ are the initial phases of the pumps. If $P_{\text{in},0}, P_{\text{in},1}$ are the powers of the two input lasers then $s_j = \sqrt{P_{\text{in},j}/\hbar\omega_{\widetilde{k}_j}}$, $j = 0, 1$ are the powers coupled to the cavity. The last term is due to four-wave mixing which happens only if $k + k''' = k' + k''$. Here, the nonlinear coupling coefficient

$$g = \frac{\hbar\omega_0^2 c n_2}{n_0^2 V_{\text{eff}}}$$

denotes a per photon frequency shift of the cavity due to the Kerr nonlinearity and thus describes the strength of the cubic nonlinearity of the system with linear refractive index $n_0$, nonlinear refractive index $n_2$ and effective cavity nonlinear volume $V_{\text{eff}}$. Finally, $c$ is the vacuum speed of light and $\hbar$ the Planck constant.

By using the transformation

$$\tilde{a}(\tau, x) := \sqrt{\frac{2g}{\kappa}} \sum_{k\in\mathbb{Z}} \hat{A}_k\left(\frac{2}{\kappa}\tau\right)\mathrm{e}^{-\mathrm{i}dk^2\tau}\mathrm{e}^{\mathrm{i}kx}$$

the system (2.1) of coupled mode equations may be rewritten in a dimensionless way as

a PDE,

$$\mathrm{i}\frac{\partial \tilde{a}}{\partial \tau} = -d\tilde{a}'' - \mathrm{i}\tilde{a} - |\tilde{a}|^2\tilde{a} + \mathrm{i}\sum_{j=0}^{1} f_j \mathrm{e}^{\mathrm{i}(\widetilde{k}_j x - \widetilde{\nu}_j \tau + \phi_j)}, \qquad \tilde{a} \ 2\pi\text{-periodic in } x, \qquad (2.2)$$

where $\tau = \kappa t/2$, $d = 2d_2/\kappa$, and $\zeta_j = 2(\omega_{\widetilde{k}_j} - \omega_{p_j})/\kappa$, $\widetilde{\nu}_j = d\widetilde{k}_j^2 - \zeta_j$, $\eta = \kappa_{\mathrm{ext}}/\kappa$, $f_j = \sqrt{8\eta g/\kappa^2}s_j$ for $j = 0,1$. To see this, first note that it can be checked that

$$|\tilde{a}(\tau,x)|^2\tilde{a}(\tau,x) = \left(\frac{2g}{\kappa}\right)^{\frac{3}{2}} \sum_{k\in\mathbb{Z}} \sum_{k'+k''-k'''=k} \hat{A}_{k'}(t)\hat{A}_{k''}(t)\bar{\hat{A}}_{k'''}(t)\mathrm{e}^{-\mathrm{i}(\omega_{k'}+\omega_{k''}-\omega_{k'''}-\omega_k+d_2k^2)t}\mathrm{e}^{\mathrm{i}kx}.$$

Equation (2.2) then follows from

$$\mathrm{i}\frac{\partial \tilde{a}}{\partial \tau}(\tau,x) = \mathrm{i}\sqrt{\frac{2g}{\kappa}}\sum_{k\in\mathbb{Z}}\left(\frac{2}{\kappa}\frac{\partial \hat{A}_k}{\partial t}(t)\mathrm{e}^{-\mathrm{i}dk^2\tau} - \mathrm{i}dk^2\hat{A}_k(t)\mathrm{e}^{-\mathrm{i}dk^2\tau}\right)\mathrm{e}^{\mathrm{i}kx}$$

$$= -d\tilde{a}''(\tau,x) + \mathrm{i}\sqrt{\frac{8g}{\kappa^3}}\sum_{k\in\mathbb{Z}}\frac{\partial \hat{A}_k}{\partial t}(t)\mathrm{e}^{-\mathrm{i}dk^2\tau}\mathrm{e}^{\mathrm{i}kx}$$

by inserting (2.1). Using the final transformation

$$a(\tau,x) := \mathrm{e}^{-\mathrm{i}(\widetilde{k}_0(x+2d\widetilde{k}_0\tau-\psi)-\widetilde{\nu}_0\tau+\phi_0)}\tilde{a}(\tau, x + 2d\widetilde{k}_0\tau - \psi) \qquad (2.3)$$

with $\psi = (\phi_1 - \phi_0)/k_1$ we find that $a$ satisfies

$$\mathrm{i}a_\tau = (\zeta - \mathrm{i})a - da'' - |a|^2 a + \mathrm{i}f_0 + \mathrm{i}f_1\mathrm{e}^{\mathrm{i}(k_1 x - \nu_1 \tau)}, \qquad a \ 2\pi\text{-periodic in } x,$$

with $k_1 = \widetilde{k}_1 - \widetilde{k}_0$, $\Delta\zeta = \zeta_0 - \zeta_1$ and $\nu_1 = \widetilde{\nu}_1 - \widetilde{\nu}_0 - 2d\widetilde{k}_0 k_1 = \Delta\zeta + dk_1^2$. Thus, we can always assume, for simplicity, that the pumped modes are $k_0 = 0$ and $k_1 \in \mathbb{N}$ and that the initial phase of both pumps is zero. Moreover we see that the change from $\tilde{a}$ to $a$ shifts the time-dependent Fourier-coefficients from $\hat{A}_k$ to $\hat{A}_{k+\widetilde{k}_0}$ and multiplies them with $\mathrm{e}^{-\mathrm{i}(\zeta_0\tau+\phi_0+k\psi)}$ so that the power in each individual mode is (up to an index shift) preserved by the transformation (2.3).

## 2. Lugiato-Lefever model for a dual-pumped ring resonator

We end this section by summarizing physical and normalized quantities in tables.

<div align="center">Physical quantities</div>

| | |
|---|---|
| Eigennumber of first pumped mode | $\widetilde{k}_0$ |
| Eigennumber of second pumped mode | $\widetilde{k}_1$ |
| Frequency of first pump | $\omega_{p_0}$ |
| Frequency of second pump | $\omega_{p_1}$ |
| FSR of resonator | $d_1$ |
| Second-order dispersion coefficient | $2d_2$ |
| Resonant modes of resonator | $\omega_k = \omega_0 + d_1 k + d_2 k^2$ |
| First pump power | $P_{\text{in},0}$ |
| Second pump power | $P_{\text{in},1}$ |
| Planck constant | $\hbar$ |
| First power coupled to cavity | $s_0 = \sqrt{\dfrac{P_{\text{in},0}}{\hbar \omega_{\widetilde{k}_0}}}$ |
| Second power coupled to cavity | $s_1 = \sqrt{\dfrac{P_{\text{in},1}}{\hbar \omega_{\widetilde{k}_1}}}$ |
| Initial phase of first pump | $\phi_0$ |
| Initial phase of second pump | $\phi_1$ |
| Intrinsic decay rate | $\kappa_0$ |
| Coupling rate to the waveguide | $\kappa_{\text{ext}}$ |
| Cavity decay rate | $\kappa = \kappa_0 + \kappa_{\text{ext}}$ |
| Coupling strength | $\eta = \dfrac{\kappa_{\text{ext}}}{\kappa}$ |
| Vacuum speed of light | $c$ |
| Linear refractive index | $n_0$ |
| Nonlinear refractive index | $n_2$ |
| Effective cavity nonlinear volume | $V_{\text{eff}}$ |
| Nonlinear coupling coefficient | $g = \dfrac{\hbar \omega_0^2 c n_2}{n_0^2 V_{\text{eff}}}$ |

## 2. Lugiato-Lefever model for a dual-pumped ring resonator

<div align="center">Normalized quantities</div>

| | |
|---|---|
| Natural time (slow time) | $\tau = \frac{\kappa}{2}t$ |
| Difference of pumped modes | $k_1 = \widetilde{k}_1 - \widetilde{k}_0$ |
| Dispersion | $d = \frac{2}{\kappa}d_2$ |
| First detuning | $\zeta_0 = \zeta = \frac{2}{\kappa}(\omega_{\widetilde{k}_0} - \omega_{p_0})$ |
| Second detuning | $\zeta_1 = \frac{2}{\kappa}(\omega_{\widetilde{k}_1} - \omega_{p_1})$ |
| Difference of detunings | $\Delta\zeta = \zeta_0 - \zeta_1$ |
| Second "detuning term" | $\nu_1 = \Delta\zeta + dk_1^2$ |
| First pump power | $f_0 = \sqrt{\frac{8\eta g}{\kappa^2}}s_0$ |
| Second pump power | $f_1 = \sqrt{\frac{8\eta g}{\kappa^2}}s_1$ |

# 3. Global continua of solutions to the Lugiato-Lefever model for frequency combs obtained by two-mode pumping

This section is based on the preprint [21], which is joint work with Tobias Jahnke, Michael Kirn and Wolfgang Reichel. Section 3.1 to Section 3.7 are taken from the preprint and were adapted in order to fit the layout and the structure of this thesis. Appendix B (Section 3.8) is not part of the preprint. It contains additional results which are of interest in comparison with results in [41].

[Start of preprint]

ELIAS GASMI, TOBIAS JAHNKE, MICHAEL KIRN, AND WOLFGANG REICHEL

ABSTRACT. We consider Kerr frequency combs in a dual-pumped microresonator as time-periodic and spatially $2\pi$-periodic traveling wave solutions of a variant of the Lugiato-Lefever equation, which is a damped, detuned and driven nonlinear Schrödinger equation given by $ia_\tau = (\zeta - i)a - da_{xx} - |a|^2 a + if_0 + if_1 e^{i(k_1 x - \nu_1 \tau)}$. The main new feature of the problem is the specific form of the source term $f_0 + f_1 e^{i(k_1 x - \nu_1 \tau)}$ which describes the simultaneously pumping of two different modes with mode indices $k_0 = 0$ and $k_1 \in \mathbb{N}$. We prove existence and uniqueness theorems for these traveling waves based on a-priori bounds and fixed point theorems. Moreover, by using the implicit function theorem and bifurcation theory, we show how non-degenerate solutions from the 1-mode case, i.e. $f_1 = 0$, can be continued into the range $f_1 \neq 0$. Our analytical findings apply both for anomalous ($d > 0$) and normal ($d < 0$) dispersion, and they are illustrated by numerical simulations.

## 3.1. Introduction

Optical frequency comb devices are extremely promising in many applications such as, e.g., optical frequency metrology [65], spectroscopy [53, 72], ultrafast optical ranging [64], and high capacity optical communications [42]. For many of these applications the Kerr soliton combs are generated by using a monochromatic pump. However, recently new pump schemes have been discussed, where more than one resonator mode is pumped, cf. [62]. The pumping of two modes can have a number of important advantages. In particular, 1-solitons arising from a dual-pump scheme can be spectrally broader and spatially more localized than 1-solitons arising from a monochromatic pump, cf. [22] for a comprehensive discussion of the theoretical advantages. Mathematically, Kerr comb dynamics are described by the Lugiato-Lefever equation (LLE), a damped, driven and detuned nonlinear Schrödinger equation [26, 39, 48]. Our analysis relies on a variant of the LLE which is modified for two-mode pumping, cf. [62] and [22] for a derivation. Using dimensionless, normalized quantities this equation takes the form

$$ia_\tau = (\zeta - i)a - da_{xx} - |a|^2 a + if_0 + if_1 e^{i(k_1 x - \nu_1 \tau)}, \qquad a \ 2\pi\text{-periodic in } x. \qquad (3.1)$$

Here, $a(\tau, x)$ represents the optical intracavity field as a function of normalized time $\tau = \frac{\kappa}{2}t$ and angular position $x \in [0, 2\pi]$ within the ring resonator. The constant $\kappa > 0$ describes the cavity decay rate and $d = \frac{2}{\kappa}d_2$ quantifies the dispersion in the system (where $\omega_k = \omega_0 + d_1 k + d_2 k^2$ is the cavity dispersion relation between the resonant frequencies $\omega_k$ and the relative indices $k \in \mathbb{Z}$). Here, the case $d < 0$ amounts to normal and the case $d > 0$ to anomalous dispersion. The resonant modes in the cavity are numbered by $k \in \mathbb{Z}$ with $k_0 = 0$ being the first and $k_1 \in \mathbb{N}$ the second pumped mode. With $f_0, f_1$ we describe the normalized power of the two input pumps and $\omega_{p_0}, \omega_{p_1}$ denote the frequencies of the two pumps. Since there are now two pumped modes there are also two normalized detuning parameters denoted by $\zeta = \frac{2}{\kappa}(\omega_0 - \omega_{p_0})$ and $\zeta_1 = \frac{2}{\kappa}(\omega_{k_1} - \omega_{p_1})$. They describe the offsets of the input pump frequencies $\omega_{p_0}$ and $\omega_{p_1}$ to the closest resonance frequency $\omega_0$ and $\omega_{k_1}$ of the microresonator. The particular form of the pump term $\mathrm{i}f_0 + \mathrm{i}f_1 \mathrm{e}^{\mathrm{i}(k_1 x - \nu_1 \tau)}$ with $\nu_1 = \zeta - \zeta_1 + dk_1^2$ suggests to change into a moving coordinate frame and to study solutions of (3.1) of the form $a(\tau, x) = u(s)$ with $s = x - \omega\tau$ and $\omega = \frac{\nu_1}{k_1}$. These traveling wave solutions propagate with speed $\omega$ in the resonator and their profiles $u$ solve the ordinary differential equation

$$-du'' + \mathrm{i}\omega u' + (\zeta - \mathrm{i})u - |u|^2 u + \mathrm{i}f_0 + \mathrm{i}f_1 \mathrm{e}^{\mathrm{i}k_1 s} = 0, \qquad u \; 2\pi\text{-periodic}. \qquad (3.2)$$

In the case $f_1 = 0$ equation (3.1) amounts to the case of pumping only one mode. This case has been thoroughly studied, e.g. in [11, 18, 25, 26, 41, 43, 48, 49, 50, 51, 59]. In this paper we are interested in the case $f_1 \neq 0$. Since the specific form of the forcing term is not essential for many of our results, we allow in the following for more general forcing terms

$$f(s) = f_0 + f_1 e(s)$$

with a $2\pi$-periodic (not necessarily continuous) function $e : \mathbb{R} \to \mathbb{C}$ and $f_0, f_1 \in \mathbb{R}$. Hence, we consider the LLE

$$-du'' + \mathrm{i}\omega u' + (\zeta - \mathrm{i})u - |u|^2 u + \mathrm{i}f(s) = 0, \qquad u \; 2\pi\text{-periodic}. \qquad (3.3)$$

Our main results on the existence of solutions to (3.3) are stated in Section 3.2. In Section 3.3 we illustrate our main analytical results by numerical simulations. The proofs of the main results are given in Section 3.4 (a-priori bounds), Section 3.5 (existence and uniqueness), and Section 3.6 (continuation results). The appendix contains a technical result and a consideration of the case where in (3.2) the value $k_1$ is not an integer but close to an integer.

## 3.2. Main results

In the following we state our main results.

- Theorem 3.1 provides existence of at least one solution of (3.3) for any choice of the parameters and any choice of $f$.

- Theorem 3.6 and Corollary 3.8 describe how trivial (constant) solutions from the

special case $f_1 = 0$ can be continued into non-trivial solutions for $f_1 \neq 0$.

- Theorem 3.9 and Corollary 3.10 show how a non-trivial solution from the case $f_1 = 0$ can be continued to $f_1 \neq 0$.

Our first theorem, which ensures the existence of a solution of (3.3) in the general case where $f_1$ does not need to vanish, is based on a-priori bounds and a variant of Schauder's fixed point theorem known as Schaefer's fixed point theorem. A corresponding uniqueness result, which applies whenever $|\zeta| \gg 1$ is sufficiently large or (essentially) $\|f\|_2 \ll 1$ is sufficiently small is given in Theorem 3.17 in Section 3.5 together with more precise details.

We will use the following Sobolev spaces. For $k \in \mathbb{N}$ the space $H^k(0, 2\pi)$ consists of all square-integrable functions on $(0, 2\pi)$ whose weak derivatives up to order $k$ exist and are square-integrable on $(0, 2\pi)$. By $H^k_{\mathrm{per}}(0, 2\pi)$ we denote all locally square-integrable $2\pi$-periodic functions on $\mathbb{R}$ whose weak derivatives up to order $k$ exist and are locally square-integrable on $\mathbb{R}$. In both spaces the norm is given by $\|u\| = \left(\sum_{j=0}^k \|(\frac{d}{ds})^j u\|^2_{L^2(0,2\pi)}\right)^{1/2}$. Clearly $H^k_{\mathrm{per}}(0, 2\pi)$ is a proper subspace of $H^k(0, 2\pi)$ since $u \in H^k_{\mathrm{per}}(0, 2\pi)$ implies that $(\frac{d}{ds})^j u(0) = (\frac{d}{ds})^j u(2\pi)$ for $j = 0, \dots, k-1$. Unless otherwise stated, all of the above Hilbert spaces are spaces of complex valued functions over the field $\mathbb{R}$. In particular, for $v, w \in L^2(0, 2\pi)$ we use the inner product $\langle v, w \rangle_2 := \mathrm{Re} \int_0^{2\pi} v\overline{w} \, ds$. The induced norm is denoted by $\| \cdot \|_2$.

**Theorem 3.1.** *Equation* (3.3) *has at least one solution* $u \in H^2_{per}(0, 2\pi)$ *for any choice of the parameters* $d \in \mathbb{R} \setminus \{0\}$, $\zeta, \omega \in \mathbb{R}$ *and any choice of* $f \in H^2(0, 2\pi)$.

Next we address the question whether a known solution $u_0$ of (3.3) for $f_1 = 0$ can be continued into the regime $f_1 \neq 0$. This continuation will be done differently depending on whether $u_0$ is constant (trivial) or non-constant (non-trivial). Moreover, we first concentrate on one-sided continuations for $f_1 > 0$ (or $f_1 < 0$). Two-sided continuations will be discussed in Section 3.2.3.

### 3.2.1. One-sided continuation of trivial solutions

In the special case $f_1 = 0$ there are trivial (constant) solutions $u_0 \in \mathbb{C}$ of (3.3) satisfying the algebraic equation

$$(\zeta - \mathrm{i})u_0 - |u_0|^2 u_0 + \mathrm{i}f_0 = 0. \tag{3.4}$$

From [41, Lemma 2.1] we know that for given $f_0 \in \mathbb{R}$ the curve of constant solutions can be parameterized by

$$\zeta(t) = (1 - t^2)f_0^2 + \frac{t}{\sqrt{1 - t^2}}, \quad u_0(t) = (1 - t^2)f_0 - \mathrm{i}f_0 t\sqrt{1 - t^2}, \quad t \in (-1, 1). \tag{3.5}$$

In Figure 6 we show the curve of the squared $L^2$-norm of all constant solutions of (3.3) for $f_1 = 0$ and $f_0 = 1$, $f_0 = \frac{2\sqrt{2}}{\sqrt[4]{27}}$ and $f_0 = 2$. The curve may or may not have turning points which are characterized by $\zeta'(t) = 0$. This condition can be formulated independently of

$t$ by the equivalent condition $\zeta^2 - 4|u_0|^2\zeta + 1 + 3|u_0|^4 = 0$. By a straightforward analysis one can show that with $f^* = \frac{2\sqrt{2}}{\sqrt[4]{27}}$ we have

- no turning point for $|f_0| < f^*$ (cf. Figure 6 green curve),

- exactly one (degenerate) turning point for $|f_0| = f^*$ (cf. Figure 6 red curve),

- exactly two turning points for $|f_0| > f^*$ (cf. Figure 6 blue curve).

Note that for $|f_0| > f^*$, as a consequence of the existence of two turning points, three different constant solutions exist for certain values of $\zeta$.

Starting from $f_1 = 0$ we use a kind of global implicit function theorem to continue a constant solution $u_0 \in \mathbb{C}$ of (3.3) with respect to $f_1$. This procedure is analyzed in Theorem 3.6. The continuation works if the constant solution $u_0 \in \mathbb{C}$ is non-degenerate in the following sense.



Figure 6. Curve of squared $L^2$-norm of all constant solutions of (3.3) for $f_1 = 0$ and $f_0 = 1$ (green), $f_0 = \frac{2\sqrt{2}}{\sqrt[4]{27}}$ (red) and $f_0 = 2$ (blue) when $\zeta \in [-1, 5]$. Turning points (if they exist) are marked with a cross.

**Definition 3.2.** A solution $u \in H^2_{\text{per}}(0, 2\pi)$ of (3.3) for $f_1 = 0$ is called non-degenerate if the kernel of the linearized operator

$$L_u\varphi := -d\varphi'' + \mathrm{i}\omega\varphi' + (\zeta - \mathrm{i} - 2|u|^2)\varphi - u^2\overline{\varphi}, \quad \varphi \in H^2_{\text{per}}(0, 2\pi)$$

consists only of span$\{u'\}$.

**Remark 3.3.** Note that $L_u : H^2_{\text{per}}(0, 2\pi) \to L^2(0, 2\pi)$ is a compact perturbation of the isomorphism $-d\frac{d^2}{dx^2} + \text{sign}(d) : H^2_{\text{per}}(0, 2\pi) \to L^2(0, 2\pi)$ and hence an index-zero Fredholm operator. Notice also that span$\{u'\}$ always belongs to the kernel of $L_u$. Non-degeneracy means that except for the obvious candidate $u'$ (and its real multiples) there is no other element of the kernel of $L_u$. Notice also that a constant solution $u_0$ is non-degenerate if the linearized operator $L_{u_0}$ is injective, and, as a consequence, invertible in suitable spaces.

**Lemma 3.4.** *A trivial solution $u_0 \in \mathbb{C}$ of (3.3) for $f_1 = 0$ is non-degenerate if and only if*

(a) *Case $\omega \neq 0$:*
$$\zeta^2 - 4|u_0|^2\zeta + 1 + 3|u_0|^4 \neq 0.$$

*(b) Case $\omega = 0$:*

$$(\zeta + dm^2)^2 - 4|u_0|^2(\zeta + dm^2) + 1 + 3|u_0|^4 \neq 0 \quad \text{for all } m \in \mathbb{N}_0.$$

*Proof.* Let $\varphi \in H^2_{\text{per}}(0, 2\pi)$ be in the kernel of the linearized operator, i.e.,

$$-d\varphi'' + \mathrm{i}\omega\varphi' + (\zeta - \mathrm{i} - 2|u_0|^2)\varphi - u_0^2\overline{\varphi} = 0.$$

This implies that the Fourier coefficients $\varphi_m$ of the Fourier series $\varphi = \sum_{m\in\mathbb{Z}} \varphi_m \mathrm{e}^{\mathrm{i}ms}$ have the property that

$$(dm^2 - \omega m + \zeta - \mathrm{i} - 2|u_0|^2)\varphi_m - u_0^2\overline{\varphi_{-m}} = 0$$

for all $m \in \mathbb{Z}$. If we also write down the complex conjugate of this equation

$$-\overline{u_0}^2\varphi_m + (dm^2 + \omega m + \zeta + \mathrm{i} - 2|u_0|^2)\overline{\varphi_{-m}} = 0$$

then we see that non-degeneracy of $u_0$ is equivalent to the non-vanishing of the determinant for this two-by-two system in the variables $\varphi_m, \overline{\varphi_{-m}}$ for all $m \in \mathbb{N}_0$. Computing the determinant we obtain the condition

$$(\zeta + dm^2)^2 - 4|u_0|^2(\zeta + dm^2) + 1 + 3|u_0|^4 - \omega^2 m^2 - 2\mathrm{i}\omega m \neq 0 \text{ for all } m \in \mathbb{N}_0. \quad (3.6)$$

In the case $\omega \neq 0$ this is trivially satisfied for all $m \neq 0$ (because then the imaginary part is non-zero) and for $m = 0$ by assumption (a) of the lemma. In the case $\omega = 0$ condition (3.6) can only be guaranteed by assumption (b). $\qquad\square$

**Remark 3.5.** Trivial solutions of (3.3) for $f_1 = 0$ are determined by (3.4). For $\omega \neq 0$ all trivial solutions $u_0$ of (3.3) for $f_1 = 0$ are non-degenerate except those at the turning points described above. In the case $\omega = 0$ all trivial solutions $u_0$ of (3.3) for $f_1 = 0$ are non-degenerate except those at the (potential) bifurcation points and the turning points. This is true (up to additional conditions ensuring transversality and simplicity of kernels) because the necessary condition for bifurcation w.r.t. $\zeta$ from the curve of trivial solutions is fulfilled if and only if the expression in (b) vanishes for at least one $m \in \mathbb{N}$, cf. [18],[41].

**Theorem 3.6.** *Let $d \in \mathbb{R} \setminus \{0\}$, $\zeta, \omega, f_0 \in \mathbb{R}$ and $e \in H^2(0, 2\pi)$ be fixed. Let furthermore $u_0 \in \mathbb{C}$ be a constant non-degenerate solution of (3.3) for $f_1 = 0$. Then the maximal continuum[1] $\mathcal{C}^+ \subset [0, \infty) \times H^2_{per}(0, 2\pi)$ of solutions $(f_1, u)$ of (3.3) with $(0, u_0) \in \mathcal{C}^+$ has the following properties:*

*(i) locally near $(0, u_0)$ the set $\mathcal{C}^+$ is the graph of a smooth curve $f_1 \mapsto (f_1, u(f_1))$,*

*(ii) $\mathcal{C}^+ \cap [0, M] \times H^2_{per}(0, 2\pi)$ is bounded for any $M > 0$.*

---

[1]A continuum is a closed and connected set.

*Moreover, if* $\mathrm{pr}_1(\mathcal{C}^+)$ *denotes the projection of* $\mathcal{C}^+$ *onto the* $f_1$*-parameter component, then at least one of the following properties hold:*

*(a)* $\mathrm{pr}_1(\mathcal{C}^+) = [0, \infty),$

*or*

*(b)* $\exists u_0^+ \neq u_0 : (0, u_0^+) \in \mathcal{C}^+.$

*A maximal continuum* $\mathcal{C}^- \subset (-\infty, 0] \times H_{per}^2(0, 2\pi)$ *with corresponding properties also exists.*

**Remark 3.7.** If property (a) of Theorem 3.6 holds, then $\mathcal{C}^+$ is unbounded in the direction of the parameter $f_1 \in [0, \infty)$ and hence this is an existence result for all $f_1 \in [0, \infty)$. Property (b) means that the continuum $\mathcal{C}^+$ returns to the $f_1 = 0$ line at a point $u_0^+ \neq u_0$.

**Corollary 3.8.** *Property (a) in Theorem 3.6 holds in any of the following three cases,*

*(i)* $\mathrm{sign}(d)\zeta < -C(d, f_0)^2 \mathbf{1}_{d<0} - 27\left(1 + \dfrac{\pi f_0^2 |\omega|}{|d|} + \dfrac{\pi^2 f_0^4}{|d|}\right)C(d, f_0)^6,$

*(ii)* $\mathrm{sign}(d)\zeta > 3C(d, f_0)^2 + \dfrac{\omega^2}{4|d|},$

*(iii)* $\sqrt{3}C(d, f_0) < 1,$

*where*

$$C(d, f_0) = |f_0|(1 + 2\pi^2 f_0^2 |d|^{-1}).$$

*In particular* $|\zeta| \gg 1$ *or* $|f_0| \ll 1$ *is sufficient.*

### 3.2.2. One-sided continuation of non-trivial solutions

One can ask the question whether also non-trivial (non-constant) solutions at $f_1 = 0$ may be continued into the regime of $f_1 > 0$. This depends on two issues: existence and non-degeneracy of a non-trivial solution of (3.3) for $f_1 = 0$. First we note that for $\omega = 0$ there is a plethora of non-trivial solutions, cf. [18],[41]. For $\omega \neq 0$ we do not know whether non-trivial solutions exist for $f_1 = 0$. The fact that for $\omega \neq 0$ there are no bifurcations from the curve of trivial solutions indicates that there may be no solutions other than the trivial ones. Although by the current state of understanding the hypotheses of Theorem 3.9 (see below) can only be fulfilled for $\omega = 0$, we allow in the following for general $\omega \in \mathbb{R}$.

In order to describe the continuation from a non-degenerate non-trivial solution, let us first state some properties of (3.3) for $f_1 = 0$: if $u_0$ solves (3.3) for $f_1 = 0$ and if we denote its shifts by $u_\sigma(s) := u_0(s - \sigma)$, then $u_\sigma$ also solves (3.3) for $f_1 = 0$. Hence

$$S : \begin{cases} \mathbb{R} & \to & \mathbb{R} \times H_{\mathrm{per}}^2(0, 2\pi), \\ \sigma & \mapsto & (0, u_\sigma) \end{cases}$$

describes a trivial curve of solutions of (3.3) from which we wish to bifurcate at some point $(0, u_{\sigma_0})$. Recall also from non-degeneracy that $\ker L_{u_\sigma} = \operatorname{span}\{u_\sigma'\}$. Since $L_{u_\sigma}^*$ also has a one-dimensional kernel, there exists $\phi_\sigma^* \in H^2_{\mathrm{per}}(0, 2\pi)$ such that $\ker L_{u_\sigma}^* = \operatorname{span}\{\phi_\sigma^*\}$. Notice that $\phi_\sigma^*(s) = \phi_0^*(s - \sigma)$. Finally, $\sigma_0$ will be determined in such a way that there exists a unique solution $\xi_{\sigma_0} \in H^2_{\mathrm{per}}(0, 2\pi)$ of

$$L_{u_0}\xi_{\sigma_0} = -\mathrm{i}e(\cdot + \sigma_0)$$

with the property that $\xi_{\sigma_0} \perp_{L^2} u_0'$. Details of the construction of $\sigma_0$ and $\xi_{\sigma_0}$ will be given in Lemma 3.21.

**Theorem 3.9.** *Let $d \in \mathbb{R} \setminus \{0\}$, $\zeta, \omega, f_0 \in \mathbb{R}$ and $e \in H^2(0, 2\pi)$ be fixed. Let furthermore $u_0 \in H^2_{per}(0, 2\pi)$ be a non-trivial non-degenerate solution of (3.3) for $f_1 = 0$. If $\sigma_0 \in \mathbb{R}$ satisfies*

$$\operatorname{Im} \int_0^{2\pi} e(s + \sigma_0)\overline{\phi_0^*(s)}\, ds = 0 \tag{3.7}$$

*and*

$$\operatorname{Im} \int_0^{2\pi} e'(s + \sigma_0)\overline{\phi_0^*(s)}\, ds \neq 0 \tag{3.8}$$

*then the maximal continuum $\mathcal{C}^+ \subset [0, \infty) \times H^2_{per}(0, 2\pi)$ of solutions $(f_1, u)$ of (3.3) with $(0, u_0) \in \mathcal{C}^+$ has the following properties:*

(i) *there exists a smooth curve $C : [0, \delta) \to \mathcal{C}^+$ with $C(t) = (f_1(t), u(t))$, $\dot{f}_1(0) = 1$, $C(0) = (0, u_{\sigma_0})$ such that locally near $(0, u_{\sigma_0})$ all solutions $(f_1, u)$ of (3.3) with $f_1 \geq 0$ lie on the curve $S$ or on the curve $C$,*

(ii) *$\mathcal{C}^+ \cap [0, M] \times H^2_{per}(0, 2\pi)$ is bounded for any $M > 0$.*

*Moreover, if zero is an algebraically simple eigenvalue of $L_{u_0}$ and if furthermore*

$$2\operatorname{Re} \int_0^{2\pi} \left(2u_0|\xi_{\sigma_0}|^2 + \overline{u_0}\xi_{\sigma_0}^2\right)\overline{\phi_0^*}\, ds \operatorname{Re} \int_0^{2\pi} \left(u_0'\overline{u_0} + 2u_0\overline{u_0'}\right)u_0'\overline{\phi_0^*}\, ds$$

$$\neq \left(\operatorname{Im} \int_0^{2\pi} e'(s + \sigma_0)\overline{\phi_0^*(s)}\, ds\right)^2, \tag{3.9}$$

*then there exists a connected set $\mathcal{C}_*^+ \subset \mathcal{C}^+$ with $\operatorname{pr}_1(\mathcal{C}_*^+) \subset (0, \infty)$ and $(0, u_{\sigma_0}) \in \overline{\mathcal{C}_*^+}$ which satisfies at least one of the following properties:*

(a) *$\operatorname{pr}_1(\mathcal{C}_*^+) = (0, \infty)$,*

*or*

(b) *$\exists u_0^+ \neq u_{\sigma_0} : (0, u_0^+) \in \overline{\mathcal{C}_*^+}$.*

*A maximal continuum $\mathcal{C}^- \subset (-\infty, 0] \times H^2_{per}(0, 2\pi)$ with corresponding properties also exists.*

For the special choice $e(s) = \mathrm{e}^{\mathrm{i}k_1 s}$ Theorem 3.9 takes the following form.

**Corollary 3.10.** *Let $k_1 \in \mathbb{N}$, $e(s) = \mathrm{e}^{\mathrm{i}k_1 s}$ and $d, \zeta, \omega, f_0, u_0$ be as in Theorem 3.9. Assume that*

$$\int_0^{2\pi} \mathrm{e}^{\mathrm{i}k_1 s} \overline{\phi_0^*(s)} \, ds \neq 0 \tag{3.10}$$

*and that $\sigma_0 \in \mathbb{R}$ satisfies*

$$\tan(k_1 \sigma_0) = \frac{\int_0^{2\pi} \cos(k_1 s) \operatorname{Im} \phi_0^*(s) - \sin(k_1 s) \operatorname{Re} \phi_0^*(s) \, ds}{\int_0^{2\pi} \sin(k_1 s) \operatorname{Im} \phi_0^*(s) + \cos(k_1 s) \operatorname{Re} \phi_0^*(s) \, ds}. \tag{3.11}$$

*Then the conditions (3.7) and (3.8) of Theorem 3.9 hold.*

**Remark 3.11.** ($\alpha$) It follows from the implicit function theorem that in the setting of Theorem 3.9 assumption (3.7) is a necessary condition for bifurcation (non-trivial kernel of the linearization). Assumption (3.8) amounts to the transversality condition. In the setting of Corollary 3.10 this means that, if (3.10) is satisfied, assumption (3.11) is a necessary condition for bifurcation.
($\beta$) Assumption (3.10) in Corollary 3.10 guarantees that the numerator and the denominator of the right-hand side of (3.11) do not vanish simultaneously. In the case where the denominator vanishes, Equation (3.11) is to be read as $\cos(k_1 \sigma_0) = 0$. In the interval $[0, \frac{\pi}{k_1})$ equation (3.11) has a unique solution $\sigma_0 \in [0, \frac{\pi}{k_1})$. All solutions of (3.11) in $[0, 2\pi)$ are then given by $\sigma_0 + j \frac{\pi}{k_1}$ for $j = 0, \ldots, 2k_1 - 1$. This can result in up to $2k_1$ bifurcation points. Smaller periodicities of $u_0$ may reduce the actual number of different bifurcation points. E.g., if $k_1 \geq 2$ and if $u_0$ has smallest period $\frac{2\pi}{k_1}$ then only two bifurcation points exist.
($\gamma$) Let $j \in \mathbb{N}$ not be a divisor of $k_1$ and $u_0$ be $\frac{2\pi}{j}$-periodic. Then assumption (3.10) is not satisfied since $\phi_0^*$ inherits the periodicity of $u_0$. We will say more about this case in the Appendix.
($\delta$) The non-trivial solutions $u_0$ of (3.3) for $f_1 = 0$ and $\omega = 0$ constructed in [18],[41] are even around $s = 0$. In this case, (3.9) is not an additional assumption because it coincides with assumption (3.8). The reason is that $\phi_0^*$ (spanning $\ker L_{u_0}^*$) inherits the parity of $u_0'$ (spanning $\ker L_{u_0}$) which implies $\int_0^{2\pi} \left( u_0' \overline{u_0} + 2u_0 \overline{u_0'} \right) u_0' \overline{\phi_0^*} \, ds = 0$, cf. Proposition 3.22. Also, the value of $\sigma_0$ in Corollary 3.10 is determined by the simpler expression

$$\tan(k_1 \sigma_0) = -\frac{\int_0^{2\pi} \sin(k_1 s) \operatorname{Re} \phi_0^*(s) \, ds}{\int_0^{2\pi} \sin(k_1 s) \operatorname{Im} \phi_0^*(s) \, ds}.$$

It is an open problem if (3.3) admits solutions for $f_1 = 0$ and $\omega = 0$ which (up to a shift) are not even around $s = 0$.
($\epsilon$) Note that in property (b) we exclude that $u_0^+ = u_{\sigma_0}$ but we do not exclude that $u_0^+$ coincides with a shift of $u_0$ different from $u_{\sigma_0}$.

### 3.2.3. Two-sided continuations

Here we explain how we can use the results of Theorem 3.6 and Theorem 3.9, Corollary 3.10 for the continua $\mathcal{C}^+$ and $\mathcal{C}^-$ in order to obtain two-sided continua w.r.t. the parameter component $f_1$.

As a first trivial observation we can construct a two-sided continuum in the following way both for the setting of Theorem 3.6 and Theorem 3.9: let $\mathcal{C} \subset \mathbb{R} \times H^2_{\mathrm{per}}(0, 2\pi)$ be the maximal continuum of solutions $(f_1, u)$ of (3.3) with $(0, u_0) \in \mathcal{C}$. Then $\mathcal{C}$ contains both $\mathcal{C}^+$ and $\mathcal{C}^-$.

Next we assume that the generalized forcing term $f(s) = f_0 + f_1 e(s)$ satisfies the symmetry condition that $e\big(s + \frac{\pi}{k_1}\big) = -e(s)$ for some $k_1 \in \mathbb{N}$. This symmetry condition is motivated by (3.2) where $e(s) = \mathrm{e}^{\mathrm{i}k_1 s}$. If we denote by $R$ the reflection operator which acts on solution pairs and is given by

$$R : (f_1, u) \mapsto \big(-f_1, u\big(\cdot + \tfrac{\pi}{k_1}\big)\big)$$

then, again both for the setting of Theorem 3.6 and Theorem 3.9, the continuum $\mathcal{C}$ has the following property:
$$(f_1, u) \in \mathcal{C} \Leftrightarrow R(f_1, u) \in \mathcal{C}.$$

This shows that globally the solution sets for positive and negative $f_1$ only differ by a phase shift. The following global structure result is a consequence of this symmetry.

**Proposition 3.12.** *Let $d \in \mathbb{R} \setminus \{0\}$, $\zeta, \omega, f_0 \in \mathbb{R}$ and $e \in H^2(0, 2\pi)$ be such that $e\big(s + \frac{\pi}{k_1}\big) = -e(s)$ for some $k_1 \in \mathbb{N}$. Let furthermore $u_0$ be a solution of (3.3) for $f_1 = 0$. Then the maximal continua $\mathcal{C}^+$, $\mathcal{C}^-$ and $\mathcal{C}$ containing $(0, u_0)$ satisfy $\mathcal{C}^- = R(\mathcal{C}^+)$ and $\mathcal{C} \supset \mathcal{C}^+ \cup \mathcal{C}^-$.*

*Proof.* It is obvious that $\mathcal{C} \supset \mathcal{C}^+ \cup \mathcal{C}^-$. Now we prove that $\mathcal{C}^- = R(\mathcal{C}^+)$. Clearly, $\mathcal{C}^+$ and $R(\mathcal{C}^+)$ contain all shifts $\{(0, u_\sigma) : \sigma \in \mathbb{R}\}$. Since additionally $R(\mathcal{C}^+) \subset (-\infty, 0] \times H^2_{\mathrm{per}}(0, 2\pi)$ is connected we find that $R(\mathcal{C}^+) \subset \mathcal{C}^-$. If we assume that $R(\mathcal{C}^+) \subsetneq \mathcal{C}^-$ then we obtain $\mathcal{C}^+ \subsetneq R^{-1}(\mathcal{C}^-)$, which contradicts the maximality of $\mathcal{C}^+$. $\qquad\square$

As another consequence, we have that either $\mathrm{pr}_1(\mathcal{C}) = (-\infty, \infty)$ or $\mathrm{pr}_1(\mathcal{C})$ is bounded from above and below. In the latter case, we call $\mathcal{C}$ a loop.

Our final result builds upon Theorem 3.6 and the resulting two-sided continuation of a trivial solution $u_0$. It describes the shape of the $L^2$-projection of the continuum $\mathcal{C}$ locally near $(0, u_0)$. In particular, local convexity or concavity can be read from this result. In Section 3.3 we will put this result into perspective with numerical simulations of the $f_1$-continuation of trivial solutions.

**Theorem 3.13.** *Assume that the assumptions of Theorem 3.6 are satisfied and that additionally $e(s) = \mathrm{e}^{\mathrm{i}k_1 s}$ is fixed for a $k_1 \in \mathbb{N}$. Then we can determine the local shape of the curve $f_1 \mapsto \|u(f_1)\|_2^2$ as follows:*

$$\frac{d}{df_1}\|u(f_1)\|_2^2 \,|_{f_1=0} = 0, \qquad \frac{d^2}{df_1^2}\|u(f_1)\|_2^2 \,|_{f_1=0} = 4\pi(\mathrm{Re}(u_0\bar{\epsilon}) + |\alpha|^2 + |\beta|^2)$$

*with*

$$\alpha = \frac{-\mathrm{i}(dk_1^2 + k_1\omega + \zeta + \mathrm{i} - 2|u_0|^2)}{(\zeta + dk_1^2 - 2|u_0|^2)^2 - (\omega k_1 + \mathrm{i})^2 - |u_0|^4},$$

$$\beta = \frac{\mathrm{i}u_0^2}{(\zeta + dk_1^2 - 2|u_0|^2)^2 - (\omega k_1 - \mathrm{i})^2 - |u_0|^4},$$

$$x = \zeta - \mathrm{i} - 2|u_0|^2,$$

$$y = -u_0^2,$$

$$z = 4u_0(|\alpha|^2 + |\beta|^2) + 4\overline{u_0}\alpha\beta,$$

$$\epsilon = \frac{-\overline{z}y + z\overline{x}}{|x|^2 - |y|^2}.$$

## 3.3. Numerical illustration of the analytical results

In this section we restrict ourselves to equation (3.2), i.e., we fix $e(s) = \mathrm{e}^{\mathrm{i}k_1 s}$. For this choice, we know from Section 3.2.3 that the one-sided continua $\mathcal{C}^+$ and $\mathcal{C}^-$ are related by $\mathcal{C}^- = R(\mathcal{C}^+)$. The following numerical examples were computed with $d = -0.1$, $f_0 = 2$, $k_1 = 1$, and $\omega = 1$.
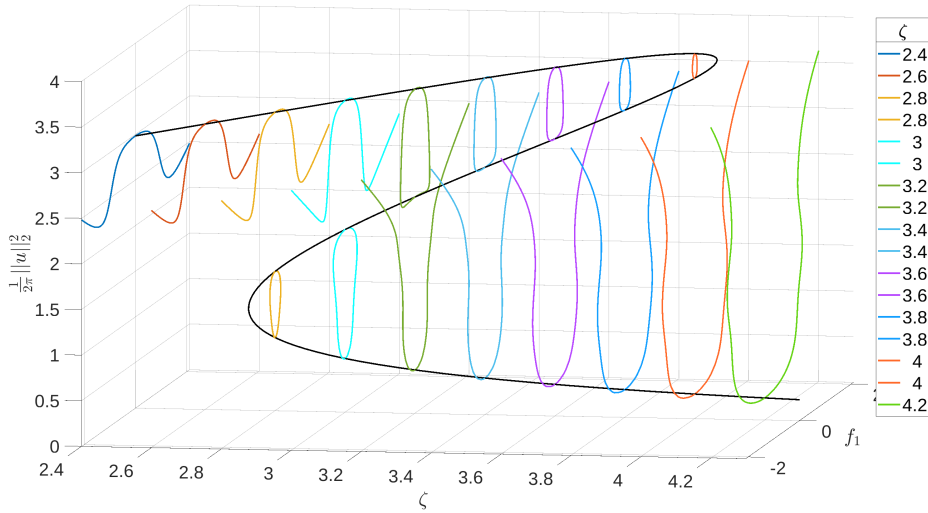


Figure 7. Continua of solutions $(f_1, u)$ of (3.2) for selected values of the detuning $\zeta$. The other parameters were set to $d = -0.1$, $f_0 = 2$, $k_1 = 1$, and $\omega = 1$.

Figure 7 illustrates some of the two-sided continua $\mathcal{C}^+ \cup \mathcal{C}^-$ obtained by continuation of trivial solutions for different values of the detuning $\zeta$. Every point on the black and colored curves corresponds to a solution $u$ of (3.2), but for the sake of visualization in a three-dimensional image every solution has to be represented by a single number. In Figure 7, the quantity $\frac{1}{2\pi}\|u\|_2^2$ was used for this purpose.

The black curve corresponds to spatially constant solutions of (3.2) obtained for $f_1 = 0$ and $\zeta \in [2.4, 4.3]$. The colored curves represent (parts of) the continua associated to

these solutions. Every trivial solution (possibly except the ones at turning points) has an associated continuum, but for the sake of visualization these continua are only shown for selected values of $\zeta$, namely $\zeta \in \{2.4, 2.6, \ldots, 4.0, 4.2\}$. The picture is symmetric with symmetry plane $\{(\zeta, 0, z) \colon \zeta \in \mathbb{R}, z \in \mathbb{R}\}$. This is an immediate consequence of the relation $\mathcal{C}^- = R(\mathcal{C}^+)$ and the fact that shifting $u$ does not change $\|u\|_2$.

For $\zeta \in \{2.4, 2.6, 4.2\}$ there is only one trivial solution, and for these three values Figure 7 shows a part of the associated two-sided continuum $\mathcal{C}^+ \cup \mathcal{C}^-$. Although $f_1$ was restricted to $[-2, 2]$, each of these continua appears to be global in $f_1$, i.e. we conjecture that the continua continue for *all* values $f_1 \in (-\infty, \infty)$. This corresponds to case (a) in Theorem 3.6.

For $\zeta \in \{2.8, 3.0, \ldots, 4.0\}$, however, there are three trivial solutions. For these values of $\zeta$, there is one colored loop which connects two solutions, and one continuum which seems to continue for all values of $f_1$. The former corresponds to case (b) in Theorem 3.6, the latter to case (a). For $\zeta \in \{2.8, 3.0\}$ the "lower" two solutions are connected, whereas for $\zeta \in \{3.2, \ldots, 4.0\}$ it is the "upper" two solutions which are connected. Hence, there seems to be a threshold value $\zeta^*$ that determines which of the two scenarios occurs. Computations with more values of $\zeta$ show that this threshold value $\zeta^*$ lies between 3.1344 and 3.1359; cf. Figure 8. The union of the continua for $\zeta$-values close to the threshold $\zeta^*$ (i.e. for $\zeta = 3.1344$ and $\zeta = 3.1359$) is nearly the same, and the two continua nearly meet in two points.[2] The mathematical mechanisms which cause this qualitative change are not yet understood. One could expect that the connectivity threshold coincides with the value where the square of the $L^2$-norm of the solutions as a function of $f_1$ changes from being locally convex to locally concave. However, Theorem 3.13 shows that this is *not* true.

Figure 9 illustrates the same application, but depicted from a different angle and with more values of $\zeta$. Repeating the simulation with $d = 0.1$ (anomalous dispersion) instead of $d = -0.1$ (normal dispersion) did not change the picture essentially.

Figures 7, 8, and 9 were generated by discretizing (3.2) with central finite differences (1000 grid points), and by applying the classical continuation method as described in, e.g., [1], to the discretized system.

The result of Theorem 3.13 can be interpreted as follows: each point on the trivial curve is a local extremum of the squared $L^2$-norm of the solution curve $f_1 \mapsto u(f_1)$. The type of local extremum is described by the sign of the second derivative $\frac{d^2}{df_1^2}\|u(f_1)\|_2^2\,|_{f_1=0}$. We visualize this by an example for $d = -0.1$, $f_0 = 2$, $k_1 = 1$, $\omega = 1$. By using the parameterization $t \mapsto \zeta(t), t \mapsto u_0(t)$ for $t \in (-1, 1)$ from (3.5) we can illustrate the sign-changes of the second derivative. In Figure 10 we are plotting the curve $t \mapsto (\zeta(t), |u_0(t)|^2)$ and indicate at each point on the curve the sign of $4\pi(\mathrm{Re}(u_0(t)\bar{\epsilon}(t)) + |\alpha(t)|^2 + |\beta(t)|^2)$, where $\epsilon(t), \alpha(t), \beta(t)$ are taken from Theorem 3.13 with $\zeta = \zeta(t)$ and $u_0 = u_0(t)$. In this particular example, as we run through the curve of trivial solutions

---

[2]As mentioned earlier, only the $L^2$-norm of solutions can be visualized in Figure 7, 8 and all other plots. The fact that two functions have (nearly) the same norm does, of course, not imply that the functions themselves are (nearly) identical. It can be checked, however, that the two solutions which correspond to the two points where the distance between the two continua is minimal are indeed very similar (data not shown).
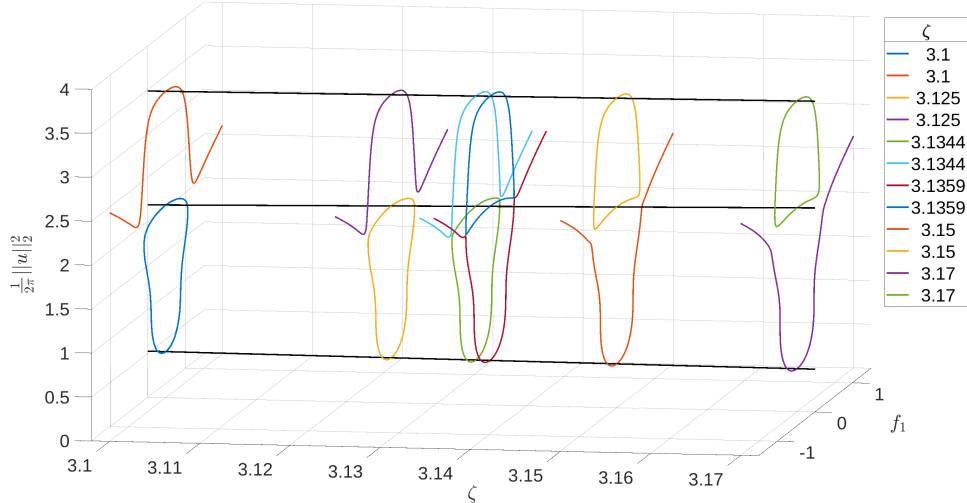
Figure 8. Same situation as in Figure 7. Zoom to the region close to the threshold where the continua change connectivity.

from left to right a first sign-change of $\frac{d^2}{df_1^2}\|u(f_1)\|_2^2\,|_{f_1=0}$ occurs at $\zeta \approx 0.8533$.

A second sign-change (in fact a singularity changing from $-\infty$ to $+\infty$) occurs at the first turning point. Then, the next sign-change occurs on the part of the branch between the two turning points at $\zeta \approx 3.34$. Finally, the second turning point generates the last sign-change from $-\infty$ to $+\infty$. Clearly, the changes in the nature of the local extremum of $f_1 \mapsto \|u(f_1)\|_2^2$ at $f_1 = 0$ do not correspond to the topology changes of the solution continua which occur near the threshold value $\zeta^* \in (3.1344, 3.1359)$.
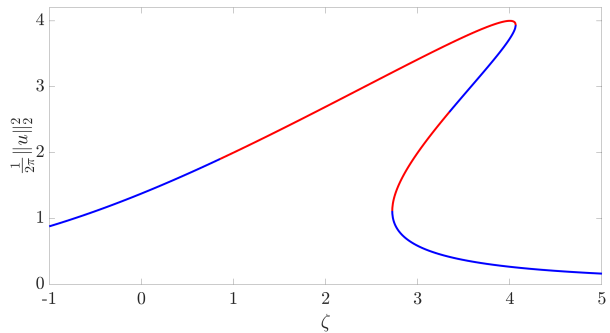


Figure 10. Sign of the second derivative of $f_1 \mapsto \|u(f_1)\|_2^2$ at $f_1 = 0$; blue=positive, red=negative.

Next, we keep the parameters $d = -0.1$, $f_0 = 2$, $k_1 = 1$ but choose $\omega = 0$ instead of $\omega = 1$. Recall that for $\omega = 0$ there is a plethora of non-trivial solutions of (3.2) for $f_1 = 0$, cf. [18],[41]. In fact, this time we find additional primary and secondary bifurcation branches for $f_1 = 0$ which are illustrated in Figure 11 in grey and brown, respectively. Bifurcation points are shown as grey dots. The bifurcation branches consist of non-trivial solutions. Further, some numerical approximations of the two-sided maximal continua $\mathcal{C}$ obtained by continuation of trivial or non-trivial solutions for different values of the detuning $\zeta$ are shown. If we start from a constant solution at $f_1 = 0$, then $\mathcal{C}^\pm$ are described by Theorem 3.6. Likewise, if we start from a non-constant solution at $f_1 = 0$ which has no smaller period than $2\pi$, then $\mathcal{C}^\pm$ are described by Theorem 3.9. In

32
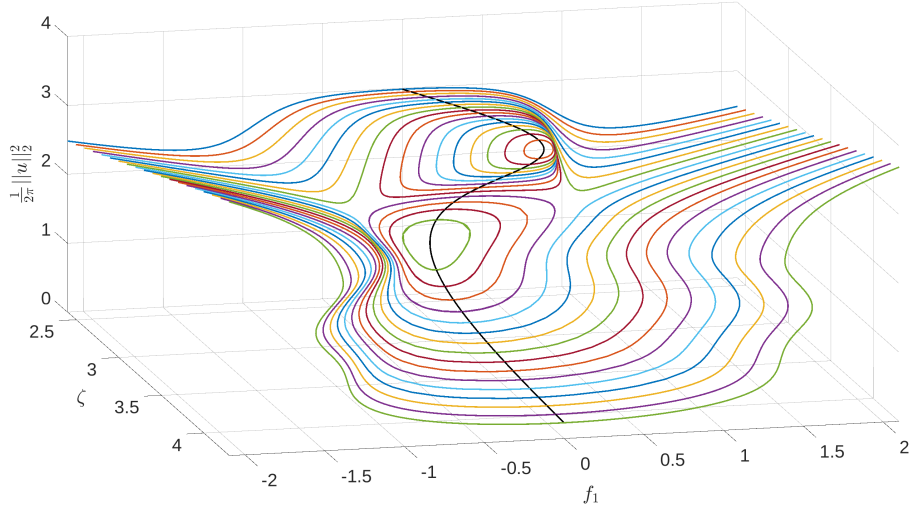
Figure 9. Same situation as in Figure 7, but depicted from a different angle and with more values of $\zeta$.

both cases, $\mathcal{C} \supset \mathcal{C}^+ \cup \mathcal{C}^-$ by Proposition 3.12, but in all examples below we observe in fact equality. If we expect a maximal continuum to contain two or more (non-trivial) different simple closed curves, then we illustrate the latter ones with different colors. Let us look at some particular values of $\zeta$ where different phenomena occur.
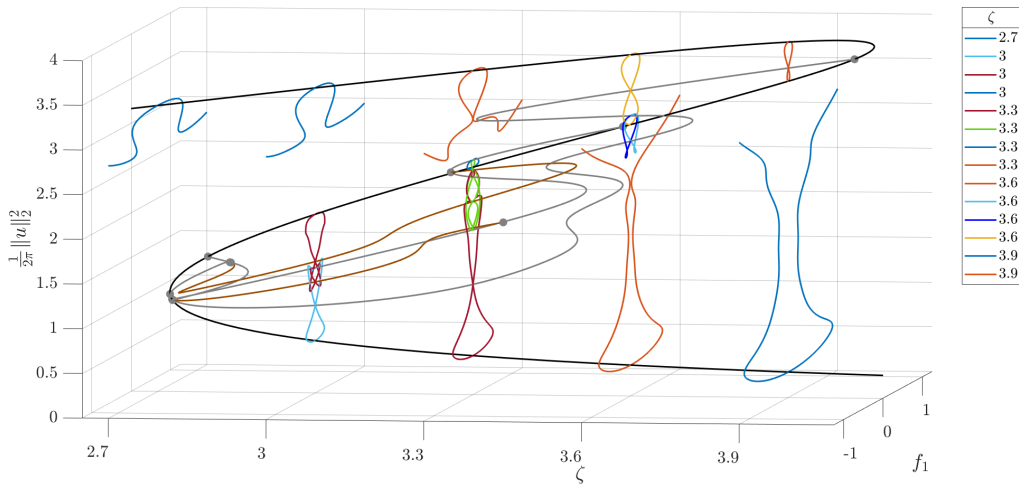


Figure 11. Continua of solutions $(f_1, u)$ of (3.2) for selected values of the detuning $\zeta$. The other parameters were set to $d = -0.1$, $f_0 = 2$, $k_1 = 1$, and $\omega = 0$.

At $\zeta = 2.7$ we see exactly one solution for $f_1 = 0$. This solution is constant and its continuation appears to be global in $f_1$. For $\zeta = 3.9$ and $f_1 = 0$ we see three constant solutions but also one non-constant solution (up to shifts) which lies on one of the grey bifurcation branches. The continuation of the constant solution with smallest magnitude

again appears to be global in $f_1$, while the other three solutions lie on the same eight-shaped maximal continuum which we will denote as *figure eight continuum*. Note that the latter continuum contains all shifts of the non-trivial solution for $f_1 = 0$.

The figure eight can be interpreted as an outcome of Theorem 3.6 applied to one of the constant solutions on the figure eight. Here, case (b) of the theorem applies. However, the figure eight can also be interpreted as an outcome of Theorem 3.9 applied to the non-constant solution $u_0$ at $f_1 = 0$. Again, case (b) of the theorem applies. A plot (which we omit) of the non-trivial solution $u_0$ at $f_1 = 0$ shows that $u_0$ has no smaller period than $2\pi$. Thus, according to Remark 3.11.($\beta$) exactly two shifts of it, which differ by $\pi$, are bifurcation points. To sum up, we observe that the figure eight continuum in fact contains a simple closed figure eight curve which exactly goes through two shifts of $u_0$ (which differ by $\pi$) in the point where the orange lines intersect the grey line of non-trivial solutions. The two shifts cannot be distinguished in the picture, because a shift does not change the $L^2$-norm. To illustrate the different continua for $\zeta = 3.6$, we
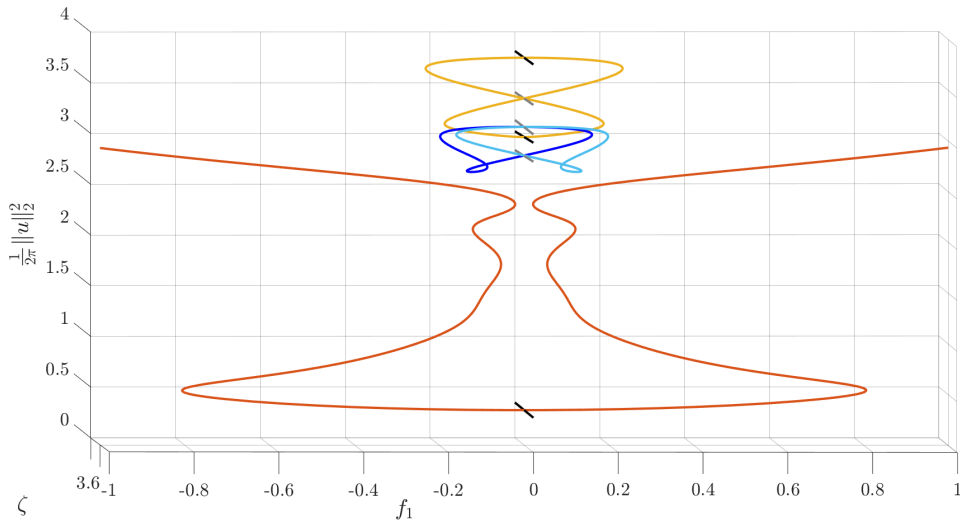


Figure 12. Zoom at $\zeta = 3.6$.

provide a zoom in Figure 12. We obtain again an unbounded continuum and a figure eight continuum. However, here we also find a third maximal continuum which cannot be found by simply continuing one of the constant solutions. This continuum consists of the blue and the light blue simple closed curve connected to each other by shifts at $f_1 = 0$. The parts of the blue and the light blue curve in the region $f_1 \geq 0$ are described by case (b) of Theorem 3.9 applied to one of the non-trivial solutions $u_0$ at $f_1 = 0$ on it. They have no smaller period than $2\pi$ (plots not shown). Going from the blue part to the light blue part is a consequence of reflection. At $f_1 = 0$ the blue curve intersects the grey line at exactly two points. The light blue curve does the same, but at $\pi$-shifts of these points.

For $\zeta = 3.3$ the situation is more complicated. In this case, we see three constant solutions for $f_1 = 0$ but also seven non-constant ones. The continuation of the upper constant solution (orange) appears to be unbounded. We observe that the blue, the

34

red and the green simple closed curve in fact form a single maximal continuum, since all curves are connected by shifts of non-constant solutions at $f_1 = 0$. Viewed from top to bottom, we find (plots not shown) that the first, the third and the last one are $\pi$-periodic while the remaining ones have smallest period $2\pi$. All together, we observe that exactly two shifts of every non-constant solution at $f_1 = 0$ are bifurcation points. For the solutions which have no smaller period than $2\pi$ this is a direct consequence of Theorem 3.9, cf. Remark 3.11.($\beta$). However, at the three remaining $\pi$-periodic solutions at $f_1 = 0$ Theorem 3.9 does not apply, cf. Remark 3.11.($\gamma$). Nevertheless, we observe continuations from these points. Interestingly, these points seem to be characterized by horizontal tangents, at least in this example.
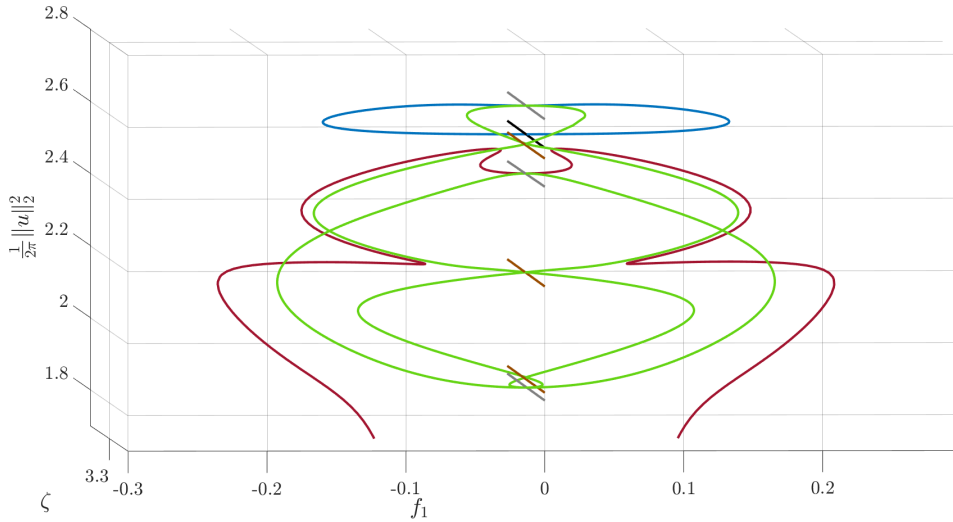


Figure 13. Zoom at $\zeta = 3.3$.

For $\zeta = 3$ we see three constant solutions and four non-constant ones at $f_1 = 0$. Again, the continuation of the upper constant solution is unbounded. We provide a more general investigation in Figure 14, where we also depict several of the continued solutions $u$ of (3.2) for $f_1 \neq 0$. Since $u$ is complex-valued, we use the quantity $|u(s)|^2$ for illustration purposes and plot it against $s \in [-\pi, \pi]$. In Figure 14(a) we show a bounded continuum consisting of the light blue and the red simple closed curve connected to each other by shifts at $f_1 = 0$. Starting from the constant solution on the light blue curve and proceeding first into the $f_1 > 0$ direction, Figure 14(b)-(c) show plots of functions corresponding to colored triangles. In Figure 14(d)-(f) functions corresponding to colored dots on the red curve are shown, where we start again at the constant solution and initially proceed in the $f_1 > 0$ direction. We observe that both curves cross the ($\pi$-periodic) non-constant solution with second largest norm, but at two different shifts: the leftmost dark-red curves in (c) and (f) only coincide after a non-zero shift. Continuations from $\pi$-periodic solutions at $f_1 = 0$ are not covered by Theorem 3.9. Nevertheless, they are observed in the numerical experiments, again with horizontal tangents. The explanation of these continuations remains open, cf. the Appendix for further discussion.
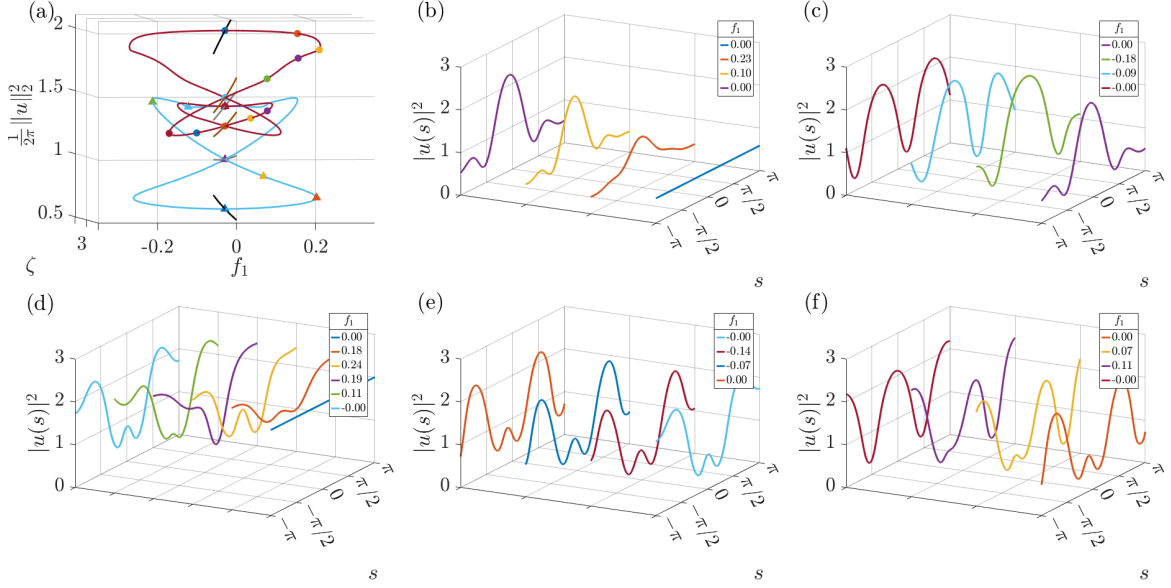
Figure 14. Zoom at $\zeta = 3$ and illustration of selected functions.

## 3.4. Proof of a-priori bounds

We use the notation $r_+ = \max\{0, r\}$ to denote the positive part of any real number $r \in \mathbb{R}$ and also $\mathbf{1}_{d<0}$ to denote (as a function of $d \in \mathbb{R}$) the characteristic function of the interval $(-\infty, 0)$. We write $\|\cdot\|_p$ for the standard norm on $L^p(0, 2\pi)$ for $p \in [1, \infty]$. A continuous map between two Banach spaces is said to be compact if it maps bounded sets into relatively compact sets.

**Theorem 3.14.** *Let $d \in \mathbb{R} \setminus \{0\}$, $\zeta, \omega \in \mathbb{R}$ and $f \in H^2(0, 2\pi)$. Then for every solution $u \in H_{per}^2(0, 2\pi)$ of (3.3) the a-priori bounds*

$$\|u\|_2 \leq F, \tag{3.12}$$

$$\|u'\|_2 \leq B\|u\|_2^{\frac{1}{4}} \leq BF^{\frac{1}{4}}, \tag{3.13}$$

$$\|u\|_\infty \leq C \tag{3.14}$$

*hold, where*

$$F = F(f) = \|f\|_2,$$

$$B = B(d, f) = \frac{F^{\frac{11}{4}}}{2|d|} + 2\|f'\|_\infty F^{\frac{1}{4}} + \sqrt{\|f''\|_2 F^{\frac{1}{2}} + 2\|f'\|_\infty \left(\sqrt{\frac{F}{2\pi}} + 1\right)},$$

$$C = C(d, f) = \frac{F}{\sqrt{2\pi}} + \sqrt{2\pi} BF^{\frac{1}{4}}.$$

*For $\zeta \operatorname{sign}(d) \ll -C^2 \mathbf{1}_{d<0}$ these bounds can be improved to*

$$\|u\|_2 \leq D, \quad \|u\|_\infty \leq \left( \frac{F^{\frac{3}{4}}}{\sqrt{2\pi}} + \sqrt{2\pi}B \right) D^{\frac{1}{4}},$$

*where*

$$D = D(d, f, \omega, \zeta) = \left( \frac{F^{\frac{3}{2}} + |\omega|BF^{\frac{3}{4}} + |d|B^2}{(-\zeta \operatorname{sign}(d) - C^2 \mathbf{1}_{d<0})_+} \right)^{\frac{2}{3}}.$$

**Remark 3.15.** The improvement in the second part of the theorem lies in the fact that the bound $D$ becomes small when the detuning $\zeta$ is such that $\zeta \operatorname{sign}(d)$ is very negative.

*Proof.* The proof is divided into five steps.

Step 1. We first prove the $L^2$ estimate

$$\|u\|_2 \leq F = \|f\|_2. \tag{3.15}$$

To this end we multiply the differential equation (3.3) with $\bar{u}$ to obtain

$$-du''\bar{u} + i\omega u'\bar{u} + (\zeta - i)|u|^2 - |u|^4 + if\bar{u} = 0. \tag{3.16}$$

Taking the imaginary part yields

$$-d \operatorname{Im}(u''\bar{u}) + \omega \operatorname{Re}(u'\bar{u}) - |u|^2 + \operatorname{Re}(f\bar{u}) = 0. \tag{3.17}$$

Let $h := |u|^2 - \operatorname{Re}(f\bar{u})$, $H := -d \operatorname{Im}(u'\bar{u}) + \frac{\omega}{2}|u|^2$. Then $H' = h$ by equation (3.17) and $H(0) = H(2\pi)$ by the periodicity of $u$. Hence

$$0 = H(2\pi) - H(0) = \int_0^{2\pi} h \, ds = \int_0^{2\pi} |u|^2 - \operatorname{Re}(f\bar{u}) \, ds$$

which implies

$$\|u\|_2^2 = \int_0^{2\pi} \operatorname{Re}(f\bar{u}) \, ds \leq \|f\|_2 \|u\|_2 = F\|u\|_2.$$

Step 2. Next we prove

$$\|u'\|_2 \leq B\|u\|_2^{\frac{1}{4}} \leq BF^{\frac{1}{4}}. \tag{3.18}$$

From (3.3) we may isolate the linear term $u$ and insert its derivative $u'$ into the following calculation for $\|u'\|_2^2$:

$$\|u'\|_2^2 = \operatorname{Re} \int_0^{2\pi} u'\bar{u}' \, ds \overset{(3.3)}{=} \operatorname{Re} \int_0^{2\pi} (idu'' + \omega u' - i\zeta u + i|u|^2 u + f)'\bar{u}' \, ds$$

$$= \operatorname{Re} \int_0^{2\pi} idu'''\bar{u}' + \omega u''\bar{u}' - i\zeta|u'|^2 + i(|u|^2 u)'\bar{u}' + f'\bar{u}' \, ds$$

$$= \int_0^{2\pi} -d(\operatorname{Im}(u''\bar{u}'))' + \left( \frac{\omega}{2}|u'|^2 \right)' \, ds - \operatorname{Im} \int_0^{2\pi} (|u|^2 u)'\bar{u}' \, ds + \operatorname{Re} \int_0^{2\pi} f'\bar{u}' \, ds$$

$$= \int_0^{2\pi} (|u|^2)' \operatorname{Im}(\bar{u}u') - \operatorname{Re}(f''\bar{u}) \, ds + \operatorname{Re} f'\bar{u}\big|_0^{2\pi}$$

$$\leq \int_0^{2\pi} \frac{1}{d}(|u|^2)'\Big(\frac{\omega}{2}|u|^2 - H\Big) + \|f''\|_2\|u\|_2 + 2\|f'\|_\infty\|u\|_\infty$$

$$= \int_0^{2\pi} \frac{\omega}{4d}(|u|^4)' - \frac{1}{d}(|u|^2)'H + \|f''\|_2\|u\|_2 + 2\|f'\|_\infty\|u\|_\infty$$

$$= \int_0^{2\pi} -\frac{1}{d}(|u|^2)'(H - H(0)) + \|f''\|_2\|u\|_2 + 2\|f'\|_\infty\|u\|_\infty.$$

Next notice the pointwise estimate

$$h = |u|^2 - \operatorname{Re}(f\bar{u}) \geq |u|^2 - |f||u| \geq -\frac{1}{4}|f|^2$$

from which we deduce the following two-sided estimate for $H - H(0)$:

$$H(s) - H(0) = \int_0^s h(r) \, dr \geq -\frac{1}{4}\|f\|_2^2 \quad (s \in [0, 2\pi]) \quad \text{and}$$

$$H(s) - H(0) = H(s) - H(2\pi) = -\int_s^{2\pi} h(r) \, dr \leq \frac{1}{4}\|f\|_2^2 \quad (s \in [0, 2\pi]).$$

Continuing the above inequality for $\|u'\|_2^2$ we conclude

$$\|u'\|_2^2 \leq \frac{\|f\|_2^2}{2|d|}\|u\|_2\|u'\|_2 + \|f''\|_2\|u\|_2 + 2\|f'\|_\infty\|u\|_\infty.$$

Next we want to get rid of the $\|u\|_\infty$ term. For that we note that there exists $s_0 \in [0, 2\pi]$ satisfying $|u^2(s_0)| \leq \frac{1}{2\pi}\|u\|_2^2$. We use this in the following way,

$$\|u\|_\infty^2 \leq |u^2(s_0)| + \sup_{s\in[0,2\pi]} |u^2(s) - u^2(s_0)| \leq \frac{1}{2\pi}\|u\|_2^2 + \int_0^{2\pi} 2|u||u'| \, ds$$

$$\leq \frac{1}{2\pi}\|u\|_2^2 + 2\|u\|_2\|u'\|_2 \overset{(3.15)}{\leq} \frac{F}{2\pi}\|u\|_2 + 2\|u\|_2\|u'\|_2$$

$$\leq \|u\|_2\Big(\frac{F}{2\pi} + 1 + \|u'\|_2^2\Big),$$

from where we find

$$\|u\|_\infty \leq \|u\|_2^{\frac{1}{2}}\Big(\sqrt{\frac{F}{2\pi} + 1} + \|u'\|_2\Big).$$

In total, we have

$$\|u'\|_2^2 \leq \frac{\|f\|_2^2}{2|d|}\|u\|_2\|u'\|_2 + \|f''\|_2\|u\|_2 + 2\|f'\|_\infty\|u\|_2^{\frac{1}{2}}\Big(\sqrt{\frac{F}{2\pi} + 1} + \|u'\|_2\Big)$$

$$\overset{(3.15)}{\leq} \frac{F^{\frac{11}{4}}}{2|d|}\|u\|_2^{\frac{1}{4}}\|u'\|_2 + \|f''\|_2 F^{\frac{1}{2}}\|u\|_2^{\frac{1}{2}} + 2\|f'\|_\infty \|u\|_2^{\frac{1}{2}}\left(\sqrt{\frac{F}{2\pi}}+1\right) + 2\|f'\|_\infty F^{\frac{1}{4}}\|u\|_2^{\frac{1}{4}}\|u'\|_2$$

$$= \left(\frac{F^{\frac{11}{4}}}{2|d|} + 2\|f'\|_\infty F^{\frac{1}{4}}\right)\|u\|_2^{\frac{1}{4}}\|u'\|_2 + \left(\|f''\|_2 F^{\frac{1}{2}} + 2\|f'\|_\infty\left(\sqrt{\frac{F}{2\pi}}+1\right)\right)\|u\|_2^{\frac{1}{2}}$$

$$=: A_1\|u\|_2^{\frac{1}{4}}\|u'\|_2 + A_2^2\|u\|_2^{\frac{1}{2}}.$$

This is a quadratic inequality in $\|u'\|_2$ which implies

$$\|u'\|_2 \leq \frac{A_1\|u\|_2^{\frac{1}{4}} + \sqrt{A_1^2\|u\|_2^{\frac{1}{2}} + 4A_2^2\|u\|_2^{\frac{1}{2}}}}{2} \leq A_1\|u\|_2^{\frac{1}{4}} + A_2\|u\|_2^{\frac{1}{4}} = B\|u\|_2^{\frac{1}{4}}$$

as claimed.

Step 3. Here we prove
$$\|u\|_\infty \leq C. \tag{3.19}$$
There exists $s_1 \in [0, 2\pi]$ satisfying $|u(s_1)| \leq \frac{\|u\|_2}{\sqrt{2\pi}}$. The claim now follows from

$$\|u\|_\infty \leq |u(s_1)| + \sup_{s\in[0,2\pi]}|u(s)-u(s_1)| \leq \frac{\|u\|_2}{\sqrt{2\pi}} + \|u'\|_1 \leq \frac{\|u\|_2}{\sqrt{2\pi}} + \sqrt{2\pi}\|u'\|_2$$

$$\overset{(3.15),(3.18)}{\leq} \left(\frac{F^{\frac{3}{4}}}{\sqrt{2\pi}} + \sqrt{2\pi}B\right)\|u\|_2^{\frac{1}{4}} \overset{(3.15)}{\leq} C.$$

Step 4. Next we show in the case $\zeta\,\mathrm{sign}(d) < -C^2\mathbf{1}_{d<0}$ the additional $L^2$-bound

$$\|u\|_2 \leq D. \tag{3.20}$$

After integrating (3.16) over $[0, 2\pi]$ and taking the real part of the resulting equation we get

$$d\|u'\|_2^2 = \omega\int_0^{2\pi}\mathrm{Im}(u'\bar{u})\,ds - \zeta\|u\|_2^2 + \|u\|_4^4 + \mathrm{Im}\int_0^{2\pi}f\bar{u}\,ds.$$

In order to prove (3.20) we first suppose $d > 0$. Then we have on one hand

$$d\|u'\|_2^2 \overset{(3.18)}{\leq} dB^2\|u\|_2^{\frac{1}{2}} \tag{3.21}$$

and on the other hand

$$
\omega \int_0^{2\pi} \operatorname{Im}(u'\bar{u}) \, ds - \zeta \|u\|_2^2 + \|u\|_4^4 + \operatorname{Im} \int_0^{2\pi} f\bar{u} \, ds
$$

$$
\geq -|\omega| \|u\|_2 \|u'\|_2 - \zeta \|u\|_2^2 - F\|u\|_2
$$

$$
\overset{(3.18)}{\geq} -|\omega| B \|u\|_2^{\frac{5}{4}} - \zeta \|u\|_2^2 - F\|u\|_2
$$

$$
\overset{(3.15)}{\geq} -|\omega| B F^{\frac{3}{4}} \|u\|_2^{\frac{1}{2}} - \zeta \|u\|_2^2 - F^{\frac{3}{2}} \|u\|_2^{\frac{1}{2}}. \tag{3.22}
$$

Combining the two estimates (3.21), (3.22) and grouping quadratic terms and terms of power $\frac{1}{2}$ of $\|u\|_2$ on separate sides of the inequality we get

$$
-\zeta \|u\|_2^2 \leq \left( F^{\frac{3}{2}} + |\omega| B F^{\frac{3}{4}} + dB^2 \right) \|u\|_2^{\frac{1}{2}}
$$

which finally implies $\|u\|_2 \leq D$ whenever $\zeta < 0$. Assuming now $d < 0$ the estimate (3.21) becomes

$$
d\|u'\|_2^2 \geq -|d| B^2 \|u\|_2^{\frac{1}{2}} \tag{3.23}
$$

whereas in (3.22) the term $\|u\|_4^4$, which was previously dropped, now has to be estimated by $\|u\|_4^4 \leq \|u\|_\infty^2 \|u\|_2^2 \leq C^2 \|u\|_2^2$. The estimate (3.22) now becomes

$$
\omega \int_0^{2\pi} \operatorname{Im}(u'\bar{u}) \, ds - \zeta \|u\|_2^2 + \|u\|_4^4 + \operatorname{Im} \int_0^{2\pi} f\bar{u} \, ds
$$

$$
\leq |\omega| B F^{\frac{3}{4}} \|u\|_2^{\frac{1}{2}} + (C^2 - \zeta) \|u\|_2^2 + F^{\frac{3}{2}} \|u\|_2^{\frac{1}{2}}. \tag{3.24}
$$

The combination of (3.23) and (3.24) leads to

$$
(\zeta - C^2) \|u\|_2^2 \leq \left( F^{\frac{3}{2}} + |\omega| B F^{\frac{3}{4}} + |d| B^2 \right) \|u\|_2^{\frac{1}{2}}
$$

which again implies $\|u\|_2 \leq D$ whenever $-\zeta < -C^2$.

Step 5. Finally we prove

$$
\|u\|_\infty \leq \left( \frac{F^{\frac{3}{4}}}{\sqrt{2\pi}} + \sqrt{2\pi} B \right) D^{\frac{1}{4}} \tag{3.25}
$$

whenever $\zeta \operatorname{sign}(d) < -C^2 \mathbf{1}_{d<0}$. For this we repeat Step 3 and use in the final estimate that $\|u\|_2 \leq D$. $\qquad \square$

## 3.5. Proof of existence (Theorem 3.1) and uniqueness (Theorem 3.17) statements

Let us consider the operator $L : H_{\mathrm{per}}^2(0, 2\pi) \to L^2(0, 2\pi)$ with $Lu = L_0 u - \mathrm{i}u$ and $L_0 u = -du'' + \mathrm{i}\omega u' + \zeta u$. Since $L_0 : H_{\mathrm{per}}^2(0, 2\pi) \to L^2(0, 2\pi)$ is self-adjoint its spectrum is real

and we see that $L$ has spectrum on the line $-\mathrm{i}+\mathbb{R}$. In particular, $L$ is invertible and $L^{-1}:$ $L^2(0,2\pi) \to H^2_{\mathrm{per}}(0,2\pi)$ is bounded. By using the compact embedding $H^2_{\mathrm{per}}(0,2\pi) \hookrightarrow$ $H^1_{\mathrm{per}}(0,2\pi)$ we see that

$$L^{-1} : L^2(0,2\pi) \to H^1_{\mathrm{per}}(0,2\pi) \text{ is compact.}$$

Since moreover $H^1_{\mathrm{per}}(0,2\pi)$ is a Banach algebra we can rewrite (3.3) as a fixed point problem $u = \Phi(u)$, where $\Phi$ denotes the compact map

$$\Phi : H^1_{\mathrm{per}}(0,2\pi) \to H^1_{\mathrm{per}}(0,2\pi), \ \ \Phi(u) = L^{-1}\big(|u|^2 u - \mathrm{i}f(s)\big).$$

In order to prove our first existence result from Theorem 3.1, let us recall Schaefer's fixed point theorem ([10, Corollary 8.1]).

**Theorem 3.16** (Schaefer's fixed point theorem)*. Let $X$ be a Banach space and $\Phi : X \to X$ be compact. Suppose that the set*

$$\{x \in X : x = \lambda\Phi(x) \text{ for some } \lambda \in (0,1)\}$$

*is bounded. Then $\Phi$ has a fixed point.*

*Proof of Theorem 3.1.* Let $u \in H^1_{\mathrm{per}}(0,2\pi)$ and $u = \lambda\Phi(u)$ for some $\lambda \in (0,1)$. Then $u \in H^2_{\mathrm{per}}(0,2\pi)$ and

$$-du'' + \mathrm{i}\omega u' + (\zeta - \mathrm{i})u - \lambda|u|^2 u + \mathrm{i}\lambda f(s) = 0.$$

Let us now define $v \in H^2_{\mathrm{per}}(0,2\pi)$ by $v(s) = \sqrt{\lambda}u(s)$. Then

$$-dv'' + \mathrm{i}\omega v' + (\zeta - \mathrm{i})v - |v|^2 v + \mathrm{i}\tilde{f}(s) = 0$$

with $\tilde{f} = \lambda^{\frac{3}{2}}f$. Estimate (3.12) of Theorem 3.14 with $\tilde{F} = F(\lambda^{\frac{3}{2}}f) = \lambda^{\frac{3}{2}}F$ implies

$$\|u\|_2 = \frac{1}{\sqrt{\lambda}}\|v\|_2 \leq \frac{1}{\sqrt{\lambda}}\tilde{F} = \lambda F \leq F.$$

Using (3.13) from Theorem 3.14 with $\tilde{B} = B(d, \lambda^{\frac{3}{2}}f)$ we also find

$$\begin{aligned}
\|u'\|_2 &= \frac{1}{\sqrt{\lambda}}\|v'\|_2 \leq \frac{1}{\sqrt{\lambda}}\tilde{B}\tilde{F}^{\frac{1}{4}} \\
&= \lambda^4 \frac{F^3}{2|d|} + 2\lambda^{\frac{7}{4}}\|f'\|_\infty F^{\frac{1}{2}} + \sqrt{\lambda^2\|f''\|_2 F + 2\lambda^{\frac{5}{4}}\|f'\|_\infty\left(\frac{\lambda^{\frac{3}{4}}F}{\sqrt{2\pi}} + \sqrt{F}\right)} \\
&\leq \frac{F^3}{2|d|} + 2\|f'\|_\infty F^{\frac{1}{2}} + \sqrt{\|f''\|_2 F + 2\|f'\|_\infty\left(\frac{F}{\sqrt{2\pi}} + \sqrt{F}\right)} = BF^{\frac{1}{4}}.
\end{aligned}$$

The assertion now follows from Theorem 3.16. $\qquad\square$

For the next uniqueness result, cf. Theorem 3.17, let us rewrite the constant $D$ from Theorem 3.14 as

$$D = D(d, f, \omega, \zeta) = \left( \frac{\tilde{D}}{(-\zeta \operatorname{sign}(d) - C^2 \mathbf{1}_{d<0})_+} \right)^{\frac{2}{3}}$$

with

$$\tilde{D} = \tilde{D}(d, f, \omega) = F^{\frac{3}{2}} + |\omega| B F^{\frac{3}{4}} + |d| B^2.$$

Our result complements the existence statement provided in Theorem 3.1 by a uniqueness statement. It consists of three cases: (i) and (ii) cover the case where $|\zeta| \gg 1$ is sufficiently large whereas (iii) builds upon $\|f\| \ll 1$ measured in a suitable norm $\|\cdot\|$ such that the constant $C = C(d, f)$ becomes small. This is the case, e.g., if $\|f\|_2 \ll 1$ and $\|f''\|_2$ remains bounded.

**Theorem 3.17.** *Let $d \in \mathbb{R} \setminus \{0\}$, $\zeta, \omega \in \mathbb{R}$ and $f \in H^2(0, 2\pi)$. Then (3.3) has a unique solution $u \in H^2_{per}(0, 2\pi)$ in the following three cases,*

*(i)*
$$\operatorname{sign}(d)\zeta < \zeta_*,$$

*(ii)*
$$\operatorname{sign}(d)\zeta > \zeta^*,$$

*(iii)*
$$\sqrt{3}C < 1,$$

*where $\zeta_* \leq 0 \leq \zeta^*$ are given by*

$$\zeta_* = \zeta_*(d, f, \omega) = -C^2 \mathbf{1}_{d<0} - \frac{27(F^{\frac{3}{4}} + 2\pi B)^6 \tilde{D}}{8\pi^3},$$

$$\zeta^* = \zeta^*(d, f, \omega) = 3C^2 + \frac{\omega^2}{4|d|},$$

*and $F = F(f)$, $B = B(d, f)$, $C = C(d, f)$ are the constants from Theorem 3.14.*

*Proof.* It suffices to consider the case $f \neq 0$. By Theorem 3.1 we know that (3.3) has at least one solution $u_1 \in H^2_{per}(0, 2\pi)$. Now let $u_2 \in H^2_{per}(0, 2\pi)$ denote an additional solution and define

$$R = R(d, f, \omega, \zeta) = \begin{cases} \min\left\{ C, \left( \frac{F^{\frac{3}{4}}}{\sqrt{2\pi}} + \sqrt{2\pi}B \right) D^{\frac{1}{4}} \right\}, & \zeta \operatorname{sign}(d) + C^2 \mathbf{1}_{d<0} < 0, \\ C, & \zeta \operatorname{sign}(d) + C^2 \mathbf{1}_{d<0} \geq 0. \end{cases}$$

Then $\|u_j\|_\infty \leq R$ for $j = 1, 2$ by Theorem 3.14, which easily implies

$$\left\| |u_1|^2 u_1 - |u_2|^2 u_2 \right\|_2 \leq 3R^2 \|u_1 - u_2\|_2.$$

Since $u_j, j = 1, 2$ solves the fixed point problem $u_j = \Phi(u_j)$ we obtain

$$\|u_1 - u_2\|_2 = \|\Phi(u_1) - \Phi(u_2)\|_2 \leq 3R^2 \|L^{-1}\| \|u_1 - u_2\|_2,$$

where $\|L^{-1}\| = \sup_{v \in L^2(0,2\pi), \|v\|_2 = 1} \|L^{-1}v\|_2$. Next we show $3R^2 \|L^{-1}\| < 1$ which implies $u_1 = u_2$ and thus finishes the proof. To this end we decompose a function $v \in L^2(0, 2\pi)$ into its Fourier series, i.e., $v = \sum_{m \in \mathbb{Z}} v_m e^{ims}$ so that

$$L^{-1}v = \sum_{m \in \mathbb{Z}} \frac{v_m}{dm^2 - \omega m + \zeta - i} e^{ims}.$$

On one hand we get $\|L^{-1}\| \leq 1$ since

$$\|L^{-1}v\|_2^2 = 2\pi \sum_{m \in \mathbb{Z}} \frac{|v_m|^2}{1 + (dm^2 - \omega m + \zeta)^2} \leq 2\pi \sum_{m \in \mathbb{Z}} |v_m|^2 = \|v\|_2^2.$$

On the other hand, if $\operatorname{sign}(d)\left(\zeta - \frac{\omega^2}{4d}\right) > 0$, we get

$$\|L^{-1}v\|_2^2 = 2\pi \sum_{m \in \mathbb{Z}} \frac{|v_m|^2}{1 + (dm^2 - \omega m + \zeta)^2} = 2\pi \sum_{m \in \mathbb{Z}} \frac{|v_m|^2}{1 + \left(d\left(m - \frac{\omega}{2d}\right)^2 + \zeta - \frac{\omega^2}{4d}\right)^2}$$

$$\leq 2\pi \sum_{m \in \mathbb{Z}} \frac{|v_m|^2}{\left(\zeta - \frac{\omega^2}{4d}\right)^2} = \frac{1}{\left(\zeta - \frac{\omega^2}{4d}\right)^2} \|v\|_2^2,$$

i.e. $\|L^{-1}\| \leq \operatorname{sign}(d)\left(\zeta - \frac{\omega^2}{4d}\right)^{-1}$.

In case (i) where $\operatorname{sign}(d)\zeta < \zeta_* < -C^2 \mathbf{1}_{d<0} \leq 0$ we use $\|L^{-1}\| \leq 1$ and find by the definition of $R$ and $\zeta_*$ that

$$3R^2 \|L^{-1}\| \leq 3\frac{(F^{\frac{3}{4}} + 2\pi B)^2}{2\pi} D^{\frac{1}{2}}$$

$$= 3\frac{(F^{\frac{3}{4}} + 2\pi B)^2}{2\pi}\left(\frac{\tilde{D}}{-\zeta \operatorname{sign}(d) - C^2 \mathbf{1}_{d<0}}\right)^{\frac{1}{3}}$$

$$< 3\frac{(F^{\frac{3}{4}} + 2\pi B)^2}{2\pi}\left(\frac{\tilde{D}}{-\zeta_* - C^2 \mathbf{1}_{d<0}}\right)^{\frac{1}{3}} = 1.$$

In case (ii) where $\operatorname{sign}(d)\zeta > \zeta^* > \frac{\omega^2}{4|d|} \geq 0$ we use $\|L^{-1}\| \leq \operatorname{sign}(d)\left(\zeta - \frac{\omega^2}{4d}\right)^{-1}$ and get by the choice of $\zeta^*$

$$3R^2 \|L^{-1}\| \leq \frac{3C^2}{\operatorname{sign}(d)\left(\zeta - \frac{\omega^2}{4d}\right)} < \frac{3C^2}{\zeta^* - \frac{\omega^2}{4|d|}} = 1.$$

In case (iii) where $\sqrt{3}C < 1$ we use $\|L^{-1}\| \le 1$ to conclude

$$3R^2\|L^{-1}\| \le 3C^2 < 1.$$

$\square$

## 3.6. Proof of the continuation results

In this section we continue to use the notion for the operator $L : H^2_{\mathrm{per}}(0, 2\pi) \to L^2(0, 2\pi)$ from Section 3.4. We also use that $L^{-1} : L^2(0, 2\pi) \to H^2_{\mathrm{per}}(0, 2\pi)$ is bounded and that $L^{-1} : L^2(0, 2\pi) \to H^1_{\mathrm{per}}(0, 2\pi)$ is compact. We first consider continuation from a trivial solution. In order to prove Theorem 3.6 let us provide the following global continuation theorem.

**Theorem 3.18.** *Let $X$ be a real Banach space and $K \in C^1(\mathbb{R} \times X, X)$ be compact. We consider the problem*

$$T(\lambda, x) := x - K(\lambda, x) = 0. \tag{3.26}$$

*Assume that $T(\lambda_0, x_0) = 0$ and that $\partial_x T(\lambda_0, x_0)$ is invertible. Then there exists a connected and closed set (=continuum) $\mathcal{C}^+ \subset [\lambda_0, \infty) \times X$ of solutions of (3.26) with $(\lambda_0, x_0) \in \mathcal{C}^+$. For $\mathcal{C}^+$ one of the following alternatives holds:*

*(a) $\mathcal{C}^+$ is unbounded,*

*or*

*(b) $\exists x_0^+ \in X \setminus \{x_0\} : (\lambda_0, x_0^+) \in \mathcal{C}^+$.*

*If one chooses $\mathcal{C}^+$ to be maximally connected then there is no more a strict alternative between (a) and (b) and instead at least one of the two (possibly both) properties holds.*

**Remark 3.19.** $(\alpha)$ The theorem follows from [2, Theorem 3.3] or [57, Theorem 1.3.2] since $\deg(T(\lambda_0, \cdot), B_\varepsilon(x_0), 0) = \deg(\partial_x T(\lambda_0, x_0), B_\varepsilon(0), 0) \ne 0$ because $\partial_x T(\lambda_0, x_0)$ is invertible.
$(\beta)$ There exists also a continuum $\mathcal{C}^- \subset (-\infty, \lambda_0] \times X$ of solutions of (3.26) with $(\lambda_0, x_0) \in \mathcal{C}^-$ satisfying one of the alternatives of the theorem.
$(\gamma)$ Alternative (a) of Theorem 3.18 means that $\mathcal{C}^+$ is unbounded either in the Banach space direction $X$ or in the parameter direction $[\lambda_0, \infty)$ or in both. If unboundedness in the Banach space direction is excluded on compact intervals $[\lambda_0, \Lambda]$, e.g., by a-priori bounds, then unboundedness in the parameter direction follows, i.e., the projection of $\mathcal{C}^+$ onto $[\lambda_0, \infty)$ denoted by $\mathrm{pr}_1(\mathcal{C}^+)$ must coincide with $[\lambda_0, \infty)$. This is an existence result for all $\lambda \ge \lambda_0$ which is one aspect of Theorem 3.6.
$(\delta)$ Alternative (b) of Theorem 3.18 means that the continuum $\mathcal{C}^+$ returns to the $\lambda = \lambda_0$ line at a point $x_0^+ \ne x_0$.

*Proof of Theorem 3.6.* Let $K : \mathbb{R} \times H^1_{\mathrm{per}}(0, 2\pi) \to H^1_{\mathrm{per}}(0, 2\pi)$, $K(f_1, u) := L^{-1}(|u|^2 u - \mathrm{i}f_0 - \mathrm{i}f_1 e(s))$ and $T(f_1, u) := u - K(f_1, u)$. Then, as explained before Theorem 3.16, $K$

44

is compact and

$$T(0, u_0) = u_0 - L^{-1}(|u_0|^2 u_0 - \mathrm{i}f_0) \overset{(3.4)}{=} u_0 - L^{-1}\big((\zeta - \mathrm{i})u_0\big) = u_0 - u_0 = 0.$$

Next we show that $\partial_u T(0, u_0)$ is invertible. To this end note that

$$\partial_u T(0, u_0)\varphi = \varphi - L^{-1}(2|u_0|^2\varphi + u_0^2\overline{\varphi}) \text{ for } \varphi \in H^1_{\mathrm{per}}(0, 2\pi)$$

and hence, as a compact perturbation of the identity, $\partial_u T(0, u_0)$ is invertible if it is injective. Since $u_0$ is constant this amounts exactly to the characterization of non-degeneracy of $u_0$ as described in Lemma 3.4.

Now assertion (i) follows from the classical implicit function theorem and Theorem 3.18 yields that the maximal continuum $\mathcal{C}^+ \subset [0, \infty) \times H^1_{\mathrm{per}}(0, 2\pi)$ of solutions $(f_1, u)$ of (3.3) with $(0, u_0) \in \mathcal{C}^+$ is unbounded or returns to another solution at $f_1 = 0$. The continuum $\mathcal{C}^+$ in fact belongs to $[0, \infty) \times H^2_{\mathrm{per}}(0, 2\pi)$ and persists as a connected and closed set in the stronger topology of $[0, \infty) \times H^2_{\mathrm{per}}(0, 2\pi)$. Next we show that the unboundedness of $\mathcal{C}^+$ coincides with $\mathrm{pr}_1(\mathcal{C}^+) = [0, \infty)$. According to Remark 3.19.$(\gamma)$ we need to show that unboundedness in the Banach space direction $H^1_{\mathrm{per}}(0, 2\pi)$ is excluded for $f_1$ in bounded intervals. To see this suppose that $0 \le f_1 \le M$ for all $(f_1, u) \in \mathcal{C}^+$ and some constant $M > 0$. Then, by the a-priori bounds (3.12) and (3.13) from Theorem 3.14 we get

$$\|u\|_2 \le \|f_0 + f_1 e(s)\|_2 \le \sqrt{2\pi}|f_0| + M\|e\|_2 =: N = N(f_0, M, e)$$

and

$$\|u'\|_2 \le \frac{N^3}{2|d|} + 2M\|e'\|_\infty N^{\frac{1}{2}} + \sqrt{M\|e''\|_2 N + 2M\|e'\|_\infty \left(\frac{N}{\sqrt{2\pi}} + \sqrt{N}\right)}$$

for all $(f_1, u) \in \mathcal{C}^+$. Hence $\mathcal{C}^+$ is bounded in the Banach space direction. Assertion (ii) follows in a similar way by using the a-priori bounds of Theorem 3.14 and the fact that by (3.3) the bounds for $\|u\|_2$, $\|u'\|_2$ and $\|u\|_\infty$ translate into a bound for $\|u''\|_2$.

According to Remark 3.19.$(\beta)$ the above line of arguments also yield that the maximal continuum $\mathcal{C}^- \subset (-\infty, 0] \times H^2_{\mathrm{per}}(0, 2\pi)$ of solutions of (3.3) with $(0, u_0) \in \mathcal{C}^-$ satisfies $\mathrm{pr}_1(\mathcal{C}^-) = (-\infty, 0]$ or returns to another solution at $f_1 = 0$. This finishes the proof. $\quad\square$

*Proof of Corollary 3.8.* The result follows from a combination of Theorem 3.6 and Theorem 3.17. For $f_1 = 0$, i.e. $f(s) = f_0$, the abbreviations $F, B, C$ from Theorem 3.14 and $\tilde{D}$ from Theorem 3.17 reduce to

$$F(f_0) = \sqrt{2\pi}|f_0|, \quad B(d, f_0) = 2^{\frac{3}{8}}\pi^{\frac{11}{8}}|f_0|^{\frac{11}{4}}|d|^{-1},$$
$$C(d, f_0) = |f_0|(1 + 2\pi^2 f_0^2|d|^{-1}),$$
$$\tilde{D}(d, f_0, \omega) = (2\pi)^{\frac{3}{4}}|f_0|^{\frac{3}{2}}(|d| + \pi f_0^2|\omega| + \pi^2 f_0^4)|d|^{-1}.$$

Hence the constants $\zeta_*, \zeta^*$ from Theorem 3.17 take the form

$$\zeta_*(d, f_0, \omega) = -C^2(d, f_0)\mathbf{1}_{d<0} - 27\left(1 + \frac{\pi f_0^2 |\omega|}{|d|} + \frac{\pi^2 f_0^4}{|d|}\right) C(d, f_0)^6,$$

$$\zeta^*(d, f_0, \omega) = 3C(d, f_0)^2 + \frac{\omega^2}{4|d|}.$$

Finally, the conditions (i), (ii), (iii) from the uniqueness result of Theorem 3.17 translate into the conditions (i), (ii), (iii) from Corollary 3.8.                                             $\square$

Now we turn to continuation from a non-trivial solution. Theorem 3.9 will follow from the Crandall-Rabinowitz Theorem of bifurcation from a simple eigenvalue, which we recall next.

**Theorem 3.20** (Crandall-Rabinowitz [9],[36]). *Let $I \subset \mathbb{R}$ be an open interval, $X,Y$ Banach spaces and let $F : I \times X \to Y$ be twice continuously differentiable such that $F(\lambda, 0) = 0$ for all $\lambda \in I$ and $\partial_x F(\lambda_0, 0) : X \to Y$ is an index-zero Fredholm operator for $\lambda_0 \in I$. Moreover assume:*

*(H1) there is $\phi \in X, \phi \neq 0$ such that $\ker \partial_x F(\lambda_0, 0) = \mathrm{span}\{\phi\}$,*

*(H2) $\partial^2_{x,\lambda} F(\lambda_0, 0)[\phi] \notin \mathrm{range}\, \partial_x F(\lambda_0, 0)$.*

*Then there exists $\epsilon > 0$ and a continuously differentiable curve $(\lambda, x) : (-\epsilon, \epsilon) \to I \times X$ with $\lambda(0) = \lambda_0$, $x(0) = 0$, $\dot{x}(0) = \phi$ and $x(t) \neq 0$ for $0 < |t| < \epsilon$ and $F(\lambda(t), x(t)) = 0$ for all $t \in (-\epsilon, \epsilon)$. Moreover, there exists a neighborhood $J \times U \subset I \times X$ of $(\lambda_0, 0)$ such that all non-trivial solutions in $J \times U$ of $F(\lambda, x) = 0$ lie on the curve. Finally,*

$$\dot{\lambda}(0) = -\frac{1}{2} \frac{\langle \partial^2_{xx} F(\lambda_0, 0)[\phi, \phi], \phi^* \rangle}{\langle \partial^2_{x,\lambda} F(\lambda_0, 0)[\phi], \phi^* \rangle},$$

*where $\mathrm{span}\{\phi^*\} = \ker \partial_x F(\lambda_0, 0)^*$ and $\langle \cdot, \cdot \rangle$ is the duality pairing between $Y$ and its dual $Y^*$.*

Next we provide the functional analytic setup. Fix the values of $d, \omega, \zeta, f_0$ and the function $e$. If $u_0 \in H^2_{\mathrm{per}}(0, 2\pi)$ is the non-trivial non-degenerate solution of (3.3) for $f_1 = 0$ (as assumed in Theorem 3.9) then for $\sigma \in \mathbb{R}$ we denote by $u_\sigma(s) := u_0(s - \sigma)$ its shifted copy, which is also a solution of (3.3) for $f_1 = 0$. Consider the mapping

$$G : \begin{cases} \mathbb{R} \times H^2_{\mathrm{per}}(0, 2\pi) & \to & L^2(0, 2\pi), \\ (f_1, u) & \mapsto & -du'' + i\omega u' + (\zeta - i)u - |u|^2 u + if_0 + if_1 e(s). \end{cases}$$

Then $G$ is twice continuously differentiable. The linearized operator $\partial_{(f_1,u)} G(0, u_\sigma) = (ie, L_{u_\sigma})$ with $L_{u_\sigma}$ as in Definition 3.2 is a Fredholm operator and $(0, u'_\sigma) \in \ker \partial_{(f_1,u)} G(0, u_\sigma)$. As we shall see there may be more elements in the kernel. Next we fix the value $\sigma_0$ (its

precise value will be given later) and let $H^2_{\mathrm{per}}(0, 2\pi) = \mathrm{span}\{u'_{\sigma_0}\} \oplus Z$ where, e.g.,

$$Z := H^2_{\mathrm{per}}(0, 2\pi) \cap \mathrm{span}\{u'_{\sigma_0}\}^{\perp_{L^2}} = \left\{ \varphi - \frac{\langle \varphi, u'_{\sigma_0} \rangle_{L^2}}{\langle u'_{\sigma_0}, u'_{\sigma_0} \rangle_{L^2}} u'_{\sigma_0} : \varphi \in H^2_{\mathrm{per}}(0, 2\pi) \right\}.$$

It will be more convenient to rewrite $u = u_\sigma + v$ with $v \in Z$. In order to justify this, note also that the map $(\sigma, v) \mapsto u_\sigma + v$ defines a diffeomorphism of a neighborhood of $(\sigma_0, 0) \in \mathbb{R} \times Z$ onto a neighborhood of $u_{\sigma_0} \in H^2_{\mathrm{per}}(0, 2\pi)$ since the derivative at $(\sigma_0, 0)$ is given by $(\lambda, \psi) \mapsto -\lambda u'_{\sigma_0} + \psi$ which is an isomorphism from $\mathbb{R} \times Z$ onto $H^2_{\mathrm{per}}(0, 2\pi)$. Now we define

$$F : \begin{cases} \mathbb{R} \times \mathbb{R} \times Z & \to & L^2(0, 2\pi), \\ (\sigma, f_1, v) & \mapsto & G(f_1, u_\sigma + v) \end{cases}$$

which is also twice continuously differentiable and where $\partial_{(f_1, v)} F(\sigma_0, 0, 0)$ is an index-zero Fredholm operator. Our goal will be to solve

$$F(\sigma, f_1, v) = 0 \tag{3.27}$$

by means of bifurcation theory, where $\sigma \in \mathbb{R}$ is the bifurcation parameter. Notice that $F(\sigma, 0, 0) = 0$ for all $\sigma \in \mathbb{R}$, i.e., $(f_1, v) = (0, 0)$ is a trivial solution of (3.27).

Next we show (H1) of Theorem 3.20.

**Lemma 3.21.** *Suppose that $\sigma_0 \in \mathbb{R}$ satisfies (3.7), i.e. $\mathrm{Im} \int_0^{2\pi} e(s + \sigma_0)\overline{\phi_0^*(s)}\, ds = 0$. Then $\dim \ker \partial_{(f_1, v)} F(\sigma_0, 0, 0) = 1$ and $\mathrm{range}\, \partial_{(f_1, v)} F(\sigma_0, 0, 0) = \mathrm{span}\{\phi_{\sigma_0}^*\}^{\perp_{L^2}}$.*

*Proof.* The fact that $\partial_{(f_1, v)} F(\sigma_0, 0, 0)$ is a Fredholm operator follows from Remark 3.3. For $(\alpha, \psi_{\sigma_0}) \in \mathbb{R} \times Z$ being non-trivial and belonging to the kernel of $\partial_{(f_1, v)} F(\sigma_0, 0, 0)$ we have

$$\partial_{(f_1, v)} F(\sigma_0, 0, 0)[\alpha, \psi_{\sigma_0}] = L_{u_{\sigma_0}} \psi_{\sigma_0} + \mathrm{i}\alpha e = 0. \tag{3.28}$$

If $\alpha = 0$ then by non-degeneracy we find $\psi_{\sigma_0} \in \mathrm{span}\{u'_{\sigma_0}\} \cap Z = \{0\}$, which is impossible. Hence we may assume w.l.o.g. that $\alpha = 1$ and $\psi_{\sigma_0}$ has to solve

$$L_{u_{\sigma_0}} \psi_{\sigma_0} = -\mathrm{i}e \tag{3.29}$$

which, by setting $\psi_{\sigma_0}(s) = \xi_{\sigma_0}(s - \sigma_0)$, is equivalent to

$$L_{u_0} \xi_{\sigma_0} = -\mathrm{i}e(\cdot + \sigma_0). \tag{3.30}$$

By the Fredholm alternative this is possible if and only if $-\mathrm{i}e(\cdot + \sigma_0) \perp_{L^2} \phi_0^*$. If this $L^2$-orthogonality holds then there exists $\psi_{\sigma_0} \in H^2_{\mathrm{per}}(0, 2\pi)$ solving (3.29) and $\psi_{\sigma_0}$ is unique up to adding a multiple of $u'_{\sigma_0}$. Hence there is a unique $\psi_{\sigma_0} \in Z$ solving (3.29). The $L^2$-orthogonality means

$$0 = -\mathrm{Re} \int_0^{2\pi} \mathrm{i}e(s + \sigma_0)\overline{\phi_0^*(s)}\, ds = \mathrm{Im} \int_0^{2\pi} e(s + \sigma_0)\overline{\phi_0^*(s)}\, ds$$

which amounts to (3.7). Finally, it remains to determine the range of $\partial_{(f_1,v)}F(\sigma_0,0,0)$. Let $\tilde{\phi} \in L^2(0,2\pi)$ be such that $\tilde{\phi} = \partial_{(f_1,v)}F(\sigma_0,0,0)[\alpha, \tilde{\psi}]$ with $\tilde{\psi} \in Z$ and $\alpha \in \mathbb{R}$. Thus

$$L_{u_{\sigma_0}}\tilde{\psi} + \mathrm{i}\alpha e = \tilde{\phi} \tag{3.31}$$

and since $\mathrm{i}e \perp_{L^2} \phi_{\sigma_0}^*$ by the definition of $\sigma_0$, the Fredholm alternative says that a necessary and sufficient condition for $\tilde{\phi}$ to satisfy (3.31) is that $\tilde{\phi} \in \mathrm{span}\{\phi_{\sigma_0}^*\}^{\perp_{L^2}}$ as claimed. Note that in this case $\tilde{\psi} \in H^2_{\mathrm{per}}(0,2\pi) = \ker L_{u_{\sigma_0}} \oplus Z$ and hence, for every given $\alpha \in \mathbb{R}$ and $\tilde{\phi} \in \mathrm{span}\{\phi_{\sigma_0}^*\}^{\perp_{L^2}}$ there is a unique element $\tilde{\psi} \in Z$ that solves (3.31). $\qquad\square$

*Proof of Theorem 3.9.* The proof is divided into three steps.

Step 1. We begin by verifying for (3.27) the conditions for the local bifurcation theorem of Crandall-Rabinowitz, cf. Theorem 3.20. By Lemma 3.21, $\partial_{(f_1,v)}F(\sigma_0,0,0): \mathbb{R} \times Z \to L^2(0,2\pi)$ is an index-zero Fredholm operator and it satisfies

$$\ker \partial_{(f_1,v)}F(\sigma_0,0,0) = \mathrm{span}\{(1, \psi_{\sigma_0})\},$$

where $\psi_{\sigma_0}$ denotes the unique element of Z which solves (3.29). Hence (H1) is satisfied. To see (H2) note that

$$\partial^2_{(f_1,v),\sigma}F(\sigma_0,0,0)[1, \psi_{\sigma_0}] = 2u'_{\sigma_0}\overline{u_{\sigma_0}}\psi_{\sigma_0} + 2\overline{u'_{\sigma_0}}u_{\sigma_0}\psi_{\sigma_0} + 2u_{\sigma_0}u'_{\sigma_0}\overline{\psi_{\sigma_0}}.$$

On the other hand, differentiation of (3.29) w.r.t. $s$ yields

$$L_{u_{\sigma_0}}\psi'_{\sigma_0} = 2u'_{\sigma_0}\overline{u_{\sigma_0}}\psi_{\sigma_0} + 2\overline{u'_{\sigma_0}}u_{\sigma_0}\psi_{\sigma_0} + 2u_{\sigma_0}u'_{\sigma_0}\overline{\psi_{\sigma_0}} - \mathrm{i}e' \tag{3.32}$$

so that

$$\partial^2_{(f_1,v),\sigma}F(\sigma_0,0,0)[1, \psi_{\sigma_0}] = L_{u_{\sigma_0}}\psi'_{\sigma_0} + \mathrm{i}e'. \tag{3.33}$$

Hence the characterization of range $\partial_{(f_1,v)}F(\sigma_0,0,0)$ from Lemma 3.21 implies that the transversality condition (H2) is satisfied if and only if $\mathrm{Re} \int_0^{2\pi} \mathrm{i}e'(s)\overline{\phi_{\sigma_0}^*(s)}\, ds \neq 0$ which amounts to assumption (3.8). This already allows us to apply Theorem 3.20 and we obtain the existence of a local curve $t \mapsto (\sigma(t), f_1(t), v(t))$, $\dot{f}_1(0) = 1$, $f_1(0) = 0$, $v(0) = 0$, $\sigma(0) = \sigma_0$ with $F(\sigma(t), f_1(t), v(t)) = 0$. Assertion (i) is then satisfied with $u(t) := u_{\sigma(t)} + v(t)$. Assertion (ii) follows like in the proof of Theorem 3.6.

Step 2. From here on let us additionally assume that zero is an algebraically simple eigenvalue of $L_{u_0}$, i.e. $u'_0 \notin \mathrm{range}\, L_{u_0}$. Next we want to show that $L_{u(t)}$ is invertible for $0 < |t| < \delta^*$ and $\delta^*$ sufficiently small, i.e. that the critical zero eigenvalue of $L_{u(0)} = L_{u_{\sigma_0}}$ moves away from zero when $t$ evolves. Let us define

$$H : \begin{cases} H^2_{\mathrm{per}}(0,2\pi) \times Z \times \mathbb{R} & \to & L^2(0,2\pi), \\ \qquad\qquad (u,v,\mu) & \mapsto & L_u(u'_{\sigma_0} + v) - \mu(u'_{\sigma_0} + v). \end{cases}$$

Then $H(u_{\sigma_0}, 0, 0) = 0$ and

$$\partial_{(v,\mu)} H(u_{\sigma_0}, 0, 0) : \begin{cases} Z \times \mathbb{R} & \to & L^2(0, 2\pi), \\ (\psi, \alpha) & \mapsto & L_{u_{\sigma_0}} \psi - \alpha u'_{\sigma_0} \end{cases}$$

clearly defines an isomorphism due to our assumption that $u'_{\sigma_0} \notin \operatorname{range} L_{u_{\sigma_0}}$. By the implicit function theorem we find neighborhoods $U \subset H^2_{\operatorname{per}}(0, 2\pi)$ of $u_{\sigma_0}$, $V \subset Z$ of $0$, $J \subset \mathbb{R}$ of $0$ and continuously differentiable functions $v^* : U \to V$, $\mu^* : U \to J$ such that $v^*(u_{\sigma_0}) = 0$, $\mu^*(u_{\sigma_0}) = 0$ and

$$\forall (u, v, \mu) \in U \times V \times J : H(u, v, \mu) = 0 \Leftrightarrow v = v^*(u), \mu = \mu^*(u).$$

Thus, for $|t|$ sufficiently small we find $L_{u(t)}\big(u'_{\sigma_0} + v^*(u(t))\big) = \mu^*(u(t))\big(u'_{\sigma_0} + v^*(u(t))\big)$. With $\varphi(t) := u'_{\sigma_0} + v^*(u(t))$ and $\mu(t) := \mu^*(u(t))$ we have $\varphi(0) = u'_{\sigma_0}$, $\mu(0) = 0$ and

$$L_{u(t)}\varphi(t) = \mu(t)\varphi(t) \tag{3.34}$$

so that we have found a parameterization of the eigenvalue $\mu(t)$ nearby $0$ with eigenfunction $\varphi(t)$ of $L_{u(t)}$. Next we want to compute $\dot{\mu}(0)$ and show that $\dot{\mu}(0) \neq 0$ so that the critical zero eigenvalue moves away from zero. Differentiating (3.34) w.r.t. $t$ and evaluating at $t = 0$ we get

$$L_{u_{\sigma_0}}\dot{\varphi}(0) - 2\dot{u}(0)\overline{u_{\sigma_0}}u'_{\sigma_0} - 2u_{\sigma_0}\overline{\dot{u}(0)}u'_{\sigma_0} - 2u_{\sigma_0}\dot{u}(0)\overline{u'_{\sigma_0}} = \dot{\mu}(0)u'_{\sigma_0}.$$

Theorem 3.20 yields $\dot{v}(0) = \psi_{\sigma_0}$ from which we find $\dot{u}(0) = -u'_{\sigma_0}\dot{\sigma}(0) + \psi_{\sigma_0}$. Thus,

$$L_{u_{\sigma_0}}\dot{\varphi}(0) - 2(\psi_{\sigma_0}\overline{u_{\sigma_0}}u'_{\sigma_0} + u_{\sigma_0}\overline{\psi_{\sigma_0}}u'_{\sigma_0} + u_{\sigma_0}\psi_{\sigma_0}\overline{u'_{\sigma_0}}) + 2\dot{\sigma}(0)u'_{\sigma_0}(\overline{u_{\sigma_0}}u'_{\sigma_0} + 2u_{\sigma_0}\overline{u'_{\sigma_0}}) = \dot{\mu}(0)u'_{\sigma_0}.$$

Using (3.32) this gives

$$L_{u_{\sigma_0}}\dot{\varphi}(0) - L_{u_{\sigma_0}}\psi'_{\sigma_0} - ie' + 2\dot{\sigma}(0)u'_{\sigma_0}(\overline{u_{\sigma_0}}u'_{\sigma_0} + 2u_{\sigma_0}\overline{u'_{\sigma_0}}) = \dot{\mu}(0)u'_{\sigma_0}.$$

Testing this equation with $\phi^*_{\sigma_0}$ and using $\dot{\mu}(0) \in \mathbb{R}$ we obtain

$$\operatorname{Re} \int_0^{2\pi} -ie'\overline{\phi^*_{\sigma_0}} + 2\dot{\sigma}(0)u'_{\sigma_0}(\overline{u_{\sigma_0}}u'_{\sigma_0} + 2u_{\sigma_0}\overline{u'_{\sigma_0}})\overline{\phi^*_{\sigma_0}}\,ds = \dot{\mu}(0)\operatorname{Re}\int_0^{2\pi} u'_{\sigma_0}\overline{\phi^*_{\sigma_0}}\,ds.$$

Due to $u'_{\sigma_0} \notin \operatorname{range} L_{u_{\sigma_0}}$ we have $\operatorname{Re}\int_0^{2\pi} u'_{\sigma_0}\overline{\phi^*_{\sigma_0}}\,ds \neq 0$ so that

$$\dot{\mu}(0) = \frac{\operatorname{Im}\int_0^{2\pi} e'(s + \sigma_0)\overline{\phi^*_0(s)}\,ds + 2\dot{\sigma}(0)\operatorname{Re}\int_0^{2\pi} u'_0(\overline{u_0}u'_0 + 2u_0\overline{u'_0})\overline{\phi^*_0}\,ds}{\operatorname{Re}\int_0^{2\pi} u'_0\overline{\phi^*_0}\,ds}.$$

From Theorem 3.20 we know that

$$\dot{\sigma}(0) = -\frac{1}{2} \frac{\left\langle \partial^2_{(f_1,v)^2} F(\sigma_0, 0, 0)[(1, \psi_{\sigma_0}), (1, \psi_{\sigma_0})], \phi^*_{\sigma_0} \right\rangle_{L^2}}{\left\langle \partial^2_{(f_1,v),\sigma} F(\sigma_0, 0, 0)[1, \psi_{\sigma_0}], \phi^*_{\sigma_0} \right\rangle_{L^2}}.$$

Therefore, using (3.33) and

$$\partial^2_{(f_1,v)^2} F(\sigma_0, 0, 0)[(1, \psi_{\sigma_0}), (1, \psi_{\sigma_0})] = -2\overline{u_{\sigma_0}} \psi^2_{\sigma_0} - 4u_{\sigma_0} |\psi_{\sigma_0}|^2$$

we find that the condition $\dot{\mu}(0) \neq 0$ amounts to assumption (3.9) of the theorem.

Finally, employing some arguments from spectral theory, we ensure that no other eigenvalue runs into zero. For $u = u_1 + iu_2 \in H^2_{\mathrm{per}}(0, 2\pi)$ let us define the $\mathbb{C}$-linear operator

$$L^{\mathbb{C}}_u : \begin{cases} H^2_{\mathrm{per}}((0, 2\pi), \mathbb{C}^2) & \to \quad L^2((0, 2\pi), \mathbb{C}^2), \\ \begin{pmatrix} \varphi_1 \\ \varphi_2 \end{pmatrix} & \mapsto \quad \begin{pmatrix} -d\varphi''_1 - \omega\varphi'_2 + \zeta\varphi_1 + \varphi_2 - 3u_1^2\varphi_1 - u_2^2\varphi_1 - 2u_1 u_2\varphi_2 \\ -d\varphi''_2 + \omega\varphi'_1 + \zeta\varphi_2 - \varphi_1 - u_1^2\varphi_2 - 3u_2^2\varphi_2 - 2u_1 u_2\varphi_1 \end{pmatrix} \end{cases}$$

which is constructed in such a way that

$$L^{\mathbb{C}}_u \begin{pmatrix} \varphi_1 \\ \varphi_2 \end{pmatrix} = \begin{pmatrix} \mathrm{Re}\, L_u(\varphi_1 + i\varphi_2) \\ \mathrm{Im}\, L_u(\varphi_1 + i\varphi_2) \end{pmatrix}$$

whenever $\varphi_1, \varphi_2 \in H^2_{\mathrm{per}}((0, 2\pi), \mathbb{R})$. Since $L^{\mathbb{C}}_u$ is an index-zero Fredholm operator, its spectrum consists of eigenvalues. The real part of these eigenvalues (weighted with $\mathrm{sign}(d)$) is bounded from below by $c \in \mathbb{R}$ which is chosen such that

$$\mathrm{Re} \left\langle \mathrm{sign}(d) L^{\mathbb{C}}_u \begin{pmatrix} \varphi_1 \\ \varphi_2 \end{pmatrix}, \begin{pmatrix} \varphi_1 \\ \varphi_2 \end{pmatrix} \right\rangle_{L^2((0,2\pi),\mathbb{C}^2)} \geq c \left\| \begin{pmatrix} \varphi_1 \\ \varphi_2 \end{pmatrix} \right\|^2_{L^2((0,2\pi),\mathbb{C}^2)}$$

holds. This implies that the resolvent set $\rho(L^{\mathbb{C}}_u)$ is non-empty and the compact embedding $H^2_{\mathrm{per}}((0, 2\pi), \mathbb{C}^2) \hookrightarrow L^2((0, 2\pi), \mathbb{C}^2)$ ensures that $L^{\mathbb{C}}_u$ has compact resolvent so that $\sigma(L^{\mathbb{C}}_u)$ consists of isolated eigenvalues. Now choose $\varepsilon > 0$ such that $\sigma(L^{\mathbb{C}}_{u(0)}) \cap \overline{B^{\mathbb{C}}_\varepsilon(0)} = \{0\}$. Using [35, Chapter Four, Theorem 3.18] we find that $\sigma(L^{\mathbb{C}}_{u(t)}) \cap B^{\mathbb{C}}_\varepsilon(0)$ exactly consists of one algebraically simple eigenvalue if $|t|$ is sufficiently small. If in addition $|t|$ is chosen so small that $\mu(t) \in (-\varepsilon, \varepsilon)$ then this means $\sigma(L^{\mathbb{C}}_{u(t)}) \cap B^{\mathbb{C}}_\varepsilon(0) = \{\mu(t)\}$. But from $\dot{\mu}(0) \neq 0$ we know that $\mu(t) \neq 0$ for small $|t| > 0$ which guarantees that $0 \notin \sigma(L^{\mathbb{C}}_{u(t)})$ for $0 < |t| < \delta^*$ and $\delta^*$ sufficiently small. Finally, $L_{u(t)}$ inherits the invertibility of $L^{\mathbb{C}}_{u(t)}$.

Step 3. Using $\dot{f}_1(0) = 1$ and Step 2 we find a local reparameterization $(\tilde{f}_1, u(\tilde{f}_1))$ of $C(t) = (f_1(t), u(t))$ such that $L_{u(\tilde{f}_1)}$ is invertible for $0 < \tilde{f}_1 < f^*_1$. Next we construct the connected set $\mathcal{C}^+_*$. For this we want to apply Theorem 3.18 to the map $T : \mathbb{R} \times H^1_{\mathrm{per}}(0, 2\pi) \to H^1_{\mathrm{per}}(0, 2\pi)$ from the proof of Theorem 3.6. Note that this theorem can not be applied directly at the point $(0, u_{\sigma_0})$ since $\partial_u T(0, u_{\sigma_0})$ is not invertible. Instead,

we apply it to the points $(\tilde{f}_1, u(\tilde{f}_1))$ with $\tilde{f}_1 \in (0, f_1^*)$ and obtain that the maximal continuum $\mathcal{C}^+(\tilde{f}_1) \subset [\tilde{f}_1, \infty) \times H^1_{\text{per}}(0, 2\pi)$ of solutions of (3.3) with $(\tilde{f}_1, u(\tilde{f}_1)) \in \mathcal{C}^+(\tilde{f}_1)$ is unbounded or returns to another solution $u^+(\tilde{f}_1) \neq u(\tilde{f}_1)$ at $f_1 = \tilde{f}_1$. As in the proof of Theorem 3.6 we see that the continuum $\mathcal{C}^+(\tilde{f}_1)$ persists as a connected and closed set in $[\tilde{f}_1, \infty) \times H^2_{\text{per}}(0, 2\pi)$. Let us define

$$\mathcal{C}^+_* := \bigcup_{\tilde{f}_1 \in (0, f_1^*)} \mathcal{C}^+(\tilde{f}_1) \subset \mathcal{C}^+.$$

Clearly, $\text{pr}_1(\mathcal{C}^+_*) \subset (0, \infty)$ and $\mathcal{C}^+_*$ is connected since $\mathcal{C}^+(\tilde{f}_1) \subset \mathcal{C}^+(\bar{f}_1)$ for $\bar{f}_1 < \tilde{f}_1$. Let us now suppose that $\text{pr}_1(\mathcal{C}^+_*) \neq (0, \infty)$ so that $\text{pr}_1(\mathcal{C}^+_*)$ is bounded. By (ii) this implies that $\mathcal{C}^+_*$ is bounded too. Hence $\mathcal{C}^+(\tilde{f}_1)$ is bounded for $\tilde{f}_1 \in (0, f_1^*)$ and contains the additional element $(\tilde{f}_1, u^+(\tilde{f}_1))$. Let us take $\tilde{f}_1 = \frac{1}{n}$ and consider the two sequences of solutions $(\frac{1}{n}, u(\frac{1}{n}))_n$ and $(\frac{1}{n}, u^+(\frac{1}{n}))_n$. Using Theorem 3.14 we obtain uniform $C^3$-bounds for both sequences $(u(\frac{1}{n}))_n$ and $(u^+(\frac{1}{n}))_n$. Therefore we can take convergent subsequences (denoted by the same index) and obtain $u(\frac{1}{n}) \to u_{\sigma_0}$ and $u^+(\frac{1}{n}) \to u_0^+$ in $C^2([0, 2\pi])$ as $n \to \infty$. In particular $(0, u_{\sigma_0}), (0, u_0^+) \in \overline{\mathcal{C}^+_*}$ and the uniqueness property from (i) guarantees that $u_0^+ \neq u_{\sigma_0}$. This finishes the proof. $\qquad\square$

*Proof of Corollary 3.10.* We first check assumption (3.7) of Theorem 3.9. For $e(s) = e^{ik_1 s}$ we have

$$\text{Im} \int_0^{2\pi} e(s + \sigma_0)\overline{\phi_0^*(s)}\, ds = \text{Im} \int_0^{2\pi} e^{ik_1(s+\sigma_0)}\overline{\phi_0^*(s)}\, ds$$

$$= \cos(k_1\sigma_0) \text{Im} \int_0^{2\pi} e^{ik_1 s}\overline{\phi_0^*(s)}\, ds + \sin(k_1\sigma_0) \text{Re} \int_0^{2\pi} e^{ik_1 s}\overline{\phi_0^*(s)}\, ds,$$

where

$$\text{Im} \int_0^{2\pi} e^{ik_1 s}\overline{\phi_0^*(s)}\, ds = \int_0^{2\pi} \sin(k_1 s) \text{Re}\, \phi_0^*(s) - \cos(k_1 s) \text{Im}\, \phi_0^*(s)\, ds,$$

$$\text{Re} \int_0^{2\pi} e^{ik_1 s}\overline{\phi_0^*(s)}\, ds = \int_0^{2\pi} \cos(k_1 s) \text{Re}\, \phi_0^*(s) + \sin(k_1 s) \text{Im}\, \phi_0^*(s)\, ds.$$

Since assumption (3.10) guarantees that $\text{Im} \int_0^{2\pi} e^{ik_1 s}\overline{\phi_0^*(s)}\, ds$ and $\text{Re} \int_0^{2\pi} e^{ik_1 s}\overline{\phi_0^*(s)}\, ds$ do not vanish simultaneously condition (3.11) ensures that assumption (3.7) of Theorem 3.9 is fulfilled.

Next we check that assumption (3.8) of Theorem 3.9 holds. For this we compute

$$\text{Im} \int_0^{2\pi} e'(s + \sigma_0)\overline{\phi_0^*(s)}\, ds = \text{Im} \int_0^{2\pi} ik_1 e^{ik_1(s+\sigma_0)}\overline{\phi_0^*(s)}\, ds = k_1 \text{Re} \int_0^{2\pi} e^{ik_1(s+\sigma_0)}\overline{\phi_0^*(s)}\, ds.$$

$$(3.35)$$

From (3.10) we know that $\int_0^{2\pi} e^{ik_1(s+\sigma_0)}\overline{\phi_0^*(s)}\, ds = e^{ik_1\sigma_0} \int_0^{2\pi} e^{ik_1 s}\overline{\phi_0^*(s)}\, ds \neq 0$ and moreover $\text{Im} \int_0^{2\pi} e^{ik_1(s+\sigma_0)}\overline{\phi_0^*(s)}\, ds = 0$ by the definition of $\sigma_0$. Therefore the expression in

(3.35) does not vanish and so assumption (3.8) of Theorem 3.9 holds. This is all we had to show. □

*Proof of Theorem 3.13.* Let us fix all parameters $d, \omega, \zeta, k_1$ and $f_0$ and consider $u : f_1 \mapsto u(f_1)$ as a function mapping the parameter $f_1 \in [-f_1^*, f_1^*]$ to the uniquely defined solution of (3.2) in the neighborhood of the trivial solution $u_0$. The existence of such a smooth function follows from the implicit function theorem applied to the equation $T(f_1, u) = 0$, cf. proof of Theorem 3.6. Similarly we consider the functions $v : f_1 \mapsto \frac{du(f_1)}{df_1}$ and $w : f_1 \mapsto \frac{d^2u(f_1)}{df_1^2}$. Then

$$\frac{d}{df_1}\|u(f_1)\|_2^2 = 2\int_0^{2\pi} \mathrm{Re}(u\overline{v})\,ds, \qquad \frac{d^2}{df_1^2}\|u(f_1)\|_2^2 = 2\int_0^{2\pi} \mathrm{Re}(u\overline{w}) + |v|^2\,ds \qquad (3.36)$$

and the differential equations for $v, w$ at $f_1 = 0$ are given by

$$-dv'' + \mathrm{i}\omega v' + (\zeta - \mathrm{i})v - 2|u_0|^2 v - u_0^2\overline{v} + \mathrm{i}e^{\mathrm{i}k_1 s} = 0, \qquad (3.37)$$

$$-dw'' + \mathrm{i}\omega w' + (\zeta - \mathrm{i})w - 4u_0|v|^2 - 2\overline{u_0}v^2 - 2|u_0|^2 w - u_0^2\overline{w} = 0 \qquad (3.38)$$

both equipped with $2\pi$-periodic boundary conditions. The first equation (3.37) has a unique solution since the homogeneous equation has a trivial kernel, cf. proof of Theorem 3.6. Thus $v(s) = \alpha e^{\mathrm{i}k_1 s} + \beta e^{-\mathrm{i}k_1 s}$ where $\alpha, \beta \in \mathbb{C}$ solve the linear system

$$(dk_1^2 - k_1\omega + \zeta - \mathrm{i} - 2|u_0|^2)\alpha - u_0^2\overline{\beta} + \mathrm{i} = 0,$$
$$(dk_1^2 + k_1\omega + \zeta - \mathrm{i} - 2|u_0|^2)\beta - u_0^2\overline{\alpha} = 0.$$

Solving for $\alpha, \beta$ leads to the formulae in the statement of the theorem. Since $v$ is the sum of two $2\pi$-periodic complex exponentials and $u_0$ is a constant we see from (3.36) that $\frac{d}{df_1}\|u(f_1)\|_2^2|_{f_1=0} = 0$. Having determined $v$ we can consider the second equation (3.38) as an inhomogeneous equation for $w$. It also has a unique solution since the homogeneous equation is the same as in (3.37). Since the inhomogeneity is of the form $c_1 e^{\mathrm{i}2k_1 s} + c_2 e^{-\mathrm{i}2k_1 s} + c_3$ the solution has the form $w(s) = \gamma e^{\mathrm{i}2k_1 s} + \delta e^{-\mathrm{i}2k_1 s} + \epsilon$. Moreover, for the determination of $\frac{d^2}{df_1^2}\|u(f_1)\|_2^2$ the values of $\gamma, \delta$ are irrelevant and only the value of $\epsilon$ matters. Using

$$|v|^2 = |\alpha|^2 + |\beta|^2 + 2\,\mathrm{Re}(\alpha\overline{\beta}e^{\mathrm{i}2k_1 s}), \quad v^2 = \alpha^2 e^{\mathrm{i}2k_1 s} + \beta^2 e^{-\mathrm{i}2k_1 s} + 2\alpha\beta$$

we find from (3.38) that the equation determining $\epsilon$ is

$$(\zeta - \mathrm{i})\epsilon - 4u_0(|\alpha|^2 + |\beta|^2) - 4\overline{u_0}\alpha\beta - 2|u_0|^2\epsilon - u_0^2\overline{\epsilon} = 0.$$

Since this is an equation of the form $x\epsilon + y\overline{\epsilon} = z$ with $x, y, z$ given in the statement of the theorem we find the solution formula $\epsilon = \frac{-\overline{z}y + z\overline{x}}{|x|^2 - |y|^2}$. Finally, only the constant contributions from $\overline{w}$ and $|v|^2$ contribute to the integral in the formula (3.36) for $\frac{d^2}{df_1^2}\|u(f_1)\|_2^2$ and lead to the claimed statement of the theorem. □

## 3.7. Appendix A

Here we raise the issue mentioned in Remark 3.11.($\gamma$) that assumption (3.10) from Corollary 3.10 is not satisfied if $u_0$ is $\frac{2\pi}{j}$-periodic and $j \in \mathbb{N}$ is not a divisor of $k_1$. Let us first prove that $\phi_0^*$ (spanning $\ker L_{u_0}^*$) inherits several properties from $u_0'$ (spanning $\ker L_{u_0}$).

**Proposition 3.22.** *Let $u_0 \in H_{per}^2(0, 2\pi)$ be a non-constant non-degenerate solution of* (3.3) *for $f_1 = 0$ and let $\ker L_{u_0}^* = \mathrm{span}\{\phi_0^*\}$. Then the following holds:*

(i) *If $u_0$ is $\frac{2\pi}{j}$-periodic with $j \in \mathbb{N}$ then $\phi_0^*$ is $\frac{2\pi}{j}$-periodic.*

(ii) *If $\omega = 0$ and if $u_0$ is even then $\phi_0^*$ is odd.*

*Proof.* (i) By assumption we have that $\ker L_{u_0} = \mathrm{span}\{u_0'\}$ and $u_0'$ is a $\frac{2\pi}{j}$-periodic function. Let us define $D := \{\varphi \in H_{per}^2(0, 2\pi) : \varphi \text{ is } \frac{2\pi}{j}\text{-periodic}\}$ and similarly $L_j^2(0, 2\pi) = \{\varphi \in L^2(0, 2\pi) : \varphi \text{ is } \frac{2\pi}{j}\text{-periodic}\}$. If we consider the restriction

$$L_{u_0}^\# : \begin{cases} D & \to & L_j^2(0, 2\pi), \\ \varphi & \mapsto & L_{u_0}\varphi, \end{cases}$$

then $L_{u_0}^\#$ is again an index-zero Fredholm operator with $\ker L_{u_0}^\# = \mathrm{span}\{u_0'\}$. Further we have $(L_{u_0}^\#)^* = (L_{u_0}^*)^\#$ where

$$(L_{u_0}^*)^\# : \begin{cases} D & \to & L_j^2(0, 2\pi), \\ \varphi & \mapsto & L_{u_0}^*\varphi \end{cases}$$

is the restriction of the adjoint. But since $1 = \dim \ker(L_{u_0}^*)^\# = \dim \ker L_{u_0}^*$ it follows that $\ker(L_{u_0}^*)^\# = \ker L_{u_0}^*$ and hence $\phi_0^* \in D$ as claimed.

The proof of (ii) is very similar. Due to the assumption $\omega = 0$ we can restrict both the domain and the codomain of $L_{u_0}$ to odd functions and observe that it is still an index-zero Fredholm operator. $\qquad\square$

Instead of $k_1 \in \mathbb{N}$ let us consider a perturbation $k_1(\epsilon) \in \mathbb{R} \setminus \{k_1\}$ with $\lim_{\epsilon \to 0} k_1(\epsilon) = k_1$. For $\epsilon \approx 0$ one may have maximally connected continua $\mathcal{C}_\epsilon^+$ as described in Theorem 3.9. In a topological sense one can describe $\liminf\{\mathcal{C}_\epsilon^+ : \epsilon^{-1} \in \mathbb{N}\}$ and $\limsup\{\mathcal{C}_\epsilon^+ : \epsilon^{-1} \in \mathbb{N}\}$ as in [70]. However, having in mind sequences of loops degenerating to one point, we do not intend to make any existence statement about a bifurcating branch obtained through such a topological limiting procedure. Let us abbreviate by $e_\epsilon(s)$ the periodic extension of $[0, 2\pi) \to \mathbb{C}$, $s \mapsto \mathrm{e}^{ik_1(\epsilon)s}$ onto $\mathbb{R}$. Note that

$$\mathrm{Im} \int_0^{2\pi} e_\epsilon(s + \sigma_{0,\epsilon})\overline{\phi_0^*(s)}\, ds = \mathrm{Im} \int_0^{2\pi} \mathrm{e}^{ik_1(\epsilon)s}\overline{\phi_{\sigma_{0,\epsilon}}^*(s)}\, ds = \mathrm{Im} \int_{-\sigma_{0,\epsilon}}^{2\pi - \sigma_{0,\epsilon}} \mathrm{e}^{ik_1(\epsilon)(s+\sigma_{0,\epsilon})}\overline{\phi_0^*(s)}\, ds$$

$$= \cos(k_1(\epsilon)\sigma_{0,\epsilon}) \mathrm{Im} \int_{-\sigma_{0,\epsilon}}^{2\pi - \sigma_{0,\epsilon}} \mathrm{e}^{ik_1(\epsilon)s}\overline{\phi_0^*(s)}\, ds + \sin(k_1(\epsilon)\sigma_{0,\epsilon}) \mathrm{Re} \int_{-\sigma_{0,\epsilon}}^{2\pi - \sigma_{0,\epsilon}} \mathrm{e}^{ik_1(\epsilon)s}\overline{\phi_0^*(s)}\, ds$$

so that assumption (3.7) from Theorem 3.9 becomes

$$\tan(k_1(\epsilon)\sigma_{0,\epsilon}) = \frac{\int_{-\sigma_{0,\epsilon}}^{2\pi-\sigma_{0,\epsilon}} \cos(k_1(\epsilon)s)\,\mathrm{Im}\,\phi_0^*(s) - \sin(k_1(\epsilon)s)\,\mathrm{Re}\,\phi_0^*(s)\,ds}{\int_{-\sigma_{0,\epsilon}}^{2\pi-\sigma_{0,\epsilon}} \sin(k_1(\epsilon)s)\,\mathrm{Im}\,\phi_0^*(s) + \cos(k_1(\epsilon)s)\,\mathrm{Re}\,\phi_0^*(s)\,ds}.$$

One may expect that if (as a result of such a limiting procedure) a bifurcating branch at $k_1 = \lim_{\epsilon\to 0} k_1(\epsilon)$ exists then it bifurcates at $\sigma_0 = \lim_{\epsilon\to 0}\sigma_{0,\epsilon}$ determined from

$$\begin{aligned}
\tan(k_1\sigma_0) &= \lim_{\epsilon\to 0} \frac{\int_{-\sigma_{0,\epsilon}}^{2\pi-\sigma_{0,\epsilon}} \cos(k_1(\epsilon)s)\,\mathrm{Im}\,\phi_0^*(s) - \sin(k_1(\epsilon)s)\,\mathrm{Re}\,\phi_0^*(s)\,ds}{\int_{-\sigma_{0,\epsilon}}^{2\pi-\sigma_{0,\epsilon}} \sin(k_1(\epsilon)s)\,\mathrm{Im}\,\phi_0^*(s) + \cos(k_1(\epsilon)s)\,\mathrm{Re}\,\phi_0^*(s)\,ds} \\
&= \frac{\int_{-\sigma_0}^{2\pi-\sigma_0} s\sin(k_1 s)\,\mathrm{Im}\,\phi_0^*(s) + s\cos(k_1 s)\,\mathrm{Re}\,\phi_0^*(s)\,ds}{\int_{-\sigma_0}^{2\pi-\sigma_0} s\sin(k_1 s)\,\mathrm{Re}\,\phi_0^*(s) - s\cos(k_1 s)\,\mathrm{Im}\,\phi_0^*(s)\,ds}.
\end{aligned}$$

However, this is not supported by our numerical experiments and we have to leave the correct determination of $\sigma_0$ in this case as an open question.

[End of preprint]

## 3.8. Appendix B: Some tailor-made results for the original two-mode equation

Clearly, the a-priori bounds from Theorem 3.14 can be used to obtain bounds for the special case $f(s) = f_0 + f_1 e^{ik_1 s}$. However, we can find tailor-made a-priori bounds in this case. For $f_1 = 0$ they recover the bounds stated in [41] for the one mode equation.

**Theorem 3.23.** *Let $d \in \mathbb{R} \setminus \{0\}, f_0, f_1, \zeta, \omega \in \mathbb{R}$ and $k_1 \in \mathbb{N}$. Then for every solution $u \in H^2_{per}(0, 2\pi)$ of (3.2) the a-priori bounds*

$$\|u\|_2 \le F, \tag{3.39}$$

$$\|u'\|_2 \le A\|u\|_2 + B\sqrt{\|u\|_2} \le AF + B\sqrt{F}, \tag{3.40}$$

$$\|u\|_\infty \le C \tag{3.41}$$

*hold, where*

$$F = F(f_0, f_1) = \sqrt{2\pi}\sqrt{f_0^2 + f_1^2}, \quad A = A(d, f_0, f_1) = \frac{F^2}{2|d|},$$

$$B = B(f_1, k_1) = \sqrt{\sqrt{2\pi}|f_1||k_1|}, \quad C = C(d, f_0, f_1, k_1) = \frac{F}{\sqrt{2\pi}} + \sqrt{2\pi}(AF + B\sqrt{F}).$$

*For $\zeta \operatorname{sign}(d) \ll -\gamma$ these bounds can be improved to*

$$\|u\|_2 \le D, \quad \|u\|_\infty \le \frac{D}{\sqrt{2\pi}} + \sqrt{2\pi}(AD + B\sqrt{D}),$$

*where*

$$D = D(d, f_0, f_1, k_1, \omega, \zeta) = \frac{F + B\sqrt{F}(|\omega| + F^2) + |d|B^2}{(-\zeta \operatorname{sign}(d) - \gamma)_+}$$

*and*

$$\gamma = \gamma(d, f_0, f_1, k_1, \omega) = \begin{cases} |d|A^2 + |\omega|A, & d > 0, \\ |d|A^2 + C^2 + |\omega|A, & d < 0. \end{cases}$$

*Proof.* The proof is divided into five steps.

Step 1. We first prove the $L^2$ estimate

$$\|u\|_2 \le F = \sqrt{2\pi}\sqrt{f_0^2 + f_1^2}. \tag{3.42}$$

To this end we multiply the differential equation (3.2) with $\bar{u}$ to obtain

$$-du''\bar{u} + \mathrm{i}\omega u'\bar{u} + (\zeta - \mathrm{i})|u|^2 - |u|^4 + \mathrm{i}f_0\bar{u} + \mathrm{i}f_1\mathrm{e}^{\mathrm{i}k_1 s}\bar{u} = 0. \tag{3.43}$$

Taking the imaginary part yields

$$-d\operatorname{Im}(u''\bar{u}) + \omega\operatorname{Re}(u'\bar{u}) - |u|^2 + f_0\operatorname{Re}(u) + f_1\operatorname{Re}(\mathrm{e}^{\mathrm{i}k_1 s}\bar{u}) = 0. \tag{3.44}$$

Let $h := |u|^2 - f_0\operatorname{Re}(u) - f_1\operatorname{Re}(\mathrm{e}^{\mathrm{i}k_1 s}\bar{u})$, $H := -d\operatorname{Im}(u'\bar{u}) + \frac{\omega}{2}|u|^2$. Then $H' = h$ by equation (3.44) and $H(0) = H(2\pi)$ by the periodicity of $u$. Hence

$$0 = H(2\pi) - H(0) = \int_0^{2\pi} h\,ds = \int_0^{2\pi} |u|^2 - f_0\operatorname{Re}(u) - f_1\operatorname{Re}(\mathrm{e}^{\mathrm{i}k_1 s}\bar{u})\,ds$$

which implies

$$
\begin{aligned}
\|u\|_2^2 &= \int_0^{2\pi} (f_0 + f_1\cos(k_1 s))\operatorname{Re}(u) + f_1\sin(k_1 s)\operatorname{Im}(u)\,ds \\
&\le \|u\|_2 \left(\int_0^{2\pi} (f_0^2 + f_1^2 + 2f_0 f_1\cos(k_1 s))\,ds\right)^{1/2} \\
&= \sqrt{2\pi}\sqrt{f_0^2 + f_1^2}\|u\|_2 = F\|u\|_2.
\end{aligned}
$$

Step 2. Next we prove

$$\|u'\|_2 \le A\|u\|_2 + B\sqrt{\|u\|_2} \le AF + B\sqrt{F}. \tag{3.45}$$

From (3.2) we may isolate the linear term $u$ and insert its derivative $u'$ into the following

calculation for $\|u'\|_2^2$:

$$
\begin{aligned}
\|u'\|_2^2 &= \operatorname{Re} \int_0^{2\pi} u'\bar{u}' \, ds \stackrel{(3.2)}{=} \operatorname{Re} \int_0^{2\pi} (\mathrm{i}du'' + \omega u' - \mathrm{i}\zeta u + \mathrm{i}|u|^2 u + f_0 + f_1 \mathrm{e}^{\mathrm{i}k_1 s})'\bar{u}' \, ds \\
&= \operatorname{Re} \int_0^{2\pi} \mathrm{i}du'''\bar{u}' + \omega u''\bar{u}' - \mathrm{i}\zeta|u'|^2 + \mathrm{i}(|u|^2 u)'\bar{u}' + \mathrm{i}k_1 f_1 \mathrm{e}^{\mathrm{i}k_1 s}\bar{u}' \, ds \\
&= -d \int_0^{2\pi} (\operatorname{Im}(u''\bar{u}'))' \, ds + \omega \int_0^{2\pi} \left(\frac{1}{2}|u'|^2\right)' ds - \operatorname{Im} \int_0^{2\pi} (|u|^2 u)'\bar{u}' + k_1 f_1 \mathrm{e}^{\mathrm{i}k_1 s}\bar{u}' \, ds \\
&= \int_0^{2\pi} (|u|^2)' \operatorname{Im}(\bar{u}u') + k_1^2 f_1 \operatorname{Re}(\mathrm{e}^{\mathrm{i}k_1 s}\bar{u}) \, ds \\
&= \int_0^{2\pi} \frac{1}{d}(|u|^2)'\left(\frac{\omega}{2}|u|^2 - H\right) + k_1^2 f_1 \operatorname{Re}(\mathrm{e}^{\mathrm{i}k_1 s}\bar{u}) \, ds \\
&= \int_0^{2\pi} \frac{\omega}{4d}(|u|^4)' - \frac{1}{d}(|u|^2)'H + k_1^2 f_1 \operatorname{Re}(\mathrm{e}^{\mathrm{i}k_1 s}\bar{u}) \, ds \\
&= \int_0^{2\pi} -\frac{1}{d}(|u|^2)'(H - H(0)) + k_1^2 f_1 \operatorname{Re}(\mathrm{e}^{\mathrm{i}k_1 s}\bar{u}) \, ds.
\end{aligned}
$$

Next notice the pointwise estimate

$$
\begin{aligned}
h &= |u|^2 - f_0 \operatorname{Re}(u) - f_1 \operatorname{Re}(\mathrm{e}^{\mathrm{i}k_1 s}\bar{u}) \\
&= |u|^2 - \operatorname{Re}((f_0 + f_1 \mathrm{e}^{\mathrm{i}k_1 s})\bar{u}) \geq |u|^2 - |f_0 + f_1 \mathrm{e}^{\mathrm{i}k_1 s}||u| \\
&\geq -\frac{1}{4}|f_0 + f_1 \mathrm{e}^{\mathrm{i}k_1 s}|^2
\end{aligned}
$$

from which we deduce the following two-sided estimate for $H - H(0)$:

$$
H(s) - H(0) = \int_0^s h(r) \, dr \geq -\frac{\pi}{2}(f_0^2 + f_1^2) \quad (s \in [0, 2\pi]) \quad \text{and}
$$

$$
H(s) - H(0) = H(s) - H(2\pi) = -\int_s^{2\pi} h(r) \, dr \leq \frac{\pi}{2}(f_0^2 + f_1^2) \quad (s \in [0, 2\pi]).
$$

Continuing the above expression for $\|u'\|_2^2$ we conclude

$$
\|u'\|_2^2 \leq \frac{\pi(f_0^2 + f_1^2)}{|d|}\|u\|_2\|u'\|_2 + \sqrt{2\pi}k_1^2|f_1|\|u\|_2 = A\|u\|_2\|u'\|_2 + B^2\|u\|_2.
$$

This is a quadratic inequality in $\|u'\|_2$ which implies

$$
\|u'\|_2 \leq \frac{A\|u\|_2 + \sqrt{A^2\|u\|_2^2 + 4B^2\|u\|_2}}{2} \leq A\|u\|_2 + B\sqrt{\|u\|_2}
$$

as claimed.

Step 3. Here we prove
$$\|u\|_\infty \le C. \tag{3.46}$$
By (3.42) there exists $s_1 \in [0, 2\pi]$ satisfying $|u(s_1)| \le \frac{F}{\sqrt{2\pi}}$. The claim now follows from

$$\|u\|_\infty \le |u(s_1)| + \sup_{s\in[0,2\pi]} |u(s) - u(s_1)| \le \frac{F}{\sqrt{2\pi}} + \|u'\|_1 \le \frac{F}{\sqrt{2\pi}} + \sqrt{2\pi}\|u'\|_2 \overset{(3.45)}{\le} C.$$

Step 4. Next we show in the case $\zeta \operatorname{sign}(d) < -\gamma$ the additional $L^2$-bound

$$\|u\|_2 \le D. \tag{3.47}$$

After integrating (3.43) over $[0, 2\pi]$ and taking the real part of the resulting equation we get

$$d\|u'\|_2^2 = \omega \int_0^{2\pi} \operatorname{Im}(u'\bar{u})\,ds - \zeta\|u\|_2^2 + \|u\|_4^4 - f_0 \int_0^{2\pi} \operatorname{Im}(u)\,ds - f_1 \int_0^{2\pi} \operatorname{Im}(e^{-ik_1 s}u)\,ds$$

$$= \omega \int_0^{2\pi} \operatorname{Im}(u'\bar{u})\,ds - \zeta\|u\|_2^2 + \|u\|_4^4$$

$$+ \int_0^{2\pi} f_1 \sin(k_1 s)\operatorname{Re}(u) - (f_0 + f_1\cos(k_1 s))\operatorname{Im}(u)\,ds.$$

In order to prove (3.47) we first suppose $d > 0$. Then we have on one hand

$$d\|u'\|_2^2 \overset{(3.45)}{\le} d\left(A\|u\|_2 + B\sqrt{\|u\|_2}\right)^2 = dA^2\|u\|_2^2 + 2dAB\|u\|_2^{\frac{3}{2}} + dB^2\|u\|_2$$

$$\overset{(3.42)}{\le} dA^2\|u\|_2^2 + 2dAB\sqrt{F}\|u\|_2 + dB^2\|u\|_2 \tag{3.48}$$

and on the other hand

$$\omega \int_0^{2\pi} \operatorname{Im}(u'\bar{u})\,ds - \zeta\|u\|_2^2 + \|u\|_4^4 + \int_0^{2\pi} f_1\sin(k_1 s)\operatorname{Re}(u) - (f_0 + f_1\cos(k_1 s))\operatorname{Im}(u)\,ds$$

$$\ge -|\omega|\|u\|_2\|u'\|_2 - \zeta\|u\|_2^2 - F\|u\|_2$$

$$\overset{(3.45)}{\ge} -|\omega|A\|u\|_2^2 - |\omega|B\|u\|_2^{\frac{3}{2}} - \zeta\|u\|_2^2 - F\|u\|_2$$

$$\overset{(3.42)}{\ge} -|\omega|A\|u\|_2^2 - |\omega|B\sqrt{F}\|u\|_2 - \zeta\|u\|_2^2 - F\|u\|_2. \tag{3.49}$$

Combining the two estimates (3.48), (3.49) and grouping quadratic terms and linear terms of $\|u\|_2$ on separate sides of the inequality we get

$$(-\zeta - dA^2 - |\omega|A)\|u\|_2^2 \le \left(F + B\sqrt{F}(|\omega| + \underbrace{2dA}_{=F^2}) + dB^2\right)\|u\|_2$$

which finally implies $\|u\|_2 \le D$ whenever $\zeta < -\gamma$. Assuming now $d < 0$ the estimate (3.48) becomes

$$d\|u'\|_2^2 \ge -|d|A^2\|u\|_2^2 - 2|d|AB\sqrt{F}\|u\|_2 - |d|B^2\|u\|_2 \tag{3.50}$$

whereas in (3.49) the term $\|u\|_4^4$, which was previously dropped, now has to be estimated by $\|u\|_4^4 \le \|u\|_\infty^2\|u\|_2^2 \le C^2\|u\|_2^2$ with $C$ from step 3. The estimate (3.49) now becomes

$$\omega\int_0^{2\pi} \mathrm{Im}(u'\bar{u})\,ds - \zeta\|u\|_2^2 + \|u\|_4^4 + \int_0^{2\pi} f_1\sin(k_1 s)\,\mathrm{Re}(u) - (f_0 + f_1\cos(k_1 s))\,\mathrm{Im}(u)\,ds$$
$$\le |\omega|A\|u\|_2^2 + |\omega|B\sqrt{F}\|u\|_2 + (C^2 - \zeta)\|u\|_2^2 + F\|u\|_2. \tag{3.51}$$

The combination of (3.23) and (3.51) leads to

$$(\zeta - |d|A^2 - C^2 - |\omega|A)\|u\|_2^2 \le \left(F + B\sqrt{F}(|\omega| + F^2) + |d|B^2\right)\|u\|_2$$

which again implies $\|u\|_2 \le D$ whenever $-\zeta < -\gamma$.

Step 5. Finally we prove

$$\|u\|_\infty \le \frac{D}{\sqrt{2\pi}} + \sqrt{2\pi}(AD + B\sqrt{D}) \tag{3.52}$$

whenever $\zeta\,\mathrm{sign}(d) < -\gamma$. For this we repeat step 3 and use instead of $\|u\|_2 \le F$ the estimate $\|u\|_2 \le D$. $\qquad\square$

Based on Theorem 3.23 we can also find a uniqueness result which is tailor-made for the case $f(s) = f_0 + f_1\mathrm{e}^{\mathrm{i}k_1 s}$. For that let us rewrite the constant $D$ from Theorem 3.23 as

$$D = D(d, f_0, f_1, k_1, \omega, \zeta) = \frac{\tilde{D}}{(-\zeta\,\mathrm{sign}(d) - \gamma)_+}$$

with

$$\tilde{D} = \tilde{D}(d, f_0, f_1, k_1, \omega) = F + B\sqrt{F}(|\omega| + F^2) + |d|B^2.$$

**Theorem 3.24.** *Let $d \in \mathbb{R} \setminus \{0\}$, $f_0, f_1, \zeta, \omega \in \mathbb{R}$ and $k_1 \in \mathbb{N}$. Then (3.2) has a unique solution $u \in H_{per}^2(0, 2\pi)$ in the following three cases,*

*(i)*
$$\mathrm{sign}(d)\zeta < \zeta_*,$$

*(ii)*
$$\mathrm{sign}(d)\zeta > \zeta^*,$$

*(iii)*
$$\sqrt{3}C < 1,$$

*where $\zeta_* \leq 0 \leq \zeta^*$ are given by*

$$\zeta_* = \zeta_*(d, f_0, f_1, k_1, \omega) = -\gamma - \frac{\tilde{D}(1 + 2\pi A)^2}{\left(\sqrt{\pi^2 B^2 + \sqrt{\frac{2}{3}\pi}(1 + 2\pi A)} - \pi B\right)^2},$$

$$\zeta^* = \zeta^*(d, f_0, f_1, k_1, \omega) = 3C^2 + \frac{\omega^2}{4|d|}$$

*and $A = A(d, f_0, f_1), B = B(f_1, k_1), C = C(d, f_0, f_1, k_1), \gamma = \gamma(d, f_0, f_1, k_1, \omega)$ are the constants from Theorem 3.23.*

*Proof.* The proof is very similar to that of Theorem 3.17. We only need to adjust the definition of $R$ in the following way,

$$R = R(d, f_0, f_1, k_1, \omega, \zeta) = \begin{cases} \min\left\{C, \frac{D}{\sqrt{2\pi}} + \sqrt{2\pi}(AD + B\sqrt{D})\right\}, & \zeta\operatorname{sign}(d) + \gamma < 0, \\ C, & \zeta\operatorname{sign}(d) + \gamma \geq 0, \end{cases}$$

and need to slightly modify the calculation made for the case (i). For this, note that it can be checked that for $f_0^2 + f_1^2 \neq 0$ the value $-\zeta_* - \gamma$ is the unique positive zero of the strictly decreasing map

$$t \mapsto 3\left(\frac{(1 + 2\pi A)\tilde{D}}{\sqrt{2\pi t}} + \sqrt{2\pi}B\sqrt{\frac{\tilde{D}}{t}}\right)^2 - 1.$$

Then, in case (i) where $\operatorname{sign}(d)\zeta < \zeta_* < -\gamma < 0$ we use $\|L^{-1}\| \leq 1$ and find by the definition of $R$ and $\zeta_*$ that

$$3R^2\|L^{-1}\| \leq 3\left(\frac{D}{\sqrt{2\pi}} + \sqrt{2\pi}(AD + B\sqrt{D})\right)^2$$

$$= 3\left(\frac{1 + 2\pi A}{\sqrt{2\pi}} \cdot \frac{\tilde{D}}{-\zeta\operatorname{sign}(d) - \gamma} + \sqrt{2\pi}B\sqrt{\frac{\tilde{D}}{-\zeta\operatorname{sign}(d) - \gamma}}\right)^2$$

$$< 3\left(\frac{1 + 2\pi A}{\sqrt{2\pi}} \cdot \frac{\tilde{D}}{-\zeta_* - \gamma} + \sqrt{2\pi}B\sqrt{\frac{\tilde{D}}{-\zeta_* - \gamma}}\right)^2 = 1.$$

$\square$

# 4. Bandwidth and conversion-efficiency analysis of Kerr soliton combs in dual-pumped resonators with anomalous dispersion

This section consists of the preprint [22]. The mentioned preprint is joint work with Christian Koos, Huanfa Peng and Wolfgang Reichel and was adapted in order to fit the layout and the structure of this thesis. In contrast to the remaining parts of this thesis we use the notation $\|u\|_2^2 = \frac{1}{2\pi} \int_0^{2\pi} |u(s)|^2 \, ds$ in this section.

[Start of preprint]

E. Gasmi, H. Peng, C. Koos, and W. Reichel

Kerr frequency combs generated in high-Q microresonators offer an immense potential in many applications, and predicting and quantifying their behavior, performance and stability is key to systematic device design. Based on an extension of the Lugiato-Lefever equation we investigate in this paper the perspectives of changing the pump scheme from the well-understood monochromatic pump to a dual-tone configuration simultaneously pumping two modes. For the case of anomalous dispersion we give a detailed study of the optimal choices of detuning offsets and division of total pump power between the two modes in order to optimize single-soliton comb states with respect to performance metrics like power conversion efficiency and bandwidth. Our approach allows also to quantify the performance metrics of the optimal single-soliton comb states and determine their trends over a wide range of technically relevant parameters.

## 4.1. Introduction and main results

Optical frequency combs have revolutionized many applications, comprising optical frequency metrology [65], spectroscopy [53, 72], optical frequency synthesizer [34, 58], optical atomic clocks [46], ultrafast optical ranging [64], and high-capacity optical communications using massively parallel wavelength-division multiplexing (WDM) [42]. The recent and rapid development of chip-scale Kerr soliton comb generators offers the prospects of realizing highly integrated devices which offer compactness, portability, and robustness, while being amenable to mass production and featuring low power consumption [37]. Whereas Kerr soliton combs have conventionally been generated by using a monochromatic pump, dual-tone pumping configurations permit to achieve threshold-less comb generation in both normal and anomalous dispersion regimes [29, 38], while stabilizing the comb-tone spacing to a well-defined frequency [47, 61]. The dual mode pumping scheme can be implemented either by using a phase- or intensity-modulated continuous-wave laser or two lasers with different wavelengths. Prior works theoretically investigated the dynamical properties of dissipative cavity soliton generation in a dual-mode-pumped Kerr microresonator by using the Lugiato-Lefever equation (LLE) with

the addition of a secondary pump term [69]. However, a comprehensive study of the optimal pumping conditions for attaining the broadest comb bandwidth and the highest power conversion efficiency in the anomalous dispersion regime is still lacking.

In this paper we study a variant of the LLE based on a modification for dual-tone pumping [62], and we use this equation for a more detailed study of the benefits of dual-tone pumping. Focussing on resonators with anomalous dispersion, we find that dual-tone pumping allows to significantly improve key performance metrics of Kerr frequency combs such as bandwidth and power conversion efficiency. Mathematically, Kerr comb dynamics with a single pumped mode have been described by the LLE, a damped, driven and detuned nonlinear Schrödinger equation [39, 26, 48]. Our modification of the LLE arises due to a forcing term which describes the pumping of two resonator modes instead of only a single one.

Using this equation as a base, we exploit numerical path continuation methods for a more detailed analysis of comb properties, the results of which can be summarized as follows:

(1) We show that pumping two modes is advantageous to pumping only one mode.

(2) We present heuristic insights for finding the optimal detuning parameters that provide the most localized single-soliton states.

(3) We determined the optimal power distribution between the two pumped modes, which corresponds to a symmetric distribution where 50% of the power is pumped into each mode[3]. This power distribution simultaneously optimizes all performance metrics (comb bandwidth, full-width at half-maximum in time domain, and power conversion efficiency) in case equal detuning offsets between pump tones and nearest resonant modes are used.

(4) Under optimal power distribution we determined trends of the performance metrics w.r.t. varying dispersion and normalized total pump power.

This paper is organized as follows: In Section 4.2 we introduce the Lugiato-Lefever model for a dual-pumped ring resonator. In Section 4.3 we present the main ideas for finding localized solitons in the case of pumping two adjacent modes. Section 4.4 is dedicated to the determination of the optimal power distribution between the two pumped modes. Here we use the comb bandwidth, the power conversion efficiency and the full-width at half-maximum as performance metrics. In Section 4.5 we provide trends for varying dispersion/forcing of this performance metrics under the provision of optimal equal power distribution between the two pumped modes. In Section 4.6 we describe the optimal solitons achieved by pumping two arbitrarily distanced modes. Appendix A is dedicated to the derivation of the Lugiato-Lefever model for a dual-pumped ring resonator. In Appendix B we explain the details of the heuristic algorithm for finding

---

[3]For purposes of simplifying the analysis this was exactly the case discussed by the authors in [29]. Our findings validate their assumption of the pumps having equal amplitude and phase detuning.

localized solitons in the case of pumping two adjacent modes and Appendix C contains the heuristic for the case of pumping two arbitrarily distanced modes.

## 4.2. Lugiato-Lefever model for a dual-pumped ring resonator

Kerr comb dynamics are described by the LLE, a damped, driven and detuned nonlinear Schrödinger equation [39, 26, 48]. As in [62] we use a variant of the LLE modified for two-mode pumping, for which we provide a derivation of equation (4.1) starting from a system of nonlinear coupled mode equations in physical quantities in Appendix A. Using dimensionless, normalized quantities, this equation takes the form

$$\mathrm{i}\frac{\partial a}{\partial \tau} = -da'' - (\mathrm{i} - \zeta_0)a - |a|^2 a + \mathrm{i}f_0 + \mathrm{i}f_1 \mathrm{e}^{\mathrm{i}(k_1 x - \nu_1 \tau)}. \tag{4.1}$$

Here, $a(\tau, x)$ is $2\pi$-periodic in $x$ and represents the optical intracavity field as a function of normalized time $\tau = \kappa t/2$ and angular position $x \in [0, 2\pi]$ within the ring resonator. The constant $\kappa > 0$ describes the cavity decay rate and $d = 2d_2/\kappa > 0$ quantifies the anomalous dispersion in the system ($2d_2$ corresponds to the difference between two neighboring FSRs at the center frequency $\omega_0$). Since the numbering $k \in \mathbb{Z}$ of the resonant modes in the cavity is relative to the first pumped mode $k_0 = 0$ we denote with $k_1 \in \mathbb{N}$ the second pumped mode (there is no loss of generality to take $k_1$ as a positive integer since $k_1$ and $-k_1$ are symmetric modes). Since there are now two pumped modes there will also be two normalized detuning parameters denoted by $\zeta_0 = 2(\omega_0 - \omega_{p_0})/\kappa$ and $\zeta_1 = 2(\omega_{k_1} - \omega_{p_1})/\kappa$. They describe the offsets of the input pump frequencies $\omega_{p_0}$ and $\omega_{p_1}$ to the closest resonance frequency $\omega_0$ and $\omega_{k_1}$ of the microresonator, respectively. Finally $f_0, f_1$ represent the normalized power of the input pumps. If we set $\Delta\zeta = \zeta_0 - \zeta_1$ and $\nu_1 = \Delta\zeta + dk_1^2$ then (after several transformations, cf. Appendix A) equation (4.1) emerges with the specific form of the second pump $f_1 \mathrm{e}^{\mathrm{i}(k_1 x - \nu_1 \tau)}$.

In the case $f_1 = 0$, equation (4.1) amounts to the case of pumping only one mode. This case has been thoroughly studied, e.g. in [18, 26, 25, 49, 50, 48, 41, 43, 11, 51]. In this paper we are interested in the case $f_1 \neq 0$. The particular form of the pump term $\mathrm{i}f_0 + \mathrm{i}f_1 \mathrm{e}^{\mathrm{i}(k_1 x - \nu_1 \tau)}$ suggests to perform a change of variables into a moving coordinate $s = x - \omega\tau$ with $\omega = \nu_1/k_1$ and study solutions of (4.1) of the form $a(\tau, x) = u(x - \omega\tau)$. These traveling-wave solutions propagate with speed $\omega$ in the resonator, and their profile $u$ solves the stationary ordinary differential equation

$$-du'' + \mathrm{i}\omega u' - (\mathrm{i} - \zeta_0)u - |u|^2 u + \mathrm{i}f_0 + \mathrm{i}f_1 \mathrm{e}^{\mathrm{i}k_1 s} = 0, \tag{4.2}$$

where $u$ is again $2\pi$-periodic in $s$. In Fourier modes $a$ and $u$ are represented as $a(\tau, x) = \sum_{k \in \mathbb{Z}} \hat{a}_k(\tau) \mathrm{e}^{\mathrm{i}kx}$, $u(s) = \sum_{k \in \mathbb{Z}} \hat{u}_k \mathrm{e}^{\mathrm{i}ks}$. The intracavity power $P$ of the field $a$ at time $\tau$ is given by

$$P = \sum_{k \in \mathbb{Z}} |\hat{a}_k(\tau)|^2 = \frac{1}{2\pi} \int_0^{2\pi} |a(\tau, x)|^2 \, dx.$$

Since the Fourier modes of $a$ and $u$ are related by $\hat{a}_k(\tau) = \hat{u}_k \mathrm{e}^{-\mathrm{i}k\omega\tau}$ one finds $P =$

$\sum_{k \in \mathbb{Z}} |\hat{u}_k|^2 = \frac{1}{2\pi} \int_0^{2\pi} |u(s)|^2 \, ds$. In particular, $P$ is independent[4] of the time, and since $\int_0^{2\pi} |u|^2 \, ds = \mathrm{Re} \int_0^{2\pi} (f_0 + f_1 e^{ik_1 s}) \bar{u} \, ds$ we see that $P \leq f^2 := f_0^2 + f_1^2$, i.e., the intracavity power cannot exceed the normalized total input power. Details are given at the end of Appendix A. Here, the notation $\bar{z}$ denotes the complex conjugate of the complex number $z \in \mathbb{C}$.

## 4.3. Heuristic for finding localized solitons in the case of pumping two adjacent modes

In the following section, we explain the main idea of the heuristic for finding strongly localized solutions of (4.2), where two adjacent modes are pumped, i.e. the pumped modes are $k_0 = 0$ and $k_1 = 1$. In Appendix B we provide a more detailed explanation, and in Appendix C we show how the heuristic can be adapted to arbitrary values of $k_1 \in \mathbb{N}$. The parameters $d > 0$, $k_1 = 1$, $f_0$ and $f_1$ are fixed, and our goal is to find optimally localized solutions by varying the parameters $\zeta_0$ and $\omega$ since they can be influenced by the choice of the pump frequencies $\omega_{p_0}$ and $\omega_{p_1}$ through the relations

$$\zeta_0 = \frac{2}{\kappa}\big(\omega_0 - \omega_{p_0}\big), \ \omega = \frac{2}{\kappa}\big(\omega_0 - \omega_{p_0} - (\omega_1 - \omega_{p_1}) + d_2\big).$$

Optimality is understood as minimality with respect to the full-width at half-maximum (FWHM) of the field distribution $|u|^2$ in the time domain. We have developed our heuristic by using the Matlab package `pde2path` (cf. [67], [15]) which has been designed to numerically treat continuation and bifurcation in boundary value problems for systems of PDEs.[5]

In short, the basic algorithm is explained as follows: First we obtain a single-peak solution for the correct value of the parameter $f_1$ (ignoring the values of the parameters $\zeta_0$ and $\omega$). Then we alternately run a continuation algorithm by varying either the $\zeta_0$- or the $\omega$-parameter (while keeping the other parameter fixed) and detect among the continued solutions the soliton $u$ with minimal FWHM of $|u|^2$ in the time domain. We denote the soliton obtained from the $j$-th $\zeta_0$-optimization as $A_j$ and the one obtained from the $j$-th $\omega$-optimization as $B_j$. We stop the algorithm when the relative change of the FWHM of $B_{j+1}$ and $B_j$ is sufficiently small. In our numerical experiments it was always sufficient to perform at most three optimizations in both of the variables $\zeta_0$ and $\omega$.

In Fig. 15(a)-(c) we plotted the spatial power distributions of the solitons $A_j$ and $B_j$ for two iteration steps $j = 1, 2$ and three different choices of the parameters $d$, $f$ and $f_1$. It is well visible that the solitons get more localized after every optimization step and

---

[4]In fact, the power $|\hat{u}_k|^2 = |\hat{a}_k(\tau)|^2$ in each mode is independent of time.

[5]Continuation and bifurcation solvers for boundary value problems (on which `pde2path` is based) allow to globally study the variety of different stationary comb states by exploiting the full range of technically available parameters. In contrast, time-integration solvers mostly only allow to access specific comb states which strongly depend on the chosen device parameters and initial conditions.
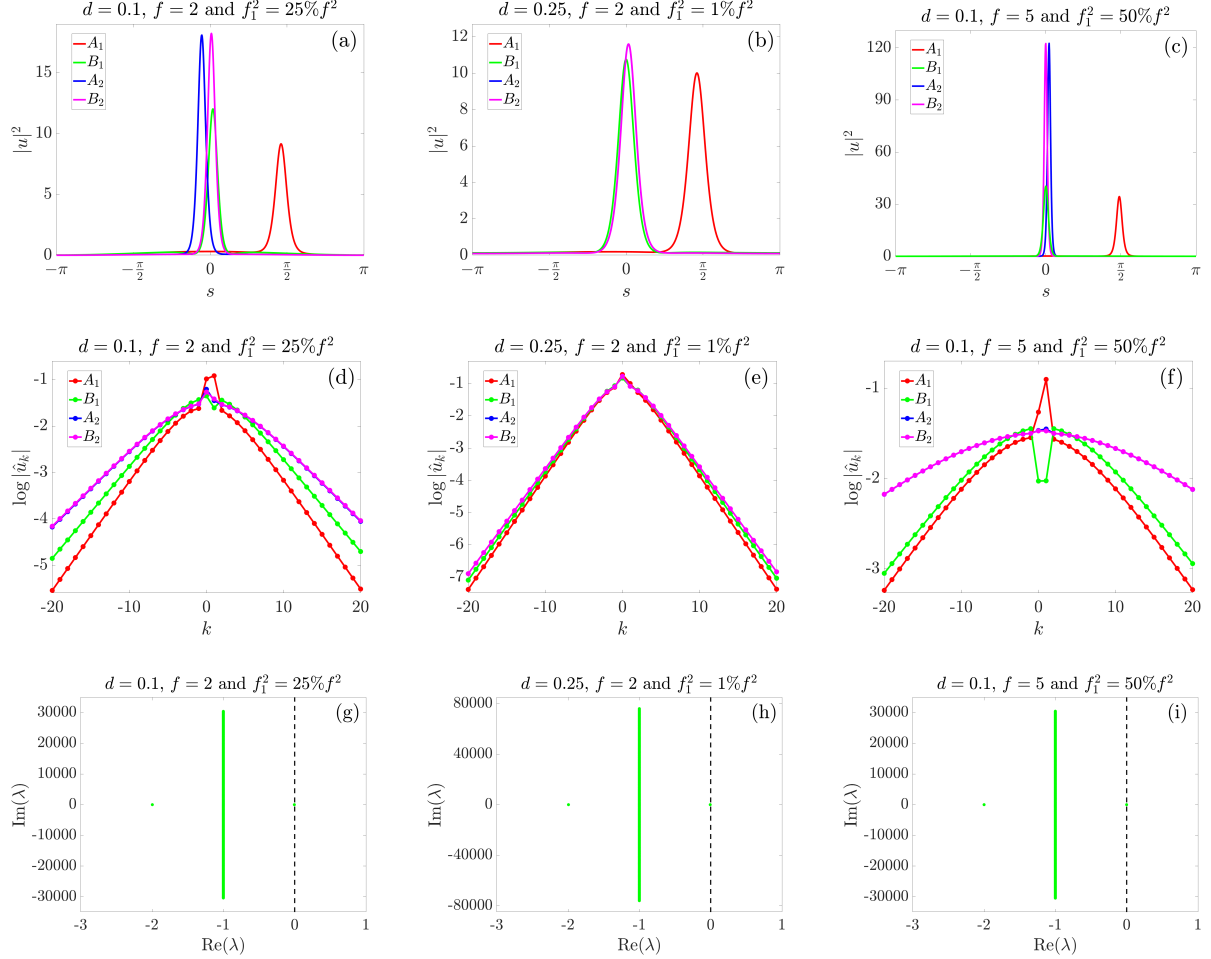
Figure 15. Spatial and spectral power distributions of the solitons obtained from two iterations (two $\zeta_0$-steps leading to $A_1$, $A_2$ and two $\omega$-steps leading to $B_1$, $B_2$) and a stability plot for $B_3$ (obtained from the third $\omega$-step) for three different choices of the parameters $d$, $f$ and $f_1$. Every column corresponds to one choice. In (g)-(i) we plotted in green the spectrum of the finite-element discretization of the linearized operator $L$ at $B_3$. The black dashed line in (g)-(i) represents the imaginary axis. The spectrum lies to the left of the imaginary axis so that the solitons are spectrally stable.

that the solitons $A_2$ and $B_2$ from the second iteration steps do not differ significantly. In the second column of Fig. 15 in (b) and (e) the blue soliton $A_2$ is not visible, since it is covered by the almost identical magenta soliton $B_2$. In the second row Fig. 15(d)-(f) we show the spectral power distributions. The final magenta comb $B_2$ covers almost entirely the blue comb $A_2$. The third row of Fig. 15 contains information on the spectral stability of the optimized solitons. This will be explained next.

*Stability of optimal solitons.* To investigate the stability of the solitons, we use the transformation $a(\tau, x) = b(\tau, x - \omega\tau)$ to rewrite (4.1) as

$$\frac{\partial b}{\partial \tau} = -\mathrm{i}\big(-db'' + \mathrm{i}\omega b' - (\mathrm{i} - \zeta_0)b - |b|^2 b + \mathrm{i}f_0 + \mathrm{i}f_1 \mathrm{e}^{\mathrm{i}k_1 s}\big), \qquad (4.3)$$

where $b$ is again $2\pi$-periodic in $s$. Solutions $u$ of (4.2) correspond to stationary solutions $b(\tau, s) = u(s)$ of (4.3). Spectral stability is based on the following considerations. Let $b(\tau, s) \approx u(s) + \phi(s)\mathrm{e}^{\lambda\tau} + \psi(s)\mathrm{e}^{\bar{\lambda}\tau}$ with $2\pi$-periodic functions $\phi, \psi$, and insert this ansatz into (4.3). After keeping only the linear terms in $\phi$ and $\psi$, we find that $\phi, \psi$ have to satisfy the eigenvalue equation

$$L\begin{pmatrix} \phi \\ \bar{\psi} \end{pmatrix} = \lambda \begin{pmatrix} \phi \\ \bar{\psi} \end{pmatrix}$$

with the linearized operator

$$L = \begin{pmatrix} \mathrm{i}d\frac{d^2}{ds^2} + \omega\frac{d}{ds} - 1 - \mathrm{i}\zeta + 2\mathrm{i}|u|^2 & \mathrm{i}u^2 \\ -\mathrm{i}\bar{u}^2 & -\mathrm{i}d\frac{d^2}{ds^2} + \omega\frac{d}{ds} - 1 + \mathrm{i}\zeta - 2\mathrm{i}|u|^2 \end{pmatrix}.$$

We see that the perturbation $\phi(s)\mathrm{e}^{\lambda\tau} + \psi(s)\mathrm{e}^{\bar{\lambda}\tau}$ will tend to zero if and only if the eigenvalues $\lambda$ of $L$ lie in the left complex plane. Using this criterion, we found that the optimized solitons (optimized w.r.t. $\zeta_0$ and $\omega$ by the above heuristic) discussed in this section are all spectrally stable. To show this, we computed the eigenvalues of the finite-element discretization of the operator $L$ and observed that they entirely belong to the left complex plane, cf. Fig. 15(g)-(i). One sees that there is always an eigenvalue very close to 0. The reason for this is the following. The optimized solitons are found near turning points along branches of the $\zeta_0$-continuation, cf. Appendix B. These turning points are necessarily associated with a 0 eigenvalue of the linearized operator $L$. Hence, for $u$ being in the vicinity of a turning point, there will be an eigenvalue of $L$ very close to 0.

## 4.4. Optimal power distribution when pumping two adjacent modes

In this section we answer the question which amount of the normalized total input power $f^2 = f_0^2 + f_1^2$ needs to be pumped into each mode in order to obtain the best soliton, i.e., we determine the optimal power distribution between the two pumped modes. The power distribution is described as $(f_0, f_1) = (f\cos\varphi, f\sin\varphi)$ with $\varphi \in [0, 2\pi)$. As before, we assume anomalous dispersion $d > 0$ and fix the indices $k_0 = 0$ and $k_1 = 1$ of the two

pumped modes. Additionally, the normalized total input power $f^2$ is given. Armed with the heuristic from Section 4.3 we are able to identify for any fixed $\varphi \in [0, 2\pi)$ a 1-soliton with the strongest spatial localization, i.e., with minimal FWHM.

Using this approach, we calculate for each such a comb state $u(s) = \sum_{k \in \mathbb{Z}} \hat{u}_k e^{iks}$ the power conversion efficiency (PCE), the comb bandwidth (CBW) and its FWHM. The PCE is defined as the ratio $P_{\mathrm{FC}}/f^2$ between intracavity comb power

$$
\begin{aligned}
P_{\mathrm{FC}} &= \sum_{k \in \mathbb{Z} \backslash \{0,1\}} |\hat{u}_k|^2 + \frac{f_1^2}{f^2} |\hat{u}_0|^2 + \frac{f_0^2}{f^2} |\hat{u}_1|^2 \\
&= \sum_{k \in \mathbb{Z} \backslash \{0,1\}} |\hat{u}_k|^2 + \sin^2(\varphi) |\hat{u}_0|^2 + \cos^2(\varphi) |\hat{u}_1|^2
\end{aligned}
$$

and the normalized total input power. Note that the intracavity comb power is a weighted sum over the power in each mode. The weights $f_j^2/f^2$, $j = 0, 1$ of the power of the zero mode and the first mode are such that $f_1 = 0$ or $f_0 = 0$ lead to the usual definition of PCE and $f_0 \to \infty$ or $f_1 \to \infty$ lead to an exclusion of the power contributed by the zero or first mode, respectively. The CBW is defined via the 3dB points, i.e.,

$$
\mathrm{CBW} = k_l^* + k_r^*
$$

with minimal integers $k_l^* > 0$ and $k_r^* > 0$ which fulfill

$$
|\hat{u}_{-k_l^*}|^2 \leq \frac{1}{2} |\hat{u}_{-1}|^2, \quad |\hat{u}_{1+k_r^*}|^2 \leq \frac{1}{2} |\hat{u}_2|^2,
$$

respectively. Note that the 3dB comb bandwidth is defined with respect to the power $|\hat{u}_{-1}|^2$ and $|\hat{u}_2|^2$ of the modes directly adjacent to the pumped modes rather than the power $|\hat{u}_0|^2$ and $|\hat{u}_1|^2$ of the pumped modes themselves.

To find the optimal power distribution between the zero mode and the first mode we performed a parameter study in $\varphi$ for three different examples, cf. Fig. 16. In the first example we chose $d = 0.1$ and $f = 2$, in the second example we kept $f = 2$ but changed the dispersion to $d = 0.25$ while in the last example we kept $d = 0.1$ and changed the forcing to $f = 5$. For these three examples we computed the most localized 1-soliton for $\varphi \in [0, 2\pi)$ based on the heuristic of Section 4.3 and evaluated the PCE, the CBW as well as the FWHM of the resulting comb state.

The results depicted in Fig. 16 clearly demonstrate the advantages of dual-tone pumping, in particular when using equal power in both modes. In all of the examples PCE and CBW increase while the FWHM decreases with $\varphi \in [0, \pi/4]$. Moreover, as we will explain at the end of this section, PCE, CBW and FWHM are $\pi/2$-periodic and symmetric w.r.t. $\pi/4$. We conclude that

  (i)  pumping two modes is advantageous to pumping only one mode,

  (ii)  PCE, CBW and FWHM are monotonic functions of $|f_0| + |f_1| = |f|(|\cos\varphi| + |\sin\varphi|)$,

(iii) the optimal case arises for equal pump powers $|f_0| = |f_1|$.

In Fig. 17(a)-(b) we plotted the optimal values of $\zeta_0$ and $\omega$ (for which the most localized soliton was found) against $\varphi$. Since $k_1 = 1$ we have $\omega = \Delta\zeta + d$ so that the optimal value of $\omega$ can be easily translated into an optimal value of $\Delta\zeta$. We added in Fig. 17(c) a plot of the optimal value of $\Delta\zeta$ against $\varphi$ since the normalized detuning difference $\Delta\zeta = \zeta_0 - \zeta_1$ is the physically more tangible quantity while from a mathematical point of view it is more convenient to work with $\omega$. In all of the examples the optimal values of $\zeta_0$, $\omega$ and $\Delta\zeta$ increase with $\varphi \in (0, \pi/4]$. Once again we observe several symmetries, which we will address in the end of this section. We further conclude that

(iv) the optimal value of $\zeta_0$ is almost independent of $d$,

(v) the optimal value of $\omega$ is almost independent of $f$,

(vi) the optimal value of $\omega$ coincides with the dispersion $d$ in case of optimal power distribution $|f_0| = |f_1|$.

As $\omega = \Delta\zeta + d$, (vi) means $\Delta\zeta = 0$, i.e., optimal solitons require equal detuning distances $\omega_0 - \omega_{p_0} = \omega_1 - \omega_{p_1}$ in case of equal power distribution $|f_0| = |f_1|$. From Fig. 17(c) we further find that the optimal values for $\zeta_0$ and $\zeta_1$ satisfy the relation $|f_0| > |f_1| \Leftrightarrow \zeta_0 < \zeta_1$, i.e., pumping more power into one mode is compensated by a larger detuning for the second mode.

For each of the three examples from Fig. 16 and Fig. 17 we added in Fig. 18 plots of the spatial and spectral power distributions of the optimal solitons for selected values of $\varphi \in [0, \pi/4]$. In this range for $\varphi$ we have $f_0, f_1 \geq 0$. The particular values of $\varphi$ are chosen as $f_0^2 = 100\% f^2$ (one mode case), $f_0^2 = 90\% f^2$ (slight perturbation of the one mode case), and $f_0^2 = 50\% f^2$ (optimal two mode case). Since for $f_1 > 0$ there is no shift-invariance in (4.2) anymore all of the depicted solitons are localized around $s = 0$, which is the unique point in the interval $[0, 2\pi)$ where the absolute value of the pump term is maximal, i.e., $f_0 + f_1 = \max_{s \in [0, 2\pi)} |\mathrm{i}f_0 + \mathrm{i}f_1 \mathrm{e}^{\mathrm{i}s}|$. In other words: the best soliton positions its maximum at the point where the pump has maximal absolute value.

Finally, we explain the symmetry properties of Fig. 16 and Fig. 17 from the symmetries of (4.2). If $u$ solves (4.2) then $u(\cdot + \pi)$ solves (4.2) with $f_1$ replaced by $-f_1$ and $-u(\cdot + \pi)$ solves (4.2) with $f_0$ replaced by $-f_0$. This means that the signs of $f_0$ and $f_1$ are not relevant for the curves in Fig. 16 and Fig. 17. The symmetry with respect to $\pi/4$ of the curves in Fig. 16 stems from the interchangeability of $f_0$ and $f_1$. Namely, if $u$ solves (4.2) with given values of $\zeta_0, \omega$ then $v(s) := u(-s)\mathrm{e}^{\mathrm{i}s}$ solves

$$-dv'' + \mathrm{i}\widetilde{\omega}v' - (\mathrm{i} - \zeta_1)v - |v|^2 v + \mathrm{i}f_1 + \mathrm{i}f_0 \mathrm{e}^{\mathrm{i}s} = 0$$

with $\zeta_1 = \zeta_0 - \omega + d$ and $\widetilde{\omega} = 2d - \omega$. Note that the roles of $f_0$ and $f_1$ are now interchanged. The fact that $\zeta_0$ and $\omega$ have changed to $\zeta_1$ and $\widetilde{\omega}$ is not relevant since we optimize anyway in these parameters. Together with (vi) this also explains that the curves in Fig. 17(b) and Fig. 17(c) are odd with respect to the points $(\pi/4, d)$ and $(\pi/4, 0)$, respectively. We
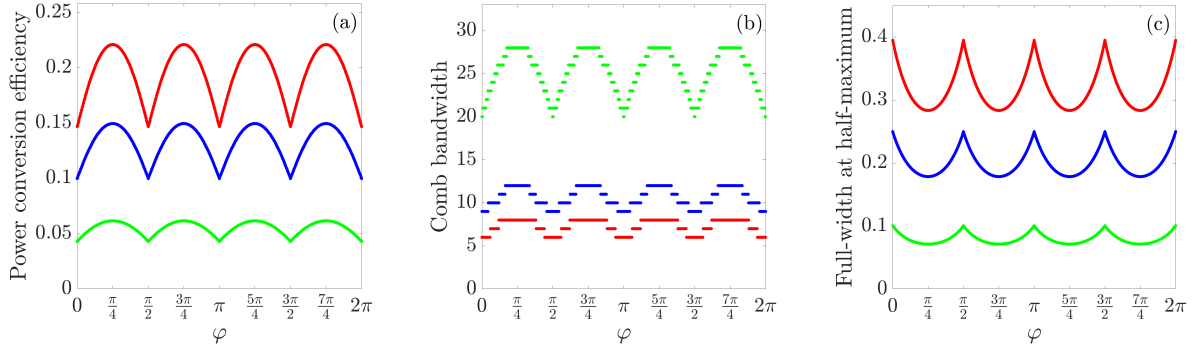
Figure 16. Power conversion efficiency, comb bandwidth and full-width at half-maximum as a function of $\varphi$ for three different examples. The blue curves correspond to $d = 0.1$ and $f = 2$, the red ones to $d = 0.25$ and $f = 2$ as well as the green ones to $d = 0.1$ and $f = 5$.
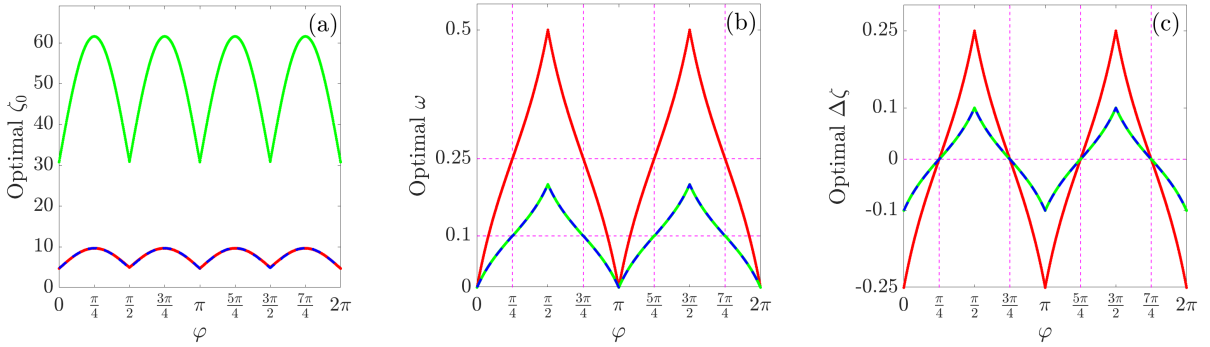


Figure 17. Optimal values of $\zeta_0$, $\omega$ and $\Delta\zeta$ as a function of $\varphi$ for three different examples. The blue curves correspond to $d = 0.1$ and $f = 2$, the red ones to $d = 0.25$ and $f = 2$ as well as the green ones to $d = 0.1$ and $f = 5$. The blue and the red curves in (a) as well as the blue and the green curves in (b) and (c) are plotted dashed so that one of the curves is not completely covered by the other one. The dashed lines colored in magenta in (b) emphasize that the optimal value of $\omega$ coincides with the dispersion $d$ in the optimal case $|f_0| = |f_1|$ where $\varphi \in \{\pi/4, 3\pi/4, 5\pi/4, 7\pi/4\}$. The dashed lines colored in magenta in (c) emphasize that the optimal value of $\Delta\zeta$ vanishes in the optimal case $|f_0| = |f_1|$ where $\varphi \in \{\pi/4, 3\pi/4, 5\pi/4, 7\pi/4\}$.
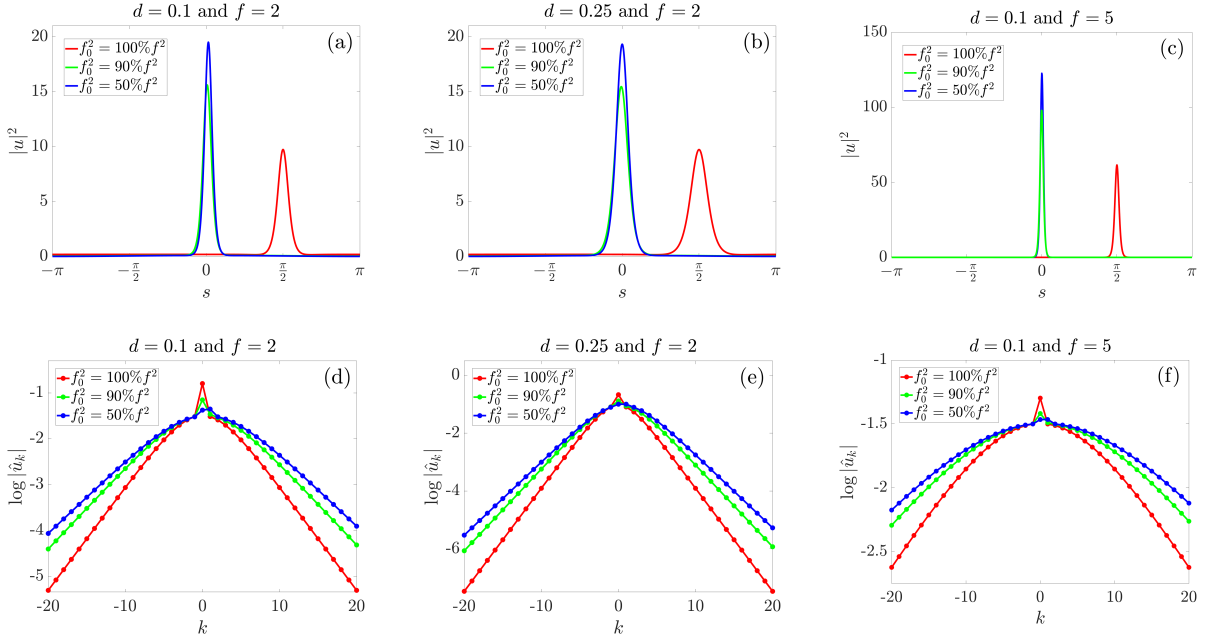
Figure 18. Spatial and spectral power distributions of optimal solitons for selected values of $\varphi \in [0, \pi/4]$ which correspond to $f_0^2 = 100\% f^2$, $f_0^2 = 90\% f^2$ as well as $f_0^2 = 50\% f^2$ for three different examples. Every column corresponds to one example.

also mention that the curves in Fig. 17(a) are not symmetric with respect to $\pi/4$ but this is not visible in the plot since the difference $\Delta\zeta = \zeta_0 - \zeta_1 = \omega - d$ is small compared to $\zeta_0$ and $\zeta_1$.

## 4.5. Trends for varying forcing and varying dispersion

For the results in this section we have carried out a parameter study w.r.t. dispersion $d$ and normalized pump amplitude $f$, considering the behavior of PCE, CBW and FWHM of the best solitons (i.e., minimal FWHM) under optimal power distribution $f_0 = f_1 = f/\sqrt{2}$. As before, we have fixed the two pumped modes to $k_0 = 0$ and $k_1 = 1$. We have considered dispersion parameters $d = 0.1, 0.15, 0.2, 0.25$ and normalized total pump amplitude $f \in (0, 10]$. From Section 4.4 we know that under optimal power distribution the solitons with minimal FWHM arise for $\omega = d$. Using this information we can reduce the optimizations from the heuristic of Section 4.3 to a single optimization step in $\zeta_0$. Since $f_0 = f_1$ we see that now PCE is the ratio between

$$P_{\mathrm{FC}} = \sum_{k \in \mathbb{Z} \setminus \{0,1\}} |\hat{u}_k|^2 + \frac{1}{2}|\hat{u}_0|^2 + \frac{1}{2}|\hat{u}_1|^2$$

and the total pump power $f^2$.

The results are shown in Fig. 19. We observe the following trends: CBW increases whereas FWHM and PCE decrease with increasing forcing $f$. Additionally, one can
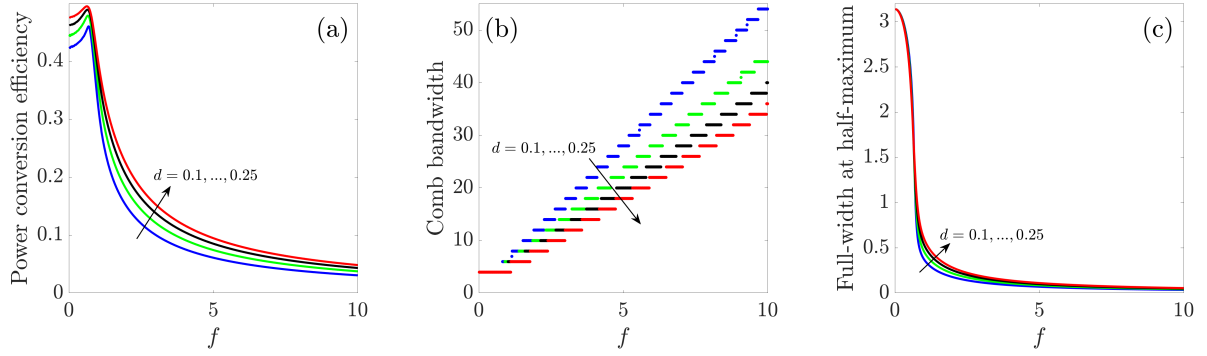
Figure 19. Power conversion efficiency, comb bandwidth and full-width at half-maximum as a function of the forcing $f$ and dispersion $d = 0.1, 0.15, 0.2, 0.25$.

see that with $d \to 0^+$ once again CBW increases and FWHM, PCE decrease. This observations are in good agreement with the trends from the one mode case, cf. [18]. Further, one can observe in Fig. 19(c) that FWHM tends to $\pi$ as $f \to 0^+$. This can be understood as follows: as $f \to 0^+$ the solutions of (4.2) tend to 0 and behave like the solutions of the linear equation

$$-du'' + i\omega u' - (i - \zeta_{0,\mathrm{opt}})u + if_0 + if_1 e^{is} = 0.$$

Since $d = \omega$ for optimal solitons under optimal power distribution $f_0 = f_1 = f/\sqrt{2}$ the above linear equation is solved by

$$u(s) = \frac{if}{\sqrt{2}(i - \zeta_{0,\mathrm{opt}})}(1 + e^{is})$$

and the latter has a FWHM of $\pi$. Similarly, in agreement with Fig. 19(a), we have

$$\mathrm{PCE}(u) \to \frac{1}{2(1 + \zeta_{0,*}^2)} \leq \frac{1}{2}$$

as $f \to 0^+$, where we assume $\zeta_{0,*} = \lim_{f \to 0^+} \zeta_{0,\mathrm{opt}}$.

Finally we mention that the jumps of size two in Fig. 19(b) could be caused by our choice of the discretization of the $f$-interval $(0, 10]$. It is possible that a finer discretization would lead to more plausible jumps of size one. Nevertheless, the finer discretization, which leads to significantly longer run times of the code, has no essential effect on the trends of the curves.

## 4.6. Pumping two arbitrarily distanced modes

Also in the case where the pumped modes are $k_0 = 0$ and $k_1 \geq 2$ we have a heuristic algorithm which enables us to identify a 1-soliton with the strongest spatial localization. The algorithm is based on a variant of the one from the case $k_1 = 1$, cf. Section 4.3, and
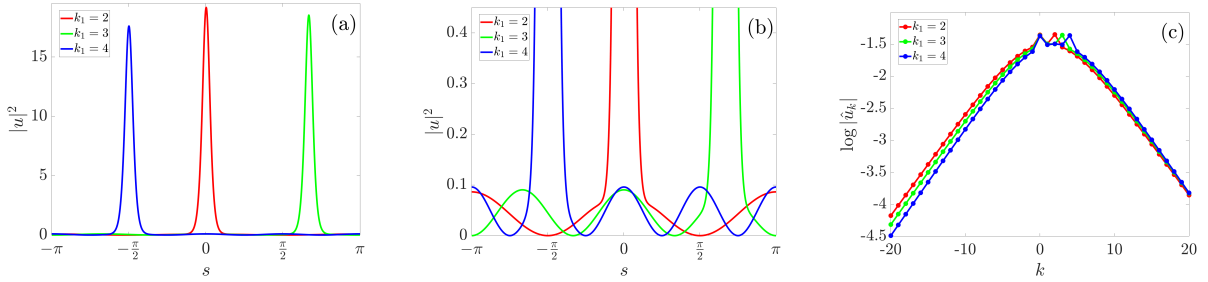
Figure 20. Spatial and spectral power distributions of the optimal 1-solitons from the case $d = 0.1$ and $f_0 = f_1 = \sqrt{2}$ for $k_1 = 2, 3, 4$. Plot (b) is a zoom of plot (a) which highlights the background of the solitons.

details can be found in Appendix C. Applying this algorithm our experiments suggest that the optimal power distribution is again given by the equal distribution $|f_0| = |f_1|$ as in the case $k_1 = 1$. Moreover, for equal power distribution, $\omega = k_1 d$ turns out to be optimal, which once again translates into equal detuning offsets $\Delta\zeta = 0$. In Fig. 20(a) we plotted the spatial power distributions of the optimal 1-solitons from the case $d = 0.1$ and $f_0 = f_1 = \sqrt{2}$ for $k_1 = 2, 3, 4$. One can observe that the optimal 1-soliton gets less localized as $k_1$ increases. In Fig. 20(b) we added a zoom-in to better point out the background of the solitons. Since with $u$ also $u(\cdot + 2\pi/k_1)$ is a solution of (4.2) optimal 1-solitons can be shifted by multiples of $2\pi/k_1$. We see that the 1-soliton localizes once again around one of the points where the absolute value of the pump term $\mathrm{i}f_0 + \mathrm{i}f_1\mathrm{e}^{\mathrm{i}k_1 s}$ is maximized. In Fig. 20(c) we added the spectral power distributions of the optimal 1-solitons. Necessarily each comb is peaked at the pumped modes $k_0 = 0$ and $k_1$.

## 4.7. Summary

We have considered pumping two different modes for a Kerr nonlinear microresonator with anomalous dispersion. Using numerical path continuation methods we found and tested a heuristic algorithm which allows to find for fixed normalized total pump power the optimal detuning offsets that provide the most localized 1-soliton. The heuristic applies in its simple form to the case of pumping two adjacent modes and in a more refined form (taking bifurcations into account) also to the case of pumping two arbitrarily distanced modes. Optimal 1-solitons appear to be spectrally stable and localize themselves around the intensity maxima of the pump. While it became clear that pumping two modes is always advantageous to pumping one mode, in the case of pumping two adjacent modes we went deeper into the question of how the normalized total input power should be divided into the two pumped modes in order to optimize quality metrics like PCE, CBW, and FWHM. A detailed parameter study shows that the optimal distribution is always the equal distribution $|f_0| = |f_1| = |f|/\sqrt{2}$ with equal detuning offsets. The situation appears to be similar in the case of pumping two arbitrarily distanced modes. Our approach has thus validated the assumptions in [29]. Finally, we determined trends of PCE, CBW, and FWHM by varying anomalous dispersion and normalized total input power. The trends are in good agreement with the case of pumping

only one mode, cf. [18]. Our approach is well-suited to determine and analyze optimal pumping schemes in the case where more than two modes are pumped.

## 4.8. Appendix A: Derivation of the Lugiato-Lefever model for a dual-pumped ring resonator

In this section we derive (4.1) from a system of coupled mode equations, cf. [62, 32]. When a resonant cavity is pumped by two continuous wave lasers with frequencies $\omega_{p_0}$ and $\omega_{p_1}$ a system of nonlinear coupled mode equations can be used to describe the evolution of the field inside the cavity. The numbering $k$ of the resonant modes in the cavity is relative to the mode $k_0 = 0$. We use the cold cavity dispersion relation $\omega_k = \omega_0 + d_1 k + d_2 k^2$ for the resonant frequencies $\omega_k$, where $d_1$ corresponds to the FSR of the resonator and $2d_2$ to the difference between two neighboring FSRs at the center frequency $\omega_0$. With $\widetilde{k}_0, \widetilde{k}_1 \in \mathbb{Z}$, $\widetilde{k}_0 < \widetilde{k}_1$, we denote the two pumped modes. If $\hat{A}_k$ is the mode amplitude of the $k$-th resonant mode normalized such that $|\hat{A}_k|^2$ is the number of quanta in the $k$-th mode, then the simplified set of equations reads as follows, cf. [62, 32]:

$$\frac{\partial \hat{A}_k}{\partial t} = -\frac{\kappa}{2}\hat{A}_k + \sum_{j=0}^{1} \delta_{k\widetilde{k}_j}\sqrt{\kappa_{\text{ext}}}\, s_j \mathrm{e}^{-\mathrm{i}(\omega_{p_j} - \omega_{\widetilde{k}_j})t}\mathrm{e}^{\mathrm{i}\phi_j} \tag{4.4}$$

$$+ \mathrm{i}g \sum_{k'+k''-k'''=k} \hat{A}_{k'}\hat{A}_{k''}\bar{\hat{A}}_{k'''}\mathrm{e}^{-\mathrm{i}(\omega_{k'}+\omega_{k''}-\omega_{k'''}-\omega_k)t}. \tag{4.5}$$

Here, $\kappa = \kappa_0 + \kappa_{\text{ext}}$ denotes the cavity decay rate as a sum of intrinsic decay rate $\kappa_0$ and coupling rate to the waveguide $\kappa_{\text{ext}}$, and $\phi_0, \phi_1$ are the initial phases of the pumps. If $P_{\text{in},0}, P_{\text{in},1}$ are the powers of the two input lasers then $s_j = \sqrt{P_{\text{in},j}/\hbar\omega_{\widetilde{k}_j}}$, $j = 0, 1$ are the powers coupled to the cavity. The nonlinear coupling coefficient

$$g = \frac{\hbar\omega_0^2 c n_2}{n_0^2 V_{\text{eff}}}$$

denotes a per photon frequency shift of the cavity due to the Kerr nonlinearity and thus describes the strength of the cubic nonlinearity of the system with linear refractive index $n_0$, nonlinear refractive index $n_2$ and effective cavity nonlinear volume $V_{\text{eff}}$. Finally, $c$ is the vacuum speed of light and $\hbar$ the Planck constant.

By using the transformation

$$\tilde{a}(\tau, x) := \sqrt{\frac{2g}{\kappa}} \sum_{k\in\mathbb{Z}} \hat{A}_k\left(\frac{2}{\kappa}\tau\right)\mathrm{e}^{-\mathrm{i}dk^2\tau}\mathrm{e}^{\mathrm{i}kx}$$

the system (4.4) of coupled mode equations may be rewritten in a dimensionless way as

a partial differential equation,

$$i\frac{\partial\tilde{a}}{\partial\tau} = -d\tilde{a}'' - i\tilde{a} - |\tilde{a}|^2\tilde{a} + i\sum_{j=0}^{1} f_j e^{i(\widetilde{k}_j x - \widetilde{\nu}_j\tau + \phi_j)}, \qquad \tilde{a}\ 2\pi\text{-periodic in } x, \qquad (4.6)$$

where $\tau = \kappa t/2$, $d = 2d_2/\kappa$, and $\zeta_j = 2(\omega_{\widetilde{k}_j} - \omega_{p_j})/\kappa$, $\widetilde{\nu}_j = d\widetilde{k}_j^2 - \zeta_j$, $\eta = \kappa_{\text{ext}}/\kappa$, $f_j = \sqrt{8\eta g/\kappa^2}s_j$ for $j = 0, 1$. By setting

$$a(\tau, x) := e^{-i(\widetilde{k}_0(x + 2d\widetilde{k}_0\tau - \psi) - \widetilde{\nu}_0\tau + \phi_0)}\tilde{a}(\tau, x + 2d\widetilde{k}_0\tau - \psi)$$

with $\psi = (\phi_1 - \phi_0)/k_1$ we find that $a$ satisfies (4.1) with $k_1 = \widetilde{k}_1 - \widetilde{k}_0$, $\Delta\zeta = \zeta_0 - \zeta_1$ and $\nu_1 = \widetilde{\nu}_1 - \widetilde{\nu}_0 - 2d\widetilde{k}_0k_1 = \Delta\zeta + dk_1^2$. Thus, we can always assume, for simplicity, that the pumped modes are $k_0 = 0$ and $k_1 \in \mathbb{N}$ and that the initial phase of both pumps is zero. Moreover we see that the change from $\tilde{a}$ to $a$ shifts the time-dependent Fourier-coefficients from $\hat{A}_k$ to $\hat{A}_{k+\widetilde{k}_0}$ and multiplies them with $e^{-i(\zeta_0\tau + \phi_0 + k\psi)}$ so that the power in each individual mode is (up to an index shift) preserved.

Finally, let us explain that the intracavity power $P = \sum_{k\in\mathbb{Z}} |\hat{u}_k|^2 = \frac{1}{2\pi}\int_0^{2\pi} |u(s)|^2\,ds$ of a $2\pi$-periodic traveling-wave comb state $u$ cannot exceed the normalized total input power $f^2 = f_0^2 + f_1^2$. To see this, we multiply the equation (4.2) for the traveling-wave profile $u$ with $\bar{u}(s)$ and take the imaginary part to obtain

$$-d\,\text{Im}(u''(s)\bar{u}(s)) + \omega\,\text{Re}(u'(s)\bar{u}(s)) - |u(s)|^2 + \text{Re}\big((f_0 + f_1 e^{ik_1 s})\bar{u}(s)\big) = 0.$$

Integration over the interval $[0, 2\pi]$, using integration by parts for the first term and $\frac{d}{ds}|u(s)|^2 = 2\,\text{Re}(u'(s)\bar{u}(s))$ for the second term together with the Cauchy-Schwarz inequality yield

$$\int_0^{2\pi} |u(s)|^2\,ds = \int_0^{2\pi} \text{Re}\big((f_0 + f_1 e^{ik_1 s})\bar{u}(s)\big)\,ds \leq \left(\int_0^{2\pi} |u(s)|^2\,ds\right)^{1/2}\sqrt{2\pi}(f_0^2 + f_1^2)^{1/2}$$

and hence $\frac{1}{2\pi}\int_0^{2\pi} |u(s)|^2\,ds \leq f_0^2 + f_1^2$.

## 4.9. Appendix B: Detailed explanation of the heuristic for finding localized solitons in the case of pumping two adjacent modes

Here we explain in detail the heuristic algorithm mentioned in Section 4.3 for finding strongly localized solutions of (4.2) in the case of anomalous dispersion $d > 0$, where two adjacent modes are pumped, i.e. the pumped modes are $k_0 = 0$ and $k_1 = 1$. We recall that the parameters $d > 0$, $k_1 = 1$, $f_0$ and $f_1$ are fixed and that the goal is to find optimally localized solutions by varying the parameters $\zeta_0$ and $\omega$ since they can be

influenced by the choice of the pump frequencies $\omega_{p_0}$ and $\omega_{p_1}$ through the relation

$$\zeta_0 = \frac{2}{\kappa}\big(\omega_0 - \omega_{p_0}\big), \qquad \omega = \frac{2}{\kappa}\big(\omega_0 - \omega_{p_0} - (\omega_1 - \omega_{p_1}) + d_2\big).$$

Without loss of generality we assume $0 < f_1 \leq f_0$. The heuristic algorithm consists of the following steps. For all our computations we carried it out by using `pde2path`.

*Step 0: Initialize with $f_1^{(0)} = 0$, $\zeta_0^{(0)} = 2 + f^2$, $\omega^{(0)} = 0$, find $u_0 = $ constant solution of (4.2) and set $j = 1$*

*Step 1 ($f_1$-continuation): with $\zeta_0^{(0)}$, $\omega^{(j-1)}$ start from $f_1^{(0)}$ and continue $u_0$ in $f_1$-parameter until desired value $f_1$ is reached, keep solution $T_j$*

*Step 2 ($\zeta_0$-optimization): with $\omega^{(j-1)}$, $f_1$ start from $\zeta_0^{(0)}$ and continue $T_j$ in $\zeta_0$-parameter until 1-solitons have been exhausted, find optimal $\zeta_0^{(j)}$, keep optimal soliton $A_j$*

*Step 3 ($\omega$-optimization): with $\zeta_0^{(j)}$, $f_1$ start from $\omega^{(j-1)}$ and continue $A_j$ in $\omega$-parameter on closed loop, find optimal $\omega^{(j)}$, keep optimal soliton $B_j$*

*$j \to j + 1$, return to Step 1 unless desired accuracy achieved*

Now we comment on the individual steps.

*Step 0:* The algorithm starts by choosing suitable initial values for the parameters $f_1$, $\zeta_0$ and $\omega$. For the values of $f_1^{(0)} = 0$ and $\zeta_0^{(0)} = 2 + f^2$ we can determine a constant solution $u_0$ of (4.2). It satisfies

$$0 = -(\mathrm{i} - \zeta_0^{(0)})u_0 - |u_0|^2 u_0 + \mathrm{i}f_0.$$

If we choose $\zeta_0^{(0)}$ sufficiently large (in all numerical experiments $\zeta_0^{(0)} = 2 + f^2$ was sufficient) then $u_0$ is uniquely determined. Since the dispersion $d$ and the difference of the normalized offsets between the pump frequencies $\omega_{p_i}$ and the resonant frequencies $\omega_i$, $i = 0, 1$ turn out to be rather small we expect that also $\omega = \Delta\zeta + d$ is rather small. Therefore the initial value $\omega^{(0)} = 0$ is feasible.

*Step 1 ($f_1$-continuation):* Starting from $\zeta_0^{(0)}$, $\omega^{(j-1)}$ and $f_1^{(0)}$ `pde2path` performs a continuation algorithm in the $f_1$-parameter. With the side constraint of always solving (4.2) the trivial state $u_0$ is continued numerically w.r.t. the $f_1$-parameter until the desired value $f_1$ is reached for the first time. Although the starting point $u_0$ is independent of $\omega$ the continuation w.r.t. the $f_1$-parameter is sensitive to the current value of $\omega$.

*Step 2 ($\zeta_0$-optimization):* Now that the $f_1$-parameter has reached its correct value we freeze the values of $\omega^{(j-1)}$ and $f_1$ and start the optimization w.r.t. the $\zeta_0$-parameter from $\zeta_0^{(0)} = 2 + f^2$. Starting from $\zeta_0^{(0)}$, the continuation of solutions of (4.2) w.r.t. $\zeta$ first provides almost trivial solutions until they develop into 1-solitons followed by less

localized higher solitons. From the point of view of FWHM-minimization it is therefore reasonable to continue from $\zeta_0^{(0)}$ until the part of the branch containing 1-solitons has been exhausted. Along this part of the branch the optimal solution $A_j$ of (4.2) with the minimal FWHM together with the optimal parameter value $\zeta_0^{(j)}$ are kept.

*Step 3 ($\omega$-optimization):* Now we freeze $f_1$ and $\zeta_0^{(j)}$. The optimal point $A_j$ from the previous step serves as starting point for the subsequent $\omega$-continuation. Beginning with $\omega^{(j-1)}$ the continuation of solutions to (4.2) in the $\omega$-parameter always delivers a closed loop. From this closed $\omega$-loop the optimal solution $B_j$ of (4.2) with the minimal FWHM together with the optimal parameter value $\omega^{(j)}$ is kept.

At this point the algorithm is not yet finished since a single optimization in $\zeta_0$ followed by a single optimization in $\omega$ is not an adequate substitute for a continuous two-parameter optimization in $\zeta_0$ and $\omega$. Therefore, the algorithm has to be suitably iterated until a desired accuracy (measured in the deviations of $A_j, B_j$ from its predecessors $A_{j-1}, B_{j-1}$) is achieved. One might think of using $B_j$ as starting point for the next $\zeta_0$-continuation. However, this turns out to be non-optimal in some cases because after the update of $\omega^{(j)}$ the solution $B_j$ no longer lies on a $\zeta_0$-branch that leads to an optimal FWHM. Instead, our strategy is to only keep the value $\omega^{(j)}$, forget the solution $B_j$ and iterate by starting again with Step 1 instead of Step 2, i.e., by starting the $f_1$-continuation from $f_1^{(0)} = 0$ (with the by now updated value of $\omega$). The subsequent $\zeta_0$-continuation of Step 2 provides a $\zeta_0$-branch with apparently smaller FWHM.

In Fig. 21 we have illustrated Step 2 and 3 for three different values of the parameters $d$, $f$ and $f_1$. In the first row Fig. 21(a)-(c) we are plotting $\zeta_0$-branches, i.e., the intracavity power of the soliton, given by $\|u\|_2^2 = \frac{1}{2\pi} \int_0^{2\pi} |u(s)|^2 \, ds$, versus the value of $\zeta_0$ (Step 2, $\zeta_0$-optimization). The points $A_1$ indicate the optimal soliton with the smallest FWHM and they are located near a turning point. They serve as starting points for the subsequent $\omega$-continuation (Step 3). The $\omega$-branches, i.e., intracavity power of the soliton versus the value of $\omega$, depicted in Fig. 21(d)-(f) turn out to be closed loops. The points $B_1$ indicate the optimal soliton on the closed $\omega$-loop. In the last row Fig. 21(g)-(i) we illustrate the optimality of the points $A_1$, $B_1$ by plotting the value of FWHM along the $\zeta_0$-branches (blue) and the $\omega$-loops (green). The FWHM is depicted as a function of normalized arc length of the corresponding curves. Since the $\zeta_0$-curves are unbounded, we decided to plot the FWHM between the reference points $S_1$ (start) before the relevant 1-solitons begin and $E_1$ (end) after the relevant 1-solitons have been passed.

An iteration of the $\zeta_0$- and $\omega$-optimization steps (until a desired accuracy is reached) provides similar pictures. In our numerical experiments we always performed three optimizations in both of the variables $\zeta_0$ and $\omega$ (unless stated otherwise).

## 4.10. Appendix C: Heuristic for finding localized solitons in the case of pumping two arbitrarily distanced modes

By considering additional bifurcations we will demonstrate how the heuristic from Section 4.3 can be adapted to arbitrary values of $k_1 \geq 2$. A first observation is that the very
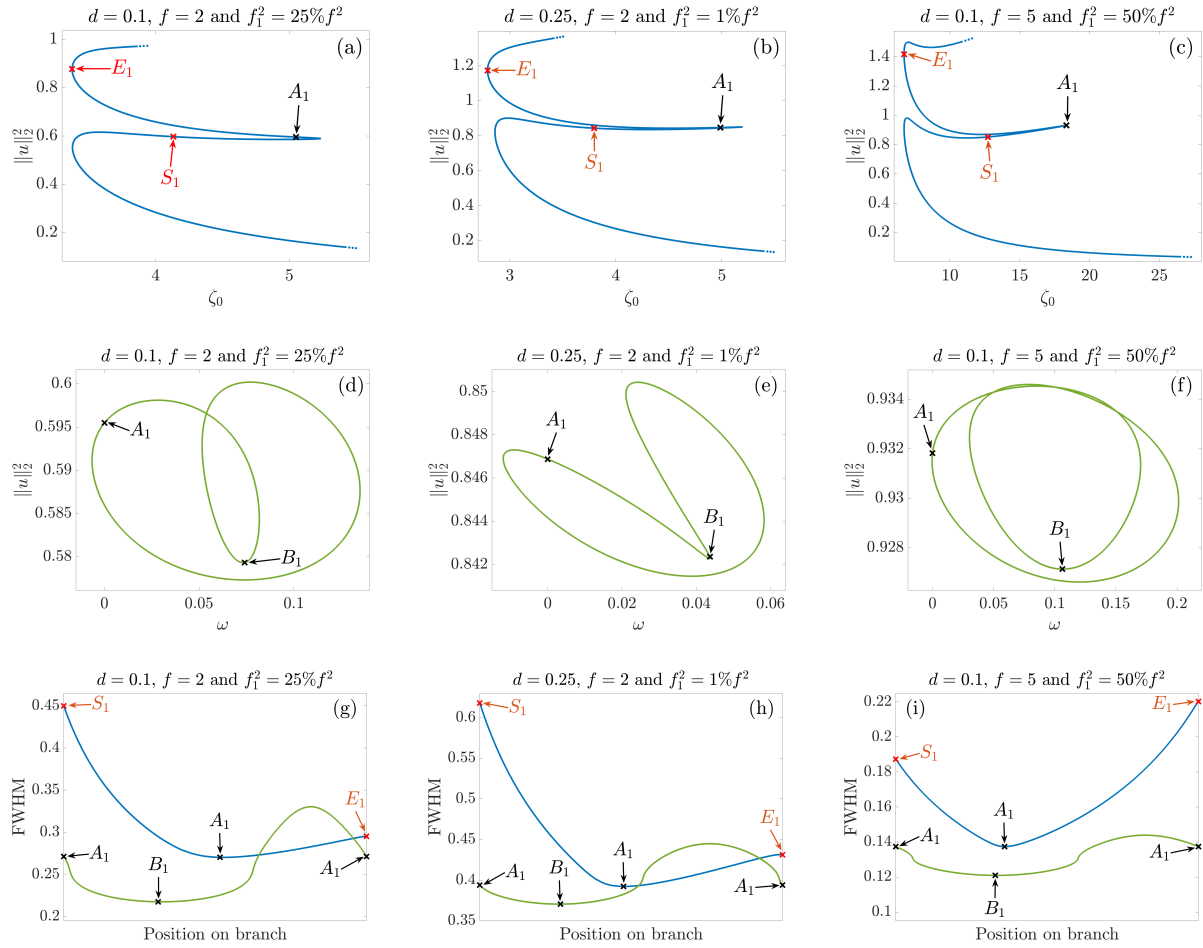
Figure 21. Branches show intracavity power $\|u\|_2^2 = \frac{1}{2\pi} \int_0^{2\pi} |u(s)|^2 \, ds$ of the soliton $u$ plotted vs. values of $\zeta_0$ or $\omega$. First row: blue branch as achieved by the first $\zeta_0$-optimization. Second row: green branch as achieved by the first $\omega$-optimization. Third row: FWHM along these branches. Columns correspond to different values of $d, f_1, f$.

same heuristic as used in Section 4.3 would lead to solitons which are not only $2\pi$- but in fact $2\pi/k_1$-periodic, i.e., the algorithm detects no 1-solitons. This is essentially due to the fact that starting from a constant solution any kind of parameter-continuation will develop solutions that have the shape of the pump.

However, in contrast to the case $k_1 = 1$, we also detect bifurcations this time. The idea of the adapted heuristic is to switch in every $\zeta_0$-optimization step to a bifurcating branch containing 1-solitons. For $d = 0.1$, $f = 2$, $f_1^2 = 25\% f^2$ this is illustrated in Fig. 22(a),(d) for $k_1 = 2, 3$. The gray branch is the new additional branch bifurcating from the first continued (blue) branch in $\zeta_0$ and $A_1$ indicates the optimal point with the minimal FWHM on that branch. The point $A_1$ is then used as starting point for the subsequent $\omega$-continuation and from here on we can once again iterate the whole process.

The mentioned bifurcations turn out to be not of simple nature in general. For example, if $k_1$ is odd, `pde2path` detects no bifurcations at all (which may be due to an even number of eigenvalues crossing zero simultaneously). However, we can easily overcome this issue by using an interpolation trick for branch-switching. For that, we consider a $\zeta_0$-value near a turning point, where we find two distinct solutions (named $X$ and $Y$) for one and the same value of $\zeta_0$. In Fig. 22(a) we used $\zeta_0 = 3.3$ and in Fig. 22(d) we used $\zeta_0 = 3.1$ for this purpose and marked the mentioned solutions in red and green, respectively. Fig. 22(b) and Fig. 22(e) show the spatial power distributions of $X$ and $Y$. It turns out that a 1-soliton-like state, which is not $2\pi/k_1$-periodic anymore, can be glued together from parts of these solutions. The resulting soliton $Z$ is marked in blue in Fig. 22(a) and Fig. 22(d) and its spatial power distribution is given in Fig. 22(c) and Fig. 22(f). The interpolated soliton serves as starting point for another $\zeta_0$-continuation yielding the gray branch which actually is a branch which bifurcates from the original curve and connects two of its turning points.
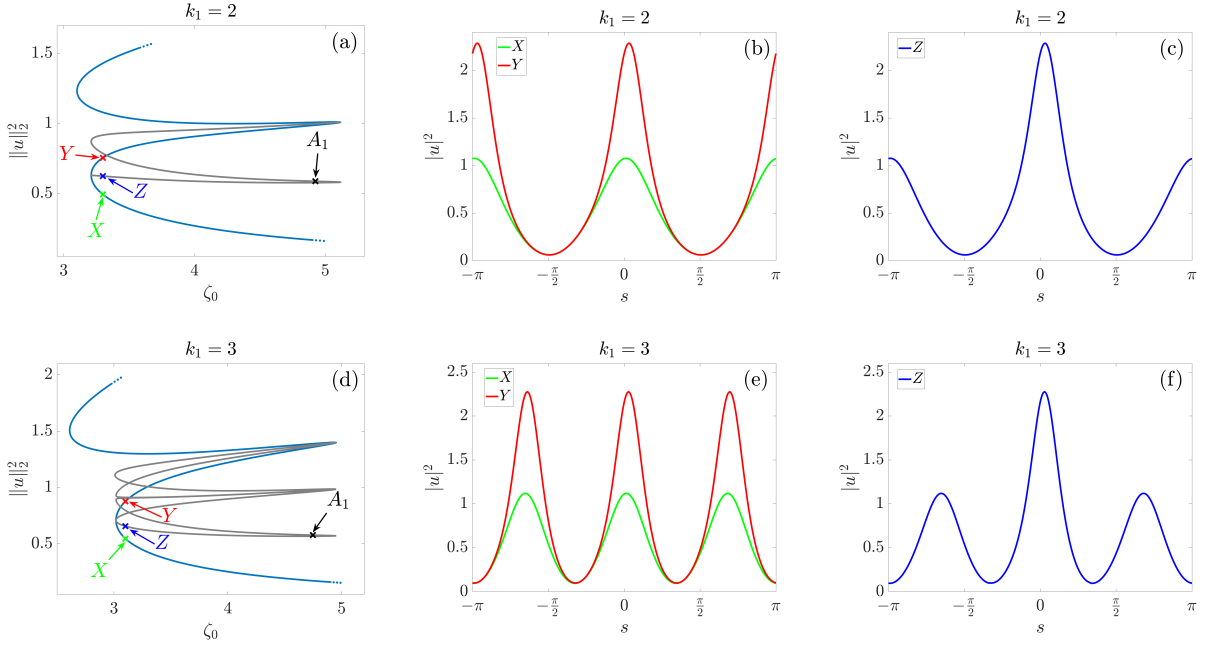
Figure 22. Example for $d = 0.1$, $f = 2$ and $f_1^2 = 25\% f^2$. First column: branches show intracavity power $\|u\|_2^2 = \frac{1}{2\pi} \int_0^{2\pi} |u(s)|^2 \, ds$ of the soliton $u$ plotted vs. $\zeta_0$. Blue branch as achieved by first $\zeta_0$-continuation and gray branch obtained from first bifurcation from blue branch. Second and third column: spatial power distribution of solutions used for branch-switching. Plots (a)-(c) correspond to the case $k_1 = 2$ while plots (d)-(f) correspond to $k_1 = 3$.

[End of preprint]

# 5. Time-dependent Lugiato-Lefever equation

In Section 5 we are interested in the time-dependent LLE

$$\mathrm{i}a_t = (-\mathrm{i} + \zeta)a - da_{xx} - |a|^2 a + \mathrm{i}f, \qquad a \; 2\pi\text{-periodic in } x, \tag{5.1}$$

and in the time-dependent two-mode modification

$$\mathrm{i}a_t = (-\mathrm{i} + \zeta)a - da_{xx} - |a|^2 a + \mathrm{i}f_0 + \mathrm{i}f_1 \mathrm{e}^{\mathrm{i}(k_1 x - \nu_1 t)}, \qquad a \; 2\pi\text{-periodic in } x. \tag{5.2}$$

In Section 5.1 we present some first results on the question if all time-periodic solutions of (5.1) are constant in $t$. This includes Theorem 5.2 which is based on Bendixson's negative criterion and which shows that this is true in the case $d = 0$, and Theorem 5.5 which is based on a-priori bounds and shows that for $|f| \ll 1$ all time-periodic solutions of (5.1) are actually constant both in $t$ and in $x$. In Section 5.2 we likewise present some first results on the question if all time-periodic solutions of (5.2) are traveling waves, i.e. of the form $a(t, x) = u(x - \omega t)$, where $\omega = \frac{\nu_1}{k_1}$ and $u$ is a solution of

$$-du'' + \mathrm{i}\omega u' + (-\mathrm{i} + \zeta)u - |u|^2 u + \mathrm{i}f_0 + \mathrm{i}f_1 \mathrm{e}^{\mathrm{i}k_1 s} = 0, \qquad u \; 2\pi\text{-periodic.} \tag{5.3}$$

In a first step towards this we establish the local uniqueness result Theorem 5.10 which is based on the implicit function theorem and the global uniqueness result Theorem 5.18 which is based on a-priori bounds and holds for $f_0^2 + f_1^2 \ll 1$.

## 5.1. One mode case

The time-dependent LLE (5.1) may or may not have time-periodic solutions which are not constant in $t$. This is a fundamental question which still needs to be answered. In a first step towards this we neglect the dispersion term, i.e. we consider the ODE

$$\mathrm{i}a_t = (-\mathrm{i} + \zeta)a - |a|^2 a + \mathrm{i}f. \tag{5.4}$$

Splitting $a = u + \mathrm{i}v$ into its real and imaginary part we obtain the first-order system

$$\begin{pmatrix} u_t \\ v_t \end{pmatrix} = \begin{pmatrix} -u + \zeta v - u^2 v - v^3 + f \\ -v - \zeta u + u^3 + v^2 u \end{pmatrix}. \tag{5.5}$$

Our next result relies on Bendixson's negative criterion (cf. [5, p. 318]).

**Theorem 5.1** (Bendixson's negative criterion). *Assume that $h \in C^1(\mathbb{R}^2, \mathbb{R}^2)$ and that* div $h$ *does not change sign in $\mathbb{R}^2$. Then the system*

$$\begin{pmatrix} u_t \\ v_t \end{pmatrix} = h(u, v) \tag{5.6}$$

*has no non-constant periodic solution.*

For the reader's convenience we repeat the short proof.

*Proof.* Assume that $(u_0, v_0)$ is a non-constant periodic solution of (5.6) with (smallest) period $T > 0$. Then
$$\Gamma := \{(u_0(t), v_0(t)) : t \in [0, T]\}$$
is a closed $C^1$-curve in $\mathbb{R}^2$ with no self-intersection points. Let $\Omega$ denote the interior of $\Gamma$ (cf. Jordan curve theorem). By the divergence theorem we have

$$
\begin{aligned}
\int_\Omega \operatorname{div} h(u, v)\, d(u, v) &= \int_0^T h(u_0(t), v_0(t)) \cdot \nu(u_0(t), v_0(t)) \left| \begin{pmatrix} u_0'(t) \\ v_0'(t) \end{pmatrix} \right| dt \\
&= \int_0^T \underbrace{\begin{pmatrix} u_0'(t) \\ v_0'(t) \end{pmatrix} \cdot \nu(u_0(t), v_0(t))}_{=0} \left| \begin{pmatrix} u_0'(t) \\ v_0'(t) \end{pmatrix} \right| dt = 0,
\end{aligned}
$$

where $\nu$ is the outward unit normal vector on $\Gamma$. On the other hand $\int_\Omega \operatorname{div} h(u, v)\, d(u, v) \neq 0$ since $\operatorname{div} h$ does not change sign, which is a contradiction. $\qquad\square$

**Theorem 5.2.** *Let $\zeta, f \in \mathbb{R}$. Then equation (5.4) has no non-constant periodic solution.*

*Proof.* We find

$$\operatorname{div} \begin{pmatrix} -u + \zeta v - u^2 v - v^3 + f \\ -v - \zeta u + u^3 + v^2 u \end{pmatrix} = -1 - 2uv + (-1 + 2vu) = -2 < 0,$$

so that the result follows immediately from Bendixson's negative criterion. $\qquad\square$

We also have the following more general result which draws a connection between the non-existence of non-constant periodic solutions and the non-vanishing of a certain potential $V$.

**Theorem 5.3.** *Let $\zeta, f \in \mathbb{R}$ and assume that $V \in C(\mathbb{R}, \mathbb{R})$ is periodic and that $V$ has no zeros. Then the differential equation*

$$\mathrm{i} V(t) a_t = (-\mathrm{i} + \zeta) a - |a|^2 a + \mathrm{i} f$$

*has no non-constant periodic solution.*

*Proof.* W.l.o.g. we can assume $V > 0$. Splitting $a = u + \mathrm{i} v$ we get

$$\begin{pmatrix} V(t) u_t \\ V(t) v_t \end{pmatrix} = \begin{pmatrix} -u + \zeta v - u^2 v - v^3 + f \\ -v - \zeta u + u^3 + v^2 u \end{pmatrix}.$$

Let us assume that $(u, v)$ is a non-constant periodic solution of this system. Consider the bijective function $H \in C^1(\mathbb{R}, \mathbb{R})$ defined by

$$H(t) := \int_0^t \frac{1}{V(\tau)}\, d\tau.$$

For $\tilde{u}, \tilde{v}$ defined via $u(t) = \tilde{u}(H(t))$ and $v(t) = \tilde{v}(H(t))$ we then find

$$\tilde{u}_t(H(t)) = V(t)\tilde{u}_t(H(t))\frac{1}{V(t)} = V(t)u_t(t) = -u(t) + \zeta v(t) - u(t)^2 v(t) - v(t)^3 + f$$

$$= -\tilde{u}(H(t)) + \zeta \tilde{v}(H(t)) - \tilde{u}(H(t))^2 \tilde{v}(H(t)) - \tilde{v}(H(t))^3 + f$$

and

$$\tilde{v}_t(H(t)) = V(t)\tilde{v}_t(H(t))\frac{1}{V(t)} = V(t)v_t(t) = -v(t) - \zeta u(t) + u(t)^3 + v(t)^2 u(t)$$

$$= -\tilde{v}(H(t)) - \zeta \tilde{u}(H(t)) + \tilde{u}(H(t))^3 + \tilde{v}(H(t))^2 \tilde{u}(H(t))$$

so that $(\tilde{u}, \tilde{v})$ solves the autonomous system (5.5). But from Theorem 5.2 we know that this system has no non-constant periodic solution so that the proof is finished if we can ensure that $(\tilde{u}, \tilde{v})$ is periodic. Note that the latter follows from the fact that $(\tilde{u}, \tilde{v})$ is a non-injective solution of an autonomous system. Observe also that $(\tilde{u}, \tilde{v})$ directly inherits its non-injectivity from $(u, v)$. □

Let us return to the general case where the dispersion term is not neglected anymore. For small values of $|f|$ we can provide a global uniqueness result for time-periodic solutions of (5.1) which is based on the following a-priori bounds. Let us abbreviate $(a(t))(x) = a(t, x)$, $\zeta^\pm = \max\{0, \pm\zeta\}$ and write $\|\cdot\|_p$ for the standard norm on $L^p(0, 2\pi)$ for $p \in [1, \infty]$.

**Theorem 5.4.** *Let $d \in \mathbb{R} \setminus \{0\}$, $f, \zeta \in \mathbb{R}$ and $T > 0$. Then for every solution $a \in C^1_{per}([0, T], H^2_{per}(0, 2\pi))$ of (5.1) the a-priori bounds*

$$\sup_{t \in [0,T]} \|a(t)\|_2^2 \leq F^2, \qquad \sup_{t \in [0,T]} \|a_x(t)\|_2^2 \leq B, \qquad \|a\|_{L^\infty((0,T) \times (0,2\pi))}^2 \leq C$$

*hold, where*

$$F = F(f) = \sqrt{2\pi}|f|,$$

$$B = B(d, f, \zeta) = \begin{cases} \frac{F^2}{|d|}(\zeta^+ + 3), & d < 0, \\ \frac{1}{4d^2}\left(4dF^2(2\zeta^- + 6 + d) + 45F^6\right), & d > 0, \end{cases}$$

$$C = C(d, f, \zeta) = \frac{F^2}{2\pi} + 2F\sqrt{B}.$$

Now we can state our global uniqueness result.

**Theorem 5.5.** *Let $d \in \mathbb{R} \setminus \{0\}$, $f, \zeta \in \mathbb{R}$ and $T > 0$. Then (5.1) has a unique solution $a \in C^1_{per}([0, T], H^2_{per}(0, 2\pi))$ if $3C < 1$, where $C = C(d, f, \zeta)$ is the constant from Theorem 5.4. In particular, $|f| \ll 1$ is sufficient. The corresponding unique solution is constant both in $t$ and in $x$.*

Theorem 5.4 and Theorem 5.5 will follow from the more general results Theorem 5.16 and Theorem 5.18 of Section 5.2 by setting $f_1 = 0$. Finally, we note that it remains

unanswered if there is a choice of the parameters $d, f, \zeta$ such that (5.1) admits a time-periodic solution which is not constant in $t$.

## 5.2. Two mode case

Every solution $u$ of (5.3) from Section 3 generates a time-periodic solution of (5.2) by setting $a(t, x) = u(x - \omega t)$ with $\omega = \frac{\nu_1}{k_1}$ and it is an open question if solutions exist which are not of that type. In a first step towards this we establish a local uniqueness result based on the implicit function theorem and a global uniqueness result (for small normalized total input power) based on a-priori bounds. Let us abbreviate $T = \frac{2\pi}{|\nu_1|}$ and $\Omega = (0, T) \times (0, 2\pi)$. Recall that in the special case $f_1 = 0$ there are trivial (constant) solutions $a_0 \in \mathbb{C}$ of (5.2) satisfying the algebraic equation

$$(-\mathrm{i} + \zeta)a_0 - |a_0|^2 a_0 + \mathrm{i}f_0 = 0,$$

cf. (3.4). As in Section 3.2.1 a constant solution $a_0 \in \mathbb{C}$ of (5.2) for $f_1 = 0$ may be continued into the regime where $f_1 \neq 0$. This relies on the properties of the linearized equation

$$\mathrm{i}\psi_t = (-\mathrm{i} + \zeta)\psi - d\psi_{xx} - 2|a_0|^2\psi - a_0^2\overline{\psi}.$$

We decompose $\psi = \sum_{k,l \in \mathbb{Z}} \psi_{k,l} \mathrm{e}^{\mathrm{i}kx} \mathrm{e}^{\mathrm{i}l\frac{2\pi}{T}t}$ and define the operator

$$L_{a_0}\psi = \sum_{k,l \in \mathbb{Z}} \left( l\frac{2\pi}{T}\psi_{k,l} - \mathrm{i}\psi_{k,l} + \zeta\psi_{k,l} + dk^2\psi_{k,l} - 2|a_0|^2\psi_{k,l} - a_0^2\psi_{-k,-l}^* \right) \mathrm{e}^{\mathrm{i}kx} \mathrm{e}^{\mathrm{i}l\frac{2\pi}{T}t} \quad (5.7)$$

on $L^2(\Omega)$ with canonical domain

$$D(L_{a_0}) = \left\{ \psi \in L^2(\Omega) : \sum_{k,l \in \mathbb{Z}} \left| l\frac{2\pi}{T} + dk^2 \right|^2 |\psi_{k,l}|^2 < \infty \right\}.$$

Here we write $\psi_{-k,-l}^* := \overline{\psi_{-k,-l}}$.

**Definition 5.6.** A constant solution $a_0 \in \mathbb{C}$ of (5.2) for $f_1 = 0$ is called non-degenerate if the linearized operator $L_{a_0}$ from (5.7) is injective.

Next we derive conditions for the invertibility of $L_{a_0}$.

**Lemma 5.7.** *A constant solution $a_0 \in \mathbb{C}$ of (5.2) for $f_1 = 0$ is non-degenerate if and only if*

$$(\zeta + dk^2)^2 - 4|a_0|^2(\zeta + dk^2) + 1 + 3|a_0|^4 \neq 0 \text{ for all } k \in \mathbb{N}_0.$$

*In this case $L_{a_0} : D(L_{a_0}) \to L^2(\Omega)$ is invertible.*

**Remark 5.8.** Note that this condition already appeared in Lemma 3.4(b) and was discussed in Remark 3.5.

*Proof of Lemma 5.7.* Let $g = \sum_{k,l \in \mathbb{Z}} g_{k,l} e^{ikx} e^{il \frac{2\pi}{T} t} \in L^2(\Omega)$ be arbitrary. The equation $L_{a_0} \psi = g$ then means

$$\left(l \frac{2\pi}{T} - i + \zeta + dk^2 - 2|a_0|^2\right) \psi_{k,l} - a_0^2 \psi_{-k,-l}^* = g_{k,l} \text{ for all } k, l \in \mathbb{Z}.$$

If we also write down the complex conjugate of this equation

$$-\overline{a_0}^2 \psi_{k,l} + \left(-l \frac{2\pi}{T} + i + \zeta + dk^2 - 2|a_0|^2\right) \psi_{-k,-l}^* = g_{-k,-l}^*$$

we find

$$\begin{pmatrix} l\frac{2\pi}{T} - i + \zeta + dk^2 - 2|a_0|^2 & -a_0^2 \\ -\overline{a_0}^2 & -l\frac{2\pi}{T} + i + \zeta + dk^2 - 2|a_0|^2 \end{pmatrix} \begin{pmatrix} \psi_{k,l} \\ \psi_{-k,-l}^* \end{pmatrix} = \begin{pmatrix} g_{k,l} \\ g_{-k,-l}^* \end{pmatrix}.$$

If we wish $L_{a_0}$ to be injective these matrices need to be invertible which leads to

$$D(k,l) := (\zeta + dk^2)^2 - 4(\zeta + dk^2)|a_0|^2 + 3|a_0|^4 + 1 - l^2 \frac{4\pi^2}{T^2} + l \frac{4\pi}{T} i \neq 0 \text{ for all } k, l \in \mathbb{Z}.$$

For $l \neq 0$ this is trivially satisfied so that this condition amounts to

$$(\zeta + dk^2)^2 - 4(\zeta + dk^2)|a_0|^2 + 3|a_0|^4 + 1 \neq 0 \text{ for all } k \in \mathbb{N}_0.$$

In this case,

$$\psi_{k,l} = \frac{(-l\frac{2\pi}{T} + dk^2 + i + \zeta - 2|a_0|^2)g_{k,l} + a_0^2 g_{-k,-l}^*}{D(k,l)}.$$

Next we want to show that this defines an element $\psi \in D(L_{a_0})$, whence $L_{a_0}$ is surjective. First we show that $\psi \in L^2(\Omega)$. Note that $|D(k,l)|^2$ is bounded away from zero since

$$|D(k,l)|^2 \geq l^2 \frac{16\pi^2}{T^2} \geq \frac{16\pi^2}{T^2} \text{ for } l \neq 0$$

and since

$$D(k,0) = (\zeta + dk^2)^2 - 4(\zeta + dk^2)|a_0|^2 + 3|a_0|^4 + 1 \to \infty \text{ for } |k| \to \infty.$$

Thus,

$$\frac{a_0^2 g_{-k,-l}^*}{D(k,l)} \in \ell^2(\mathbb{Z}^2)$$

and it remains to show

$$h_{k,l} := \frac{(-l\frac{2\pi}{T} + dk^2 + i + \zeta - 2|a_0|^2)g_{k,l}}{D(k,l)} \in \ell^2(\mathbb{Z}^2).$$

For $k, l \in \mathbb{Z}$ with $|-l\frac{2\pi}{T} + dk^2 + i + \zeta - 2|a_0|^2| \leq |a_0|^4 + 1$ we can use once again that

$D(k, l)$ is bounded away from zero to get $|h_{k,l}| \leq C|g_{k,l}|$ for some constant $C > 0$. In the case $|-l\frac{2\pi}{T} + dk^2 + \mathrm{i} + \zeta - 2|a_0|^2| > |a_0|^4 + 1$ we get

$$
\begin{aligned}
|h_{k,l}| &= \left| \frac{(-l\frac{2\pi}{T} + dk^2 + \mathrm{i} + \zeta - 2|a_0|^2)g_{k,l}}{(-l\frac{2\pi}{T} + dk^2 + \mathrm{i} + \zeta - 2|a_0|^2)(l\frac{2\pi}{T} + dk^2 - \mathrm{i} + \zeta - 2|a_0|^2) - |a_0|^4} \right| \\
&\leq \frac{|-l\frac{2\pi}{T} + dk^2 + \mathrm{i} + \zeta - 2|a_0|^2|}{|-l\frac{2\pi}{T} + dk^2 + \mathrm{i} + \zeta - 2|a_0|^2||l\frac{2\pi}{T} + dk^2 - \mathrm{i} + \zeta - 2|a_0|^2| - |a_0|^4} |g_{k,l}| \\
&\leq \frac{|-l\frac{2\pi}{T} + dk^2 + \mathrm{i} + \zeta - 2|a_0|^2|}{|-l\frac{2\pi}{T} + dk^2 + \mathrm{i} + \zeta - 2|a_0|^2| - |a_0|^4} |g_{k,l}| \\
&= \left( 1 + \frac{|a_0|^4}{|-l\frac{2\pi}{T} + dk^2 + \mathrm{i} + \zeta - 2|a_0|^2| - |a_0|^4} \right) |g_{k,l}| \\
&\leq (1 + |a_0|^4)|g_{k,l}|
\end{aligned}
$$

so that $h_{k,l} \in \ell^2(\mathbb{Z}^2)$ and thus $\psi \in L^2(\Omega)$ is proven. Finally, to obtain $\psi \in D(L_{a_0})$ note that by construction we have

$$
\sum_{k,l \in \mathbb{Z}} \left| \left( l\frac{2\pi}{T} - \mathrm{i} + \zeta + dk^2 - 2|a_0|^2 \right) \psi_{k,l} - a_0^2 \psi_{-k,-l}^* \right|^2 = \sum_{k,l \in \mathbb{Z}} |g_{k,l}|^2 < \infty
$$

which due to $\psi \in L^2(\Omega)$ easily implies

$$
\sum_{k,l \in \mathbb{Z}} \left| l\frac{2\pi}{T} + dk^2 \right|^2 |\psi_{k,l}|^2 < \infty.
$$

$\square$

**Remark 5.9.** Note that the above proof in fact shows that $L_{a_0}^{-1} : L^2(\Omega) \to L^2(\Omega)$ is continuous which also implies the continuity of $L_{a_0}^{-1} : H^2_{\mathrm{per}}(\Omega) \to H^2_{\mathrm{per}}(\Omega)$ since $L_{a_0}$ commutes with derivatives. Roughly speaking, we do not know how much regularity we gain by applying $L_{a_0}^{-1}$ but at least we do not lose regularity.

From the implicit function theorem we find the following continuation result.

**Theorem 5.10.** *Let $d \in \mathbb{R} \setminus \{0\}$, $\zeta, f_0, \nu_1 \in \mathbb{R}$ and $k_1 \in \mathbb{N}$ be fixed. Let furthermore $a_0 \in \mathbb{C}$ be a constant non-degenerate solution of (5.2) for $f_1 = 0$. Then there exist neighborhoods $(-\delta, \delta) \subset \mathbb{R}$ of 0 and $B_\varepsilon(a_0) \subset H^2_{per}(\Omega)$ of $a_0$ and a continuously differentiable curve $\tilde{a} : (-\delta, \delta) \to B_\varepsilon(a_0)$ with $\tilde{a}(0) = a_0$ such that all solutions $(f_1, a)$ of (5.2) in $(-\delta, \delta) \times B_\varepsilon(a_0)$ are exactly given by $\{(\tilde{f}_1, \tilde{a}(\tilde{f}_1)) : \tilde{f}_1 \in (-\delta, \delta)\}$.*

*Proof.* The operator $L_{a_0} : D(L_{a_0}) \to L^2(\Omega)$ is invertible by the non-degeneracy assumption. Consider the map

$$
A : \begin{cases} \mathbb{R} \times H^2_{\mathrm{per}}(\Omega) & \to \quad L_{a_0}(H^2_{\mathrm{per}}(\Omega)), \\ (f_1, a) & \mapsto \quad -\mathrm{i}a_t + (-\mathrm{i} + \zeta)a - da_{xx} - |a|^2 a + \mathrm{i}f_0 + \mathrm{i}f_1 \mathrm{e}^{\mathrm{i}(k_1 x - \nu_1 t)}. \end{cases}
$$

Note that $A$ is well-defined since

$$A(f_1, a) = L_{a_0} a + 2|a_0|^2 a + a_0^2 \bar{a} - |a|^2 a + \mathrm{i} f_0 + \mathrm{i} f_1 \mathrm{e}^{\mathrm{i}(k_1 x - \nu_1 t)}$$

and

$$2|a_0|^2 a + a_0^2 \bar{a} - |a|^2 a + \mathrm{i} f_0 + \mathrm{i} f_1 \mathrm{e}^{\mathrm{i}(k_1 x - \nu_1 t)} \in H^2_{\mathrm{per}}(\Omega) \subset L_{a_0}(H^2_{\mathrm{per}}(\Omega)),$$

cf. Remark 5.9. We equip $L_{a_0}(H^2_{\mathrm{per}}(\Omega))$ with the norm $\|g\|_{L_{a_0}(H^2_{\mathrm{per}}(\Omega))} = \|L_{a_0}^{-1} g\|_{H^2_{\mathrm{per}}(\Omega)}$ so that $L_{a_0}|_{H^2_{\mathrm{per}}(\Omega)} : H^2_{\mathrm{per}}(\Omega) \to L_{a_0}(H^2_{\mathrm{per}}(\Omega))$ becomes an isometric isomorphism and $L_{a_0}(H^2_{\mathrm{per}}(\Omega))$ a Banach space. Since $A(0, a_0) = 0$ and $\partial_a A(0, a_0) = L_{a_0}|_{H^2_{\mathrm{per}}(\Omega)} : H^2_{\mathrm{per}}(\Omega) \to L_{a_0}(H^2_{\mathrm{per}}(\Omega))$ is invertible, the assertion follows from the implicit function theorem. □

In fact, we can provide some more information about the deduced solutions.

**Corollary 5.11.** *In the setting of Theorem 5.10, $\tilde{a}(\tilde{f}_1)$ is a traveling wave of the form $u(x - \omega t)$ for $|\tilde{f}_1|$ sufficiently small. Here, $\omega = \frac{\nu_1}{k_1}$ and $u$ is a $\frac{2\pi}{k_1}$-periodic solution of (5.3).*

*Proof.* Note that Theorem 3.6 provides continuations $u$ of $a_0$ which are not only $2\pi$- but in fact $\frac{2\pi}{k_1}$-periodic[6], cf. Section 4.10. Thus, $a(t, x) = u(x - \omega t)$ has time-periodicity $\frac{2\pi}{k_1|\omega|} = T$ and space-periodicity $\frac{2\pi}{k_1}$. In particular, $a \in H^2_{\mathrm{per}}(\Omega)$. By uniqueness, the assertion follows. □

**Remark 5.12.** The benefit of Theorem 5.10 lies less in the existence part but rather in the statement that the locally uniqueness of $\tilde{a}(\tilde{f}_1)$ is no longer restricted to traveling waves but holds for all space- and time-periodic solutions.

Next we want to analyze the domain $D(L_{a_0})$ and point out why global continuation results seem to be challenging in this setting. For this we introduce the norm

$$\|\psi\|^2_{D(L_{a_0})} = \sum_{k,l \in \mathbb{Z}} \left( 1 + \left| l\frac{2\pi}{T} + dk^2 \right|^2 \right) |\psi_{k,l}|^2$$

on $D(L_{a_0})$ which makes the operator $L_{a_0} : (D(L_{a_0}), \| \cdot \|_{D(L_{a_0})}) \to L^2(\Omega)$ continuous.

**Proposition 5.13.** *The embedding $(D(L_{a_0}), \| \cdot \|_{D(L_{a_0})}) \hookrightarrow L^2(\Omega)$ is not compact.*

*Proof.* For every $k \in \mathbb{N}$ we can choose $l(k) \in \mathbb{Z}$ such that

$$\left| l(k)\frac{2\pi}{T} + dk^2 \right|^2 \leq \frac{\pi^2}{T^2}.$$

The sequence $\left( \mathrm{e}^{\mathrm{i}kx} \mathrm{e}^{\mathrm{i}l(k)\frac{2\pi}{T}t} \right)_{k \in \mathbb{N}}$ is bounded in $(D(L_{a_0}), \| \cdot \|_{D(L_{a_0})})$ since

$$\left\| \mathrm{e}^{\mathrm{i}kx} \mathrm{e}^{\mathrm{i}l(k)\frac{2\pi}{T}t} \right\|^2_{D(L_{a_0})} = 1 + \left| l(k)\frac{2\pi}{T} + dk^2 \right|^2 \leq 1 + \frac{\pi^2}{T^2}.$$

---

[6]In case of $e(s) = \mathrm{e}^{\mathrm{i}k_1 s}$ we can work in $H^2_{\mathrm{per}}(0, \frac{2\pi}{k_1})$ instead of $H^2_{\mathrm{per}}(0, 2\pi)$ in Theorem 3.6.

But due to

$$\left\| e^{ik_1 x} e^{il(k_1)\frac{2\pi}{T}t} - e^{ik_2 x} e^{il(k_2)\frac{2\pi}{T}t} \right\|_{L^2(\Omega)}^2 = 4\pi T \text{ for } k_1 \neq k_2$$

this sequence has no convergent subsequence in $L^2(\Omega)$. $\square$

Next we want to show that there are no choices of $T > 0$ and $d \neq 0$ such that

$$\left| l\frac{2\pi}{T} + dk^2 \right| \geq \varepsilon_0$$

for some $\varepsilon_0 > 0$ and almost all $(k,l) \in \mathbb{Z}^2$. Note that in the case $\frac{Td}{2\pi} \in \mathbb{Q}$ this is easily proven. In fact, if $\frac{Td}{2\pi} = \frac{m}{n}$ for some $m \in \mathbb{Z}$ and $n \in \mathbb{N}$, then with $(k(r), l(r)) = (rn, -r^2 mn)$, $r \in \mathbb{Z}$ one finds

$$\left| l(r)\frac{2\pi}{T} + dk(r)^2 \right| = \frac{2\pi}{T}\left| l(r) + \frac{Td}{2\pi}k(r)^2 \right| = \frac{2\pi}{T}\left| -r^2 mn + \frac{m}{n}r^2 n^2 \right| = 0.$$

The case $\frac{Td}{2\pi} \notin \mathbb{Q}$ is more complicated. Note that here the assertion can be reformulated as

$$\inf_{(k,l)\in\mathbb{Z}^2\setminus\{(0,0)\}} \left| l\frac{2\pi}{T} + dk^2 \right| = 0.$$

To show this we will need the following result from Heilbronn (cf. [30]).

**Theorem 5.14.** *For every integer $N \geq 1$ and every real $\theta$, integers $n$ and $g$ can be found such that*

$$1 \leq n \leq N, \qquad |n^2\theta - g| \leq c(\eta)N^{-\frac{1}{2}+\eta},$$

*where $\eta$ is an arbitrarily small positive number and where $c(\eta)$ depends on $\eta$ only.*

We can use Theorem 5.14 to obtain the following statement.

**Proposition 5.15.** *Let $T > 0$ and $d \neq 0$ be such that $\frac{Td}{2\pi} \notin \mathbb{Q}$. Then*

$$\inf_{(k,l)\in\mathbb{Z}^2\setminus\{(0,0)\}} \left| l\frac{2\pi}{T} + dk^2 \right| = 0.$$

*Proof.* Choose $\theta = -\frac{Td}{2\pi}$, $\eta = \frac{1}{4}$ and consider $N \to \infty$ in Theorem 5.14. $\square$

Next we want to establish a global uniqueness result which is based on the following a-priori bounds.

**Theorem 5.16.** *Let $d \in \mathbb{R} \setminus \{0\}$, $f_0, f_1, \zeta, \nu_1 \in \mathbb{R}$ and $k_1 \in \mathbb{N}$. Then for every solution $a \in C_{per}^1([0,T], H_{per}^2(0, 2\pi))$ of (5.2) the a-priori bounds*

$$\sup_{t\in[0,T]} \|a(t)\|_2^2 \leq F^2, \qquad \sup_{t\in[0,T]} \|a_x(t)\|_2^2 \leq B, \qquad \|a\|_{L^\infty(\Omega)}^2 \leq C$$

*hold, where*

$$F = F(f_0, f_1) = \sqrt{2\pi(f_0^2 + f_1^2)},$$

88

$$B = B(d, f_0, f_1, \nu_1, \zeta) = \begin{cases} \frac{F}{|d|}\left(\sqrt{F^2 + 2\pi\nu_1^2 f_1^2} + (\zeta^+ + 2)F\right), & d < 0, \\ \frac{8dF\left(\sqrt{F^2 + 2\pi\nu_1^2 f_1^2} + (\zeta^- + 2)F\right) + 4d^2 F^2 + 45F^6}{4d^2}, & d > 0, \end{cases}$$

$$C = C(d, f_0, f_1, \nu_1, \zeta) = \frac{F^2}{2\pi} + 2F\sqrt{B}.$$

*Proof.* The proof is divided into three steps.

Step 1. We first prove the estimate

$$\sup_{t \in [0,T]} \|a(t)\|_2^2 \leq F^2 = 2\pi(f_0^2 + f_1^2). \tag{5.8}$$

To this end note that

$$\frac{\mathrm{d}}{\mathrm{d}t}\|a(t)\|_2^2 = 2\operatorname{Re}\int_0^{2\pi} \overline{a}a_t \, dx$$

$$\overset{(5.2)}{=} -2\operatorname{Re}\int_0^{2\pi} \overline{a}\,\mathrm{i}\big((-\mathrm{i}+\zeta)a - da_{xx} - |a|^2 a + \mathrm{i}f_0 + \mathrm{i}f_1 \mathrm{e}^{\mathrm{i}(k_1 x - \nu_1 t)}\big)\,dx$$

$$= -2\operatorname{Re}\int_0^{2\pi} \overline{a}\big(a + \zeta\mathrm{i}a - \mathrm{i}da_{xx} - \mathrm{i}|a|^2 a - f_0 - f_1 \mathrm{e}^{\mathrm{i}(k_1 x - \nu_1 t)}\big)\,dx$$

$$= -2\|a(t)\|_2^2 + 2\operatorname{Re}\int_0^{2\pi} \overline{a}\big(f_0 + f_1 \mathrm{e}^{\mathrm{i}(k_1 x - \nu_1 t)}\big)\,dx$$

$$\leq -2\|a(t)\|_2^2 + 2\|a(t)\|_2\big\|f_0 + f_1 \mathrm{e}^{\mathrm{i}(k_1 \cdot - \nu_1 t)}\big\|_2$$

$$= -2\|a(t)\|_2^2 + 2\|a(t)\|_2\sqrt{2\pi(f_0^2 + f_1^2)}$$

$$\leq -\|a(t)\|_2^2 + 2\pi(f_0^2 + f_1^2)$$

so that

$$\frac{\mathrm{d}}{\mathrm{d}t}\big(\mathrm{e}^t\|a(t)\|_2^2\big) \leq 2\pi(f_0^2 + f_1^2)\mathrm{e}^t.$$

By integration this yields

$$\|a(t)\|_2^2 \leq \mathrm{e}^{-t}\|a(0)\|_2^2 + 2\pi(f_0^2 + f_1^2)(1 - \mathrm{e}^{-t}).$$

Now let $t \in [0, T]$. Then, for $m \in \mathbb{N}$, we get

$$\|a(t)\|_2^2 = \|a(t + mT)\|_2^2 \leq \mathrm{e}^{-(t+mT)}\|a(0)\|_2^2 + 2\pi(f_0^2 + f_1^2)\big(1 - \mathrm{e}^{-(t+mT)}\big)$$

by the time-periodicity of $a$. Finally, $m \to \infty$ yields

$$\|a(t)\|_2^2 \leq 2\pi(f_0^2 + f_1^2).$$

Step 2. Next we show

$$\sup_{t \in [0,T]} \|a_x(t)\|_2^2 \leq B = \begin{cases} \frac{F}{|d|}\left(\sqrt{F^2 + 2\pi\nu_1^2 f_1^2} + (\zeta^+ + 2)F\right), & d < 0, \\ \frac{8dF\left(\sqrt{F^2 + 2\pi\nu_1^2 f_1^2} + (\zeta^- + 2)F\right) + 4d^2 F^2 + 45F^6}{4d^2}, & d > 0. \end{cases} \tag{5.9}$$

For this let us introduce the modified energy (cf. [33])

$$\mathcal{E}(t,b) = \frac{d}{2}\|b_x\|_2^2 - \frac{1}{4}\|b\|_4^4 + \text{Re}\int_0^{2\pi}(\mathrm{i}f_0 + \mathrm{i}f_1 \mathrm{e}^{\mathrm{i}(k_1 x - \nu_1 t)})\bar{b}\,dx + \frac{\zeta}{2}\|b\|_2^2$$

for $t \geq 0$ and $b \in H^1_{\text{per}}(0, 2\pi)$. Then,

$$\frac{\mathrm{d}}{\mathrm{d}t}\mathcal{E}(t, a(t)) = \text{Re}\int_0^{2\pi} da_x\bar{a}_{xt} - |a|^2 a\bar{a}_t + (\mathrm{i}f_0 + \mathrm{i}f_1 \mathrm{e}^{\mathrm{i}(k_1 x - \nu_1 t)})\bar{a}_t + \zeta a\bar{a}_t + \nu_1 f_1 \mathrm{e}^{\mathrm{i}(k_1 x - \nu_1 t)}\bar{a}\,dx$$

$$= \text{Re}\int_0^{2\pi}\left(-da_{xx} - |a|^2 a + \mathrm{i}f_0 + \mathrm{i}f_1 \mathrm{e}^{\mathrm{i}(k_1 x - \nu_1 t)} + \zeta a\right)\bar{a}_t + \nu_1 f_1 \mathrm{e}^{\mathrm{i}(k_1 x - \nu_1 t)}\bar{a}\,dx$$

$$\overset{(5.2)}{=} \text{Re}\int_0^{2\pi} \mathrm{i}(a_t + a)\bar{a}_t + \nu_1 f_1 \mathrm{e}^{\mathrm{i}(k_1 x - \nu_1 t)}\bar{a}\,dx$$

$$= \text{Re}\int_0^{2\pi} \mathrm{i}a\bar{a}_t + \nu_1 f_1 \mathrm{e}^{\mathrm{i}(k_1 x - \nu_1 t)}\bar{a}\,dx$$

$$= \text{Re}\int_0^{2\pi} -\mathrm{i}a_t\bar{a} + \nu_1 f_1 \mathrm{e}^{\mathrm{i}(k_1 x - \nu_1 t)}\bar{a}\,dx$$

$$\overset{(5.2)}{=} \text{Re}\int_0^{2\pi}\left((\mathrm{i} - \zeta)a + da_{xx} + |a|^2 a - \mathrm{i}f_0 - \mathrm{i}f_1 \mathrm{e}^{\mathrm{i}(k_1 x - \nu_1 t)}\right)\bar{a} + \nu_1 f_1 \mathrm{e}^{\mathrm{i}(k_1 x - \nu_1 t)}\bar{a}\,dx$$

$$= -\zeta\|a(t)\|_2^2 - d\|a_x(t)\|_2^2 + \|a(t)\|_4^4 - \text{Re}\int_0^{2\pi} \mathrm{i}f_0 + (\mathrm{i} - \nu_1)f_1 \mathrm{e}^{\mathrm{i}(k_1 x - \nu_1 t)}\bar{a}\,dx$$

$$= -2\mathcal{E}(t, a(t)) + \frac{1}{2}\|a(t)\|_4^4 + \text{Re}\int_0^{2\pi} \mathrm{i}f_0 + (\mathrm{i} + \nu_1)f_1 \mathrm{e}^{\mathrm{i}(k_1 x - \nu_1 t)}\bar{a}\,dx.$$

In order to prove (5.9) we first suppose $d < 0$. In this case

$$\frac{\mathrm{d}}{\mathrm{d}t}\mathcal{E}(t, a(t)) \geq -2\mathcal{E}(t, a(t)) - \sqrt{2\pi}\sqrt{f_0^2 + f_1^2 + \nu_1^2 f_1^2}\|a(t)\|_2 \tag{5.10}$$

$$\overset{(5.8)}{\geq} -2\mathcal{E}(t, a(t)) - 2\pi\sqrt{f_0^2 + f_1^2 + \nu_1^2 f_1^2}\sqrt{f_0^2 + f_1^2}$$

so that

$$\frac{\mathrm{d}}{\mathrm{d}t}\left(\mathrm{e}^{2t}\mathcal{E}(t, a(t))\right) \geq -2\pi\sqrt{f_0^2 + f_1^2 + \nu_1^2 f_1^2}\sqrt{f_0^2 + f_1^2}\mathrm{e}^{2t}.$$

By integration we find

$$\mathcal{E}(t, a(t)) \geq \mathrm{e}^{-2t}\mathcal{E}(0, a(0)) - \pi\sqrt{f_0^2 + f_1^2 + \nu_1^2 f_1^2}\sqrt{f_0^2 + f_1^2}(1 - \mathrm{e}^{-2t}).$$

Now let $t \in [0, T]$. Then, for $m \in \mathbb{N}$, we get

$$\mathcal{E}(t, a(t)) = \mathcal{E}(t + mT, a(t + mT))$$
$$\geq \mathrm{e}^{-2(t+mT)}\mathcal{E}(0, a(0)) - \pi\sqrt{f_0^2 + f_1^2 + \nu_1^2 f_1^2}\sqrt{f_0^2 + f_1^2}(1 - \mathrm{e}^{-2(t+mT)})$$

by the periodicity of $\mathcal{E}(\cdot, a(\cdot))$ and hence

$$\mathcal{E}(t, a(t)) \geq -\pi\sqrt{f_0^2 + f_1^2 + \nu_1^2 f_1^2}\sqrt{f_0^2 + f_1^2}.$$

Thus,

$$-\pi\sqrt{f_0^2 + f_1^2 + \nu_1^2 f_1^2}\sqrt{f_0^2 + f_1^2}$$
$$\leq \frac{d}{2}\|a_x(t)\|_2^2 - \frac{1}{4}\|a(t)\|_4^4 + \mathrm{Re}\int_0^{2\pi}(\mathrm{i}f_0 + \mathrm{i}f_1 \mathrm{e}^{\mathrm{i}(k_1 x - \nu_1 t)})\overline{a}\,dx + \frac{\zeta}{2}\|a(t)\|_2^2$$
$$\overset{(5.8)}{\leq} \frac{d}{2}\|a_x(t)\|_2^2 + \sqrt{2\pi(f_0^2 + f_1^2)}\|a(t)\|_2 + \pi\zeta^+(f_0^2 + f_1^2)$$
$$\overset{(5.8)}{\leq} \frac{d}{2}\|a_x(t)\|_2^2 + 2\pi(f_0^2 + f_1^2) + \pi\zeta^+(f_0^2 + f_1^2)$$

from where we finally deduce

$$\|a_x(t)\|_2^2 \leq \frac{2\pi\sqrt{f_0^2 + f_1^2}}{|d|}\left(\sqrt{f_0^2 + f_1^2 + \nu_1^2 f_1^2} + (\zeta^+ + 2)\sqrt{f_0^2 + f_1^2}\right)$$
$$= \frac{F}{|d|}\left(\sqrt{F^2 + 2\pi\nu_1^2 f_1^2} + (\zeta^+ + 2)F\right).$$

Assuming now $d > 0$ the estimate (5.10) becomes

$$\frac{\mathrm{d}}{\mathrm{d}t}\mathcal{E}(t, a(t)) \leq -2\mathcal{E}(t, a(t)) + \frac{1}{2}\sup_{r \in [0,T]}\|a(r)\|_4^4 + 2\pi\sqrt{f_0^2 + f_1^2 + \nu_1^2 f_1^2}\sqrt{f_0^2 + f_1^2}$$

so that

$$\frac{\mathrm{d}}{\mathrm{d}t}\left(\mathrm{e}^{2t}\mathcal{E}(t, a(t))\right) \leq \frac{\mathrm{e}^{2t}}{2}\sup_{r \in [0,T]}\|a(r)\|_4^4 + 2\pi\sqrt{f_0^2 + f_1^2 + \nu_1^2 f_1^2}\sqrt{f_0^2 + f_1^2}\mathrm{e}^{2t}.$$

By integration,

$$\mathcal{E}(t, a(t)) \leq \mathrm{e}^{-2t}\mathcal{E}(0, a(0)) + \frac{1 - \mathrm{e}^{-2t}}{4}\left(\sup_{r \in [0,T]}\|a(r)\|_4^4 + 4\pi\sqrt{f_0^2 + f_1^2 + \nu_1^2 f_1^2}\sqrt{f_0^2 + f_1^2}\right)$$

and hence

$$\mathcal{E}(t, a(t)) \leq \frac{1}{4} \sup_{r \in [0,T]} \|a(r)\|_4^4 + \pi \sqrt{f_0^2 + f_1^2 + \nu_1^2 f_1^2} \sqrt{f_0^2 + f_1^2}.$$

Thus,

$$\frac{1}{4} \sup_{r \in [0,T]} \|a(r)\|_4^4 + \pi \sqrt{f_0^2 + f_1^2 + \nu_1^2 f_1^2} \sqrt{f_0^2 + f_1^2}$$

$$\geq \frac{d}{2} \|a_x(t)\|_2^2 - \frac{1}{4} \|a(t)\|_4^4 + \mathrm{Re} \int_0^{2\pi} (\mathrm{i} f_0 + \mathrm{i} f_1 \mathrm{e}^{\mathrm{i}(k_1 x - \nu_1 t)}) \overline{a} \, dx + \frac{\zeta}{2} \|a(t)\|_2^2$$

$$\overset{(5.8)}{\geq} \frac{d}{2} \|a_x(t)\|_2^2 - \frac{1}{4} \sup_{r \in [0,T]} \|a(r)\|_4^4 - 2\pi(f_0^2 + f_1^2) - \pi \zeta^-(f_0^2 + f_1^2)$$

from where we find

$$d\|a_x(t)\|_2^2 \leq \sup_{r \in [0,T]} \|a(r)\|_4^4 + 2\pi \sqrt{f_0^2 + f_1^2} \left( \sqrt{f_0^2 + f_1^2 + \nu_1^2 f_1^2} + (\zeta^- + 2) \sqrt{f_0^2 + f_1^2} \right)$$

$$= \sup_{r \in [0,T]} \|a(r)\|_4^4 + F \left( \sqrt{F^2 + 2\pi \nu_1^2 f_1^2} + (\zeta^- + 2)F \right).$$

Using the Gagliardo-Nirenberg inequality (cf. Lemma 5.17 below) and Young's inequality we can control the fourth order term,

$$\|a(r)\|_4^4 \leq \frac{64}{27} \sqrt{2} \|a(r)\|_2^3 \|a(r)\|_{H^1(0,2\pi)}$$

$$\leq \frac{64}{27} \sqrt{2} \left( \frac{27d}{128\sqrt{2}} \|a(r)\|_{H^1(0,2\pi)}^2 + \frac{32\sqrt{2}}{27d} \|a(r)\|_2^6 \right)$$

$$= \frac{d}{2} \|a_x(r)\|_2^2 + \frac{d}{2} \|a(r)\|_2^2 + \frac{4096}{729d} \|a(r)\|_2^6$$

$$\overset{(5.8)}{\leq} \frac{d}{2} \|a_x(r)\|_2^2 + \frac{F^2 d}{2} + \frac{45}{8d} F^6.$$

Combining the previous two estimates we find

$$\sup_{t \in [0,T]} \|a_x(t)\|_2^2 \leq \frac{8dF \left( \sqrt{F^2 + 2\pi \nu_1^2 f_1^2} + (\zeta^- + 2)F \right) + 4d^2 F^2 + 45F^6}{4d^2}.$$

**Step 3.** Finally we prove

$$\|a\|_{L^\infty(\Omega)}^2 \leq C = \frac{F^2}{2\pi} + 2F\sqrt{B}.$$

Using (5.8) we find for every $t \in [0, T]$ an element $x_t \in [0, 2\pi]$ such that

$$|a(t, x_t)|^2 \leq \frac{F^2}{2\pi}.$$

Now we can conclude

$$|a(t, x)^2| \leq |a(t, x_t)^2| + |a(t, x)^2 - a(t, x_t)^2| \leq \frac{F^2}{2\pi} + 2 \int_0^{2\pi} |a(t, y) a_x(t, y)| \, dy$$

$$\leq \frac{F^2}{2\pi} + 2\|a(t)\|_2 \|a_x(t)\|_2 \leq \frac{F^2}{2\pi} + 2F\sqrt{B}.$$

$\square$

Let us provide the Gagliardo-Nirenberg inequality used in the above proof. Recall that $\|\cdot\|_p$ denotes the standard norm on $L^p(0, 2\pi)$ for $p \in [1, \infty]$.

**Lemma 5.17.** *Let $b \in H^1(0, 2\pi)$. Then the inequality*

$$\|b\|_4^4 \leq \frac{64}{27}\sqrt{2}\|b\|_2^3 \|b\|_{H^1(0,2\pi)}$$

*holds.*

*Proof.* From [44, Corollary 5.15] we find

$$\|v\|_{L^4(\mathbb{R})}^4 \leq \frac{16}{27}\|v\|_{L^2(\mathbb{R})}^3 \|v'\|_{L^2(\mathbb{R})} \tag{5.11}$$

for $v \in H^1(\mathbb{R})$. Now let $b \in H^1(0, 2\pi)$. We want to construct an extension $c_* \in H^1(\mathbb{R})$ with $c_*|_{(0,2\pi)} = b$. First we extend $b$ to a function $b_* \in H^1(-\pi, 3\pi)$ in the following way,

$$b_*(x) = \begin{cases} b(-x), & -\pi \leq x \leq 0, \\ b(x), & 0 \leq x \leq 2\pi, \\ b(4\pi - x), & 2\pi \leq x \leq 3\pi \end{cases}$$

and observe $\|b_*\|_{L^2(-\pi,3\pi)}^2 = 2\|b\|_2^2$ as well as $\|b_*'\|_{L^2(-\pi,3\pi)}^2 = 2\|b'\|_2^2$. Consider the function $\psi \in H^1(-\pi, 3\pi) \cap C_c(-\pi, 3\pi)$ defined by

$$\psi(x) = \begin{cases} 0, & -\pi \leq x \leq -1, \\ 1 + x, & -1 \leq x \leq 0, \\ 1, & 0 \leq x \leq 2\pi, \\ 2\pi + 1 - x, & 2\pi \leq x \leq 2\pi + 1, \\ 0, & 2\pi + 1 \leq x \leq 3\pi. \end{cases}$$

Note that $c := \psi b_* \in H^1(-\pi, 3\pi) \cap C_c(-\pi, 3\pi)$ is an extension of $b$ and that $0 \leq \psi \leq 1$

as well as

$$|\psi'(x)| \le 1 \text{ for almost all } x \in (-\pi, 3\pi). \tag{5.12}$$

Finally, $c_* \in H^1(\mathbb{R})$ will be defined by

$$c_*(x) = \begin{cases} c(x), & -\pi \le x \le 3\pi, \\ 0, & \text{otherwise.} \end{cases}$$

Clearly, $c_*|_{(0,2\pi)} = b$, $\|c_*\|_{L^2(\mathbb{R})} = \|c\|_{L^2(-\pi,3\pi)}$ as well as $\|c'_*\|_{L^2(\mathbb{R})} = \|c'\|_{L^2(-\pi,3\pi)}$. Hence,

$$
\begin{aligned}
\|b\|_4^4 \le \|c_*\|_{L^4(\mathbb{R})}^4 &\overset{(5.11)}{\le} \frac{16}{27}\|c_*\|_{L^2(\mathbb{R})}^3\|c'_*\|_{L^2(\mathbb{R})} = \frac{16}{27}\|c\|_{L^2(-\pi,3\pi)}^3\|c'\|_{L^2(-\pi,3\pi)} \\
&= \frac{16}{27}\|\psi b_*\|_{L^2(-\pi,3\pi)}^3\|(\psi b_*)'\|_{L^2(-\pi,3\pi)} \le \frac{16}{27}\|b_*\|_{L^2(-\pi,3\pi)}^3\|\psi b'_* + \psi' b_*\|_{L^2(-\pi,3\pi)} \\
&\le \frac{32}{27}\sqrt{2}\|b\|_2^3\big(\|\psi b'_*\|_{L^2(-\pi,3\pi)} + \|\psi' b_*\|_{L^2(-\pi,3\pi)}\big) \\
&\overset{(5.12)}{\le} \frac{32}{27}\sqrt{2}\|b\|_2^3\big(\|b'_*\|_{L^2(-\pi,3\pi)} + \|b_*\|_{L^2(-\pi,3\pi)}\big) = \frac{64}{27}\|b\|_2^3\big(\|b'\|_2 + \|b\|_2\big) \\
&\le \frac{64}{27}\sqrt{2}\|b\|_2^3\|b\|_{H^1(0,2\pi)}
\end{aligned}
$$

which finishes the proof. $\qquad\square$

Now we can state our global uniqueness result.

**Theorem 5.18.** *Let $d \in \mathbb{R} \setminus \{0\}$, $f_0, f_1, \zeta, \nu_1 \in \mathbb{R}$ and $k_1 \in \mathbb{N}$. Then (5.2) has a unique solution $a \in C^1_{per}([0,T], H^2_{per}(0,2\pi))$ if $3C < 1$, where $C = C(d, f_0, f_1, \nu_1, \zeta)$ is the constant from Theorem 5.16. In particular, $f_0^2 + f_1^2 \ll 1$ is sufficient.*

**Remark 5.19.** The corresponding unique solution is of the form $a(t,x) = u(x - \omega t)$ where $u$ is a $\frac{2\pi}{k_1}$-periodic[7] solution of (5.3) and $\omega = \frac{\nu_1}{k_1}$. Thus, it has the shape of the pump.

*Proof.* Equation (5.2) has at least one solution $a_1 \in C^1_{\mathrm{per}}([0,T], H^2_{\mathrm{per}}(0,2\pi))$ due to Theorem 3.1. Now let $a_2 \in C^1_{\mathrm{per}}([0,T], H^2_{\mathrm{per}}(0,2\pi))$ denote an additional solution. Then $\|a_j\|_{L^\infty(\Omega)}^2 \le C$ for $j = 1, 2$ by Theorem 5.16, which easily implies

$$\big\||a_1|^2 a_1 - |a_2|^2 a_2\big\|_{L^2(\Omega)} \le 3C\|a_1 - a_2\|_{L^2(\Omega)}.$$

Note that $a_j, j = 1, 2$ solves the fixed point problem

$$a_j = L^{-1}\big(|a_j|^2 a_j - \mathrm{i}f_0 - \mathrm{i}f_1 e^{\mathrm{i}(k_1 x - \nu_1 t)}\big),$$

where

$$L = -\mathrm{i}\frac{\partial}{\partial t} + (-\mathrm{i} + \zeta) - d\frac{\partial^2}{\partial x^2}.$$

---

[7]In case of $e(s) = e^{\mathrm{i}k_1 s}$ we can work in $H^2_{\mathrm{per}}(0, \frac{2\pi}{k_1})$ instead of $H^2_{\mathrm{per}}(0, 2\pi)$ in Theorem 3.1.

Hence,

$$\|a_1 - a_2\|_{L^2(\Omega)} \le 3C\|L^{-1}\|\|a_1 - a_2\|_{L^2(\Omega)},$$

where $\|L^{-1}\| = \sup_{v \in L^2(\Omega), \|v\|_{L^2(\Omega)}=1} \|L^{-1}v\|_{L^2(\Omega)}$. Next we show $3C\|L^{-1}\| < 1$ which implies $a_1 = a_2$ and thus finishes the proof. To this end we decompose a function $b \in L^2(\Omega)$ into its Fourier series, i.e., $b = \sum_{k,l \in \mathbb{Z}} b_{k,l} \mathrm{e}^{\mathrm{i}kx} \mathrm{e}^{\mathrm{i}l\frac{2\pi}{T}t}$ so that

$$L^{-1}b = \sum_{k,l \in \mathbb{Z}} \frac{b_{k,l}}{l\frac{2\pi}{T} + dk^2 - \mathrm{i} + \zeta} \, \mathrm{e}^{\mathrm{i}kx} \mathrm{e}^{\mathrm{i}l\frac{2\pi}{T}t}.$$

Since

$$\|L^{-1}b\|_{L^2(\Omega)}^2 = 2\pi T \sum_{k,l \in \mathbb{Z}} \frac{|b_{k,l}|^2}{1 + \left(l\frac{2\pi}{T} + dk^2 + \zeta\right)^2} \le 2\pi T \sum_{k,l \in \mathbb{Z}} |b_{k,l}|^2 = \|b\|_{L^2(\Omega)}^2$$

we get $\|L^{-1}\| \le 1$ which, due to our assumption $3C < 1$, is all we had to show. $\qquad \square$

Note that it remains unanswered if there is a choice of the parameters $d, f_0, \zeta, k_1, \nu_1, f_1$ such that (5.2) admits a time-periodic solution which is not of the form $a(t,x) = u(x - \omega t)$ where $u$ is a solution of (5.3) and $\omega = \frac{\nu_1}{k_1}$.

# 6. Approximation formulas

## 6.1. One mode case

In [68], Wabnitz used an approximation formula for soliton solutions of the following variant of the stationary LLE

$$-da'' + (-\mathrm{i}\alpha + \zeta)a - |a|^2 a + \mathrm{i}f_* = 0 \text{ on } \mathbb{R}, \qquad a'(0) = 0, \tag{6.1}$$

where we assume $\alpha, d, \zeta > 0$ and $f_* \neq 0$, cf. also [31]. Note that in the anomalous dispersion regime it is reasonable to consider the LLE on the real line since strongly localized solutions of (6.1) serve as good approximations for periodic solutions, cf. [31]. Note also that the condition $a'(0) = 0$ breaks the shift invariance. An advantage of this approach is that for $\alpha = 0$ and $f_* = 0$ the explicit solution family

$$a_\theta(x) = \sqrt{2\zeta}\,\mathrm{sech}\left(\sqrt{\frac{\zeta}{d}}x\right)\mathrm{e}^{\mathrm{i}\theta}, \quad \theta \in [0, 2\pi)$$

is known, where sech denotes the hyperbolic secant. It serves as the basis for the approximation formula used by Wabnitz which reads

$$a(x) \approx a_\infty + a_{\theta^*}(x),$$

where $\cos\theta^* = \frac{\alpha\sqrt{8\zeta}}{\pi f_*}$ and where the constant background $a_\infty \in \mathbb{C}$ is the solution with smallest magnitude of

$$(-\mathrm{i}\alpha + \zeta)a_\infty - |a_\infty|^2 a_\infty + \mathrm{i}f_* = 0.$$

Here, the parameters have to be chosen such that $\alpha\sqrt{8\zeta} < \pi|f_*|$.

Our goal is to provide a mathematically rigorous approximation theorem. We use a bifurcation approach and consider the equation

$$-dw'' + (-\mathrm{i}\varepsilon + \zeta)w - |w|^2 w + \mathrm{i}\varepsilon f = 0 \text{ on } \mathbb{R}, \quad w'(0) = 0, \tag{6.2}$$

where $\varepsilon$ is considered as bifurcation parameter. Compared with (6.1) we have $\alpha = \varepsilon$ and $f_* = \varepsilon f$ so that $\cos\theta^* = \frac{\sqrt{8\zeta}}{\pi f}$ in our setting. We fix $\zeta > 0$, $f \neq 0$ such that $\sqrt{8\zeta} < \pi|f|$ and denote by $w_\infty = w_\infty(\varepsilon) \in \mathbb{C}$ the solution with smallest magnitude of

$$(-\mathrm{i}\varepsilon + \zeta)w_\infty - |w_\infty|^2 w_\infty + \mathrm{i}\varepsilon f = 0. \tag{6.3}$$

This choice of $w_\infty$ is made since we want to have a curve with $w_\infty(0) = 0$. We will work with the real Hilbert spaces $\mathcal{H} := \{\phi \in H^2(\mathbb{R}) : \phi(x) = \phi(-x)\}$ and $\mathcal{L} := \{\phi \in L^2(\mathbb{R}) : \phi(x) = \phi(-x)\}$ and the scalar product

$$\langle\phi, \psi\rangle_{L^2(\mathbb{R})} := \mathrm{Re}\int_{\mathbb{R}}\phi\overline{\psi}\,dx.$$

# 6. Approximation formulas

Roughly speaking, we can formulate our approximation result in the following way.

**Approximation result 6.1.** Let $d, \zeta > 0$, $f \neq 0$ such that

$$\frac{\sqrt{8\zeta}}{\pi|f|} < 1 \ \text{ and } \ \cos\theta^* = \frac{\sqrt{8\zeta}}{\pi f}.$$

Then, localized solutions of (6.2) have the form

$$w(\varepsilon) = w_\infty(\varepsilon) + a_{\theta^*} + \varepsilon\psi + \mathcal{O}(\varepsilon^2)$$
$$= a_{\theta^*} + \varepsilon\left(\psi - \frac{\mathrm{i}f}{\zeta}\right) + \mathcal{O}(\varepsilon^2),$$

where

$$a_{\theta^*}(x) = \sqrt{2\zeta}\,\mathrm{sech}\left(\sqrt{\frac{\zeta}{d}}\,x\right)\mathrm{e}^{\mathrm{i}\theta^*}$$

and where $\psi \in \mathcal{H}$ is a suitable solution of

$$-d\psi'' + \zeta\psi - 2|a_{\theta^*}|^2\psi - a_{\theta^*}^2\overline{\psi} = \mathrm{i}a_{\theta^*} - \frac{2\mathrm{i}f}{\zeta}|a_{\theta^*}|^2 + \frac{\mathrm{i}f}{\zeta}a_{\theta^*}^2.$$

**Remark 6.2.** ($\alpha$) Compared to the approximation formula used by Wabnitz, our result also provides a first order correction term $\varepsilon\psi$. Details of the function $\psi$ will be explained in Theorem 6.6.
($\beta$) In physical constants the LLE reads

$$-d_2 a'' + \left(-\mathrm{i}\frac{\kappa}{2} + \omega_0 - \omega_p\right)a - g|a|^2 a + \mathrm{i}\sqrt{\frac{\kappa\eta P_{\mathrm{in}}}{\hbar\omega_0}} = 0,$$

cf. Section 2. By $a(x) = \sqrt{\frac{\kappa}{2g\varepsilon}}\tilde{a}\left(\sqrt{\frac{\kappa}{4d_2\varepsilon}}x\right)$ we get

$$-\frac{1}{2}\tilde{a}'' + \left(-\mathrm{i}\varepsilon + \frac{2\varepsilon}{\kappa}(\omega_0 - \omega_p)\right)\tilde{a} - |\tilde{a}|^2\tilde{a} + \mathrm{i}\sqrt{\frac{8g\eta P_{\mathrm{in}}}{\hbar\omega_0\kappa^2}}\varepsilon^{\frac{3}{2}} = 0.$$

Comparing the last equation with (6.2) we see $\zeta = \frac{2\varepsilon}{\kappa}(\omega_0 - \omega_p)$ and $f = \sqrt{\frac{8g\eta P_{\mathrm{in}}}{\hbar\omega_0\kappa^2}}\sqrt{\varepsilon}$. Now the condition $\sqrt{8\zeta} < \pi|f|$ leads to

$$\frac{2(\omega_0 - \omega_p)\hbar\omega_0\kappa}{\pi^2\eta g} < P_{\mathrm{in}}.$$

Next we want to find and prove a mathematically more precise formulation of Ap-

proximation result 6.1. We decompose $w = w_\infty + \tilde{w}$ with $\tilde{w} \in \mathcal{H}$ and define the map

$$
G : \begin{cases} \mathbb{R} \times \mathcal{H} & \to & \mathcal{L}, \\ (\varepsilon, \tilde{w}) & \mapsto & -d\tilde{w}'' + (-\mathrm{i}\varepsilon + \zeta)\tilde{w} - |w_\infty + \tilde{w}|^2 (w_\infty + \tilde{w}) + |w_\infty|^2 w_\infty. \end{cases}
$$

Note that

$$
T : \begin{cases} \mathbb{R} & \to & \mathbb{R} \times \mathcal{H}, \\ \theta & \mapsto & (0, a_\theta) \end{cases}
$$

describes a trivial curve of solutions $(\varepsilon, w)$ of (6.2), i.e. $G(T(\theta)) = 0$ for $\theta \in \mathbb{R}$, from where we wish to bifurcate at some point $(0, a_{\theta^*})$. In particular, $(0, \partial_\theta a_\theta) = (0, \mathrm{i}a_\theta)$ lies in the kernel of $\partial_{(\varepsilon, \tilde{w})} G(0, a_\theta)$. As we shall see there may be more elements in the kernel. Next let us fix the value $\theta^*$ such that $\cos \theta^* = \frac{\sqrt{8\zeta}}{\pi f}$ and let $\mathcal{H} = \mathrm{span}\{\mathrm{i}a_{\theta^*}\} \oplus Z$ where, e.g., $Z := \mathcal{H} \cap \mathrm{span}\{\mathrm{i}a_{\theta^*}\}^{\perp_{L^2}}$. It will be more convenient to rewrite $\tilde{w} = a_\theta + v$ with $v \in Z$, cf. Section 3.6. In order to justify this, note also that the map $(\theta, v) \mapsto a_\theta + v$ defines a diffeomorphism of a neighborhood of $(\theta^*, 0) \in \mathbb{R} \times Z$ onto a neighborhood of $a_{\theta^*} \in \mathcal{H}$ since the derivative at $(\theta^*, 0)$ is given by $(\lambda, \psi) \mapsto \lambda \mathrm{i}a_{\theta^*} + \psi$ which is an isomorphism from $\mathbb{R} \times Z$ onto $\mathcal{H}$. Let us define

$$
F : \begin{cases} \mathbb{R} \times \mathbb{R} \times Z & \to & \mathcal{L}, \\ (\theta, \varepsilon, v) & \mapsto & G(\varepsilon, a_\theta + v) \end{cases}
$$

which is twice continuously differentiable. Our goal is to solve

$$
F(\theta, \varepsilon, v) = 0 \tag{6.4}
$$

by means of bifurcation theory, where $\theta \in \mathbb{R}$ serves as artificial bifurcation parameter. Notice that $F(\theta, 0, 0) = 0$ for all $\theta \in \mathbb{R}$, i.e., $(\varepsilon, v) = (0, 0)$ is a trivial solution of (6.4). We will use the following formulation of the Crandall-Rabinowitz Theorem of bifurcation from a simple eigenvalue [9, Theorem 1.7].

**Theorem 6.3** (Crandall-Rabinowitz). *Let $I \subset \mathbb{R}$ be an open interval, $X,Y$ Banach spaces and let $F : I \times X \to Y$ be twice continuously differentiable such that $F(\lambda, 0) = 0$ for all $\lambda \in I$ and $\partial_x F(\lambda_0, 0) : X \to Y$ is an index-zero Fredholm operator for $\lambda_0 \in I$. Moreover assume:*

*(H1) there is $\phi \in X, \phi \neq 0$ such that $\ker \partial_x F(\lambda_0, 0) = \mathrm{span}\{\phi\}$,*

*(H2) $\partial_{x,\lambda}^2 F(\lambda_0, 0)[\phi] \notin \mathrm{range}\, \partial_x F(\lambda_0, 0)$.*

*If $K$ is any complement of $\ker \partial_x F(\lambda_0, 0)$ in $X$, then there is a neighborhood $U$ of $(\lambda_0, 0)$ in $I \times X$, an interval $(-a, a)$, and continuously differentiable functions $\lambda : (-a, a) \to I$, $\xi : (-a, a) \to K$ such that $\lambda(0) = \lambda_0$, $\xi(0) = 0$ and*

$$
F^{-1}(0) \cap U = \{(\lambda(\alpha), \alpha\phi + \alpha\xi(\alpha)) : |\alpha| < a\} \cup \{(\lambda, 0) : (\lambda, 0) \in U\}.
$$

*Finally,*

$$\dot{\lambda}(0) = -\frac{1}{2}\frac{\langle \partial^2_{xx} F(\lambda_0, 0)[\phi, \phi], \phi^* \rangle}{\langle \partial^2_{x,\lambda} F(\lambda_0, 0)[\phi], \phi^* \rangle},$$

*where* $\mathrm{span}\{\phi^*\} = \ker \partial_x F(\lambda_0, 0)^*$ *and* $\langle \cdot, \cdot \rangle$ *is the duality pairing between* $Y$ *and its dual* $Y^*$.

In order to show (H1) let us define the operator

$$A : \begin{cases} \mathcal{H} & \to & \mathcal{L}, \\ \psi & \mapsto & -d\psi'' + \zeta\psi - 2|a_{\theta^*}|^2\psi - a_{\theta^*}^2\overline{\psi} \end{cases}$$

and

$$b := -\mathrm{i}a_{\theta^*} + \frac{2\mathrm{i}f}{\zeta}|a_{\theta^*}|^2 - \frac{\mathrm{i}f}{\zeta}a_{\theta^*}^2.$$

Observe that $\partial_v F(\theta^*, 0, 0)\psi = A\psi$ for $\psi \in Z$. Within the next lemma we will show that $\partial_\varepsilon F(\theta^*, 0, 0) = b$ and that $\theta^*$ is chosen in such a way that

$$A\psi = -b \tag{6.5}$$

has a unique solution in $Z$, which we denote by $\psi^*$.

**Lemma 6.4.** *Let* $d, \zeta > 0$, $f \neq 0$ *such that* $\sqrt{8\zeta} < \pi|f|$ *and* $\cos\theta^* = \frac{\sqrt{8\zeta}}{\pi f}$. *Then, the kernel of* $\partial_{(\varepsilon,v)} F(\theta^*, 0, 0)$ *is one-dimensional and* range $\partial_{(\varepsilon,v)} F(\theta^*, 0, 0) = \mathrm{span}\{\mathrm{i}a_{\theta^*}\}^{\perp_{L^2}}$.

*Proof.* From [19, Lemma 3.5] it follows that $A$ is a self-adjoint index-zero Fredholm operator with $\ker A = \mathrm{span}\{\mathrm{i}a_{\theta^*}\}$ (cf. also [20]). Further,

$$\partial_\varepsilon F(\theta^*, 0, 0) = -\mathrm{i}a_{\theta^*} - 2|a_{\theta^*}|^2 w'_\infty(0) - a_{\theta^*}^2\overline{w'_\infty(0)},$$

where $w'_\infty(0)$ denotes the derivate of $\varepsilon \mapsto w_\infty(\varepsilon)$ at $\varepsilon = 0$. From (6.3) one finds $\zeta w'_\infty(0) + \mathrm{i}f = 0$, whence

$$\partial_\varepsilon F(\theta^*, 0, 0) = -\mathrm{i}a_{\theta^*} + \frac{2\mathrm{i}f}{\zeta}|a_{\theta^*}|^2 - \frac{\mathrm{i}f}{\zeta}a_{\theta^*}^2 = b.$$

For $(\delta, \psi) \in \mathbb{R} \times Z$ belonging to the kernel of $\partial_{(\varepsilon,v)} F(0, 0, 0)$ we have

$$\partial_{(\varepsilon,v)} F(\theta^*, 0, 0)[\delta, \psi] = A\psi + \delta b = 0.$$

If $\delta = 0$ we find $A\psi = 0$, i.e. $\psi \in \mathrm{span}\{\mathrm{i}a_{\theta^*}\} \cap Z = \{0\}$. Hence we may assume w.l.o.g. that $\delta = 1$ and $\psi$ has to solve (6.5). By the Fredholm alternative and the self-adjointness of $A$ this is possible if and only if $b \perp_{L^2} \mathrm{i}a_{\theta^*}$. This is true due to the choice of $\theta^*$, in fact,

$$\langle b, \mathrm{i}a_{\theta^*}\rangle_{L^2(\mathbb{R})} = \mathrm{Re}\int_\mathbb{R}\left(-\mathrm{i}a_{\theta^*} + \frac{2\mathrm{i}f}{\zeta}|a_{\theta^*}|^2 - \frac{\mathrm{i}f}{\zeta}a_{\theta^*}^2\right)(-\mathrm{i}\overline{a_{\theta^*}})\,dx$$

$$= \mathrm{Re}\int_\mathbb{R} -2\zeta\,\mathrm{sech}^2\left(\sqrt{\frac{\zeta}{d}}x\right) + f\sqrt{8\zeta}(2\mathrm{e}^{-\mathrm{i}\theta^*} - \mathrm{e}^{\mathrm{i}\theta^*})\,\mathrm{sech}^3\left(\sqrt{\frac{\zeta}{d}}x\right)\,dx$$

$$= \int_{\mathbb{R}} -2\zeta \operatorname{sech}^2\left(\sqrt{\frac{\zeta}{d}}x\right) + f\sqrt{8\zeta}\cos\theta^* \operatorname{sech}^3\left(\sqrt{\frac{\zeta}{d}}x\right) dx$$

$$= \int_{\mathbb{R}} -2\zeta \operatorname{sech}^2\left(\sqrt{\frac{\zeta}{d}}x\right) + \frac{8\zeta}{\pi} \operatorname{sech}^3\left(\sqrt{\frac{\zeta}{d}}x\right) dx$$

$$= -2\sqrt{d\zeta} \underbrace{\int_{\mathbb{R}} \operatorname{sech}^2(x)\, dx}_{=2} + \frac{8\sqrt{d\zeta}}{\pi} \underbrace{\int_{\mathbb{R}} \operatorname{sech}^3(x)\, dx}_{=\frac{\pi}{2}}$$

$$= 0.$$

Thus, there exists $\psi \in \mathcal{H}$ solving (6.5) and $\psi$ is unique up to adding a real multiple of $ia_{\theta^*}$. Hence, there is a unique $\psi^* \in Z$ solving (6.5) so that $\dim\ker\partial_{(\varepsilon,v)}F(\theta^*,0,0) = 1$ and it remains to determine the range of $\partial_{(\varepsilon,v)}F(\theta^*,0,0)$. Since $b \in \operatorname{range} A$ we find $\operatorname{range}\partial_{(\varepsilon,v)}F(\theta^*,0,0) = \operatorname{range} A = \operatorname{span}\{ia_{\theta^*}\}^{\perp_{L^2}}$ which is all we had to show. $\qquad\square$

From the proof of Lemma 6.4 we know that $\ker\partial_{(\varepsilon,v)}F(\theta^*,0,0) = \operatorname{span}\{(1,\psi^*)\}$, where $\psi^* \in Z$ denotes the unique element of $Z$ which solves (6.5). Let us prove the transversality condition (H2) in the next lemma.

**Lemma 6.5.** *Let $d,\zeta > 0$, $f \neq 0$ such that $\sqrt{8\zeta} < \pi|f|$ and $\cos\theta^* = \frac{\sqrt{8\zeta}}{\pi f}$. Then,*

$$\partial^2_{(\varepsilon,v),\theta}F(\theta^*,0,0)[1,\psi^*] \notin \operatorname{range}\partial_{(\varepsilon,v)}F(\theta^*,0,0).$$

*Proof.* Recall that

$$\partial_{(\varepsilon,v)}F(\theta,0,0)[1,\psi^*] = -d(\psi^*)'' + \zeta\psi^* - 2|a_\theta|^2\psi^* - a_\theta^2\overline{\psi^*} - ia_\theta + \frac{2if}{\zeta}|a_\theta|^2 - \frac{if}{\zeta}a_\theta^2,$$

whence

$$\partial^2_{(\varepsilon,v),\theta}F(\theta^*,0,0)[1,\psi^*] = a_{\theta^*} - 2ia_{\theta^*}^2\overline{\psi^*} + \frac{2f}{\zeta}a_{\theta^*}^2.$$

Further, $\operatorname{range}\partial_{(\varepsilon,v)}F(\theta^*,0,0) = \operatorname{span}\{ia_{\theta^*}\}^{\perp_{L^2}}$ by Lemma 6.4 so that it suffices to show

$$\operatorname{Re}\int_{\mathbb{R}}\left(a_{\theta^*} - 2ia_{\theta^*}^2\overline{\psi^*} + \frac{2f}{\zeta}a_{\theta^*}^2\right)(-i\overline{a_{\theta^*}})\, dx \neq 0.$$

In fact, using $Aa_{\theta^*} = -2|a_{\theta^*}|^2a_{\theta^*}$, we find

$$\operatorname{Re}\int_{\mathbb{R}}\left(a_{\theta^*} - 2ia_{\theta^*}^2\overline{\psi^*} + \frac{2f}{\zeta}a_{\theta^*}^2\right)(-i\overline{a_{\theta^*}})\, dx$$

$$= \operatorname{Re}\int_{\mathbb{R}} -i|a_{\theta^*}|^2 - 2|a_{\theta^*}|^2a_{\theta^*}\overline{\psi^*} - \frac{2if}{\zeta}|a_{\theta^*}|^2a_{\theta^*}\, dx$$

$$= \operatorname{Re}\int_{\mathbb{R}} Aa_{\theta^*}\overline{\psi^*} - \frac{2if}{\zeta}|a_{\theta^*}|^2a_{\theta^*}\, dx$$

101

$$= \operatorname{Re} \int_{\mathbb{R}} a_{\theta^*} \overline{A\psi^*} - \frac{2\mathrm{i}f}{\zeta}|a_{\theta^*}|^2 a_{\theta^*}\, dx$$

$$= \operatorname{Re} \int_{\mathbb{R}} a_{\theta^*} \left( -\mathrm{i}\overline{a_{\theta^*}} + \frac{2\mathrm{i}f}{\zeta}|a_{\theta^*}|^2 - \frac{\mathrm{i}f}{\zeta}\overline{a_{\theta^*}}^2 \right) - \frac{2\mathrm{i}f}{\zeta}|a_{\theta^*}|^2 a_{\theta^*}\, dx$$

$$= \operatorname{Re} \int_{\mathbb{R}} -\frac{\mathrm{i}f}{\zeta}|a_{\theta^*}|^2 \overline{a_{\theta^*}}\, dx = \frac{f}{\zeta} \operatorname{Im} \int_{\mathbb{R}} |a_{\theta^*}|^2 \overline{a_{\theta^*}}\, dx$$

$$= 2\sqrt{2\zeta}\, f \operatorname{Im} \int_{\mathbb{R}} \operatorname{sech}^3\left( \sqrt{\frac{\zeta}{d}}x \right) \mathrm{e}^{-\mathrm{i}\theta^*}\, dx$$

$$= -2\sqrt{2d}\, f \sin\theta^* \underbrace{\int_{\mathbb{R}} \operatorname{sech}^3(x)\, dx}_{= \frac{\pi}{2}} = -\pi f\sqrt{2d}\sin\theta^* \neq 0$$

since $|\cos\theta^*| < 1$. $\qquad\qquad\square$

Now we can state our approximation theorem.

**Theorem 6.6.** *Let $d, \zeta > 0$, $f \neq 0$ such that*

$$\frac{\sqrt{8\zeta}}{\pi|f|} < 1 \text{ and } \cos\theta^* = \frac{\sqrt{8\zeta}}{\pi f}.$$

*Then, there is $a > 0$ and a continuously differentiable curve $\mathcal{C} : (-a, a) \to \mathbb{R} \times \mathcal{H}$ with $\mathcal{C}(\varepsilon) = (\varepsilon, \tilde{w}(\varepsilon))$, $\mathcal{C}(0) = (0, a_{\theta^*})$ such that $G(\mathcal{C}(\varepsilon)) = 0$ for $|\varepsilon| < a$ and such that locally near $(0, a_{\theta^*})$ all solutions of $G(\varepsilon, \tilde{w}) = 0$ lie on the curve $T$ or on the curve $\mathcal{C}$. More precisely,*

$$\tilde{w}(\varepsilon) = a_{\theta^*} + \varepsilon(\psi^* + \mathrm{i}\gamma a_{\theta^*}) + \mathcal{O}(\varepsilon^2),$$

*where $\psi^* \in \mathcal{H}$ is the unique solution of (6.5) with $\psi^* \perp_{L^2} \mathrm{i}a_{\theta^*}$ and where*

$$\gamma = \frac{\operatorname{Re} \int_{\mathbb{R}} \mathrm{i}\overline{a_{\theta^*}}^2 (\psi^*)^2 - \psi^* \overline{a_{\theta^*}} + \frac{2f}{\zeta}\overline{a_{\theta^*}}^2 \psi^*\, dx}{\pi f\sqrt{2d}\sin\theta^*} + \frac{\pi^2 - 16}{\pi^2\zeta}.$$

*Proof.* The assumptions of Theorem 6.3 are satisfied due to Lemma 6.4 and Lemma 6.5. If $\mathcal{K}$ is any complement of $\operatorname{span}\{\psi^*\}$ in $Z$ then $K := \mathbb{R} \times \mathcal{K}$ is a complement of $\operatorname{span}\{(1, \psi^*)\}$ in $\mathbb{R} \times Z$. Thus, Theorem 6.3 provides an interval $(-a_*, a_*)$ and continuously differentiable functions $\theta : (-a_*, a_*) \to \mathbb{R}$, $\xi_1 : (-a_*, a_*) \to \mathbb{R}$, $\xi_2 : (-a_*, a_*) \to \mathcal{K}$ with $\theta(0) = \theta^*$, $\xi_1(0) = 0$, $\xi_2(0) = 0$ such that

$$F(\theta(\alpha), \alpha(1, \psi^*) + \alpha(\xi_1(\alpha), \xi_2(\alpha))) = F(\theta(\alpha), \alpha + \alpha\xi_1(\alpha), \alpha\psi^* + \alpha\xi_2(\alpha)) = 0$$

for $|\alpha| < a_*$ and such that locally near $(\theta^*, 0, 0)$ all non-trivial solutions of $F(\theta, \varepsilon, v) = 0$ are of that form. Let us abbreviate $\varepsilon(\alpha) = \alpha + \alpha\xi_1(\alpha)$ and $v(\alpha) = \alpha\psi^* + \alpha\xi_2(\alpha)$ so that $F(\theta(\alpha), \varepsilon(\alpha), v(\alpha)) = 0$. Next, observe that $G(\varepsilon(\alpha), \tilde{w}_*(\alpha)) = 0$ for $\tilde{w}_*(\alpha) := a_{\theta(\alpha)} + v(\alpha)$. Since $\dot{\varepsilon}(0) = 1$ we find a local reparameterization $(\varepsilon, \tilde{w}(\varepsilon))$ of $(\varepsilon(\alpha), \tilde{w}_*(\alpha))$ on some

interval $(-a, a)$. Note that

$$\tilde{w}(\varepsilon) = a_{\theta^*} + \varepsilon\left(\psi^* + \mathrm{i}\dot{\theta}(0)a_{\theta^*}\right) + \mathcal{O}(\varepsilon^2),$$

so that the proof is finished if we can show $\dot{\theta}(0) = \gamma$. Theorem 6.3 yields

$$\dot{\theta}(0) = -\frac{1}{2}\frac{\left\langle \partial^2_{(\varepsilon,v)^2}F(\theta^*, 0, 0)[(1, \psi^*), (1, \psi^*)], \mathrm{i}a_{\theta^*}\right\rangle_{L^2(\mathbb{R})}}{\left\langle \partial^2_{(\varepsilon,v),\theta}F(\theta^*, 0, 0)[1, \psi^*], \mathrm{i}a_{\theta^*}\right\rangle_{L^2(\mathbb{R})}}.$$

From the proof of Lemma 6.5 we already know

$$\left\langle \partial^2_{(\varepsilon,v),\theta}F(\theta^*, 0, 0)[1, \psi^*], \mathrm{i}a_{\theta^*}\right\rangle_{L^2(\mathbb{R})} = -\pi f\sqrt{2d}\sin\theta^*.$$

Further,

$$\partial^2_{(\varepsilon,v)^2}F(\theta^*, 0, 0)[(1, \psi^*), (1, \psi^*)]$$
$$= -2\overline{a_{\theta^*}}(\psi^*)^2 - 4a_{\theta^*}|\psi^*|^2 - 2\mathrm{i}\psi^* + \frac{4\mathrm{i}f}{\zeta}\overline{a_{\theta^*}}\psi^* + \frac{8f}{\zeta}a_{\theta^*}\,\mathrm{Im}\,\psi^*$$
$$- \frac{4f}{\zeta^2}|a_{\theta^*}|^2 + \frac{2f^2}{\zeta^2}\overline{a_{\theta^*}} - \frac{2f^2}{\zeta^2}a_{\theta^*} - \frac{2f}{\zeta^2}a_{\theta^*}^2,$$

whence

$$\left\langle \partial^2_{(\varepsilon,v)^2}F(\theta^*, 0, 0)[(1, \psi^*), (1, \psi^*)], \mathrm{i}a_{\theta^*}\right\rangle_{L^2(\mathbb{R})}$$
$$= \mathrm{Re}\int_{\mathbb{R}} 2\mathrm{i}\overline{a_{\theta^*}}^2(\psi^*)^2 - 2\psi^*\overline{a_{\theta^*}} + \frac{4f}{\zeta}\overline{a_{\theta^*}}^2\psi^*\,dx + \frac{\sqrt{8d}f}{\pi\zeta}\sin\theta^*(\pi^2 - 16)$$

which is all we had to show. $\qquad\qquad\qquad\qquad\qquad\qquad\qquad\qquad\qquad\square$

## 6.2. Two mode case

Here we want to provide an approximation result for a simplified version of the following two mode equation

$$-du'' + \mathrm{i}\omega u' + (-\mathrm{i} + \zeta)u - |u|^2u + \mathrm{i}f_0 + \mathrm{i}f_1\mathrm{e}^{\mathrm{i}k_1x} = 0. \tag{6.6}$$

The simplified equation will hold in the case $|f_1| \ll |f_0|$ and will have the advantage of admitting constant solutions. We start with the derivation of this model which is due to Huanfa Peng[8]. The main idea is that

$$f_0 + f_1\mathrm{e}^{\mathrm{i}k_1x} = \sqrt{f_0^2 + 2f_0f_1\cos(k_1x) + f_1^2}\,\mathrm{e}^{\mathrm{i}\arctan\frac{f_1\sin(k_1x)}{f_0+f_1\cos(k_1x)}} \approx f_0\mathrm{e}^{\mathrm{i}\frac{f_1}{f_0}\sin(k_1x)}$$

---

[8]Institute of Photonics and Quantum Electronics (IPQ), Karlsruhe Institute of Technology, 76131 Karlsruhe, Germany

in the case $|f_1| \ll |f_0|$, where we made use of $\arctan x \approx x$ for $x \to 0$. Equation (6.6) then becomes

$$-du'' + \mathrm{i}\omega u' + (-\mathrm{i} + \zeta)u - |u|^2 u + \mathrm{i}f_0 \mathrm{e}^{\mathrm{i}\frac{f_1}{f_0}\sin(k_1 x)} = 0.$$

The ansatz $u(x) = v(x)\mathrm{e}^{\mathrm{i}\frac{f_1}{f_0}\sin(k_1 x)}$ leads to

$$-dv'' + \mathrm{i}V(x)v' + (-\mathrm{i}W(x) + U(x))v - |v|^2 v + \mathrm{i}f_0 = 0,$$

where $V(x) = \omega - 2dk_1\frac{f_1}{f_0}\cos(k_1 x)$, $W(x) = 1 - d\frac{f_1}{f_0}k_1^2\sin(k_1 x)$, $U(x) = \zeta + dk_1^2\frac{f_1^2}{f_0^2}\cos^2(k_1 x) - \omega k_1\frac{f_1}{f_0}\cos(k_1 x)$. Next we use the realistic simplifications $W(x) \approx 1$ and $U(x) \approx \zeta$ leading to

$$-dv'' + \mathrm{i}V(x)v' + (-\mathrm{i} + \zeta)v - |v|^2 v + \mathrm{i}f_0 = 0. \tag{6.7}$$

In order to fit (6.7) into a mathematical theory similar to the one used in the previous section we need to restrict to the special case where $\omega = 0$, i.e.

$$-dv'' - 2\mathrm{i}dk_1\frac{f_1}{f_0}\cos(k_1 x)v' + (-\mathrm{i} + \zeta)v - |v|^2 v + \mathrm{i}f_0 = 0. \tag{6.8}$$

We use a bifurcation approach and consider the equation

$$-dw'' + 2\mathrm{i}\varepsilon\beta\sin(k_1 x)w' + (-\mathrm{i}\varepsilon + \zeta)w - |w|^2 w + \mathrm{i}\varepsilon f = 0 \text{ on } \mathbb{R}, \qquad w'(0) = 0, \tag{6.9}$$

where $\varepsilon$ serves as bifurcation parameter. Note that the sine term of (6.9) can be transformed into a cosine term like it appears in (6.8) by a simple shifting argument. Roughly speaking, we can formulate our generalized approximation result in the following way.

**Approximation result 6.7.** Let $d, \zeta > 0$, $f \neq 0$, $\beta \in \mathbb{R}$, $k_1 \in \mathbb{N}$ such that

$$\frac{\sqrt{8\zeta}}{\pi|f|}\left|1 - \frac{R}{4\sqrt{\zeta d}}\right| < 1 \text{ and } \cos\theta^* = \frac{\sqrt{8\zeta}}{\pi f}\left(1 - \frac{R}{4\sqrt{\zeta d}}\right),$$

where

$$R = R(\beta, \zeta, d, k_1) = -4\beta\zeta\int_{\mathbb{R}}\sin\left(\sqrt{\frac{d}{\zeta}}k_1 x\right)\frac{\sinh(x)}{\cosh^3(x)}\,dx.$$

Then, localized solutions of (6.9) have the form

$$w(\varepsilon) = w_\infty(\varepsilon) + a_{\theta^*} + \varepsilon\psi + \mathcal{O}(\varepsilon^2)$$
$$= a_{\theta^*} + \varepsilon\left(\psi - \frac{\mathrm{i}f}{\zeta}\right) + \mathcal{O}(\varepsilon^2),$$

where

$$a_{\theta^*}(x) = \sqrt{2\zeta}\operatorname{sech}\left(\sqrt{\frac{\zeta}{d}}x\right)\mathrm{e}^{\mathrm{i}\theta^*}$$

and where $\psi \in \mathcal{H}$ is a suitable solution of

$$-d\psi'' + \zeta\psi - 2|a_{\theta^*}|^2\psi - a_{\theta^*}^2\overline{\psi} = \mathrm{i}a_{\theta^*} - \frac{2\mathrm{i}f}{\zeta}|a_{\theta^*}|^2 + \frac{\mathrm{i}f}{\zeta}a_{\theta^*}^2 - 2\mathrm{i}\beta\sin(k_1 x)a_{\theta^*}'.$$

**Remark 6.8.** The counterpart of (6.7) in physical constants (pumped modes: $\widetilde{k}_0, \widetilde{k}_1$) reads

$$-d_2 v'' + \mathrm{i}V(x)v' + \left(-\mathrm{i}\frac{\kappa}{2} + \omega_{\widetilde{k}_0} - \omega_{p_0}\right)v - g|v|^2 v + \mathrm{i}\sqrt{\frac{\kappa\eta P_{\mathrm{in},0}}{\hbar\omega_{\widetilde{k}_0}}} = 0,$$

where

$$k_1 = \widetilde{k}_1 - \widetilde{k}_0 \text{ and } V(x) = \frac{\omega_{\widetilde{k}_0} - \omega_{p_0} - \omega_{\widetilde{k}_1} + \omega_{p_1}}{k_1} + d_2 k_1 - 2d_2 k_1\sqrt{\frac{P_{\mathrm{in},1}\omega_{\widetilde{k}_0}}{P_{\mathrm{in},0}\omega_{\widetilde{k}_1}}}\cos(k_1 x),$$

cf. Section 2. By $v(x) = \sqrt{\frac{\kappa}{2g\varepsilon}}z\left(x - \frac{\pi}{2k_1}\right)$, we get

$$-\frac{2d_2\varepsilon}{\kappa}z'' + \frac{2\mathrm{i}\varepsilon}{\kappa}\widetilde{V}(x)z' + \left(-\mathrm{i}\varepsilon + \frac{2\varepsilon}{\kappa}(\omega_{\widetilde{k}_0} - \omega_{p_0})\right)z - |z|^2 z + \mathrm{i}\sqrt{\frac{8g\eta P_{\mathrm{in},0}}{\hbar\omega_{\widetilde{k}_0}\kappa^2}}\varepsilon^{\frac{3}{2}} = 0, \quad (6.10)$$

where

$$\widetilde{V}(x) = \frac{\omega_{\widetilde{k}_0} - \omega_{p_0} - \omega_{\widetilde{k}_1} + \omega_{p_1}}{k_1} + d_2 k_1 + 2d_2 k_1\sqrt{\frac{P_{\mathrm{in},1}\omega_{\widetilde{k}_0}}{P_{\mathrm{in},0}\omega_{\widetilde{k}_1}}}\sin(k_1 x).$$

In order to fit our mathematical situation, we need to restrict to the case where

$$\frac{\omega_{\widetilde{k}_0} - \omega_{p_0} - \omega_{\widetilde{k}_1} + \omega_{p_1}}{k_1} + d_2 k_1 = 0,$$

i.e.

$$\widetilde{V}(x) = 2d_2 k_1\sqrt{\frac{P_{\mathrm{in},1}\omega_{\widetilde{k}_0}}{P_{\mathrm{in},0}\omega_{\widetilde{k}_1}}}\sin(k_1 x).$$

Physically, this means that if the frequency $\omega_{p_0}$ of the first pump is tuned arbitrarily, the frequency of the second pump needs to be tuned to $\omega_{p_1} = \omega_{p_0} + \omega_{\widetilde{k}_1} - \omega_{\widetilde{k}_0} - d_2 k_1^2$. Comparing (6.10) with (6.9) we see $\zeta = \frac{2\varepsilon}{\kappa}(\omega_{\widetilde{k}_0} - \omega_{p_0})$, $f = \sqrt{\frac{8g\eta P_{\mathrm{in},0}}{\hbar\omega_{\widetilde{k}_0}\kappa^2}}\sqrt{\varepsilon}$ and $\beta = \frac{2}{\kappa}d_2 k_1\sqrt{\frac{P_{\mathrm{in},1}\omega_{\widetilde{k}_0}}{P_{\mathrm{in},0}\omega_{\widetilde{k}_1}}}$. Using $\sin x \approx x$ for $x \to 0$ and

$$\int_{\mathbb{R}} \frac{x\sinh(x)}{\cosh^3(x)}\, dx = 1$$

# 6. Approximation formulas

we can approximate $R \approx -4\beta k_1 \sqrt{\zeta d}$. The condition $\frac{\sqrt{8\zeta}}{\pi|f|}\left|1 - \frac{R}{4\sqrt{\zeta d}}\right| < 1$ then simplifies to

$$\left(1 + \frac{2}{\kappa} d_2 k_1^2 \sqrt{\frac{P_{\text{in},1}\omega_{\widetilde{k}_0}}{P_{\text{in},0}\omega_{\widetilde{k}_1}}}\right) \sqrt{\frac{2(\omega_{\widetilde{k}_0} - \omega_{p_0})\hbar\omega_{\widetilde{k}_0}\kappa}{g\eta P_{\text{in},0}}} < \pi.$$

In order to find a mathematically more precise formulation of Approximation result 6.7 we can proceed analogously to the last section and only need to do some slight modifications. In the definition of $G$ we need to include one extra term, i.e.

$$G(\varepsilon, \tilde{w}) = -\frac{1}{2}\tilde{w}'' + 2i\varepsilon\beta\sin(k_1 x)\tilde{w}' + (-i\varepsilon + \zeta)\tilde{w} - |w_\infty + \tilde{w}|^2(w_\infty + \tilde{w}) + |w_\infty|^2 w_\infty.$$

Thus, the operator $A$ remains the same but the function $b$ becomes

$$b = -ia_{\theta^*} + \frac{2if}{\zeta}|a_{\theta^*}|^2 - \frac{if}{\zeta}a_{\theta^*}^2 + 2i\beta\sin(k_1 x)a'_{\theta^*}.$$

The change of $b$ also effects the definition of $\theta^*$ which is determined by $\langle b, ia_{\theta^*}\rangle_{L^2(\mathbb{R})} \overset{!}{=} 0$. In fact, with

$$R = R(\beta, \zeta, d, k_1) = -4\beta\zeta\int_{\mathbb{R}}\sin\left(\sqrt{\frac{d}{\zeta}}k_1 x\right)\frac{\sinh(x)}{\cosh^3(x)}\,dx \approx -4\beta k_1\sqrt{\zeta d}$$

we find this time

$$\langle b, ia_{\theta^*}\rangle_{L^2(\mathbb{R})} = \sqrt{2d}(-\sqrt{8\zeta} + \pi f\cos\theta^*) + R,$$

whence

$$\cos\theta^* = \frac{\sqrt{8\zeta}}{\pi f}\left(1 - \frac{R}{4\sqrt{\zeta d}}\right) \approx \frac{\sqrt{8\zeta}}{\pi f}(1 + \beta k_1).$$

Note that the change of $b$ also effects the definition of $\psi^*$, cf. (6.5). In order to prove the transversality condition (H2) we now find

$$\partial^2_{(\varepsilon,v),\theta}F(\theta^*, 0, 0)[1, \psi^*] = a_{\theta^*} - 2ia_{\theta^*}^2\overline{\psi^*} + \frac{2f}{\zeta}a_{\theta^*}^2 - 2\beta\sin(k_1 x)a'_{\theta^*}$$

instead of

$$\partial^2_{(\varepsilon,v),\theta}F(\theta^*, 0, 0)[1, \psi^*] = a_{\theta^*} - 2ia_{\theta^*}^2\overline{\psi^*} + \frac{2f}{\zeta}a_{\theta^*}^2.$$

But since

$$\langle -2\beta\sin(k_1 x)a'_{\theta^*}, ia_{\theta^*}\rangle_{L^2(\mathbb{R})} = 0$$

we once again see that (H2) is satisfied. For the determination of $\gamma$ notice that this time

$$\left\langle \partial^2_{(\varepsilon,v)^2}F(\theta^*, 0, 0)[(1, \psi^*), (1, \psi^*)], ia_{\theta^*}\right\rangle_{L^2(\mathbb{R})}$$

$$= \operatorname{Re} \int_{\mathbb{R}} 2\mathrm{i}\overline{a_{\theta^*}}^2(\psi^*)^2 - 2\psi^*\overline{a_{\theta^*}} + \frac{4f}{\zeta}\overline{a_{\theta^*}}^2\psi^* + 4\beta\sin(k_1 x)(\psi^*)'\overline{a_{\theta^*}}\,dx$$
$$+ \frac{\sqrt{8d}f}{\pi\zeta}\sin\theta^*\left(\pi^2 - 16\left(1 - \frac{R}{4\sqrt{\zeta d}}\right)\right)$$

instead of

$$\left\langle \partial^2_{(\varepsilon,v)^2}F(\theta^*,0,0)[(1,\psi^*),(1,\psi^*)],\mathrm{i}a_{\theta^*}\right\rangle_{L^2(\mathbb{R})}$$
$$= \operatorname{Re}\int_{\mathbb{R}} 2\mathrm{i}\overline{a_{\theta^*}}^2(\psi^*)^2 - 2\psi^*\overline{a_{\theta^*}} + \frac{4f}{\zeta}\overline{a_{\theta^*}}^2\psi^*\,dx + \frac{\sqrt{8d}f}{\pi\zeta}\sin\theta^*(\pi^2 - 16).$$

Hence,

$$\gamma = \frac{\operatorname{Re}\int_{\mathbb{R}}\mathrm{i}\overline{a_{\theta^*}}^2(\psi^*)^2 - \psi^*\overline{a_{\theta^*}} + \frac{2f}{\zeta}\overline{a_{\theta^*}}^2\psi^* + 2\beta\sin(k_1 s)(\psi^*)'\overline{a_{\theta^*}}\,dx}{\pi f\sqrt{2d}\sin\theta^*}$$
$$+ \frac{1}{\pi^2\zeta}\left(\pi^2 - 16\left(1 - \frac{R}{4\sqrt{\zeta d}}\right)\right).$$

Now we can state our generalized approximation result.

**Theorem 6.9.** *Let $d,\zeta > 0$, $f \neq 0$, $\beta \in \mathbb{R}$, $k_1 \in \mathbb{N}$ such that*

$$\frac{\sqrt{8\zeta}}{\pi|f|}\left|1 - \frac{R}{4\sqrt{\zeta d}}\right| < 1 \text{ and } \cos\theta^* = \frac{\sqrt{8\zeta}}{\pi f}\left(1 - \frac{R}{4\sqrt{\zeta d}}\right).$$

*Then the conclusions stated in Theorem 6.6 hold with*

$$\gamma = \frac{\operatorname{Re}\int_{\mathbb{R}}\mathrm{i}\overline{a_{\theta^*}}^2(\psi^*)^2 - \psi^*\overline{a_{\theta^*}} + \frac{2f}{\zeta}\overline{a_{\theta^*}}^2\psi^* + 2\beta\sin(k_1 s)(\psi^*)'\overline{a_{\theta^*}}\,dx}{\pi f\sqrt{2d}\sin\theta^*}$$
$$+ \frac{1}{\pi^2\zeta}\left(\pi^2 - 16\left(1 - \frac{R}{4\sqrt{\zeta d}}\right)\right).$$

# 7. Outlook - Pumping multiple modes

In Section 4 we have illustrated that 1-solitons arising in a dual-pumped resonator are spectrally broader and spatially more localized than 1-solitons achieved by pumping only a single mode. Therefore, it is natural to ask what happens if more than two modes are pumped. Here we write again $\zeta_0$ instead of $\zeta$ for the detuning of the first pump. Let us denote by $\widetilde{k}_j \in \mathbb{Z}$, $j \in \{0, ..., n-1\}$ the $n$ distinct pumped modes. If we assume (for simplicity) that the initial phases of all pumps are zero then the evolution of the field inside the cavity is described by the following nonlinear coupled mode equations

$$\frac{\partial \hat{A}_k}{\partial t} = -\frac{\kappa}{2}\hat{A}_k + \sum_{j=0}^{n-1} \delta_{k\widetilde{k}_j} \sqrt{\kappa_{\text{ext}}} s_j \mathrm{e}^{-\mathrm{i}(\omega_{p_j}-\omega_{\widetilde{k}_j})t} + \mathrm{i}g \sum_{k'+k''-k'''=k} \hat{A}_{k'}\hat{A}_{k''}\bar{\hat{A}}_{k'''}\mathrm{e}^{-\mathrm{i}(\omega_{k'}+\omega_{k''}-\omega_{k'''}-\omega_k)t},$$

cf. Section 2. The description of the physical quantities is the same as in Section 2 with the only difference that $j = 0,1$ has to be replaced by $j = 0, ..., n-1$. By using the transformation

$$\tilde{a}(\tau, x) := \sqrt{\frac{2g}{\kappa}} \sum_{k \in \mathbb{Z}} \hat{A}_k\left(\frac{2}{\kappa}\tau\right)\mathrm{e}^{-\mathrm{i}dk^2\tau}\mathrm{e}^{\mathrm{i}kx}$$

we find the partial differential equation

$$\mathrm{i}\frac{\partial \tilde{a}}{\partial \tau} = -d\tilde{a}'' - \mathrm{i}\tilde{a} - |\tilde{a}|^2\tilde{a} + \mathrm{i}\sum_{j=0}^{n-1} f_j \mathrm{e}^{\mathrm{i}(\widetilde{k}_j x - \widetilde{\nu}_j \tau)}, \qquad \tilde{a} \ 2\pi\text{-periodic in } x,$$

where $\tau = \kappa t/2$, $d = 2d_2/\kappa$, and $\zeta_j = 2(\omega_{\widetilde{k}_j} - \omega_{p_j})/\kappa$, $\widetilde{\nu}_j = d\widetilde{k}_j^2 - \zeta_j$, $\eta = \kappa_{\text{ext}}/\kappa$, $f_j = \sqrt{8\eta g/\kappa^2}s_j$ for $j = 0, ..., n-1$. Setting

$$a(\tau, x) := \mathrm{e}^{-\mathrm{i}(\widetilde{k}_0(x+2d\widetilde{k}_0\tau)-\widetilde{\nu}_0\tau)}\tilde{a}(\tau, x + 2d\widetilde{k}_0\tau)$$

leads to

$$\mathrm{i}\frac{\partial a}{\partial \tau} = -da'' - (\mathrm{i} - \zeta_0)a - |a|^2 a + \mathrm{i}f_0 + \mathrm{i}\sum_{j=1}^{n-1} f_j \mathrm{e}^{\mathrm{i}(k_j x - \nu_j \tau)}, \qquad a \ 2\pi\text{-periodic in } x$$

with $k_j = \widetilde{k}_j - \widetilde{k}_0$ and $\nu_j = \zeta_0 - \zeta_j + dk_j^2$ for $j = 1, ..., n-1$.

In the two mode case the traveling wave ansatz was crucial for simplifying both the analysis and the numerical computations. In the general case of pumping multiple modes such a traveling wave ansatz is not possible for arbitrary parameter choices. However, by imposing the following side constraints we can overcome this issue,

$$\nu_j = \frac{k_j}{k_1}\nu_1 \text{ for } j = 2, ..., n-1. \tag{7.1}$$

Note that in this case

$$k_j x - \nu_j \tau = k_j x - \frac{k_j}{k_1}\nu_1\tau = \frac{k_j}{k_1}(k_1 x - \nu_1\tau) \text{ for } j = 2, ..., n-1.$$

The conditions (7.1) translate to

$$\zeta_j = \frac{k_j}{k_1}\zeta_1 + \left(1 - \frac{k_j}{k_1}\right)\zeta_0 + dk_j(k_j - k_1) \text{ for } j = 2, ..., n-1, \qquad (7.2)$$

or, in terms of physical quantities,

$$\omega_{\widetilde{k}_j} - \omega_{p_j} = \frac{\widetilde{k}_j - \widetilde{k}_0}{\widetilde{k}_1 - \widetilde{k}_0}(\omega_{\widetilde{k}_1} - \omega_{p_1}) + \frac{\widetilde{k}_1 - \widetilde{k}_j}{\widetilde{k}_1 - \widetilde{k}_0}(\omega_{\widetilde{k}_0} - \omega_{p_0}) + d_2(\widetilde{k}_j - \widetilde{k}_0)(\widetilde{k}_j - \widetilde{k}_1) \text{ for } j = 2, ..., n-1.$$

Physically, this means that if the first two lasers are set to arbitrary detunings $\omega_{\widetilde{k}_0} - \omega_{p_0}$ and $\omega_{\widetilde{k}_1} - \omega_{p_1}$ then the detunings of the remaining lasers must be tuned in the unique way imposed by (7.1). The traveling wave ansatz $a(\tau, x) = u(x - \omega\tau)$ with $s = x - \omega\tau$ and $\omega = \nu_1/k_1$ now leads to

$$-du'' + i\omega u' - (i - \zeta_0)u - |u|^2 u + if_0 + i\sum_{j=1}^{n-1} f_j e^{ik_j s} = 0, \qquad u \text{ } 2\pi\text{-periodic.}$$

First numerical experiments with `pde2path` suggest that as in Section 4 pumping of adjacent modes with equal power distribution between the modes leads to optimal combs. Thus, from here on we choose the pumped modes as $k_j = j$ with $j = 0, ..., n-1$ for some $n \in \mathbb{N}$ and consider the problem

$$-du'' + i\omega u' - (i - \zeta_0)u - |u|^2 u + if_0 + if_1\sum_{j=1}^{n-1} e^{ijs} = 0, \qquad u \text{ } 2\pi\text{-periodic}, \qquad (7.3)$$

where $f_j = f_1 > 0$ for $j = 2, ..., n-1$. Note that the side constraints (7.2) then read

$$\zeta_j = j\zeta_1 + (1 - j)\zeta_0 + d(j - 1)j \text{ for } j = 2, ..., n-1$$

and observe also that several of the theoretical results stated in Section 3 hold for equation (7.3) due to the general forcing term used there. In order to find localized solutions of (7.3) we can apply a heuristic algorithm similar to the one mentioned in Section 4.3. That is, starting from $f_1 = 0$ and a constant solution $u_0 \in \mathbb{C}$ we perform a continuation w.r.t. the $f_1$-parameter until $f_1 = f_0$ is reached, whence we alternately run a continuation algorithm by varying either the $\zeta_0$- or the $\omega$-parameter. Since our experiments suggest that the choice $\omega = (n - 1)d$ is optimal in the case of equal power distribution $f_0 = ... = f_{n-1}$ we can in fact reduce the optimizations from the algorithm to a single optimization step in $\zeta_0$. Let us denote the normalized total input power by $f^2 = \sum_{j=0}^{n-1} f_j^2$. For the example $d = 0.1$, $f = 2$ we computed the most localized

soliton (i.e., minimal FWHM) for the expected optimal power distribution $f_0 = ... = f_{n-1} = f/\sqrt{n}$ for any choice of $n = 1, ..., 50$ and evaluated the PCE, the CBW as well as the FWHM of the resulting comb state $u(s) = \sum_{k\in\mathbb{Z}} \hat{u}_k e^{iks}$. The results are depicted in Figure 23. We see that PCE and CBW increase while the FWHM decreases with increasing number of pumped modes. Hence, it seems to be beneficial to pump as many modes as possible. Here, the PCE is defined as ratio $P_{\text{FC}}/f^2$ between intracavity comb power

$$P_{\text{FC}} = \sum_{k\in\mathbb{Z}} |\hat{u}_k|^2 - \sum_{k=0}^{n-1} \frac{f_k^2}{f^2} |\hat{u}_k|^2$$

and the normalized total input power. In the special case $f_0 = ... = f_{n-1} = f/\sqrt{n}$ we find

$$P_{\text{FC}} = \sum_{k\in\mathbb{Z}} |\hat{u}_k|^2 - \frac{1}{n} \sum_{k=0}^{n-1} |\hat{u}_k|^2.$$

The CBW is again defined via the 3dB points of the adjacent non-pumped modes, i.e.,

$$\text{CBW} = k_l^* + k_r^*$$

with minimal integers $k_l^* > 0$ and $k_r^* > 0$ that fulfill

$$|\hat{u}_{-k_l^*}|^2 \leq \frac{1}{2}|\hat{u}_{-1}|^2, \quad |\hat{u}_{n-1+k_r^*}|^2 \leq \frac{1}{2}|\hat{u}_n|^2$$

respectively.
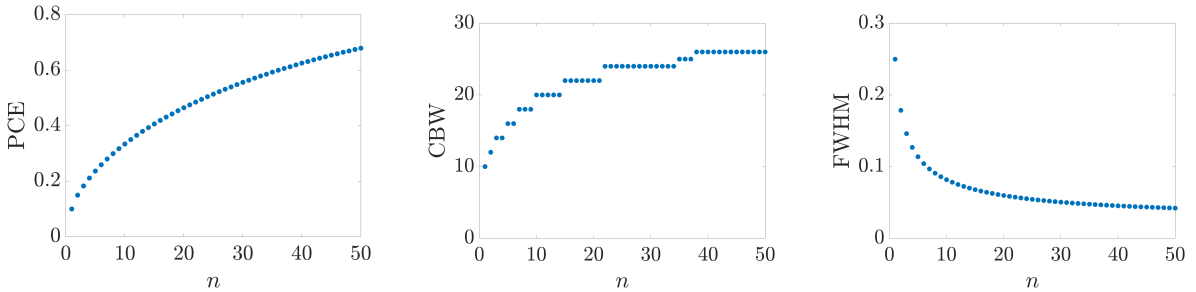


Figure 23. Power conversion efficiency, comb bandwidth and full-width at half-maximum of expected optimal soliton for $d = 0.1$ and $f = 2$ as function of number of pumped modes.

In Figure 24 we added plots of the spatial and spectral power distributions of the expected optimal solitons for $d = 0.1$ and $f = 2$ for $n = 3, 4, 5, 6$. One can observe that the soliton gets spatially more localized and spectrally broader as $n$ increases. Note that for $k \in \mathbb{N}$ the power in the mode $k$ is higher than the one in the mode $-k$ since we only pump modes with nonnegative indices.
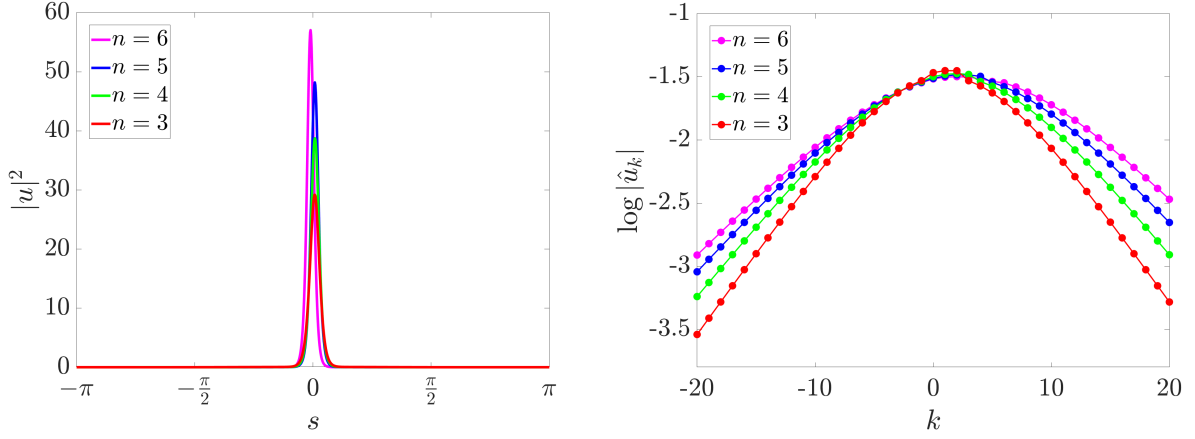
Figure 24. Spatial and spectral power distributions of optimal solitons for $d = 0.1$ and $f = 2$ for $n = 3, 4, 5, 6$.

In order to formulate a limit equation for the case $n \to \infty$ let us consider $u_n$ as an optimal solution of

$$-du'' + \mathrm{i}\omega u' - (\mathrm{i} - \zeta_0)u - |u|^2 u + \frac{\mathrm{i}f}{\sqrt{2n+1}} \sum_{j=-n}^{n} \mathrm{e}^{\mathrm{i}js} = 0, \quad u \; 2\pi\text{-periodic.}$$

Note that here we are summing from $j = -n$ to $j = n$ in order to include all modes for $n \to \infty$. In this case the optimal choice of $\omega$ for equal power distribution translates into $\omega = 0$, whence

$$-du_n'' - (\mathrm{i} - \zeta_{0,n})u_n - |u_n|^2 u_n + \frac{\mathrm{i}f}{\sqrt{2n+1}} \sum_{j=-n}^{n} \mathrm{e}^{\mathrm{i}js} = 0, \quad u_n \; 2\pi\text{-periodic,}$$

where $\zeta_{0,n}$ denotes the optimized $\zeta_0$. For $v_n(s) = \sqrt{2n+1}u_n(s)$ we find

$$-dv_n'' - (\mathrm{i} - \zeta_{0,n})v_n - \frac{1}{2n+1}|v_n|^2 v_n + \mathrm{i}f \sum_{j=-n}^{n} \mathrm{e}^{\mathrm{i}js} = 0, \quad v_n \; 2\pi\text{-periodic.}$$

Since $\sum_{j=-n}^{n} \mathrm{e}^{\mathrm{i}js}$ tends to a delta potential $2\pi\delta_0$ for $n \to \infty$ it would be interesting to find and analyze an appropriate limit equation for $n \to \infty$. Note that Theorem 3.14 only implies $\|u_n\|_2^2 \le 2\pi f^2$, whence $(v_n)_{n \in \mathbb{N}}$ does not seem to be bounded in $L^2(0, 2\pi)$. But due to better $L^1(0, 2\pi)$-bounds of the pump one may find boundedness in the $L^1(0, 2\pi)$-setting. This is currently not yet understood and it would be interesting to see more detailed research in this direction in the future.

# A. Band structures for periodic fractional Schrödinger operators

## A.1. Introduction

Appendix A is not related to frequency combs. Here, we study the spectrum of fractional Schrödinger operators with periodic potentials. The operators formally read as $L = (-\Delta)^s + V(x) + \alpha\delta_{\mathrm{per}}(x_n)$. Here, $s \in (1/2, 1)$, $\alpha \in \mathbb{R}$, $V \in L^\infty(\mathbb{R}^n, \mathbb{R})$ is $2\pi$-periodic in $x_1, ..., x_n$ and $\delta_{\mathrm{per}}$ denotes a $2\pi$-periodic Dirac comb. In the case $\alpha = 0$ we even allow $s \in (0, 1)$. We give an exact definition of these operators using sesquilinear forms. Our goal is to generalize the well-known band structure of the spectrum of periodic differential operators to the fractional case. We use Floquet-Bloch theory to give a representation of the spectrum $\sigma(L)$ in terms of the spectra of associated operators $L_k$ acting on the periodicity cell $\mathcal{P}^n := (0, 2\pi)^n$. Note that $L_k$ can not be simply defined by acting via the same expression since $L$ is a nonlocal operator. We show that the spectral definition of the fractional Laplacian, denoted by $(-\Delta)_k^s$, leads to the right operators $L_k = (-\Delta)_k^s + V(x) + \alpha\delta(x_n)$. Our main result is given in Theorem A.14 and states

$$\sigma(L) = \bigcup_{k \in \mathcal{B}^n} \sigma(L_k),$$

where $\mathcal{B}^n := [-1/2, 1/2]^n$ denotes the Brillouin zone. The operators $L_k$ have purely discrete spectrum $\sigma(L_k) = \{\lambda_l(k) : l \in \mathbb{N}\}$ with real eigenvalues

$$\lambda_1(k) \le \lambda_2(k) \le ... \le \lambda_l(k) \xrightarrow{l \to \infty} \infty.$$

The sets $I_l := \{\lambda_l(k) : k \in \mathcal{B}^n\}$ are compact intervals, whence $\sigma(L) = \bigcup_{l \in \mathbb{N}} I_l$ has so-called band structure. Floquet-Bloch theory does not answer the question whether gaps really occur in the spectrum or whether the bands actually overlap. Using the one-dimensional examples $L = (-\Delta)^s \pm 2\pi\delta_{\mathrm{per}}(x)$, we show the existence of at least one spectral gap in the fractional case $s \in (1/2, 1)$. In Section A.2 we collect some important facts about fractional Sobolev spaces. Section A.3 is dedicated to direct integrals which occur in a natural way in Floquet-Bloch theory. Section A.4 introduces the Floquet transformation which is the right tool for connecting the whole space problem with a family of problems on the periodicity cell. In Section A.5 we start our spectral theory in one dimension and we provide a multidimensional generalization in Section A.6. In Section A.7 we treat our one-dimensional examples in which a spectral gap occurs. Section A.8 contains the proofs of some technical results. Finally, in Section A.9 we prove that the eigenvalues $\lambda_l(k)$ of the periodicity cell operators depend continuously on the parameter $k$.

## A.2. Some background on fractional Sobolev spaces

In Section A.2 we collect some important facts about fractional Sobolev spaces. A detailed introduction can be found in [13].

Let $\Omega \subset \mathbb{R}^n$ be open and $s \in (0,1)$. The fractional Sobolev space $H^s(\Omega)$ is defined as

$$H^s(\Omega) := \left\{ u \in L^2(\Omega) : \int_\Omega \int_\Omega \frac{|u(x) - u(y)|^2}{|x-y|^{n+2s}} \, dx \, dy < \infty \right\}.$$

This space is endowed with the natural norm

$$\|u\|_{H^s(\Omega)} := \left( \int_\Omega |u(x)|^2 \, dx + \int_\Omega \int_\Omega \frac{|u(x) - u(y)|^2}{|x-y|^{n+2s}} \, dx \, dy \right)^{\frac{1}{2}},$$

where the term

$$[u]_{H^s(\Omega)} := \left( \int_\Omega \int_\Omega \frac{|u(x) - u(y)|^2}{|x-y|^{n+2s}} \, dx \, dy \right)^{\frac{1}{2}}$$

is the so-called Gagliardo seminorm of $u$.

If $\Omega = \mathbb{R}^n$, there is an equivalent definition via the Fourier transform,

$$\mathcal{F}\varphi(\xi) := \widehat{\varphi}(\xi) := \frac{1}{(2\pi)^{n/2}} \int_{\mathbb{R}^n} \varphi(x) \mathrm{e}^{-\mathrm{i}\xi^\mathrm{T} x} \, dx \quad \text{for } \varphi \in L^1(\mathbb{R}^n), \xi \in \mathbb{R}^n.$$

As usual, $\mathcal{F}$ extends to a unitary map $\mathcal{F} : L^2(\mathbb{R}^n) \to L^2(\mathbb{R}^n)$. By [13, Proposition 3.4],

$$H^s(\mathbb{R}^n) = \left\{ u \in L^2(\mathbb{R}^n) : \int_{\mathbb{R}^n} \left( 1 + |\xi|^2 \right)^s |\widehat{u}(\xi)|^2 \, d\xi < \infty \right\}$$

and

$$[u]_{H^s(\mathbb{R}^n)}^2 = C_1(n,s) \int_{\mathbb{R}^n} |\xi|^{2s} |\widehat{u}(\xi)|^2 \, d\xi \tag{A.1}$$

for the constant

$$C_1(n,s) := 2 \int_{\mathbb{R}^n} \frac{1 - \cos(z_1)}{|z|^{n+2s}} \, dz. \tag{A.2}$$

Therefore,

$$\|u\|_{H^s(\mathbb{R}^n)} := \left( \int_{\mathbb{R}^n} \left( 1 + |\xi|^2 \right)^s |\widehat{u}(\xi)|^2 \, d\xi \right)^{\frac{1}{2}}$$

defines an equivalent norm on $H^s(\mathbb{R}^n)$. We define the fractional Laplacian $(-\Delta)^{s/2}$ by $(-\Delta)^{s/2} u := \mathcal{F}^{-1}\left( |\xi|^s \widehat{u}(\xi) \right)$ for $u \in H^s(\mathbb{R}^n)$. Note that although $(-\Delta)^s$ appears in the formal definition of $L$, we will only need to deal with $(-\Delta)^{s/2}$ since we follow a sesquilinear

form approach.

By [13, Proposition 3.8], any function $u \in H^s(\mathbb{R}^n)$ for $s \in (1/2, 1)$ has a trace $v$ on the hyperplane $\{x_n = 0\}$, such that $v \in L^2(\mathbb{R}^{n-1})$. In order to study our sesquilinear forms, we will need the following inequality. The proof is given in Section A.8.

**Theorem A.1.** *Let $s \in (1/2, 1)$ and $\varepsilon > 0$. Then there exists a constant $D = D(n, s) > 0$ such that $u \in H^s(\mathbb{R}^n)$ has a trace at $\{x_n = 0\}$ and*

$$\|u(\cdot, 0)\|_{L^2(\mathbb{R}^{n-1})}^2 \leq D\Big(\varepsilon^{-2s/2s-1}\|u\|_{L^2(\mathbb{R}^n)}^2 + \varepsilon^{2s}[u]_{H^s(\mathbb{R}^n)}^2\Big).$$

Next, we move to the periodicity cell $\mathcal{P}^n = (0, 2\pi)^n$ and want to equip $H^s(\mathcal{P}^n)$ with quasiperiodic boundary conditions. For this purpose, if $u \in L^2(\mathcal{P}^n)$, $k \in \mathcal{B}^n = [-1/2, 1/2]^n$ and $l \in \mathbb{Z}^n$, then we write

$$\widehat{u}_{k,l} := \frac{1}{(2\pi)^{n/2}}\Big\langle u, \mathrm{e}^{\mathrm{i}(k+l)^{\mathrm{T}}(\cdot)}\Big\rangle_{L^2(\mathcal{P}^n)} = \frac{1}{(2\pi)^{n/2}}\int_{\mathcal{P}^n} u(x)\mathrm{e}^{-\mathrm{i}(k+l)^{\mathrm{T}}x}\,dx.$$

Observe that $\big((2\pi)^{-n/2}\mathrm{e}^{\mathrm{i}(k+l)^{\mathrm{T}}(\cdot)}\big)_{l \in \mathbb{Z}^n}$ forms an orthonormal basis in $L^2(\mathcal{P}^n)$ and

$$u = \frac{1}{(2\pi)^{n/2}}\sum_{l \in \mathbb{Z}^n}\widehat{u}_{k,l}\mathrm{e}^{\mathrm{i}(k+l)^{\mathrm{T}}(\cdot)}.$$

Let $s \in (0, 1)$ and $k \in \mathcal{B}^n$. By means of a discrete Fourier characterization, we define the space $H_k^s(\mathcal{P}^n)$ as

$$H_k^s(\mathcal{P}^n) := \left\{u \in L^2(\mathcal{P}^n) : \sum_{l \in \mathbb{Z}^n}\big(1 + |k + l|^2\big)^s|\widehat{u}_{k,l}|^2 < \infty\right\},$$

with norm

$$\|u\|_{H_k^s(\mathcal{P}^n)} := \left(\sum_{l \in \mathbb{Z}^n}\big(1 + |k + l|^2\big)^s|\widehat{u}_{k,l}|^2\right)^{\frac{1}{2}}.$$

Further, the quasiperiodic fractional Laplacian $(-\Delta)_k^{s/2} : H_k^s(\mathcal{P}^n) \subset L^2(\mathcal{P}^n) \to L^2(\mathcal{P}^n)$ is defined by

$$(-\Delta)_k^{s/2}u := \frac{1}{(2\pi)^{n/2}}\sum_{l \in \mathbb{Z}^n}|k + l|^s\widehat{u}_{k,l}\mathrm{e}^{\mathrm{i}(k+l)^{\mathrm{T}}(\cdot)}. \tag{A.3}$$

Note that (A.3) holds for $s = 2$, i.e. for the usual Laplacian, which motivates this definition. Note also that $(-\Delta)_k^{s/2}$ is self-adjoint and that $H_k^s(\mathcal{P}^n)$ is a Hilbert space. The following lemma shows that, in fact, $H_k^s(\mathcal{P}^n)$ is a subspace of $H^s(\mathcal{P}^n)$. The proof is an adaption of [13, Proposition 3.4].

A. *Band structures for periodic fractional Schrödinger operators*

**Lemma A.2.** *Let $s \in (0,1)$ and $k \in \mathcal{B}^n$. Then, for $u \in H^s_k(\mathcal{P}^n)$,*

$$[u]^2_{H^s(\mathcal{P}^n)} \le C_1(n,s)\big\|(-\Delta)^{s/2}_k u\big\|^2_{L^2(\mathcal{P}^n)}, \tag{A.4}$$

*where the constant $C_1(n,s)$ is defined by (A.2).*

*Proof.* We consider $u$ as quasiperiodically extended to $\mathbb{R}^n$. Then,

$$[u]^2_{H^s(\mathcal{P}^n)} = \int_{\mathcal{P}^n}\int_{\mathcal{P}^n} \frac{|u(x)-u(y)|^2}{|x-y|^{n+2s}}\,dx\,dy = \int_{\mathcal{P}^n}\int_{\mathcal{P}^n-y} \frac{|u(z+y)-u(y)|^2}{|z|^{n+2s}}\,dz\,dy$$

$$\le \int_{\mathcal{P}^n}\int_{\mathbb{R}^n} \frac{|u(z+y)-u(y)|^2}{|z|^{n+2s}}\,dz\,dy = \int_{\mathbb{R}^n} \frac{1}{|z|^{n+2s}}\int_{\mathcal{P}^n} |u(z+y)-u(y)|^2\,dy\,dz.$$

By the Plancherel theorem we further conclude

$$[u]^2_{H^s(\mathcal{P}^n)} \le \int_{\mathbb{R}^n} \frac{1}{|z|^{n+2s}} \sum_{l\in\mathbb{Z}^n} |\widehat{(u(z+\cdot)-u)}_{k,l}|^2\,dz$$

$$= \int_{\mathbb{R}^n} \frac{1}{|z|^{n+2s}} \sum_{l\in\mathbb{Z}^n} |e^{i(k+l)^{\mathrm{T}}z}-1|^2|\widehat{u}_{k,l}|^2\,dz$$

$$= 2\sum_{l\in\mathbb{Z}^n} \int_{\mathbb{R}^n} \frac{1-\cos((k+l)^{\mathrm{T}}z)}{|z|^{n+2s}}\,dz\,|\widehat{u}_{k,l}|^2.$$

Now choose an orthogonal matrix $R \in \mathbb{R}^{n\times n}$ with $R(k+l) = |k+l|e_1$, where $e_1 = (1,0,...,0)^{\mathrm{T}}$. Using the transformation $z = R^{\mathrm{T}}\zeta$ we have

$$\int_{\mathbb{R}^n} \frac{1-\cos((k+l)^{\mathrm{T}}z)}{|z|^{n+2s}}\,dz = \int_{\mathbb{R}^n} \frac{1-\cos(|k+l|\zeta_1)}{|\zeta|^{n+2s}}\,d\zeta.$$

A further transformation $\zeta = |k+l|^{-1}\xi$ (we can assume $|k+l|\ne 0$) yields

$$\int_{\mathbb{R}^n} \frac{1-\cos((k+l)^{\mathrm{T}}z)}{|z|^{n+2s}}\,dz = \int_{\mathbb{R}^n} \frac{1-\cos(\xi_1)}{|\xi|^{n+2s}}\,d\xi|k+l|^{2s} = \frac{1}{2}C_1(n,s)|k+l|^{2s},$$

so that finally

$$[u]^2_{H^s(\mathcal{P}^n)} \le C_1(n,s)\sum_{l\in\mathbb{Z}^n} |k+l|^{2s}|\widehat{u}_{k,l}|^2 = C_1(n,s)\big\|(-\Delta)^{s/2}_k u\big\|^2_{L^2(\mathcal{P}^n)}. \qquad \square$$

We can also prove an analogon of Theorem A.1 for functions acting on the periodicity cell. The proof is given in Section A.8.

**Theorem A.3.** *Let $s \in (1/2, 1)$ and $\varepsilon > 0$. Then there exists a constant $C = C(n,s) > 0$*

*such that $u \in H^s(\mathcal{P}^n)$ has a trace at $\{x_n = 0\}$ and*

$$\|u(\cdot,0)\|_{L^2(\mathcal{P}^{n-1})}^2 \le C\Big(\big(\varepsilon^{2s} + \varepsilon^{-2s/2s-1}\big)\|u\|_{L^2(\mathcal{P}^n)}^2 + \varepsilon^{2s}[u]_{H^s(\mathcal{P}^n)}^2\Big).$$

## A.3. Direct integrals

Direct integrals occur in a natural way in Floquet-Bloch theory. We limit ourselves to the most important facts and refer the reader to [55] for more details.

Let $H$ be a separable Hilbert space and $(\Omega, \mathfrak{M}, \mu)$ a $\sigma-$finite measure space. We call

$$\int_\Omega^\oplus H \, d\mu := L^2(\Omega, H)$$

a constant direct integral. We say that a map $k \mapsto B_k$ from $\Omega$ to the space $L(H)$ of bounded linear operators on $H$ is measurable if $\Omega \to \mathbb{C}, k \mapsto \langle B_k \varphi, \psi \rangle_H$ is measurable for all $\varphi, \psi \in H$. Further, we call a map $k \mapsto A_k$ from $\Omega$ to the space of (possibly unbounded) self-adjoint operators on $H$ measurable if the map $\Omega \to L(H), k \mapsto (A_k + \mathrm{i}\,\mathrm{Id})^{-1}$ is measurable. For such a map we define an operator

$$A : D(A) \subset \int_\Omega^\oplus H \, d\mu \to \int_\Omega^\oplus H \, d\mu$$

with domain

$$D(A) = \left\{ \psi \in \int_\Omega^\oplus H \, d\mu : \ \psi(k) \in D(A_k) \text{ for a.a. } k \in \Omega, \int_\Omega \|A_k \psi(k)\|_H^2 \, dk < \infty \right\}$$

by

$$(A\psi)(k) := A_k \psi(k).$$

We write

$$A = \int_\Omega^\oplus A_k \, dk.$$

In this situation we have the following result, see [55, Theorem XIII.85].

**Theorem A.4.**

*(a) The operator $A$ is self-adjoint.*

*(b) For every $\lambda \in \mathbb{R}$ one has*

$$\lambda \in \sigma(A) \Leftrightarrow \forall \varepsilon > 0 : \mu\big(\{k \in \Omega : \sigma(A_k) \cap (\lambda - \varepsilon, \lambda + \varepsilon) \ne \emptyset\}\big) > 0.$$

## A.4. Floquet transformation

For simplicity, we start our investigations in one dimension, i.e. in Section A.4 and Section A.5 we fix $n = 1$. For a local differential operator, its restriction to a periodicity

cell can be defined on suitable function spaces (i.e. with included quasiperiodic boundary conditions) by acting via the same differential expression. It is a-priori not clear how this can be done for the nonlocal operator $(-\Delta)^{s/2}$. Here, we show that the spectral definition of $(-\Delta)_k^{s/2}$ from (A.3) is the right one.

The Floquet transformation

$$\mathcal{U} : L^2(\mathbb{R}) \to L^2(\mathcal{P} \times \mathcal{B}), \ (\mathcal{U}f)(x,k) = \sum_{m \in \mathbb{Z}} f(x - 2\pi m)\mathrm{e}^{2\pi \mathrm{i} k m}$$

is the right tool for transforming a problem on the whole space into a family of problems on the periodicity cell and vice versa. For $k \in \mathcal{B}$, let us define the quasiperiodic extension operator

$$E_k : L^2(\mathcal{P}) \to L^2_{\mathrm{loc}}(\mathbb{R}), \ (E_k u)(x + 2\pi l) := u(x)\mathrm{e}^{2\pi \mathrm{i} k l} \text{ for } x \in \mathcal{P}, l \in \mathbb{Z}.$$

Then, by [16, Lemma 3.4.1], we have the following result.

**Lemma A.5.** *The operator $\mathcal{U}$ is unitary and its inverse is given by*

$$\left(\mathcal{U}^{-1}g\right)(x) = \int_{\mathcal{B}} \left(E_k\ g(\cdot,k)\right)(x) \, dk \text{ for } x \in \mathbb{R}.$$

With the help of $\mathcal{U}$, we find the following important relation between the operator $(-\Delta)^{s/2}$ and the operators $(-\Delta)_k^{s/2}$.

**Theorem A.6.** *Let $s \in (0,1)$ and $f \in H^s(\mathbb{R})$. Then, for a.a. $k \in \mathcal{B}$ and all $g \in H_k^s(\mathcal{P})$,*

$$\left\langle \left(\mathcal{U}(-\Delta)^{s/2}f\right)(\cdot,k), g\right\rangle_{L^2(\mathcal{P})} = \left\langle (\mathcal{U}f)(\cdot,k), (-\Delta)_k^{s/2}g\right\rangle_{L^2(\mathcal{P})}.$$

For the proof we need the following lemma, see [4].

**Lemma A.7.** *Let $s \in (0,1)$, $\varphi \in \mathcal{S}(\mathbb{R})$ be a Schwartz function and*

$$\mathcal{S}_{s/2}(\mathbb{R}) := \left\{ f \in C^\infty(\mathbb{R}) : \sup_{x \in \mathbb{R}} \left(1 + |x|^{1+s}\right)\left|f^{(m)}(x)\right| < \infty \text{ for all } m \in \mathbb{N}_0 \right\}.$$

*Then, $(-\Delta)^{s/2}\varphi \in \mathcal{S}_{s/2}(\mathbb{R})$.*

Notice that in general $(-\Delta)^{s/2}\varphi \notin \mathcal{S}(\mathbb{R})$ for $\varphi \in \mathcal{S}(\mathbb{R})$ because $|\xi|^s$ introduces a lack of differentiability at the origin, so that $|\xi|^s\widehat{\varphi}(\xi)$ no longer need to be a Schwartz function. Transforming back via $\mathcal{F}^{-1}$, the lack of differentiability translates into a lack of rapid decay.

*Proof of Theorem A.6.* First, let $f \in C_c^\infty(\mathbb{R})$ and $g = (2\pi)^{-1/2}\mathrm{e}^{\mathrm{i}(k+j)(\cdot)}$ for an integer $j \in \mathbb{Z}$. Then,

$$\left\langle (\mathcal{U}f)(\cdot,k), (-\Delta)_k^{s/2}g\right\rangle_{L^2(\mathcal{P})}$$

$$= \frac{1}{\sqrt{2\pi}}|k+j|^s \left\langle (\mathcal{U}f)(\cdot,k), \mathrm{e}^{\mathrm{i}(k+j)(\cdot)} \right\rangle_{L^2(\mathcal{P})}$$

$$= \frac{1}{\sqrt{2\pi}}|k+j|^s \int_0^{2\pi} \sum_{m\in\mathbb{Z}} f(x-2\pi m)\mathrm{e}^{2\pi\mathrm{i}km}\mathrm{e}^{-\mathrm{i}(k+j)x}\, dx$$

$$= \frac{1}{\sqrt{2\pi}}|k+j|^s \sum_{m\in\mathbb{Z}} \int_0^{2\pi} f(x-2\pi m)\mathrm{e}^{2\pi\mathrm{i}km}\mathrm{e}^{-\mathrm{i}(k+j)x}\, dx$$

$$= \frac{1}{\sqrt{2\pi}}|k+j|^s \sum_{m\in\mathbb{Z}} \int_{-2\pi m}^{-2\pi m+2\pi} f(x)\mathrm{e}^{2\pi\mathrm{i}km}\mathrm{e}^{-\mathrm{i}(k+j)(x+2\pi m)}\, dx$$

$$= \frac{1}{\sqrt{2\pi}}|k+j|^s \int_{\mathbb{R}} f(x)\mathrm{e}^{-\mathrm{i}(k+j)x}\, dx$$

$$= |k+j|^s \widehat{f}(k+j).$$

On the other hand, since $(-\Delta)^{s/2}f \in \mathcal{S}_{s/2}(\mathbb{R})$ by Lemma A.7, via a similar calculation,

$$\left\langle \left( \mathcal{U}(-\Delta)^{s/2}f \right)(\cdot,k), g \right\rangle_{L^2(\mathcal{P})}$$

$$= \frac{1}{\sqrt{2\pi}} \int_0^{2\pi} \sum_{m\in\mathbb{Z}} \left( (-\Delta)^{s/2}f \right)(x-2\pi m)\mathrm{e}^{2\pi\mathrm{i}km}\mathrm{e}^{-\mathrm{i}(k+j)x}\, dx$$

$$= \widehat{(-\Delta)^{s/2}f}(k+j)$$

$$= |k+j|^s \widehat{f}(k+j). \tag{A.5}$$

Next, to generalize the result to arbitrary $g \in H_k^s(\mathcal{P})$, we define for $M \in \mathbb{N}$,

$$g_M := \frac{1}{\sqrt{2\pi}} \sum_{l=-M}^{M} \widehat{g}_{k,l}\mathrm{e}^{\mathrm{i}(k+l)(\cdot)}.$$

By linearity, we have

$$\left\langle \left( \mathcal{U}(-\Delta)^{s/2}f \right)(\cdot,k), g_M \right\rangle_{L^2(\mathcal{P})} = \left\langle (\mathcal{U}f)(\cdot,k), (-\Delta)_k^{s/2} g_M \right\rangle_{L^2(\mathcal{P})}.$$

Since $g_M \to g$ in $L^2(\mathcal{P})$ as $M \to \infty$ and

$$(-\Delta)_k^{s/2} g_M = \frac{1}{\sqrt{2\pi}} \sum_{l=-M}^{M} |k+l|^s \widehat{g}_{k,l}\mathrm{e}^{\mathrm{i}(k+l)(\cdot)} \to (-\Delta)_k^{s/2} g \text{ in } L^2(\mathcal{P})$$

as $M \to \infty$, the claim follows for $f \in C_c^\infty(\mathbb{R})$. Finally, let $f \in H^s(\mathbb{R})$. Then, we find $f_m \in C_c^\infty(\mathbb{R})$ with $f_m \to f$ in $H^s(\mathbb{R})$. In particular, $f_m \to f$ and $(-\Delta)^{s/2}f_m \to (-\Delta)^{s/2}f$ in $L^2(\mathbb{R})$. By Lemma A.5, $\mathcal{U}f_m \to \mathcal{U}f$ and $\mathcal{U}(-\Delta)^{s/2}f_m \to \mathcal{U}(-\Delta)^{s/2}f$ in $L^2(\mathcal{P}\times\mathcal{B})$. Since $L^2(\mathcal{P}\times\mathcal{B}) \cong L^2(\mathcal{B}, L^2(\mathcal{P}))$ we can assume (up to a subsequence) by the Riesz-Fischer theorem that $(\mathcal{U}f_m)(\cdot,k) \to (\mathcal{U}f)(\cdot,k)$ and $\left( \mathcal{U}(-\Delta)^{s/2}f_m \right)(\cdot,k) \to \left( \mathcal{U}(-\Delta)^{s/2}f \right)(\cdot,k)$ in

$L^2(\mathcal{P})$ for a.a. $k \in \mathcal{B}$. The assertion follows from

$$\left\langle \left( \mathcal{U}(-\Delta)^{s/2} f_m \right)(\cdot, k), g \right\rangle_{L^2(\mathcal{P})} = \left\langle (\mathcal{U} f_m)(\cdot, k), (-\Delta)_k^{s/2} g \right\rangle_{L^2(\mathcal{P})}$$

by taking the limit $m \to \infty$. $\qquad\qquad\qquad\qquad\qquad\qquad\qquad\qquad \square$

**Remark A.8.** Inspired by [56, Theorem A] and armed with Theorem A.6, we can provide an alternative view onto the operator $(-\Delta)_k^{s/2}$. The canonical way to define the periodicity cell operator $(-\Delta)_k^{s/2}$ is the following: Take a function $g \in H_k^s(\mathcal{P})$, extend it quasiperiodically to the whole of $\mathbb{R}$, insert it into the whole-space operator $(-\Delta)^{s/2}$ and finally restrict the obtained function again to the periodicity cell $\mathcal{P}$. The fact that $E_k g \notin L^2(\mathbb{R})$ for $g \neq 0$ now requires a definition of $(-\Delta)^{s/2}$ for a larger class of functions. For this, we notice that $(-\Delta)^{s/2} : \mathcal{S}(\mathbb{R}) \to \mathcal{S}_{s/2}(\mathbb{R})$ is not only well-defined (cf. Lemma A.7) but also continuous if we equip $\mathcal{S}_{s/2}(\mathbb{R})$ with the family of seminorms (see [4])

$$[f]_m := \sup_{x \in \mathbb{R}} \left( 1 + |x|^{1+s} \right) \left| f^{(m)}(x) \right|.$$

The symmetry of $(-\Delta)^{s/2}$ allows us to define $(-\Delta)^{s/2} : \mathcal{S}'_{s/2}(\mathbb{R}) \to \mathcal{S}'(\mathbb{R})$ by duality, i.e.

$$\left\langle (-\Delta)^{s/2} f, \varphi \right\rangle := \left\langle f, (-\Delta)^{s/2} \varphi \right\rangle, \ f \in \mathcal{S}'_{s/2}(\mathbb{R}), \varphi \in \mathcal{S}(\mathbb{R}).$$

Next note that $E_k g$ defines a distribution in $\mathcal{S}'_{s/2}(\mathbb{R})$. In fact, for $\psi \in \mathcal{S}_{s/2}(\mathbb{R})$,

$$
\begin{aligned}
\int_{\mathbb{R}} |E_k g| |\psi| \, dx &= \int_{\mathbb{R}} |E_k g| \frac{1}{1 + |x|^{1+s}} \left( 1 + |x|^{1+s} \right) |\psi| \, dx \\
&\leq \sum_{j=1}^{\infty} \int_{2\pi(j-1) \leq |x| \leq 2\pi j} |E_k g| \frac{1}{1 + |x|^{1+s}} \, dx \, [\psi]_0 \\
&\leq \sum_{j=1}^{\infty} \frac{1}{1 + (2\pi(j-1))^{1+s}} \int_{2\pi(j-1) \leq |x| \leq 2\pi j} |E_k g| \, dx \, [\psi]_0 \\
&\leq 2 \sum_{j=1}^{\infty} \frac{1}{1 + (2\pi(j-1))^{1+s}} \|g\|_{L^1(\mathcal{P})} \, [\psi]_0,
\end{aligned}
$$

and the last series converges since $s > 0$. Further, for $\varphi \in \mathcal{S}(\mathbb{R})$,

$$
\begin{aligned}
\left\langle E_k g, (-\Delta)^{s/2} \varphi \right\rangle &= \int_{\mathbb{R}} E_k g \, (-\Delta)^{s/2} \varphi \, dx = \sum_{m \in \mathbb{Z}} \int_{2\pi m}^{2\pi(m+1)} g(x - 2\pi m) e^{2\pi i k m} (-\Delta)^{s/2} \varphi \, dx \\
&= \sum_{m \in \mathbb{Z}} \int_0^{2\pi} g(x) e^{2\pi i k m} \left( (-\Delta)^{s/2} \varphi \right)(x + 2\pi m) \, dx \\
&= \int_0^{2\pi} g(x) \sum_{m \in \mathbb{Z}} \left( (-\Delta)^{s/2} \varphi \right)(x + 2\pi m) e^{2\pi i k m} \, dx
\end{aligned}
$$

$$= \int_0^{2\pi} g(x) \big(\mathcal{U}(-\Delta)^{s/2}\varphi\big)(x,-k)\,dx = \int_0^{2\pi} g(x)\overline{\big(\mathcal{U}(-\Delta)^{s/2}\overline{\varphi}\big)(x,k)}\,dx$$

$$= \big\langle g, \big(\mathcal{U}(-\Delta)^{s/2}\overline{\varphi}\big)(\cdot,k)\big\rangle_{L^2(\mathcal{P})} = \big\langle (-\Delta)_k^{s/2}g, \big(\mathcal{U}\overline{\varphi}\big)(\cdot,k)\big\rangle_{L^2(\mathcal{P})}$$

$$= \int_0^{2\pi} (-\Delta)_k^{s/2} g\,\big(\mathcal{U}\varphi\big)(x,-k)\,dx \overset{(*)}{=} \int_{\mathbb{R}} E_k(-\Delta)_k^{s/2}g\,\varphi\,dx$$

$$= \big\langle E_k(-\Delta)_k^{s/2}g, \varphi\big\rangle.$$

Therefore, $(-\Delta)^{s/2}E_k g = E_k(-\Delta)_k^{s/2}g$, whence $(-\Delta)_k^{s/2}g = \big((-\Delta)^{s/2}E_k g\big)\big|_{\mathcal{P}}$. Note that $(*)$ follows in a similar way as

$$\int_{\mathbb{R}} E_k g\,(-\Delta)^{s/2}\varphi\,dx = \int_0^{2\pi} g(x)\big(\mathcal{U}(-\Delta)^{s/2}\varphi\big)(x,-k)\,dx,$$

which was proven during the first steps of the calculation.

## A.5. One-dimensional spectral theory

Next, we turn to the analysis of the operator $L = (-\Delta)^s + V(x) + \alpha\delta_{\mathrm{per}}(x)$. We assume $s \in (1/2, 1), \alpha \in \mathbb{R}$ and that $V \in L^\infty(\mathbb{R},\mathbb{R})$ is $2\pi$-periodic. First we define the corresponding sesquilinear form $B_L : H^s(\mathbb{R}) \times H^s(\mathbb{R}) \to \mathbb{C}$ by

$$B_L[u,v] := \int_{\mathbb{R}} |\xi|^{2s}\widehat{u}(\xi)\overline{\widehat{v}(\xi)}\,d\xi + \int_{\mathbb{R}} V(x)u(x)\overline{v(x)}\,dx + \alpha\sum_{l\in\mathbb{Z}} u(2\pi l)\overline{v(2\pi l)}.$$

Recall that $s > 1/2$ implies the embedding $H^s(\mathbb{R}) \hookrightarrow C_0(\mathbb{R})$. By Theorem A.3 we find for any $\varepsilon > 0$ and $l \in \mathbb{Z}$,

$$|u(2\pi l)|^2 \leq C\Big(\big(\varepsilon^{2s} + \varepsilon^{-2s/2s-1}\big)\|u\|^2_{L^2(2\pi l, 2\pi(l+1))} + \varepsilon^{2s}[u]^2_{H^s(2\pi l, 2\pi(l+1))}\Big) \tag{A.6}$$

for a constant $C = C(s) > 0$. Therefore, using (A.1), we find,

$$\sum_{l\in\mathbb{Z}} |u(2\pi l)|^2 \leq C\Big(\big(\varepsilon^{2s} + \varepsilon^{-2s/2s-1}\big)\|u\|^2_{L^2(\mathbb{R})} + \varepsilon^{2s}\big\|(-\Delta)^{s/2}u\big\|^2_{L^2(\mathbb{R})}\Big) \tag{A.7}$$

for a new constant $C = C(s) > 0$. For a suitable choice of $\varepsilon$, this results in

$$B_L[u,u] \geq \frac{1}{2}\big\|(-\Delta)^{s/2}u\big\|^2_{L^2(\mathbb{R})} - C_2\|u\|^2_{L^2(\mathbb{R})} \text{ for a constant } C_2 = C_2(\alpha, s, V), \tag{A.8}$$

whence $B_L$ is semibounded and closed. By [54, Theorem VIII.15] we may view $L$ as a self-adjoint operator on a suitable domain $D(L) \subset H^s(\mathbb{R})$ given by the relation that for

## A. Band structures for periodic fractional Schrödinger operators

$u \in H^s(\mathbb{R}), w \in L^2(\mathbb{R})$,

$$u \in D(L) \text{ and } Lu = w \Leftrightarrow \forall v \in H^s(\mathbb{R}) : B_L[u, v] = \langle w, v \rangle_{L^2(\mathbb{R})}.$$

We note that

$$D(L) = \left\{ u \in H^s(\mathbb{R}) : |\xi|^{2s} \widehat{u}(\xi) + \frac{\alpha}{\sqrt{2\pi}} \sum_{l \in \mathbb{Z}} u(2\pi l) e^{-2\pi i l \xi} \in L^2(\mathbb{R}) \right\},$$

$$Lu = \mathcal{F}^{-1}\left[ |\xi|^{2s} \widehat{u}(\xi) + \frac{\alpha}{\sqrt{2\pi}} \sum_{l \in \mathbb{Z}} u(2\pi l) e^{-2\pi i l \xi} \right] + V(x)u.$$

Here, $\sum_{l \in \mathbb{Z}} u(2\pi l) e^{-2\pi i l \xi}$ converges in $L^2_{\text{loc}}(\mathbb{R})$ since $\sum_{l \in \mathbb{Z}} |u(2\pi l)|^2 < \infty$ for $u \in H^s(\mathbb{R})$ by (A.7).

We proceed by introducing the associated periodicity cell operators $L_k = (-\Delta)_k^s + V(x) + \alpha \delta(x)$, $k \in \mathcal{B}$. The corresponding sesquilinear form $B_{L_k} : H^s_k(\mathcal{P}) \times H^s_k(\mathcal{P}) \to \mathbb{C}$ is defined by

$$B_{L_k}[u, v] := \sum_{l \in \mathbb{Z}} |k + l|^{2s} \widehat{u}_{k,l} \overline{\widehat{v}_{k,l}} + \int_0^{2\pi} V(x) u(x) \overline{v(x)} \, dx + \alpha u(0) \overline{v(0)}.$$

We note that $s \in (1/2, 1)$ implies the embedding $H^s(\mathcal{P}) \hookrightarrow C^{0,\beta}(\mathcal{P})$ for $\beta = s - 1/2$, see [13, Theorem 8.2]. Combining (A.6) for $l = 0$ and (A.4), we find, for $u \in H^s_k(\mathcal{P})$,

$$|u(0)|^2 \leq C\left( \left( \varepsilon^{2s} + \varepsilon^{-2s/2s-1} \right) \|u\|_{L^2(\mathcal{P})}^2 + \varepsilon^{2s} \left\| (-\Delta)_k^{s/2} u \right\|_{L^2(\mathcal{P})}^2 \right)$$

for a constant $C = C(s) > 0$. Again, for a suitable choice of $\varepsilon$, this results in

$$B_{L_k}[u, u] \geq \frac{1}{2} \left\| (-\Delta)_k^{s/2} u \right\|_{L^2(\mathcal{P})}^2 - C_2 \|u\|_{L^2(\mathcal{P})}^2 \tag{A.9}$$

for the constant $C_2 = C_2(\alpha, s, V)$ from (A.8), whence $B_{L_k}$ is semibounded and closed. The corresponding self-adjoint operator is given by

$$D(L_k) = \left\{ u \in H^s_k(\mathcal{P}) : |k + l|^{2s} \widehat{u}_{k,l} + \frac{\alpha}{\sqrt{2\pi}} u(0) \in \ell^2(\mathbb{Z}) \right\},$$

$$L_k u = \frac{1}{\sqrt{2\pi}} \sum_{l \in \mathbb{Z}} \left( |k + l|^{2s} \widehat{u}_{k,l} + \frac{\alpha}{\sqrt{2\pi}} u(0) \right) e^{i(k+l)(\cdot)} + V(x)u.$$

Since $\mathcal{P}$ is bounded, compactness arguments can be used to prove the existence of a $L^2(\mathcal{P})$ orthonormal basis $(\varphi_l(\cdot, k))_{l \in \mathbb{N}}$ of eigenfunctions from $L_k$ with corresponding (real) eigenvalues satisfying

$$\lambda_1(k) \leq \lambda_2(k) \leq \ldots \leq \lambda_l(k) \xrightarrow{l \to \infty} \infty$$

*A. Band structures for periodic fractional Schrödinger operators*

and

$$\sigma(L_k) = \{\lambda_l(k) : l \in \mathbb{N}\}. \tag{A.10}$$

Proving the analogon of Theorem A.6 for $L$ and $L_k$ directly seems to be hard by the complicated structure of $D(L)$. Therefore, we follow [3] and choose a sesquilinear form approach. Since we are studying a spectral problem, we may assume w.l.o.g. (introducing a shift by $C_2 + 1/2$) that $B_L$ and $B_{L_k}$ define scalar products on $H^s(\mathbb{R})$ and $H^s_k(\mathcal{P})$, which are equivalent to the usual scalar products on $H^s(\mathbb{R})$ and $H^s_k(\mathcal{P})$.

An important step is to prove that $\mathcal{U}$ is also a unitary map between $(H^s(\mathbb{R}), B_L[\cdot, \cdot])$ and the Hilbert space $(\mathcal{H}, \langle \cdot, \cdot \rangle_{\mathcal{H}})$ defined by

$$\mathcal{H} := \{u \in L^2(\mathcal{P} \times \mathcal{B}) : u(\cdot, k) \in H^s_k(\mathcal{P}) \text{ for a.a. } k \in \mathcal{B}, \|u\|_{\mathcal{H}} < \infty\},$$
$$\langle u, v \rangle_{\mathcal{H}} := \int_{\mathcal{B}} B_{L_k}[u(\cdot, k), v(\cdot, k)]\, dk, \quad \|u\|_{\mathcal{H}} := \sqrt{\langle u, u \rangle_{\mathcal{H}}}.$$

Note that $\mathcal{H} = D\left(\int_{\mathcal{B}}^{\oplus} (-\Delta)_k^{s/2}\, dk\right)$ and that the graph norm of $\int_{\mathcal{B}}^{\oplus} (-\Delta)_k^{s/2}\, dk$ defines an equivalent norm on $\mathcal{H}$. Here, using $L^2(\mathcal{P} \times \mathcal{B}) \cong L^2(\mathcal{B}, L^2(\mathcal{P}))$, we interpret $\int_{\mathcal{B}}^{\oplus} (-\Delta)_k^{s/2}\, dk$ as an operator in $L^2(\mathcal{P} \times \mathcal{B})$. Part (a) of Theorem A.4 now implies the completeness of $\mathcal{H}$.

**Theorem A.9.** *The map $\mathcal{U} : (H^s(\mathbb{R}), B_L[\cdot, \cdot]) \to (\mathcal{H}, \langle \cdot, \cdot \rangle_{\mathcal{H}})$ is well-defined and unitary.*

*Proof.* Let $u \in C_c^\infty(\mathbb{R})$. Since $\widehat{(\mathcal{U}u)(\cdot, k)}_{k,l} = \widehat{u}(k+l)$, cf. (A.5) for $s = 0$, and $\widehat{u} \in \mathcal{S}(\mathbb{R})$, we conclude $(\mathcal{U}u)(\cdot, k) \in H^s_k(\mathcal{P})$ for all $k \in \mathcal{B}$. Further, for $u, v \in C_c^\infty(\mathbb{R})$,

$$B_{L_k}[(\mathcal{U}u)(\cdot, k), (\mathcal{U}v)(\cdot, k)]$$
$$= \sum_{l \in \mathbb{Z}} |k+l|^{2s} \widehat{u}(k+l)\overline{\widehat{v}(k+l)} + \sum_{m,\widetilde{m} \in \mathbb{Z}} e^{2\pi ik(m-\widetilde{m})} \int_0^{2\pi} V(x)u(x-2\pi m)\overline{v(x-2\pi\widetilde{m})}\, dx$$
$$+ \alpha \sum_{m,\widetilde{m} \in \mathbb{Z}} e^{2\pi ik(m-\widetilde{m})} u(-2\pi m)\overline{v(-2\pi\widetilde{m})}.$$

Integration over $\mathcal{B}$ yields

$$\int_{\mathcal{B}} B_{L_k}[(\mathcal{U}u)(\cdot, k), (\mathcal{U}v)(\cdot, k)]\, dk$$
$$= \sum_{l \in \mathbb{Z}} \int_{-\frac{1}{2}}^{\frac{1}{2}} |k+l|^{2s} \widehat{u}(k+l)\overline{\widehat{v}(k+l)}\, dk + \sum_{m \in \mathbb{Z}} \int_0^{2\pi} V(x)u(x-2\pi m)\overline{v(x-2\pi m)}\, dx$$
$$+ \alpha \sum_{m \in \mathbb{Z}} u(-2\pi m)\overline{v(-2\pi m)}$$
$$= \sum_{l \in \mathbb{Z}} \int_{-\frac{1}{2}+l}^{\frac{1}{2}+l} |k|^{2s} \widehat{u}(k)\overline{\widehat{v}(k)}\, dk + \sum_{m \in \mathbb{Z}} \int_{-2\pi m}^{-2\pi m + 2\pi} V(x)u(x)\overline{v(x)}\, dx + \alpha \sum_{l \in \mathbb{Z}} u(2\pi l)\overline{v(2\pi l)}$$

123

$$= \int_{\mathbb{R}} |\xi|^{2s} \widehat{u}(\xi) \overline{\widehat{v}(\xi)} \, d\xi + \int_{\mathbb{R}} V(x) u(x) \overline{v(x)} \, dx + \alpha \sum_{l \in \mathbb{Z}} u(2\pi l) \overline{v(2\pi l)} = B_L[u, v].$$

Hence, $\mathcal{U}u, \mathcal{U}v \in \mathcal{H}$ and $B_L[u, v] = \langle \mathcal{U}u, \mathcal{U}v \rangle_{\mathcal{H}}$. Now let $u \in H^s(\mathbb{R})$. We find $u_m \in C_c^\infty(\mathbb{R})$ with $u_m \to u$ in $H^s(\mathbb{R})$. Since $B_L[u_m - u_l, u_m - u_l] = \|\mathcal{U}u_m - \mathcal{U}u_l\|_{\mathcal{H}}^2$, we conclude that $(\mathcal{U}u_m)_{m \in \mathbb{N}}$ is a Cauchy sequence in $\mathcal{H}$ and thus converges to some $w \in \mathcal{H}$. In particular, $\mathcal{U}u_m \to w$ in $L^2(\mathcal{P} \times \mathcal{B})$. On the other hand, by Lemma A.5, $\mathcal{U}u_m \to \mathcal{U}u$ in $L^2(\mathcal{P} \times \mathcal{B})$. Thus, $\mathcal{U}u = w \in \mathcal{H}$ and $\mathcal{U}u_m \to \mathcal{U}u$ in $\mathcal{H}$, so that $B_L[u, v] = \langle \mathcal{U}u, \mathcal{U}v \rangle_{\mathcal{H}}$ follows for all $u, v \in H^s(\mathbb{R})$. Conversely, let $g \in \mathcal{H}$. It remains to show that $\mathcal{U}^{-1}g \in H^s(\mathbb{R})$. For $\psi \in H^s(\mathbb{R})$,

$$\left\langle (-\Delta)^{s/2} \psi, \mathcal{U}^{-1} g \right\rangle_{L^2(\mathbb{R})} = \left\langle \mathcal{U}(-\Delta)^{s/2} \psi, g \right\rangle_{L^2(\mathcal{P} \times \mathcal{B})}$$

$$= \int_{\mathcal{B}} \left\langle (\mathcal{U}(-\Delta)^{s/2} \psi)(\cdot, k), g(\cdot, k) \right\rangle_{L^2(\mathcal{P})} dk = \int_{\mathcal{B}} \left\langle (\mathcal{U}\psi)(\cdot, k), (-\Delta)_k^{s/2} (g(\cdot, k)) \right\rangle_{L^2(\mathcal{P})} dk$$

$$= \left\langle \mathcal{U}\psi, \int_{\mathcal{B}}^{\oplus} (-\Delta)_k^{s/2} \, dk \, g \right\rangle_{L^2(\mathcal{P} \times \mathcal{B})} = \left\langle \psi, \mathcal{U}^{-1} \int_{\mathcal{B}}^{\oplus} (-\Delta)_k^{s/2} \, dk \, g \right\rangle_{L^2(\mathbb{R})},$$

where we used Theorem A.6 and twice that $\mathcal{U} : L^2(\mathbb{R}) \to L^2(\mathcal{P} \times \mathcal{B})$ is unitary, cf. Lemma A.5. Using that $(-\Delta)^{s/2} : H^s(\mathbb{R}) \subset L^2(\mathbb{R}) \to L^2(\mathbb{R})$ is self-adjoint, the assertion is proved since $\mathcal{U}^{-1}g \in D\big(((-\Delta)^{s/2})^*\big) = D((-\Delta)^{s/2}) = H^s(\mathbb{R})$. $\qquad \square$

Armed with Theorem A.9, we get the following result at operator level.

**Corollary A.10.** *The relation*

$$\mathcal{U}(D(L)) = D\left( \int_{\mathcal{B}}^{\oplus} L_k \, dk \right)$$

*holds and*

$$L = \mathcal{U}^{-1} \int_{\mathcal{B}}^{\oplus} L_k \, dk \, \mathcal{U}|_{D(L)}.$$

*In particular,*

$$\sigma(L) = \sigma\left( \int_{\mathcal{B}}^{\oplus} L_k \, dk \right).$$

*Proof.* Let $f \in D(L) \subset H^s(\mathbb{R})$. Then, for $\psi \in D\big(\int_{\mathcal{B}}^{\oplus} L_k \, dk\big) \subset \mathcal{H}$,

$$\left\langle \int_{\mathcal{B}}^{\oplus} L_k \, dk \, \psi, \mathcal{U}f \right\rangle_{L^2(\mathcal{P} \times \mathcal{B})} = \int_{\mathcal{B}} \left\langle L_k \big(\psi(\cdot, k)\big), (\mathcal{U}f)(\cdot, k) \right\rangle_{L^2(\mathcal{P})} dk$$

$$= \int_{\mathcal{B}} B_{L_k}[\psi(\cdot, k), (\mathcal{U}f)(\cdot, k)] \, dk = \langle \psi, \mathcal{U}f \rangle_{\mathcal{H}} = B_L\big[\mathcal{U}^{-1}\psi, f\big]$$

$$= \left\langle \mathcal{U}^{-1}\psi, Lf \right\rangle_{L^2(\mathbb{R})} = \left\langle \psi, \mathcal{U}Lf \right\rangle_{L^2(\mathcal{P} \times \mathcal{B})}$$

by Theorem A.9 and Lemma A.5. Using part (a) of Theorem A.4, we conclude

$$\mathcal{U}f \in D\left(\int_{\mathcal{B}}^{\oplus} L_k \, dk\right) \text{ and } \int_{\mathcal{B}}^{\oplus} L_k \, dk \, \mathcal{U}f = \mathcal{U}Lf.$$

Conversely, let $g \in D\big(\int_{\mathcal{B}}^{\oplus} L_k \, dk\big) \subset \mathcal{H}$. Then, for $\psi \in D(L) \subset H^s(\mathbb{R})$,

$$\left\langle L\psi, \mathcal{U}^{-1}g \right\rangle_{L^2(\mathbb{R})} = B_L\left[\psi, \mathcal{U}^{-1}g\right] = \langle \mathcal{U}\psi, g \rangle_{\mathcal{H}} = \int_{\mathcal{B}} B_{L_k}[(\mathcal{U}\psi)(\cdot, k), g(\cdot, k)] \, dk$$

$$= \int_{\mathcal{B}} \left\langle (\mathcal{U}\psi)(\cdot, k), L_k\big(g(\cdot, k)\big) \right\rangle_{L^2(\mathcal{P})} dk = \left\langle \mathcal{U}\psi, \int_{\mathcal{B}}^{\oplus} L_k \, dk \, g \right\rangle_{L^2(\mathcal{P} \times \mathcal{B})}$$

$$= \left\langle \psi, \mathcal{U}^{-1} \int_{\mathcal{B}}^{\oplus} L_k \, dk \, g \right\rangle_{L^2(\mathbb{R})}$$

by Theorem A.9 and Lemma A.5. Using that $L$ is self-adjoint, we conclude

$$\mathcal{U}^{-1}g \in D(L) \text{ and } L\mathcal{U}^{-1}g = \mathcal{U}^{-1} \int_{\mathcal{B}}^{\oplus} L_k \, dk \, g. \qquad \square$$

As a last step towards $\sigma(L) = \bigcup_{k \in \mathcal{B}} \sigma(L_k)$ we show that

$$\sigma\left(\int_{\mathcal{B}}^{\oplus} L_k \, dk\right) = \bigcup_{k \in \mathcal{B}} \sigma(L_k).$$

A crucial step towards this is the a-priori closedness of $\bigcup_{k \in \mathcal{B}} \sigma(L_k)$. For this, for $l \in \mathbb{N}$, we set $I_l := \{\lambda_l(k) : k \in \mathcal{B}\}$. Then, by (A.10),

$$\bigcup_{k \in \mathcal{B}} \sigma(L_k) = \bigcup_{l \in \mathbb{N}} I_l. \tag{A.11}$$

**Lemma A.11.** *The set $\bigcup_{k \in \mathcal{B}} \sigma(L_k)$ is closed.*

*Proof.* Each $I_l$ is a compact interval since $\lambda_l(k)$ depends continuously on the parameter $k$, see Theorem A.20 in Section A.9. Next, we show that

$$\min I_l \xrightarrow{l \to \infty} \infty. \tag{A.12}$$

For this, we recall that $B_{L_k}[u, u] \geq \frac{1}{2}\big\|(-\Delta)_k^{s/2}u\big\|_{L^2(\mathcal{P})}^2$ since we introduced a shift. Therefore, by the min-max characterization of eigenvalues, it suffices to consider the case $\alpha = 0, V = 0$. In this case,

$$\{\lambda_l(k) : l \in \mathbb{N}\} = \big\{|k + j|^{2s} : j \in \mathbb{Z}\big\},$$

and one finds

$$\min I_l = \min_{k \in \mathcal{B}} \lambda_l(k) = \left( \frac{l-1}{2} \right)^{2s},$$

whence (A.12) follows. Finally, let $(x_m)_{m \in \mathbb{N}}$ be a sequence in $\bigcup_{l \in \mathbb{N}} I_l$ converging to some $x_0 \in \mathbb{R}$. By (A.12) and the boundedness of the sequence, we find $l_0 \in \mathbb{N}$ with $\{x_m : m \in \mathbb{N}\} \cap I_l = \emptyset$ for all $l > l_0$. Thus, there exists a number $m_0 \in \mathbb{N}$ satisfying that $x_m \in I_{m_0}$ for infinitely many $m \in \mathbb{N}$. As the corresponding subsequence converges also to $x_0$, we conclude $x_0 \in I_{m_0}$ by the closedness of $I_{m_0}$. In particular, $x_0 \in \bigcup_{l \in \mathbb{N}} I_l$.  $\square$

**Lemma A.12.** *The relation*

$$\sigma \left( \int_{\mathcal{B}}^{\oplus} L_k \, dk \right) = \bigcup_{k \in \mathcal{B}} \sigma(L_k)$$

*is true.*

*Proof.* First, let $\mu \in \bigcup_{k \in \mathcal{B}} \sigma(L_k)$, i.e. $\mu = \lambda_{l_0}(k_0)$ for some $l_0 \in \mathbb{N}$ and some $k_0 \in \mathcal{B}$. Let $\varepsilon > 0$. By the continuity of $k \mapsto \lambda_{l_0}(k)$ (see Theorem A.20), we find $\delta > 0$ such that $\lambda_{l_0}(k) \in (\mu - \varepsilon, \mu + \varepsilon)$ for all $k \in \mathcal{B} \cap (k_0 - \delta, k_0 + \delta)$. In particular,

$$\sigma(L_k) \cap (\mu - \varepsilon, \mu + \varepsilon) \supset \{\lambda_{l_0}(k)\} \neq \emptyset$$

for all $k \in \mathcal{B} \cap (k_0 - \delta, k_0 + \delta)$, whence (with $\lambda$ denoting the Lebesgue measure)

$$\lambda\big(\{k \in \mathcal{B} : \sigma(L_k) \cap (\mu - \varepsilon, \mu + \varepsilon) \neq \emptyset\}\big) \geq \lambda\big(\mathcal{B} \cap (k_0 - \delta, k_0 + \delta)\big) > 0.$$

Part (b) of Theorem A.4 now implies $\mu \in \sigma\big(\int_{\mathcal{B}}^{\oplus} L_k \, dk\big)$. Conversely, let $\mu \in \mathbb{R} \setminus \bigcup_{k \in \mathcal{B}} \sigma(L_k)$. By Lemma A.11 we find $\varepsilon_0 > 0$ satisfying that $|\nu - \mu| \geq \varepsilon_0$ for all $\nu \in \bigcup_{k \in \mathcal{B}} \sigma(L_k)$. In particular,

$$\sigma(L_k) \cap (\mu - \varepsilon_0, \mu + \varepsilon_0) = \emptyset$$

for $k \in \mathcal{B}$, whence

$$\lambda\big(\{k \in \mathcal{B} : \sigma(L_k) \cap (\mu - \varepsilon_0, \mu + \varepsilon_0) \neq \emptyset\}\big) = \lambda(\emptyset) = 0.$$

Again, part (b) of Theorem A.4 implies $\mu \in \mathbb{R} \setminus \sigma\big(\int_{\mathcal{B}}^{\oplus} L_k \, dk\big)$.  $\square$

Combining Corollary A.10 and Lemma A.12, we obtain the main result of this section.

**Theorem A.13.** *Let $s \in (1/2, 1)$, $\alpha \in \mathbb{R}$ and $V \in L^{\infty}(\mathbb{R}, \mathbb{R})$ be $2\pi$-periodic. Further, let $L = (-\Delta)^s + V(x) + \alpha \delta_{per}(x)$ and $L_k = (-\Delta)_k^s + V(x) + \alpha \delta(x)$ for $k \in \mathcal{B}$. Then,*

$$\sigma(L) = \bigcup_{k \in \mathcal{B}} \sigma(L_k).$$

Remembering (A.11), we can write the last equation also as

$$\sigma(L) = \bigcup_{l \in \mathbb{N}} I_l.$$

Thus, we proved the so-called band structure of the spectrum of $L$, i.e. $\sigma(L)$ is a countable union of compact intervals.

## A.6. Multidimensional spectral theory

As stated before, for simplicity we restricted the previous considerations to one dimension. Here, we provide a multidimensional generalization.

We start with the analysis of the operator $L = (-\Delta)^s + V(x) + \alpha\delta_{\mathrm{per}}(x_n)$. Now we assume $s \in (\mathrm{^1/_2}, 1)$, $\alpha \in \mathbb{R}$ and that $V \in L^\infty(\mathbb{R}^n, \mathbb{R})$ is $2\pi$-periodic in $x_1, ..., x_n$. First we define the corresponding sesquilinear form $B_L : H^s(\mathbb{R}^n) \times H^s(\mathbb{R}^n) \to \mathbb{C}$ by

$$B_L[u, v] := \int_{\mathbb{R}^n} |\xi|^{2s}\widehat{u}(\xi)\overline{\widehat{v}(\xi)}\, d\xi + \int_{\mathbb{R}^n} V(x)u(x)\overline{v(x)}\, dx + \alpha\sum_{l \in \mathbb{Z}} \int_{\mathbb{R}^{n-1}} u(x', 2\pi l)\overline{v(x', 2\pi l)}\, dx'.$$

By Theorem A.3 we find for any $\varepsilon > 0$, $l \in \mathbb{Z}$ and $m \in \mathbb{Z}^{n-1}$,

$$\|u(\cdot, 2\pi l)\|^2_{L^2(\mathcal{P}^{n-1}+2\pi m)} \le C\Big(\big(\varepsilon^{2s} + \varepsilon^{-2s/2s-1}\big)\|u\|^2_{L^2(\mathcal{P}^n+2\pi(l,m))} + \varepsilon^{2s}[u]^2_{H^s(\mathcal{P}^n+2\pi(l,m))}\Big) \tag{A.13}$$

for a constant $C = C(n, s) > 0$. Therefore, using (A.1) we find,

$$\sum_{l \in \mathbb{Z}} \|u(\cdot, 2\pi l)\|^2_{L^2(\mathbb{R}^{n-1})} = \sum_{l \in \mathbb{Z}} \sum_{m \in \mathbb{Z}^{n-1}} \|u(\cdot, 2\pi l)\|^2_{L^2(\mathcal{P}^{n-1}+2\pi m)}$$

$$\le C\Big(\big(\varepsilon^{2s} + \varepsilon^{-2s/2s-1}\big)\|u\|^2_{L^2(\mathbb{R}^n)} + \varepsilon^{2s}\big\|(-\Delta)^{s/2}u\big\|^2_{L^2(\mathbb{R}^n)}\Big)$$

for a new constant $C = C(n, s) > 0$. From here, we can proceed as in one dimension, in order to see that $B_L$ is semibounded and closed.

Next, we introduce the associated periodicity cell operators $L_k = (-\Delta)^s_k + V(x) + \alpha\delta(x_n)$, $k \in \mathcal{B}^n$. The corresponding sesquilinear form $B_{L_k} : H^s_k(\mathcal{P}^n) \times H^s_k(\mathcal{P}^n) \to \mathbb{C}$ is defined by

$$B_{L_k}[u, v] := \sum_{l \in \mathbb{Z}^n} |k + l|^{2s}\widehat{u}_{k,l}\overline{\widehat{v}_{k,l}} + \int_{\mathcal{P}^n} V(x)u(x)\overline{v(x)}\, dx + \alpha\int_{\mathcal{P}^{n-1}} u(x', 0)\overline{v(x', 0)}\, dx'.$$

Combining (A.13) for $l = 0, m = 0$ and (A.4), we find, for $u \in H_k^s(\mathcal{P}^n)$,

$$\|u(\cdot, 0)\|_{L^2(\mathcal{P}^{n-1})}^2 \leq C\Big( \big(\varepsilon^{2s} + \varepsilon^{-2s/2s-1}\big)\|u\|_{L^2(\mathcal{P}^n)}^2 + \varepsilon^{2s}\big\|(-\Delta)_k^{s/2}u\big\|_{L^2(\mathcal{P}^n)}^2 \Big).$$

Again, by proceeding as in one dimension, we see that $B_{L_k}$ is semibounded and closed.

Next, we present a multidimensional generalization of Theorem A.13. We omit the proof since the main ideas are completely covered by the one-dimensional case. We only note that the Floquet transformation now reads

$$\mathcal{U} : L^2(\mathbb{R}^n) \to L^2(\mathcal{P}^n \times \mathcal{B}^n), \ (\mathcal{U}f)(x, k) = \sum_{m \in \mathbb{Z}^n} f(x - 2\pi m)\mathrm{e}^{2\pi \mathrm{i}k^T m}.$$

**Theorem A.14.** *Let $s \in (1/2, 1)$, $\alpha \in \mathbb{R}$ and $V \in L^\infty(\mathbb{R}^n, \mathbb{R})$ be $2\pi$-periodic in $x_1, ..., x_n$. Further, let $L = (-\Delta)^s + V(x) + \alpha\delta_{per}(x_n)$ and $L_k = (-\Delta)_k^s + V(x) + \alpha\delta(x_n)$ for $k \in \mathcal{B}^n$. Then,*

$$\sigma(L) = \bigcup_{k \in \mathcal{B}^n} \sigma(L_k).$$

The restriction $s > 1/2$ is only due to the delta potential term. In fact, in the case $\alpha = 0$, we have the following result. Again, we omit the proof.

**Theorem A.15.** *Let $s \in (0, 1)$ and $V \in L^\infty(\mathbb{R}^n, \mathbb{R})$ be $2\pi$-periodic in $x_1, ..., x_n$. Further, let $L = (-\Delta)^s + V(x)$ and $L_k = (-\Delta)_k^s + V(x)$ for $k \in \mathcal{B}^n$. Then,*

$$\sigma(L) = \bigcup_{k \in \mathcal{B}^n} \sigma(L_k).$$

## A.7. One-dimensional examples

Floquet-Bloch theory does not answer the question whether gaps really occur in the spectrum or whether the bands actually overlap. Using examples, we show the existence of at least one spectral gap in the fractional case $s \in (1/2, 1)$. We work again in one dimension.

Note that $\overline{L_k u} = L_{-k}\overline{u}$. From this, we conclude $\lambda_l(k) = \lambda_l(-k)$. Therefore, it suffices to consider $k \in [0, 1/2]$ instead of $k \in \mathcal{B}$, i.e. $I_l = \{\lambda_l(k) : k \in [0, 1/2]\}$.

As a first example, we set $V = 0$ and $\alpha = 2\pi$, i.e. $L = (-\Delta)^s + 2\pi\delta_{per}(x)$ and $L_k = (-\Delta)_k^s + 2\pi\delta(x)$. Calculating the eigenvalues of $L_k$ results in an infinite system of equations,

$$|k + l|^{2s}\widehat{u}_{k,l} + \sqrt{2\pi}u(0) = \lambda\widehat{u}_{k,l} \text{ for } l \in \mathbb{Z}.$$

Using $u(0) = (2\pi)^{-1/2} \sum_{j \in \mathbb{Z}} \widehat{u}_{k,j}$, it suffices to consider

$$\big(\lambda - |k + l|^{2s}\big)\widehat{u}_{k,l} = \sum_{j \in \mathbb{Z}} \widehat{u}_{k,j}, \tag{A.14}$$

whence

$$\widehat{u}_{k,l} = \frac{1}{\lambda - |k+l|^{2s}} \sum_{j \in \mathbb{Z}} \widehat{u}_{k,j}$$

for $\lambda \neq |k+l|^{2s}$. From this, one finds that for $\lambda \neq |k+l|^{2s}$,

$$\lambda \in \sigma(L_k) \Leftrightarrow \sum_{l \in \mathbb{Z}} \frac{1}{\lambda - |k+l|^{2s}} = 1,$$

and that $\lambda$ is a simple eigenvalue in this case. The case in which $\lambda = |k+l|^{2s}$ for an integer $l \in \mathbb{Z}$ must be treated separately. One can check that this leads to no additional eigenvalues for $k \in (0, 1/2)$, but to the additional simple eigenvalues $|l|^{2s}$, $l \in \mathbb{N}$ in the case $k = 0$ and to the additional simple eigenvalues $|1/2 + l|^{2s}$, $l \in \mathbb{N}_0$ in the case $k = 1/2$. Indeed, if for example $k = 0$ and $\lambda = 0$, then (A.14) reduces to $-|l|^{2s}\widehat{u}_{0,l} = \sum_{j \in \mathbb{Z}} \widehat{u}_{0,j}$ for $l \in \mathbb{Z}$. For $l = 0$ this leads to $\sum_{j \in \mathbb{Z}} \widehat{u}_{0,j} = 0$, which then for $l \neq 0$ implies $\widehat{u}_{0,l} = 0$. But from $\sum_{j \in \mathbb{Z}} \widehat{u}_{0,j} = 0$, we then also find $\widehat{u}_{0,0} = 0$, i.e. $\lambda = 0$ is no eigenvalue for $k = 0$. If in contrast $\lambda = 1$, then we find again $\sum_{j \in \mathbb{Z}} \widehat{u}_{0,j} = 0$ (this time for $l = \pm 1$), but only that $\widehat{u}_{0,l} = 0$ for $l \neq \pm 1$. Hence, $\widehat{u}_{0,-1} + \widehat{u}_{0,1} = 0$, i.e. $\lambda = 1$ is a simple eigenvalue for $k = 0$.

We can interpret

$$D(k,\lambda) := 1 + \sum_{l \in \mathbb{Z}} \frac{1}{|k+l|^{2s} - \lambda}$$

as some kind of infinite determinant. For more information on infinite determinants appearing in such a context (in the non-fractional case), we refer the reader to [40, Section 2.3]. We also note that

$$\sum_{l \in \mathbb{Z}} \frac{1}{|k+l|^2 - \lambda} = \frac{\pi}{2\sqrt{\lambda}} \left( \cot(\pi(k - \sqrt{\lambda})) - \cot(\pi(k + \sqrt{\lambda})) \right), \qquad \text{(A.15)}$$

i.e. in the non-fractional case $s = 1$ it is possible to replace the infinite series by a trigonometric term, cf. [40, Section 2.3]. Figure 25 shows a plot of $D(1/4, \cdot)$ in the non-fractional case $s = 1$. The spectrum $\sigma(L_{1/4})$ consists exactly of the zeros of $D(1/4, \cdot)$. Note that $D(k, \cdot)$ has the poles

$$k^{2s} < (1-k)^{2s} < (1+k)^{2s} < (2-k)^{2s} < (2+k)^{2s} < ...$$

for $k \in (0, 1/2)$. For $k \in \{0, 1/2\}$ some of the mentioned poles coincide.

Next, we show that there is a spectral gap between $I_1$ and $I_2$, i.e. $\max I_1 < \min I_2$. First, we observe that $D(k, \lambda) \to 1$ as $\lambda \to -\infty$ and that $D(k, \cdot)$ is strictly increasing in every branch cut. Thus, there is exactly one zero between two adjacent poles. Note that $\sigma(L_k)$ consists exactly of these zeros for $k \in (0, 1/2)$. In contrast, for $k = 1/2$, the spectrum $\sigma(L_{1/2})$ also contains all the poles themselves. The same holds for $k = 0$ except for the pole at $\lambda = 0$. Therefore, $4^{-s} \leq (1-k)^{2s} < \lambda_2(k) < (1+k)^{2s}$ for $k \in (0, 1/2]$. Combining this with $\lambda_2(0) = 1 > 4^{-s}$, this results in $\min I_2 > 4^{-s}$. Hence, the assertion
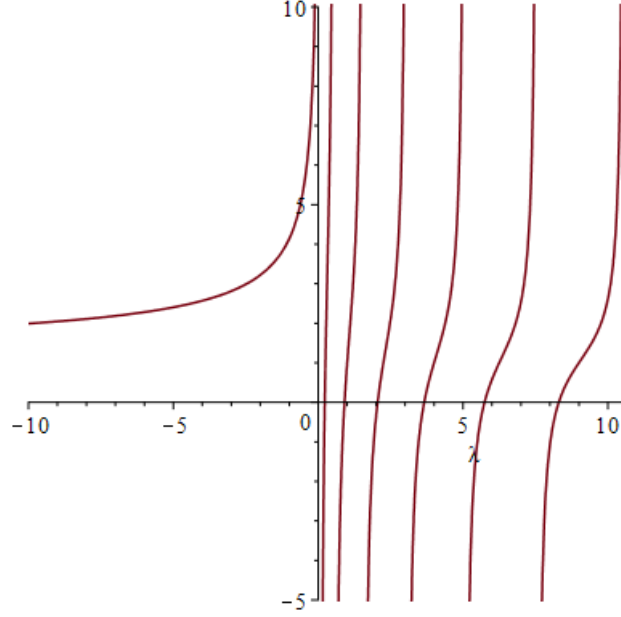
Figure 25. Plot of $D(\sfrac{1}{4}, \cdot)$ for $s = 1$.

is proven once we show that $\max I_1 = 4^{-s}$. Clearly, $\lambda_1(\sfrac{1}{2}) = 4^{-s}$, whence it remains to show that $\lambda_1(k) \le 4^{-s}$ for $k \in [0, \sfrac{1}{2})$. By the monotonicity of $D(k, \cdot)$, the latter is the case if $D(k, 4^{-s}) \ge 0$ for $k \in [0, \sfrac{1}{2})$. In the non-fractional case $s = 1$, we have $D(k, 4^{-1}) = 1$, which follows using (A.15). However, in the fractional case $s \in (\sfrac{1}{2}, 1)$ the situation is slightly more complicated. The main idea is to use a comparison with the case $s = 1$. For $k \in [0, \sfrac{1}{2})$ and $s \in (\sfrac{1}{2}, 1)$,

$$
D(k, 4^{-s}) = 1 + \sum_{l \in \mathbb{Z}} \frac{1}{|k + l|^{2s} - 4^{-s}}
$$

$$
= 1 + \frac{1}{k^{2s} - 4^{-s}} + \frac{1}{(1 - k)^{2s} - 4^{-s}} + \sum_{l \in \mathbb{Z} \setminus \{-1, 0\}} \frac{1}{|k + l|^{2s} - 4^{-s}}
$$

$$
> 1 + \frac{1}{k^{2s} - 4^{-s}} + \frac{1}{(1 - k)^{2s} - 4^{-s}} + \sum_{l \in \mathbb{Z} \setminus \{-1, 0\}} \frac{1}{|k + l|^2 - 4^{-1}}
$$

$$
= 1 + \frac{1}{k^{2s} - 4^{-s}} + \frac{1}{(1 - k)^{2s} - 4^{-s}} - \frac{1}{k^2 - 4^{-1}} - \frac{1}{(1 - k)^2 - 4^{-1}}.
$$

Further,

$$
1 + \frac{1}{k^{2s} - 4^{-s}} + \frac{1}{(1 - k)^{2s} - 4^{-s}} - \frac{1}{k^2 - 4^{-1}} - \frac{1}{(1 - k)^2 - 4^{-1}} \ge 0
$$

$$
\Leftrightarrow \quad (k^{2s} - 4^{-s})((1 - k)^{2s} - 4^{-s})(k^2 - 4^{-1})((1 - k)^2 - 4^{-1})
$$
$$
+ ((1 - k)^{2s} - 4^{-s})(k^2 - 4^{-1})((1 - k)^2 - 4^{-1})
$$

130

$$+ (k^{2s} - 4^{-s})(k^2 - 4^{-1})((1 - k)^2 - 4^{-1})$$
$$- (k^{2s} - 4^{-s})((1 - k)^{2s} - 4^{-s})((1 - k)^2 - 4^{-1})$$
$$- (k^{2s} - 4^{-s})((1 - k)^{2s} - 4^{-s})(k^2 - 4^{-1}) \geq 0.$$

For $k \in [0, {}^1\!/_4]$ and $s \in ({}^1\!/_2, 1)$, we rewrite the left side of the last inequality as

$$\underbrace{((1 - k)^{2s} - 4^{-s})((1 - k)^2 - 4^{-1})}_{\geq 0}(k^2 - 4^{-1} - k^{2s} + 4^{-s})$$
$$+ \underbrace{(k^{2s} - 4^{-s})(k^2 - 4^{-1})}_{\geq 0}\Big[\underbrace{((1 - k)^{2s} - 4^{-s})((1 - k)^2 - 4^{-1})}_{\geq 0}$$
$$+ (1 - k)^2 - 4^{-1} - (1 - k)^{2s} + 4^{-s}\Big].$$

By checking monotonicity in $k$ one can find that the remaining terms, i.e. $k^2 - 4^{-1} - k^{2s} + 4^{-s}$ and $(1 - k)^2 - 4^{-1} - (1 - k)^{2s} + 4^{-s}$, are also nonnegative for $k \in [0, {}^1\!/_4]$ and $s \in ({}^1\!/_2, 1)$. On the other hand, for $k \in [{}^1\!/_4, {}^1\!/_2)$ and $s \in ({}^1\!/_2, 1)$, we use the representation

$$\underbrace{\left[3(k^{2s} - 4^{-s})((1 - k)^{2s} - 4^{-s}) + (1 - k)^{2s} + k^{2s} - 2 \cdot 4^{-s}\right]}_{=:h(k,s)}\underbrace{(k - 2^{-1})^2(k + 2^{-1})\left(k - \frac{3}{2}\right)}_{\leq 0}$$
$$+ \underbrace{2(4^{-s} - k^{2s})((1 - k)^{2s} - 4^{-s})(k - 2^{-1})^4}_{\geq 0},$$

whence it suffices to show that $h(k, s) \leq 0$. We have

$$\frac{1}{2s}\frac{\partial h}{\partial k}(k, s) = 3k^{2s-1}(1 - k)^{2s-1}(1 - 2k) + (3 \cdot 4^{-s} - 1)((1 - k)^{2s-1} - k^{2s-1})$$
$$\geq 3k^{2s-1}(1 - k)^{2s-1}(1 - 2k) - 4^{-1}((1 - k)^{2s-1} - k^{2s-1})$$
$$= 3k^{2s-1}(1 - k)^{2s-1}(1 - 2k) - 4^{-1}\int_k^{1-k}(2s - 1)x^{2s-2}\,dx$$
$$\geq 3k^{2s-1}(1 - k)^{2s-1}(1 - 2k) - 4^{-1}(2s - 1)k^{2s-2}(1 - 2k)$$
$$= \underbrace{k^{2s-2}(1 - 2k)}_{\geq 0}(3k(1 - k)^{2s-1} - 4^{-1}(2s - 1))$$

and by checking monotonicity in $k$ one can show that

$$3k(1 - k)^{2s-1} - 4^{-1}(2s - 1) \geq 0$$

for $k \in [{}^1\!/_4, {}^1\!/_2)$ and $s \in ({}^1\!/_2, 1)$. The assertion finally follows since $h(2^{-1}, s) = 0$.

As a second example, we set $V = 0$ and $\alpha = -2\pi$, i.e. $L = (-\Delta)^s - 2\pi\delta_{\mathrm{per}}(x)$ and $L_k = (-\Delta)_k^s - 2\pi\delta(x)$. Now, we set

$$\widetilde{D}(k, \lambda) := 1 - \sum_{l \in \mathbb{Z}} \frac{1}{|k + l|^{2s} - \lambda}$$

and observe that, for $\lambda \neq |k + l|^{2s}$,

$$\lambda \in \sigma(L_k) \Leftrightarrow \widetilde{D}(k, \lambda) = 0$$

and that $\lambda$ is a simple eigenvalue in this case. Again, the case in which $\lambda = |k + l|^{2s}$ for an integer $l \in \mathbb{Z}$ must be treated separately and leads to no additional eigenvalues for $k \in (0, 1/2)$, but to the additional simple eigenvalues $|l|^{2s}$, $l \in \mathbb{N}$ in the case $k = 0$ and to the additional simple eigenvalues $|1/2 + l|^{2s}$, $l \in \mathbb{N}_0$ in the case $k = 1/2$. Figure 26 shows a plot of $\widetilde{D}(1/4, \cdot)$ in the non-fractional case $s = 1$.
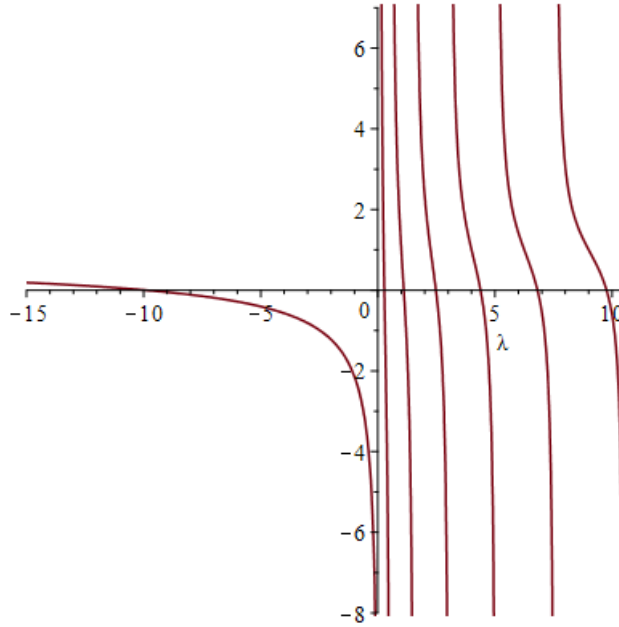


Figure 26. Plot of $\widetilde{D}(1/4, \cdot)$ for $s = 1$.

Again, we show that there is a spectral gap between $I_1$ and $I_2$. First, we observe that $\widetilde{D}(k, \lambda) \to 1$ as $\lambda \to -\infty$ and that $\widetilde{D}(k, \cdot)$ is strictly decreasing in every branch cut. Therefore, $0 \leq k^{2s} < \lambda_2(k) < (1 - k)^{2s}$ for $k \in [0, 1/2)$. Combining this with $\lambda_2(1/2) = 4^{-s} > 0$, this results in $\min I_2 > 0$. Hence, the assertion is proven once we show that $\max I_1 < 0$. Clearly, $\lambda_1(0) < 0$, whence it remains to show that $\lambda_1(k) < 0$ for $k \in (0, 1/2]$. By the monotonicity of $\widetilde{D}(k, \cdot)$, the latter is the case if $\widetilde{D}(k, 0) < 0$ for

$k \in (0, \nicefrac{1}{2}]$. In fact, for $k \in (0, \nicefrac{1}{2}]$ and $s \in (\nicefrac{1}{2}, 1)$,

$$\widetilde{D}(k,0) = 1 - \sum_{l \in \mathbb{Z}} \frac{1}{|k+l|^{2s}} < 1 - \frac{1}{k^{2s}} \le 1 - 4^s < -1,$$

whence the assertion follows.

## A.8. Proofs of Theorem A.1 and Theorem A.3

This section contains the proofs of Theorem A.1 and Theorem A.3.

*Proof of Theorem A.1.* By the Gagliardo-Nirenberg inequality (see [44]), for $w \in H^s(\mathbb{R})$,

$$\|w\|_{L^\infty(\mathbb{R})} \le M \|w\|_{L^2(\mathbb{R})}^{1-\frac{1}{2s}} \|(-\Delta)^{s/2} w\|_{L^2(\mathbb{R})}^{\frac{1}{2s}}$$

with a constant $M = M(s) > 0$. Using Young's inequality, we conclude

$$|w(0)|^2 \le M^2 \Big( \varepsilon^{-2s/2s-1} \|w\|_{L^2(\mathbb{R})}^2 + \varepsilon^{2s} \|(-\Delta)^{s/2} w\|_{L^2(\mathbb{R})}^2 \Big).$$

Now let $u \in C_c^\infty(\mathbb{R}^n)$. Then,

$$\begin{aligned}
\|u(\cdot,0)\|_{L^2(\mathbb{R}^{n-1})}^2 &= \int_{\mathbb{R}^{n-1}} |u(x',0)|^2 \, dx' \\
&\le M^2 \int_{\mathbb{R}^{n-1}} \Big( \varepsilon^{-2s/2s-1} \|u(x',\cdot)\|_{L^2(\mathbb{R})}^2 + \varepsilon^{2s} \big\|(-\Delta)^{s/2}[u(x',\cdot)]\big\|_{L^2(\mathbb{R})}^2 \Big) \, dx' \\
&\overset{(*)}{=} M^2 \Big( \varepsilon^{-2s/2s-1} \|u\|_{L^2(\mathbb{R}^n)}^2 + \varepsilon^{2s} \big\||\xi_n|^s \widehat{u}(\xi)\big\|_{L^2(\mathbb{R}^n)}^2 \Big) \\
&\le M^2 \Big( \varepsilon^{-2s/2s-1} \|u\|_{L^2(\mathbb{R}^n)}^2 + \varepsilon^{2s} \big\||\xi|^s \widehat{u}(\xi)\big\|_{L^2(\mathbb{R}^n)}^2 \Big) \\
&\le D \Big( \varepsilon^{-2s/2s-1} \|u\|_{L^2(\mathbb{R}^n)}^2 + \varepsilon^{2s} [u]_{H^s(\mathbb{R}^n)}^2 \Big)
\end{aligned}$$

for a constant $D = D(n,s) > 0$, whence the general assertion follows by an approximation argument. Note that the equality $(*)$ is not obvious and needs an explanation, which follows now. For this, we first notice that

$$\mathcal{F}[u(x',\cdot)](\xi_n) = \mathcal{F}^{-1}[\widehat{u}(\cdot,\xi_n)](x')$$

for $x' \in \mathbb{R}^{n-1}$ and $\xi_n \in \mathbb{R}$ by the $(n-1)$-dimensional Fourier inversion formula. In fact,

$$\begin{aligned}
\mathcal{F}^{-1}[\widehat{u}(\cdot,\xi_n)](x') &= \frac{1}{(2\pi)^{\frac{n-1}{2}}} \int_{\mathbb{R}^{n-1}} \widehat{u}(\xi',\xi_n) e^{i\xi'^{\mathrm{T}} x'} \, d\xi' \\
&= \frac{1}{(2\pi)^{\frac{n-1}{2}}} \int_{\mathbb{R}^{n-1}} \frac{1}{(2\pi)^{\frac{n}{2}}} \int_{\mathbb{R}^n} u(y',y_n) e^{-i(y',y_n)^{\mathrm{T}}(\xi',\xi_n)} \, d(y',y_n) \, e^{i\xi'^{\mathrm{T}} x'} \, d\xi'
\end{aligned}$$

$$= \frac{1}{(2\pi)^{\frac{1}{2}}} \int_{\mathbb{R}} \underbrace{\frac{1}{(2\pi)^{n-1}} \int_{\mathbb{R}^{n-1}} \int_{\mathbb{R}^{n-1}} u(y', y_n) \mathrm{e}^{-\mathrm{i}y'^{\mathrm{T}}\xi'} \mathrm{e}^{\mathrm{i}\xi'^{\mathrm{T}}x'} \, dy' \, d\xi'}_{=u(x',y_n)} \, \mathrm{e}^{-\mathrm{i}y_n\xi_n} \, dy_n$$

$$= \mathcal{F}[u(x', \cdot)](\xi_n).$$

Using the Plancherel identity this finally results in

$$\int_{\mathbb{R}^{n-1}} \left\| (-\Delta)^{s/2}[u(x', \cdot)] \right\|_{L^2(\mathbb{R})}^2 \, dx' = \int_{\mathbb{R}^{n-1}} \left\| |\xi_n|^s \mathcal{F}[u(x', \cdot)](\xi_n) \right\|_{L^2(\mathbb{R})}^2 \, dx'$$

$$= \int_{\mathbb{R}^{n-1}} \left\| |\xi_n|^s \mathcal{F}^{-1}[\widehat{u}(\cdot, \xi_n)](x') \right\|_{L^2(\mathbb{R})}^2 \, dx'$$

$$= \int_{\mathbb{R}} \left\| |\xi_n|^s \mathcal{F}^{-1}[\widehat{u}(\cdot, \xi_n)](x') \right\|_{L^2(\mathbb{R}^{n-1})}^2 \, d\xi_n$$

$$= \int_{\mathbb{R}} \left\| |\xi_n|^s \widehat{u}(\xi', \xi_n) \right\|_{L^2(\mathbb{R}^{n-1})}^2 \, d\xi_n$$

$$= \left\| |\xi_n|^s \widehat{u}(\xi) \right\|_{L^2(\mathbb{R}^n)}^2. \qquad \square$$

*Proof of Theorem A.3.* From [13, Theorem 5.4] it follows that $\mathcal{P}^n$ is an extension domain for $H^s$, i.e. there is a constant $M = M(n,s) > 0$ such that for every function $u \in H^s(\mathcal{P}^n)$ there exists $\widetilde{u} \in H^s(\mathbb{R}^n)$ with $\widetilde{u}|_{\mathcal{P}^n} = u$ and $\|\|\widetilde{u}\|\|_{H^s(\mathbb{R}^n)} \leq M \|\|u\|\|_{H^s(\mathcal{P}^n)}$. Here, we need to know that the last inequality in fact decomposes in $[\widetilde{u}]_{H^s(\mathbb{R}^n)} \leq L \|\|u\|\|_{H^s(\mathcal{P}^n)}$ and $\|\widetilde{u}\|_{L^2(\mathbb{R}^n)} \leq L \|u\|_{L^2(\mathcal{P}^n)}$ for a constant $L = L(n,s) > 0$. This follows easily by studying the proofs of [13, Section 5]. Using Theorem A.1 we conclude

$$\|u(\cdot, 0)\|_{L^2(\mathcal{P}^{n-1})}^2 \leq \|\widetilde{u}(\cdot, 0)\|_{L^2(\mathbb{R}^{n-1})}^2 \leq D\Big( \varepsilon^{-2s/2s-1} \|\widetilde{u}\|_{L^2(\mathbb{R}^n)}^2 + \varepsilon^{2s} [\widetilde{u}]_{H^s(\mathbb{R}^n)}^2 \Big)$$

$$\leq DL^2 \Big( \varepsilon^{-2s/2s-1} \|u\|_{L^2(\mathcal{P}^n)}^2 + \varepsilon^{2s} \|\|u\|\|_{H^s(\mathcal{P}^n)}^2 \Big)$$

$$= C\Big( (\varepsilon^{2s} + \varepsilon^{-2s/2s-1}) \|u\|_{L^2(\mathcal{P}^n)}^2 + \varepsilon^{2s} [u]_{H^s(\mathcal{P}^n)}^2 \Big)$$

for a constant $C = C(n,s) > 0$. $\qquad \square$

## A.9. Continuity of eigenvalue functions

We follow [35, Chapter 4] to prove that the eigenvalues $\lambda_l(k)$ of the periodicity cell operators $L_k$ depend continuously on the parameter $k$. For this we first introduce the concept of generalized convergence for closed operators, which generalizes the norm convergence of bounded operators.

**Definition A.16.**

(a) For Banach spaces $X, Y$ the set of all bounded operators $A : X \to Y$ will be denoted by $L(X, Y)$ and the set of all closed operators $T : D(T) \subset X \to Y$ by $\mathscr{C}(X, Y)$. In particular, $\mathscr{C}(X) := \mathscr{C}(X, X)$.

(b) For any two closed subspaces $M, N$ of a Banach space $Z$ we set

$$\delta(M, N) := \begin{cases} 0 & , \ M = \{0\} \\ \displaystyle\sup_{u \in M, \|u\|_Z = 1} \text{dist}(u, N) & , \ M \neq \{0\} \end{cases}$$

and

$$\widehat{\delta}(M, N) := \max\{\delta(M, N), \delta(N, M)\}.$$

(c) If $T, S \in \mathscr{C}(X, Y)$, their graphs $G(T), G(S)$ are closed subspaces of $X \times Y$ and we define

$$\delta(T, S) := \delta(G(T), G(S))$$

as well as

$$\widehat{\delta}(T, S) := \widehat{\delta}(G(T), G(S)) = \max\{\delta(T, S), \delta(S, T)\}.$$

(d) We say that $T_n \in \mathscr{C}(X, Y)$ converges to $T \in \mathscr{C}(X, Y)$ in the generalized sense if $\widehat{\delta}(T_n, T) \to 0$.

We have the following lemma, see Theorems 2.23 and 3.1 in [35, Chapter 4].

**Lemma A.17.**

(a) *If $T_n \in \mathscr{C}(X, Y)$ converges to $T \in \mathscr{C}(X, Y)$ in the generalized sense and if $A \in L(X, Y)$, then $T_n + A \to T + A$ in the generalized sense.*

(b) *Let $T \in \mathscr{C}(X)$ and let $\Gamma$ be a compact subset of the resolvent set $\rho(T)$. Then there is an $\varepsilon > 0$ such that $\Gamma \subset \rho(S)$ for any $S \in \mathscr{C}(X)$ with $\widehat{\delta}(S, T) < \varepsilon$. In particular, $\Gamma \subset \rho(T_n)$ for sufficiently large $n \in \mathbb{N}$ if $T_n \to T$ in the generalized sense.*

Next, we show the continuity of the map $\mathcal{B} \to \mathscr{C}(L^2(\mathcal{P}))$, $k \mapsto L_k$.

**Lemma A.18.** *Let $k_n \in \mathcal{B}$ converge to $k \in \mathcal{B}$. Then, $L_{k_n} \to L_k$ in the generalized sense.*

*Proof.* By part (a) of Lemma A.17 it suffices to show that $T_n := (-\Delta)^s_{k_n} + \alpha\delta(x)$ converges to $T := (-\Delta)^s_k + \alpha\delta(x)$ in the generalized sense. For this, we first show that $\delta(T, T_n) \to 0$. Let $u = (f, Tf) \in G(T)$ with

$$\|u\|^2_{L^2(\mathcal{P}) \times L^2(\mathcal{P})} = \|f\|^2_{L^2(\mathcal{P})} + \|Tf\|^2_{L^2(\mathcal{P})} = 1.$$

Then, it is easy to see that $\left(e^{i(k_n - k)(\cdot)}f, T_n e^{i(k_n - k)(\cdot)}f\right) \in G(T_n)$, whence

$$|\text{dist}(u, G(T_n))|^2 \leq \|f - e^{i(k_n - k)(\cdot)}f\|^2_{L^2(\mathcal{P})} + \|Tf - T_n e^{i(k_n - k)(\cdot)}f\|^2_{L^2(\mathcal{P})}.$$

Further,

$$\|f - e^{i(k_n - k)(\cdot)}f\|^2_{L^2(\mathcal{P})} \leq \sup_{x \in (0, 2\pi)} |1 - e^{i(k_n - k)x}|^2 \|f\|^2_{L^2(\mathcal{P})} \leq 4\pi^2 |k_n - k|^2 \xrightarrow{n \to \infty} 0.$$

On the other hand,

$$\|Tf - T_n e^{i(k_n-k)(\cdot)}f\|_{L^2(\mathcal{P})}^2 = \|Tf - e^{i(k_n-k)(\cdot)}Tf + e^{i(k_n-k)(\cdot)}Tf - T_n e^{i(k_n-k)(\cdot)}f\|_{L^2(\mathcal{P})}^2$$
$$\le 2\|Tf - e^{i(k_n-k)(\cdot)}Tf\|_{L^2(\mathcal{P})}^2 + 2\|e^{i(k_n-k)(\cdot)}Tf - T_n e^{i(k_n-k)(\cdot)}f\|_{L^2(\mathcal{P})}^2.$$

For the first part, we have

$$\|Tf - e^{i(k_n-k)(\cdot)}Tf\|_{L^2(\mathcal{P})}^2 \le \sup_{x\in(0,2\pi)}|1 - e^{i(k_n-k)x}|^2\|Tf\|_{L^2(\mathcal{P})}^2 \le 4\pi^2|k_n - k|^2 \xrightarrow{n\to\infty} 0.$$

By taking into account

$$e^{i(k_n-k)(\cdot)}Tf = \frac{1}{\sqrt{2\pi}}\sum_{l\in\mathbb{Z}}\left(|k+l|^{2s}\widehat{f}_{k,l} + \frac{\alpha}{\sqrt{2\pi}}f(0)\right)e^{i(k_n+l)(\cdot)}$$

and

$$T_n e^{i(k_n-k)(\cdot)}f = \frac{1}{\sqrt{2\pi}}\sum_{l\in\mathbb{Z}}\left(|k_n+l|^{2s}\widehat{f}_{k,l} + \frac{\alpha}{\sqrt{2\pi}}f(0)\right)e^{i(k_n+l)(\cdot)}$$

we conclude for the second part,

$$\|e^{i(k_n-k)(\cdot)}Tf - T_n e^{i(k_n-k)(\cdot)}f\|_{L^2(\mathcal{P})}^2 = \sum_{l\in\mathbb{Z}}\left||k_n+l|^{2s} - |k+l|^{2s}\right|^2|\widehat{f}_{k,l}|^2.$$

Using the mean value theorem, we find

$$\left||k_n+l|^{2s} - |k+l|^{2s}\right|^2 \le 4s^2(1+|k+l|)^{4s-2}|k_n-k|^2 \le 4s^2(1+|k+l|)^{2s}|k_n-k|^2.$$

Hence,

$$\|e^{i(k_n-k)(\cdot)}Tf - T_n e^{i(k_n-k)(\cdot)}f\|_{L^2(\mathcal{P})}^2 \le 4s^2|k_n-k|^2\sum_{l\in\mathbb{Z}}(1+|k+l|)^{2s}|\widehat{f}_{k,l}|^2$$

$$\le 8s^2|k_n-k|^2\left(\|(-\Delta)_k^{s/2}f\|_{L^2(\mathcal{P})}^2 + \|f\|_{L^2(\mathcal{P})}^2\right)$$

$$\le 8s^2|k_n-k|^2\left(2\langle Tf,f\rangle_{L^2(\mathcal{P})} + (2C_2+1)\|f\|_{L^2(\mathcal{P})}^2\right)$$

$$\le 8s^2|k_n-k|^2\left(2\|Tf\|_{L^2(\mathcal{P})}\|f\|_{L^2(\mathcal{P})} + (2C_2+1)\|f\|_{L^2(\mathcal{P})}^2\right)$$

$$\le 8s^2\max\{2C_2+3,2\}|k_n-k|^2 \xrightarrow{n\to\infty} 0$$

with the constant $C_2 = C_2(\alpha,s)$ from (A.9). Thus, $\delta(T,T_n) \to 0$. By a similar calculation, $\delta(T_n,T) \to 0$, whence $\widehat{\delta}(T_n,T) \to 0$. $\square$

Before we can prove the continuity of the eigenvalue functions, we need a final lemma (see § 3.5 and Theorem 3.16 in [35, Chapter 4]). For an operator $T \in \mathscr{C}(X)$ we denote by $\sigma_d(T)$ its discrete spectrum (consisting of all isolated eigenvalues in $\sigma(T)$ with finite algebraic multiplicity).

**Lemma A.19.** *Let $T_n \in \mathscr{C}(X)$ converge to $T \in \mathscr{C}(X)$ in the generalized sense. Further, let $\lambda_0 \in \sigma_d(T)$ with algebraic multiplicity $m_a(\lambda_0, T) \in \mathbb{N}$ and $\varepsilon > 0$ such that*

$$\sigma(T) \cap \overline{B_\varepsilon(\lambda_0)} = \{\lambda_0\}.$$

*Then, for sufficiently large $n \in \mathbb{N}$,*

$$\sigma(T_n) \cap B_\varepsilon(\lambda_0) \subset \sigma_d(T_n)$$

*and*

$$\sum_{\lambda \in \sigma(T_n) \cap B_\varepsilon(\lambda_0)} m_a(\lambda, T_n) = m_a(\lambda_0, T).$$

**Theorem A.20.** *Let $l_0 \in \mathbb{N}$ and $k_n \in \mathcal{B}$ converge to $k_0 \in \mathcal{B}$. Then, $\lambda_{l_0}(k_n) \to \lambda_{l_0}(k_0)$.*

*Proof.* First of all, we have $\lambda_l(k) \geq 1/2$ since we introduced a shift. For $k \in \mathcal{B}$ we denote by $(\mu_l(k))_{l \in \mathbb{N}}$ the strictly increasing sequence of eigenvalues from $L_k$ which counts each eigenvalue exactly once and we choose $l' \leq l_0$ with $\mu_{l'}(k_0) = \lambda_{l_0}(k_0)$. Moreover, we choose $\varepsilon_1, ..., \varepsilon_{l'} > 0$ such that the intervals $J_j := (\mu_j(k_0) - \varepsilon_j, \mu_j(k_0) + \varepsilon_j)$ are disjoint and such that $\mu_{l'}(k_0) + \varepsilon_{l'} < d := 2^{-1}(\mu_{l'}(k_0) + \mu_{l'+1}(k_0))$ as well as $\mu_1(k_0) - \varepsilon_1 > 0$. Now let $\varepsilon \in (0, \varepsilon_{l'}]$ be arbitrary. The set

$$\Gamma := [0, d] \setminus \left( (\mu_{l'}(k_0) - \varepsilon, \mu_{l'}(k_0) + \varepsilon) \cup \bigcup_{j=1}^{l'-1} J_j \right)$$

is a compact subset of $\rho(L_{k_0})$, thus a subset of $\rho(L_{k_n})$ for $n \geq N = N(\varepsilon)$ by part (b) of Lemma A.17 and Lemma A.18. Next, we use Lemma A.19. For $j = 1, ..., l' - 1$ we find $n_j \in \mathbb{N}$ such that, for $n \geq n_j$, $\sigma(L_{k_n}) \cap J_j$ consists of eigenvalues from $L_{k_n}$ whose multiplicities add up to that of $\mu_j(k_0)$. Further, we choose $n_{l'} = n_{l'}(\varepsilon) \in \mathbb{N}$ such that, for $n \geq n_{l'}$, $\sigma(L_{k_n}) \cap (\mu_{l'}(k_0) - \varepsilon, \mu_{l'}(k_0) + \varepsilon)$ consists of eigenvalues from $L_{k_n}$ whose multiplicities add up to those of $\mu_{l'}(k_0)$. Finally, let $n \geq n_0 := \max\{N, n_1, ..., n_{l'}\}$. The operator $L_{k_n}$ has no negative eigenvalue since $\lambda_l(k) \geq 1/2$. Further, since $n \geq N$, there are no eigenvalues of $L_{k_n}$ in $\Gamma$. In what follows we write $m_l := m_a(\mu_l(k_0), L_{k_0})$. Since $n \geq n_1$, the interval $J_1$ contains exactly the eigenvalues $\lambda_1(k_n), ..., \lambda_{m_1}(k_n)$. Similarly, since $n \geq n_j$, the interval $J_j$ contains exactly the eigenvalues $\lambda_{m_1+...+m_{j-1}+1}(k_n), ..., \lambda_{m_1+...+m_{j-1}+m_j}(k_n)$ for $j = 2, ..., l' - 1$. Finally, since $n \geq n_{l'}$, the interval $(\mu_{l'}(k_0) - \varepsilon, \mu_{l'}(k_0) + \varepsilon)$ contains exactly the eigenvalues $\lambda_{m_1+...+m_{l'-1}+1}(k_n), ..., \lambda_{m_1+...+m_{l'-1}+m_{l'}}(k_n)$. In particular, this includes $\lambda_{l_0}(k_n)$ so that $|\lambda_{l_0}(k_n) - \lambda_{l_0}(k_0)| = |\lambda_{l_0}(k_n) - \mu_{l'}(k_0)| < \varepsilon$. $\square$

# References

[1] Eugene L. Allgower and Kurt Georg. *Numerical continuation methods*, volume 13 of *Springer Series in Computational Mathematics*. Springer-Verlag, Berlin, 1990. An introduction. `doi:10.1007/978-3-642-61257-2`.

[2] Catherine Bandle and Wolfgang Reichel. Solutions of quasilinear second-order elliptic boundary value problems via degree theory. In *Stationary partial differential equations. Vol. I*, Handb. Differ. Equ., pages 1–70. North-Holland, Amsterdam, 2004. `doi:10.1016/S1874-5733(04)80003-2`.

[3] B. M. Brown, V. Hoang, M. Plum, and I. G. Wood. Floquet-bloch theory for elliptic problems with discontinuous coefficients. In Jan Janas, Pavel Kurasov, Ari Laptev, Sergei Naboko, and Günter Stolz, editors, *Spectral Theory and Analysis*, pages 1–20, Basel, 2011. Springer Basel.

[4] Claudia Bucur. Some observations on the Green function for the ball in the fractional Laplace framework. *Communications on Pure and Applied Analysis*, 15:657–699, 2016.

[5] T. A. (Theodore Allen) Burton. *Volterra integral and differential equations*. Mathematics in science and engineering, v. 202. Elsevier, Amsterdam, 2nd ed. edition, 2005.

[6] Yanne K. Chembo and Curtis R. Menyuk. Spatiotemporal Lugiato-Lefever formalism for Kerr-comb generation in whispering-gallery-mode resonators. *Phys. Rev. A*, 87:053852, May 2013. URL: `https://link.aps.org/doi/10.1103/PhysRevA.87.053852`, `doi:10.1103/PhysRevA.87.053852`.

[7] Yanne K. Chembo, Dmitry V. Strekalov, and Nan Yu. Spectrum and dynamics of optical frequency combs generated with monolithic whispering gallery mode resonators. *Phys. Rev. Lett.*, 104:103902, Mar 2010. URL: `https://link.aps.org/doi/10.1103/PhysRevLett.104.103902`, `doi:10.1103/PhysRevLett.104.103902`.

[8] Yanne K. Chembo and Nan Yu. Modal expansion approach to optical-frequency-comb generation with monolithic whispering-gallery-mode resonators. *Phys. Rev. A*, 82:033801, Sep 2010. URL: `https://link.aps.org/doi/10.1103/PhysRevA.82.033801`, `doi:10.1103/PhysRevA.82.033801`.

[9] Michael G. Crandall and Paul H. Rabinowitz. Bifurcation from simple eigenvalues. *J. Functional Analysis*, 8:321–340, 1971.

[10] Klaus Deimling. *Nonlinear functional analysis*. Springer-Verlag, Berlin, 1985. `doi:10.1007/978-3-662-00547-7`.

# References

[11] Lucie Delcey and Mariana Haragus. Periodic waves of the Lugiato-Lefever equation at the onset of Turing instability. *Philos. Trans. of the Roy. Soc. A*, 376(2117):20170188, 2018. doi:10.1098/rsta.2017.0188.

[12] P. Del'Haye, A. Schliesser, O. Arcizet, T. Wilken, R. Holzwarth, and T. J. Kippenberg. Optical frequency comb generation from a monolithic microresonator. *Nature*, 450(7173):1214–1217, dec 2007. URL: https://doi.org/10.1038%2Fnature06401, doi:10.1038/nature06401.

[13] Eleonora Di Nezza, Giampiero Palatucci, and Enrico Valdinoci. Hitchhiker's guide to the fractional sobolev spaces. *Bulletin des Sciences Mathématiques*, 136(5):521–573, 2012. URL: https://www.sciencedirect.com/science/article/pii/S0007449711001254, doi:https://doi.org/10.1016/j.bulsci.2011.12.004.

[14] Scott A. Diddams. The evolving optical frequency comb. *J. Opt. Soc. Am. B*, 27(11):B51–B62, Nov 2010. URL: http://opg.optica.org/josab/abstract.cfm?URI=josab-27-11-B51, doi:10.1364/JOSAB.27.000B51.

[15] Tomas Dohnal, Jens Rademacher, Hannes Uecker, and Daniel Wetzel. pde2path 2.0: multi-parameter continuation and periodic domains. 2014.

[16] Willy Dörfler, Armin Lechleiter, Michael Plum, Guido Schneider, and Christian Wieners. *Photonic Crystals. Mathematical Analysis and Numerical Approximation.* 01 2011. doi:10.1007/978-3-0348-0113-3.

[17] Tara Fortier and Esther Baumann. 20 years of developments in optical frequency comb technology and applications. *Communications Physics*, 2(1), dec 2019. URL: https://doi.org/10.1038%2Fs42005-019-0249-y, doi:10.1038/s42005-019-0249-y.

[18] J. Gärtner, P. Trocha, R. Mandel, C. Koos, T. Jahnke, and W. Reichel. Bandwidth and conversion efficiency analysis of dissipative kerr soliton frequency combs based on bifurcation theory. *Phys. Rev. A*, 100:033819, Sep 2019. URL: https://link.aps.org/doi/10.1103/PhysRevA.100.033819, doi:10.1103/PhysRevA.100.033819.

[19] Janina Gärtner. *Continuation and Bifurcation of Frequency Combs Modeled by the Lugiato-Lefever Equation.* PhD thesis, Karlsruher Institut für Technologie (KIT), 2019. doi:10.5445/IR/1000092286.

[20] Janina Gärtner and Wolfgang Reichel. Soliton solutions for the Lugiato–Lefever equation by analytical and numerical continuation methods. In Willy Dörfler, Marlis Hochbruck, Dirk Hundertmark, Wolfgang Reichel, Andreas Rieder, Roland Schnaubelt, and Birgit Schörkhuber, editors, *Mathematics of Wave Phenomena*, Trends in Mathematics, pages 179–195. Birkhäuser Basel, oct 2020. doi:10.1007/978-3-030-47174-3_11.

## References

[21] E. Gasmi, T. Jahnke, M. Kirn, and W. Reichel. Global continua of solutions to the Lugiato-Lefever model for frequency combs obtained by two-mode pumping. Preprint, 2022. URL: https://www.math.kit.edu/iana2/~reichel/seite/publ/media/gasmi_jahnke_kirn_reichel.pdf.

[22] E. Gasmi, H. Peng, C. Koos, and W. Reichel. Bandwidth and conversion-efficiency analysis of Kerr soliton combs in dual-pumped resonators with anomalous dispersion. Preprint, 2022. URL: https://www.math.kit.edu/iana2/~reichel/seite/publ/media/gasmi_peng_koos_reichel.pdf.

[23] Elias Gasmi. Bandstrukturen bei periodischen fraktionalen Schrödingeroperatoren und Anwendungen auf nichtlineare Grundzustände. Masterarbeit, Karlsruher Institut für Technologie (KIT), 2018.

[24] Michele Giunta, Marc Fischer, Wolfgang Hänsel, Tilo Steinmetz, Maurice Lessing, Simon Holzberger, Carsten Cleff, Theodor W. Hänsch, Michael Mei, and Ronald Holzwarth. 20 years and 20 decimal digits: A journey with optical frequency combs. *IEEE Photonics Technology Letters*, 31(23):1898–1901, 2019. doi:10.1109/LPT.2019.2955096.

[25] Cyril Godey. A bifurcation analysis for the Lugiato-Lefever equation. *The European Physical Journal D*, 71(5):131, May 2017. doi:10.1140/epjd/e2017-80057-2.

[26] Cyril Godey, Irina V. Balakireva, Aurélien Coillet, and Yanne K. Chembo. Stability analysis of the spatiotemporal Lugiato-Lefever model for Kerr optical frequency combs in the anomalous and normal dispersion regimes. *Phys. Rev. A*, 89:063814, 2014. URL: http://link.aps.org/doi/10.1103/PhysRevA.89.063814, doi:10.1103/PhysRevA.89.063814.

[27] John L. Hall. Nobel lecture: Defining and measuring optical frequencies. *Rev. Mod. Phys.*, 78:1279–1295, Nov 2006. URL: https://link.aps.org/doi/10.1103/RevModPhys.78.1279, doi:10.1103/RevModPhys.78.1279.

[28] Theodor W. Hänsch. Nobel lecture: Passion for precision. *Rev. Mod. Phys.*, 78:1297–1309, Nov 2006. URL: https://link.aps.org/doi/10.1103/RevModPhys.78.1297, doi:10.1103/RevModPhys.78.1297.

[29] T. Hansson and S. Wabnitz. Bichromatically pumped microresonator frequency combs. *Phys. Rev. A*, 90:013811, Jul 2014. URL: https://link.aps.org/doi/10.1103/PhysRevA.90.013811, doi:10.1103/PhysRevA.90.013811.

[30] H. Heilbronn. On the distribution of the sequence $n^2\theta \pmod 1$. *The Quarterly Journal of Mathematics*, os-19(1):249–256, 01 1948. arXiv:https://academic.oup.com/qjmath/article-pdf/os-19/1/249/4572309/os-19-1-249.pdf, doi:10.1093/qmath/os-19.1.249.

[31] T. Herr, V. Brasch, J. D. Jost, C. Y. Wang, N. M. Kondratiev, M. L. Gorodet-sky, and T. J. Kippenberg. Temporal solitons in optical microresonators. *Nature Photonics*, 8(2):145–152, dec 2013. URL: https://doi.org/10.1038%2Fnphoton.2013.343, doi:10.1038/nphoton.2013.343.

[32] T. Herr, K. Hartinger, J. Riemensberger, C. Y. Wang, E. Gavartin, R. Holzwarth, M. L. Gorodetsky, and T. J. Kippenberg. Universal Dynamics of Kerr-Frequency Comb Formation in Microresonators. In *Conference on Lasers and Electro-Optics 2012*, page QF3G.7. Optica Publishing Group, 2012. URL: http://opg.optica.org/abstract.cfm?URI=QELS-2012-QF3G.7, doi:10.1364/QELS.2012.QF3G.7.

[33] Tobias Jahnke, Marcel Mikl, and Roland Schnaubelt. Strang splitting for a semi-linear Schrödinger equation with damping and forcing. *J. Math. Anal. Appl.*, 455(2):1051–1071, nov 2017. doi:10.1016/j.jmaa.2017.06.004.

[34] David J Jones, Scott A Diddams, Jinendra K Ranka, Andrew Stentz, Robert S Windeler, John L Hall, and Steven T Cundiff. Carrier-envelope phase control of femtosecond mode-locked lasers and direct optical frequency synthesis. *Science*, 288(5466):635–639, 2000.

[35] Tosio Kato. *Perturbation theory for linear operators; 2nd ed.* Grundlehren der mathematischen Wissenschaften : a series of comprehensive studies in mathematics. Springer, Berlin, 1976. URL: https://cds.cern.ch/record/101545.

[36] H. Kielhöfer. *Bifurcation Theory: An Introduction with Applications to Partial Differential Equations*. Applied Mathematical Sciences. Springer New York, 2011. URL: https://books.google.de/books?id=wrqZj3BYZ7YC.

[37] T. J. Kippenberg, R. Holzwarth, and S. A. Diddams. Microresonator-based optical frequency combs. *Science*, 332(6029):555–559, 2011. URL: https://www.science.org/doi/abs/10.1126/science.1193968, arXiv:https://www.science.org/doi/pdf/10.1126/science.1193968, doi:10.1126/science.1193968.

[38] Valery E Lobanov, Grigory Lihachev, and Michael L Gorodetsky. Generation of platicons and frequency combs in optical microresonators with normal gvd by mod-ulated pump. *EPL (Europhysics Letters)*, 112(5):54008, 2015.

[39] L. A. Lugiato and R. Lefever. Spatial dissipative structures in passive optical sys-tems. *Phys. Rev. Lett.*, 58:2209–2211, 1987. URL: http://link.aps.org/doi/10.1103/PhysRevLett.58.2209, doi:10.1103/PhysRevLett.58.2209.

[40] Wilhelm Magnus and Stanley Winkler. *Hill's equation*. Interscience Tracts in Pure and Applied Mathematics, No. 20. Interscience Publishers John Wiley & Sons, New York-London-Sydney, 1966.

[41] Rainer Mandel and Wolfgang Reichel. A priori bounds and global bifurcation results for frequency combs modeled by the Lugiato-Lefever equation. *SIAM J. Appl. Math.*, 77(1):315–345, 2017. doi:10.1137/16M1066221.

[42] Pablo Marin-Palomo, Juned N Kemal, Maxim Karpov, Arne Kordts, Joerg Pfeifle, Martin HP Pfeiffer, Philipp Trocha, Stefan Wolf, Victor Brasch, Miles H Anderson, et al. Microresonator-based solitons for massively parallel coherent optical communications. *Nature*, 546(7657):274–279, 2017.

[43] T. Miyaji, I. Ohnishi, and Y. Tsutsumi. Bifurcation analysis to the Lugiato-Lefever equation in one space dimension. *Phys. D*, 239(23-24):2066–2083, 2010. URL: http://dx.doi.org/10.1016/j.physd.2010.07.014, doi:10.1016/j.physd.2010.07.014.

[44] Carlo Morosi and Livio Pizzocchero. On the constants for some fractional Gagliardo–Nirenberg and Sobolev inequalities. *Expositiones Mathematicae*, 36(1):32–77, 2018. URL: https://www.sciencedirect.com/science/article/pii/S0723086917300592, doi:https://doi.org/10.1016/j.exmath.2017.08.007.

[45] Nils Nemitz, Takuya Ohkubo, Masao Takamoto, Ichiro Ushijima, Manoj Das, Noriaki Ohmae, and Hidetoshi Katori. Frequency ratio of yb and sr clocks with $5 \times 10$-17 uncertainty at 150 seconds averaging time. *Nature Photonics*, 10(4):258–261, feb 2016. URL: https://doi.org/10.1038%2Fnphoton.2016.20, doi:10.1038/nphoton.2016.20.

[46] Zachary L Newman, Vincent Maurice, Tara Drake, Jordan R Stone, Travis C Briles, Daryl T Spencer, Connor Fredrick, Qing Li, Daron Westly, Bojan R Ilic, et al. Architecture for the photonic integration of an optical atomic clock. *Optica*, 6(5):680–685, 2019.

[47] Scott B Papp, Pascal Del'Haye, and Scott A Diddams. Parametric seeding of a microresonator optical frequency comb. *Optics Express*, 21(15):17615–17624, 2013.

[48] P. Parra-Rivas, D. Gomila, L. Gelens, and E. Knobloch. Bifurcation structure of localized states in the Lugiato-Lefever equation with anomalous dispersion. *Phys. Rev. E*, 97:042204, Apr 2018. URL: https://link.aps.org/doi/10.1103/PhysRevE.97.042204, doi:10.1103/PhysRevE.97.042204.

[49] Pedro Parra-Rivas, Damià Gomila, François Leo, Stéphane Coen, and Lendert Gelens. Third-order chromatic dispersion stabilizes Kerr frequency combs. *Opt. Lett.*, 39(10):2971–2974, 2014. URL: http://ol.osa.org/abstract.cfm?URI=ol-39-10-2971, doi:10.1364/OL.39.002971.

[50] Pedro Parra-Rivas, Edgar Knobloch, Damià Gomila, and Lendert Gelens. Dark solitons in the Lugiato-Lefever equation with normal dispersion. *Phys. Rev. A*, 93(6):1–17, 2016. URL: https://journals.aps.org/pra/abstract/10.1103/PhysRevA.93.063839, doi:10.1103/PhysRevA.93.063839.

[51] Nicolas Périnet, Nicolas Verschueren, and Saliya Coulibaly. Eckhaus instability in the Lugiato-Lefever model. *The European Physical Journal D*, 71(9):243, Sep 2017. `doi:10.1140/epjd/e2017-80078-9`.

[52] Joerg Pfeifle, Aurélien Coillet, Rémi Henriet, Khaldoun Saleh, Philipp Schindler, Claudius Weimann, Wolfgang Freude, Irina V. Balakireva, Laurent Larger, Christian Koos, and Yanne K. Chembo. Optimally Coherent Kerr Combs Generated with Crystalline Whispering Gallery Mode Resonators for Ultrahigh Capacity Fiber Communications. *Phys. Rev. Lett.*, 114:093902, Mar 2015. URL: `https://link.aps.org/doi/10.1103/PhysRevLett.114.093902`, `doi:10.1103/PhysRevLett.114.093902`.

[53] Nathalie Picqué and Theodor W Hänsch. Frequency comb spectroscopy. *Nature Photonics*, 13(3):146–157, 2019.

[54] M. Reed. *Methods of Modern Mathematical Physics: Functional Analysis*. Elsevier Science, 2012. URL: `https://books.google.de/books?id=78ROoxSZNl8C`.

[55] M. Reed and B. Simon. *Methods of Modern Mathematical Physics. IV Analysis of Operators*. Academic Press, New York, 1978.

[56] Luz Roncal and Pablo Raúl Stinga. Transference of fractional Laplacian regularity. In *Special functions, partial differential equations, and harmonic analysis*, volume 108 of *Springer Proc. Math. Stat.*, pages 203–212. Springer, Cham, 2014. URL: `https://doi.org/10.1007/978-3-319-10545-1_14`, `doi:10.1007/978-3-319-10545-1\_14`.

[57] Klaus Schmitt. Positive solutions of semilinear elliptic boundary value problems. In *Topological methods in differential equations and inclusions (Montreal, PQ, 1994)*, volume 472 of *NATO Adv. Sci. Inst. Ser. C: Math. Phys. Sci.*, pages 447–500. Kluwer Acad. Publ., Dordrecht, 1995.

[58] Daryl T Spencer, Tara Drake, Travis C Briles, Jordan Stone, Laura C Sinclair, Connor Fredrick, Qing Li, Daron Westly, B Robert Ilic, Aaron Bluestone, et al. An optical-frequency synthesizer using integrated photonics. *Nature*, 557(7703):81–85, 2018.

[59] Milena Stanislavova and Atanas G. Stefanov. Asymptotic stability for spectrally stable Lugiato-Lefever solitons in periodic waveguides. *J. Math. Phys.*, 59(10):101502, 12, 2018. `doi:10.1063/1.5048017`.

[60] Brian Stern, Xingchen Ji, Yoshitomo Okawachi, Alexander L. Gaeta, and Michal Lipson. Battery-operated integrated frequency comb generator. *Nature*, 562:401–405, 2018.

[61] Dmitry V Strekalov and Nan Yu. Generation of optical combs in a whispering gallery mode resonator from a bichromatic pump. *Physical Review A*, 79(4):041805, 2009.

## References

[62] Hossein Taheri, Andrey B. Matsko, and Lute Maleki. Optical lattice trap for Kerr solitons. *The European Physical Journal D*, 71(6), jun 2017. URL: https://doi.org/10.1140%2Fepjd%2Fe2017-80150-6, doi:10.1140/epjd/e2017-80150-6.

[63] Philipp Trocha. *Kerr-Nonlinear Microresonators and Frequency Combs: Modelling, Design, and Applications*. PhD thesis, Karlsruher Institut für Technologie (KIT), 2022. doi:10.5445/IR/1000142186.

[64] Philipp Trocha, M Karpov, D Ganin, Martin HP Pfeiffer, Arne Kordts, S Wolf, J Krockenberger, Pablo Marin-Palomo, Claudius Weimann, Sebastian Randel, et al. Ultrafast optical ranging using microresonator soliton frequency combs. *Science*, 359(6378):887–891, 2018.

[65] Th. Udem, R. Holzwarth, and T. W. Hänsch. Optical frequency metrology. *Nature*, 416(6877):233–237, 2002. URL: http://www.nature.com/doifinder/10.1038/416233a, doi:10.1038/416233a.

[66] Th. Udem, J. Reichert, R. Holzwarth, and T. W. Hänsch. Absolute optical frequency measurement of the cesium $d_1$ line with a mode-locked laser. *Phys. Rev. Lett.*, 82:3568–3571, May 1999. URL: https://link.aps.org/doi/10.1103/PhysRevLett.82.3568, doi:10.1103/PhysRevLett.82.3568.

[67] Hannes Uecker, Daniel Wetzel, and Jens D.M. Rademacher. pde2path - a Matlab package for continuation and bifurcation in 2D elliptic systems. *NMTMA*, (7):58–106, 2014.

[68] S. Wabnitz. Suppression of interactions in a phase-locked soliton optical memory. *Opt. Lett.*, 18(8):601–603, Apr 1993. URL: http://opg.optica.org/ol/abstract.cfm?URI=ol-18-8-601, doi:10.1364/OL.18.000601.

[69] Wenle Weng, Romain Bouchand, and Tobias J Kippenberg. Formation and collision of multistability-enabled composite dissipative Kerr solitons. *Physical Review X*, 10(2):021017, 2020.

[70] Gordon Thomas Whyburn. *Analytic topology*. American Mathematical Society Colloquium Publications, Vol. XXVIII. American Mathematical Society, Providence, R.I., 1963.

[71] Tobias Wilken, Gaspare Lo Curto, Rafael A Probst, Tilo Steinmetz, Antonio Manescau, Luca Pasquini, Jonay I González Hernández, Rafael Rebolo, Theodor W Hänsch, Thomas Udem, and Ronald Holzwarth. A spectrograph for exoplanet observations calibrated at the centimetre-per-second level. *Nature*, 485(7400):611—614, May 2012. doi:10.1038/nature11092.

[72] Qi-Fan Yang, Myoung-Gyun Suh, Ki Youl Yang, Xu Yi, and Kerry J Vahala. Microresonator soliton dual-comb spectroscopy. In *CLEO: Science and Innovations*, pages SM4D–4. Optica Publishing Group, 2017.

## Eidesstattliche Erklärung:

Hiermit erkläre ich an Eides statt, dass ich die vorliegende Arbeit selbstständig und nur unter Zuhilfenahme der ausgewiesenen Hilfsmittel angefertigt habe. Sämtliche Stellen der Arbeit, die im Wortlaut oder dem Sinn nach anderen gedruckten oder im Internet veröffentlichten Werken entnommen sind, habe ich durch genaue Quellenangaben kenntlich gemacht.


Karlsruhe, den 17. Oktober 2022